1-1-2010

Enhanced Lipid Production And Biodiesel Yields From Activated Sludge Via Fermentation Of Lignocellulose Hydrolyzate

Andro Hernandez Mondala

ENHANCED LIPID PRODUCTION AND BIODIESEL YIELDS FROM ACTIVATED SLUDGE VIA FERMENTATION OF LIGNOCELLULOSE HYDROLYZATE

By

Andro Hernandez Mondala

A Dissertation
Submitted to the Faculty of
Mississippi State University
in Partial Fulfillment of the Requirements
for the Degree of Doctor of Philosophy
in Engineering
in the Dave C. Swalm School of Chemical Engineering

Mississippi State, Mississippi

December 2010

ENHANCED LIPID PRODUCTION AND BIODIESEL YIELDS FROM ACTIVATED SLUDGE VIA FERMENTATION OF LIGNOCELLULOSE HYDROLYZATE

By

Andro Hernandez Mondala

Approved:

Rafael Hernandez Associate Professor Dave C. Swalm School of Chemical Engineering (Director of Dissertation and Advisor)	W. Todd French Assistant Professor Dave C. Swalm School of Chemical Engineering (Committee Member)
R. Mark Bricka Associate Professor Dave C. Swalm School of Chemical Engineering (Committee Member)	Bill Elmore Interim Director and Henry Hunter Chair Dave C. Swalm School of Chemical Engineering (Committee Member)
Benjamin S. Magbanua, Jr. Associate Professor Department of Civil and Environmental Engineering (Committee Member)	Keisha B. Walters Assistant Professor Dave C. Swalm School of Chemical Engineering (Committee Member)
Rafael Hernandez Associate Professor Dave C. Swalm School of Chemical Engineering (Graduate Coordinator)	Sarah A. Rajala Dean of the Bagley College of Engineering

Name: Andro Hernandez Mondala

Date of Degree: December 10, 2010

Institution: Mississippi State University

Major Field: Engineering

Major Professor: Rafael Hernandez, Ph.D.

Title of Study: ENHANCED LIPID PRODUCTION AND BIODIESEL YIELDS FROM ACTIVATED SLUDGE VIA FERMENTATION OF LIGNOCELLULOSE HYDROLYZATE

Pages in Study: 316

Candidate for Degree of Doctor of Philosophy

The potential of enhancing lipid accumulation in municipal sewage activated sludge via fermentation of lignocellulose biomass hydrolyzate was investigated. The overall objective was to increase the levels of feedstock lipids in the activated sludge biomass and increase its biodiesel yield via *in situ* or *ex situ* transesterification; and improve its cost competitiveness as an abundant feedstock source for biofuels production. To reduce production costs and maintain environmental sustainability, influent wastewater and waste lignocellulose biomass hydrolyzate were used as cultivation media and substrate, respectively. However, lignocellulose hydrolyzates also contain degradation by-products such as furfural and acetic acid that are known to exert inhibitory effects on microorganisms; hence their effects on the fermentative performance of activated sludge were investigated and fermentation strategies were proposed and evaluated to counteract the microbial toxicity of these compounds. The utilization rate and efficiency of xylose by activated sludge microorganisms for lipid production was

also evaluated as pentose sugars such as xylose usually constitute a major percentage of lignocellulose hydrolyzates. Furthermore, variations in the population profile of activated sludge microbiota were determined via 16S rRNA sequence analysis to determine the effect of sugar fermentation at different initial conditions. Results show that activated sludge lipid contents and biodiesel yield could be enhanced by fermentation of sugars at a high initial C:N ratio (70:1). Furfural was found to be highly inhibitory to microbial growth and lipid accumulation while high initial acetic acid concentrations enhanced biomass production but not lipid formation. Xylose was also utilized more efficiently than glucose by the activated sludge microorganisms for biomass and lipid production albeit at relatively slower rates; hence sugar mixtures derived from lignocellulose could be utilized for the process. Semicontinuous and continuous fermentation modes were proposed and evaluated as strategies to reduce inhibitory effect of furfural and acetic acid and improve lipid productivity, but the lack of nutrient supplementation prevented the cultures from sustaining microbial growth and lipid production, leading to cell death and washout. Finally, the reduction in the diversity of the activated sludge microbiota could point to specific microbial strains that are mainly responsible for lipid accumulation.

DEDICATION

This work is dedicated to my parents, who have sacrificed so much that I may have this opportunity to succeed in my all endeavors; to Sandy, my better half and my inspiration; and to God, with whom all things are possible.

ACKNOWLEDGEMENTS

The author would like to thank the following agencies for providing the funding for this research: the U.S. Department of Energy, U.S. Environmental Protection Agency, and the National Science Foundation; as well as to the City of Tuscaloosa, AL Hillard Fletcher Wastewater Treatment Plant for providing the activated sludges used in this study.

Special thanks are also given to the members of the author's dissertation committee. First and foremost, to Dr. Rafael Hernandez; a great mentor, teacher, and leader in whom the author looks up to and hopes to model his future academic career after. Many thanks also to Dr. Todd French, who has been a source of invaluable knowledge in the field of microbiology and also in life. Furthermore, the author thanks Dr. Bill Elmore, Dr. Mark Bricka, Dr. Keisha B. Walters, and Dr. Benjamin Magbanua, for all the invaluable inputs, comments, suggestions, and criticisms that contributed greatly for the improvement of this work.

This work would not have been possible without the hard work and dedication of the Renewable Fuels and Chemicals Laboratory (RFCL) staff and students who have worked on the project over the four and a half years since its inception. Many thanks to Ms. Linda McFarland, an excellent lab manager who always worked hard to instill in us a sense of discipline in research; Mr. William Holmes, whose expertise in analytical

instrumentation has contributed greatly to the analytical results in this study; the late Dr. Earl Alley, whose extensive knowledge in analytical chemistry continues to inspire and influence the group's research in that aspect and everything else; and to the following undergraduate and high school students: Colin Gurtowski, Marlene Trillo, Courtney Ramsey, Otis Malone, Vicdaly Williams, Leni Alex, Monica Haque, and David Batchelor. Many thanks are also given to the rest of the RFCL staff and students, current and former, for all the support and likewise the invaluable comments, criticisms, and suggestions that have contributed in one way or another to the development of this work: Dr. Darrell Sparks (now with the Department of Biochemistry and Molecular Biology, Mississippi State University), Dr. Patrisha Pham, Mr. Jimmie Cain, Dr. Alexei Iretski (Lake Superior State University, Sault Ste. Marie, MI), Jacqueline Hall, Mary Hetrick, Maria Paraschivescu, Emmanuel Revellame, Adebola Coker, and Scott Crymble.

The author also thanks the U.S. Environmental Protection Agency, National Risk Management Research Laboratory (NRMRL) group in Cincinnati, OH composed of Dr. Jorge W. Santo Domingo, Dr. Mark Meckes, Dr. Hodon Ryu, and Brandon Iker for performing most of the microbial community analysis and for their hospitality during the author's stay in Cincinnati to undergo training on molecular methods. Special thanks also to Jacqueline Hall and Mary Hetrick, who have likewise contributed greatly to this part of the overall work and for being such great company during the 10-day training period at the U.S. EPA Cincinnati office.

The author would also like to thank the faculty and staff of the Dave C. Swalm School of Chemical Engineering, most especially to Ms. Sandra Shumaker and Ms. Ellen Weeks for all the purchase and trip requests that they made and for their extreme

patience; to Mr. Mike Hillhouse, Ms. Sherre Denson, and Dr. Bill Elmore, Interim Director of the Department.

Special thanks are given to Dr. Chay Binh Pham and Dr Laura Pham, for all their support and for being instrumental in all of these successes; and to Dr. Patrisha Pham, a great friend and colleague, with whom the author had the pleasure of working with on the many challenging aspects of our field of research.

Most special thanks to Ms. Alessandra Pham (Sandy), for all the love, support, and patience, and for being the inspiration for all of these endeavors.

Furthermore, the author expresses his sincerest gratitude to his family: Mom, Dad, Anna, and Adrian for all the love, support, patience, and sacrifice that we may be able to achieve our dreams for a better life.

Finally, thanks to God Almighty; for without His grace, all of these successes and life itself will not be possible.

To those who were not mentioned but have contributed in one way or another to the success of this project and the development of this dissertation, the author extends his sincerest appreciation and best regards.

AHM

November 3, 2010

Mississippi State, MS

TABLE OF CONTENTS

APPENDIX

LIST OF TABLES

LIST OF FIGURES

CHAPTER I

INTRODUCTION

In his September 2006 State of the Union address, former U.S. President George W. Bush stressed the problem of America's addiction to oil [Center for American Progress, 2006]. The United States currently has one-third of the world's automobiles (roughly 230 million) and consumes 25 % of the world's total oil supplies in order to drive its economy through transportation, heat, and electric power [Biomass Research and Development Board, 2008]. As shown in Figure 1.1, the total oil consumption of the U.S. has reached a high of approximately 20,000 barrels per day in the last five years, whereas domestic oil production exhibited a declining trend within the last 30 years to less than half of the oil consumption. Majority of these oil demands are currently met by importing oil from foreign countries as evident in the negative net export/import values within the last 30 years. Carbon dioxide emissions in the US are also on the rise due to the combustion of these fossil fuels, reaching around 6,000 million metric tons in 2008. It has been projected that in the absence of alternatives to petroleum, the country's reliance of foreign oil will increase by 30 % through 2030 and the transportation sector's greenhouse gas emissions will increase by 40 % [Biomass Research and Development Board, 2008]. Therefore, energy security and environmental impacts are the two main

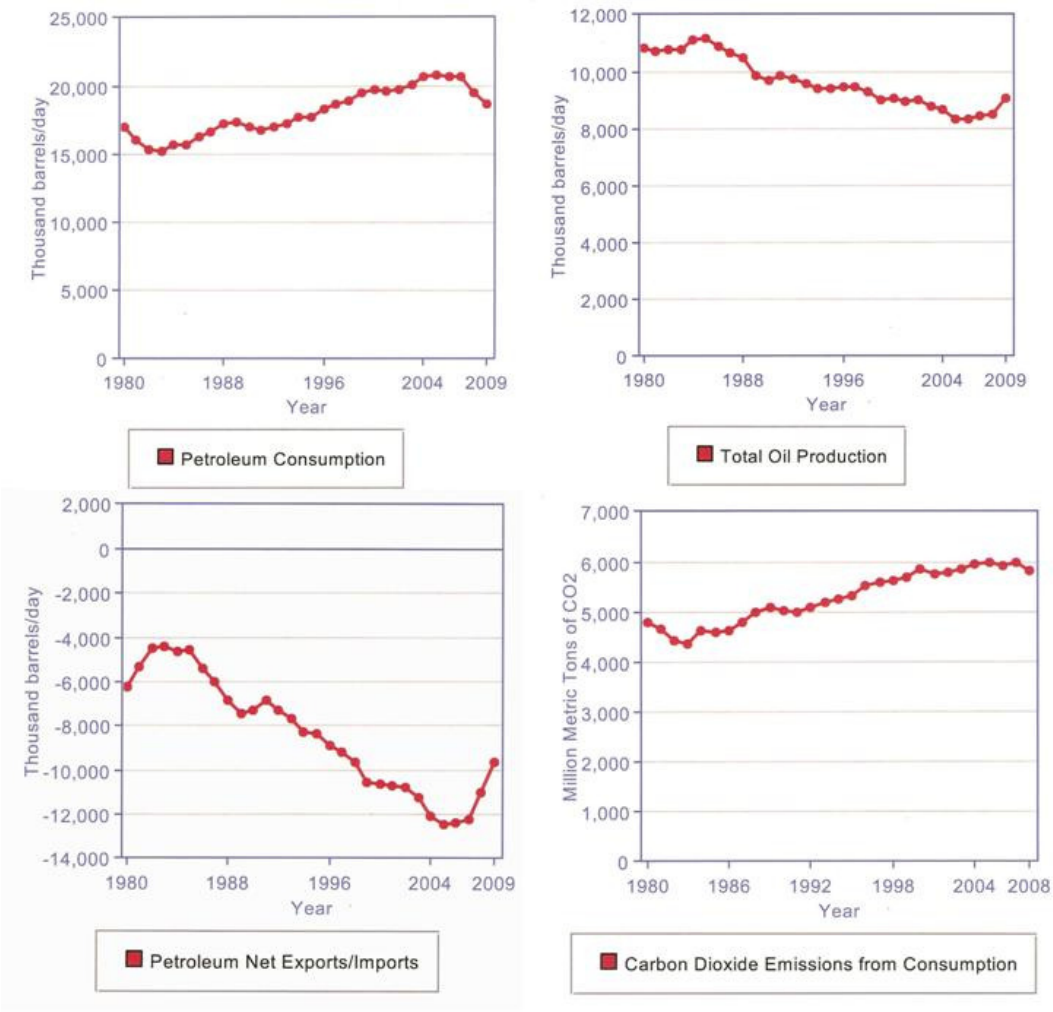

Figure 1.1: U.S. petroleum consumption, production, imports/exports, and CO_2 emission profiles [U.S. DOE-EIA, 2010].

driving forces that have led to the increased amount of interest and research activities on the development of alternative biofuels derived from domestic renewable biomass. As part of the *Twenty in Ten* initiative by the Bush administration in 2007, biofuels have been considered as one of the near-term strategies to address these energy security and climate change [Biomass Research and Development Board, 2008]. The goal of the program was to reduce the country's gasoline consumption by 20 % in the next ten years with a mandate to increase domestic production of renewable biofuels such as bioethanol and biodiesel to 35 billion gallons per year by 2017.

Biodiesel

One of the most familiar first-generation biofuels that have been extensively studied and commercially produced is biodiesel. Biodiesel is a petroleum diesel substitute produced through *transesterification* of vegetable oils or animal fats [Knothe, 2005]. This reaction is shown in Figure 1.2, where triacylglycerols (TAG) in the oil react with an alcohol (usually methanol) to separate glycerol from the TAG molecule and the resulting fatty acyl residues are converted into fatty acid alkyl esters (fatty acid methyl esters or FAME when methanol is used). The overall reaction however, is a sequence of three consecutive and reversible reactions, in which di- (DAG) and monoacyglycerols (MAG) are formed as intermediates [Freedman, et al., 1986]. In a general sense, the term transesterification is used to describe a class of organic reactions where an ester is transformed into another through interchange of the alkoxy moiety [Schuchardt, et al., 1998]. Therefore, in addition to TAG, DAG, and MAG, any other lipid with an ester

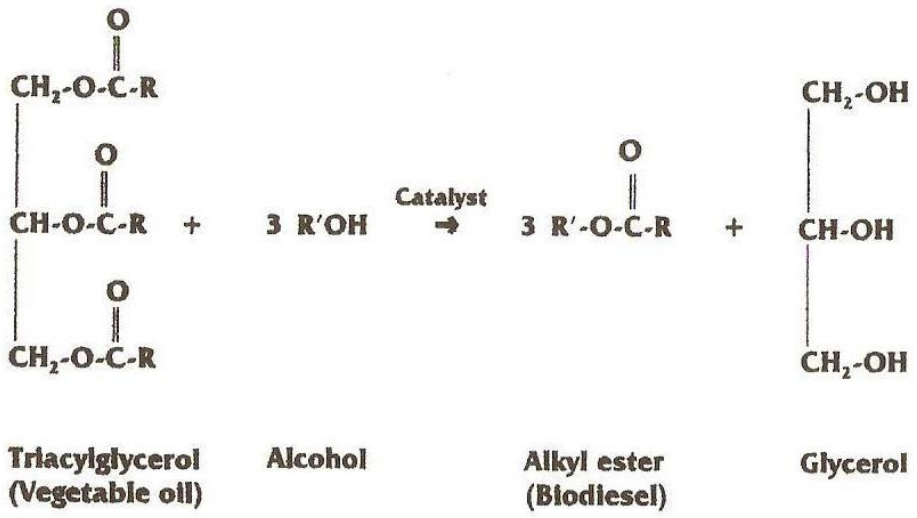

Figure 1.2: Overall scheme of the transesterification reaction, where R represents a mixture of various fatty acid chains [Van Gerpen and Knothe, 2005].

functional group such as free fatty acids (FFA), phospholipids, glycolipids, sphingolipids, and waxes can undergo transesterification (esterification for FFA) to yield alkyl ester derivatives. These lipids (Figure 1.3) are also classified as saponifiable lipids or those that can undergo hydrolysis under alkaline conditions and from hereon will also be used to refer to lipids that can be converted to methyl esters (biodiesel).

The transesterification reaction can also be either base- or acid-catalyzed depending on the nature of the oil feedstock. Although base-catalyzed transesterification occurs more rapidly than acid-catalysis, the latter is more applicable when using oils or fats containing > 5 % free fatty acids (FFA) due to soap formation during base-catalyzed transesterification as shown in the reaction below [Van Gerpen and Knothe, 2005]:

$$\underset{\text{Free fatty acid}}{\text{R-COOH}} + \underset{\text{Base}}{\text{KOH}} \rightarrow \underset{\text{Soap}}{\text{R-COOK}} + \underset{\text{Water}}{\text{H}_2\text{O}} \qquad (1.1)$$

At FFA levels above 5 %, it was found that soap inhibits the separation of the glycerol from the methyl esters and contributes to emulsion formation during water washes. Hence in these cases, acid catalysts such as sulfuric acid are used to esterify the FFA to alkyl esters. At the same time, this can be used as a pretreatment process to reduce the FFA level in the oil followed by alkali-catalyzed transesterification to convert the TAG to alkyl esters. Additionally, alternate methods to conventional base- and acid-catalyzed transesterification have been developed with the objectives of reducing catalyst cost, waste and by-product (glycerol) output, and extensive product purification requirements. These methods include alkali-catalyzed monophasic transesterification, enzymatic conversion, and *in situ* transesterification [Haas and Foglia, 2005].

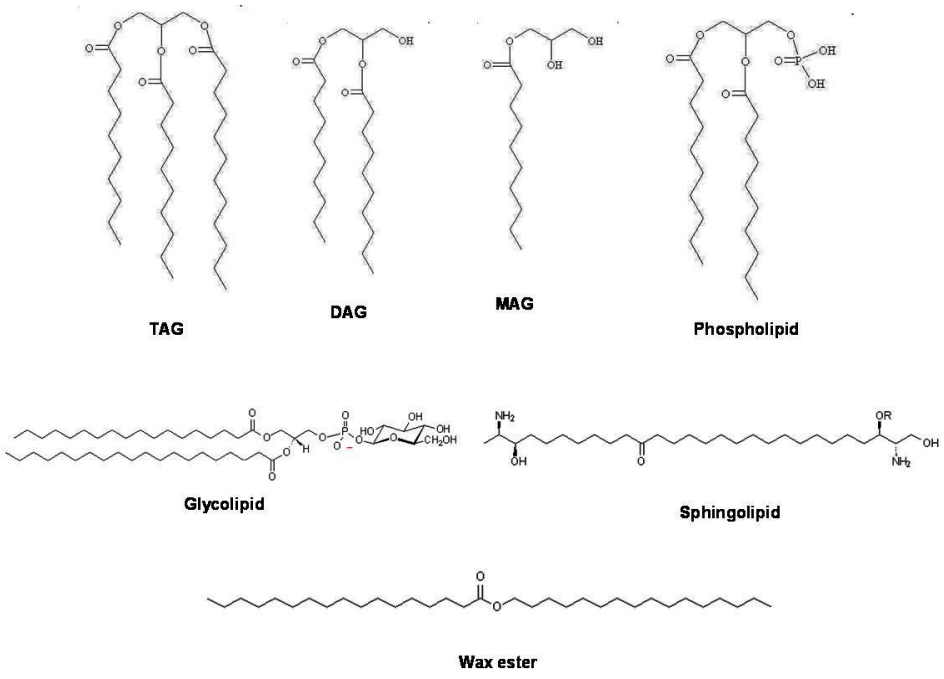

Figure 1.3: Chemical structures of some common saponifiable lipids that can undergo transesterification for biodiesel production [AOCS, 2010].

Some of the benefits of biodiesel that have contributed to its popularity are the following:

- *Environmental Impact and Safety:* Biodiesel combustion results into a significant reduction in carbon dioxide emissions (78.5 %), unburned hydrocarbons (67 %), carbon monoxide (48 %), and particulate matter (47 %) compared with petroleum diesel [National Biodiesel Board, 2009]. In addition to this, biodiesel has been shown to be nontoxic, more biodegradable than petroleum diesel, and has a flashpoint (200°F) higher than petroleum diesel (125°F), making it safer to use, handle, and store [National Biodiesel Board, 2010b]
- *Economic and Energy Security:* The use of renewable domestic feedstock sources and the capability to manufacture biodiesel using existing production capacity and conventional equipment provides substantial opportunities to immediately address energy security issues as well as create and support around 52,000 jobs in the U.S. [National Biodiesel Board, 2009].
- *Performance:* Biodiesel has an energy content comparable to No. 2 diesel (128,000 BTU/gal) when used as B20 blend [National Biodiesel Board, 2010a], at the same time provides up to a 65 % increase in lubricity and is compatible with most engine components [National Biodiesel Board, 2010c].

However, in spite of these advantages, several issues that are limiting the realization of biodiesel's full commercial potential remain. These issues are mainly related to economics and feedstock sources and are discussed in the next section.

Current Status of Biodiesel

Economics

As of 2009, there are 173 biodiesel manufacturing and marketing companies in the United States with a total combined maximum annual production capacity of 2.69 billion gallons per year [National Biodiesel Board, 2010e]. The actual biodiesel production trend in million gallons per year shown in Figure 1.4 indicates an exponentially increasing trend between the fiscal years 2000 and 2008. However, recent data estimates suggested a decrease in production from 700 million gallons in 2008 to 545 million gallons in 2009 possibly due to the recent economic recession [National Biodiesel Board, 2010f]. In spite of this, it has been reported that at least 29 companies have started construction of new biodiesel plants, which would result in another 427.8 million gallons per year of biodiesel production capacity [National Biodiesel Board, 2010f].

A major challenge to the commercialization of biodiesel is its relatively higher manufacturing cost compared with petroleum-based diesel [You, et al., 2008]. The data presented in Table 1.1 suggest that this discrepancy can be attributed to the type of feedstock, which typically constitutes 70-85 % of the overall production cost [Haas and Foglia, 2005]. This implies that the nature of the feedstock used for the production of biodiesel is a crucial factor in determining the economic feasibility of biodiesel as an alternative renewable fuel.

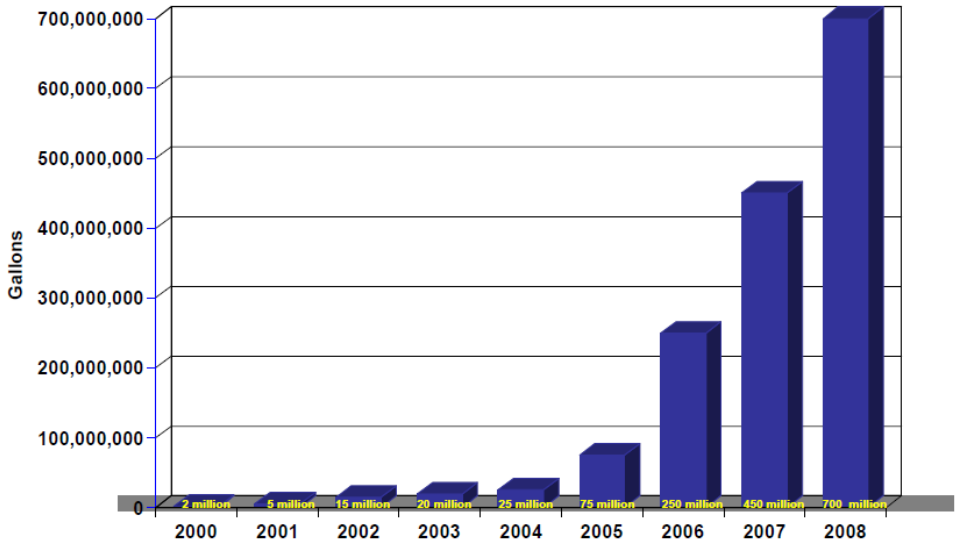

Figure 1.4: Estimated US biodiesel production by fiscal year [National Biodiesel Board, 2010d].

Table 1.1 Projected production costs for diesel fuel by feedstock, 2004-2013 in 2002 dollars per gallon [U.S. Energy Information Administration, 2004].

Marketing Year	Soybean Oil	Yellow Grease	Petroleum
2004/05	2.54	1.41	0.67
2005/06	2.49	1.39	0.78
2006/07	2.47	1.38	0.77
2007/08	2.44	1.37	0.78
2008/09	2.52	1.40	0.78
2009/10	2.57	1.42	0.75
2010/11	2.67	1.47	0.76
2011/12	2.73	1.51	0.76
2012/13	2.80	1.55	0.75

Feedstock

Biodiesel can be produced from a wide variety of feedstocks, the most common of which are vegetable oils such as soybean, cottonseed, palm, rapeseed/canola, peanut, sunflower, safflower, and coconut; and animal fats such as tallow [Knothe, 2005]. The choice of oil from biodiesel production largely depends on local availability and affordability. In United States, soybean oil and animal fats are the major feedstocks used. An estimated 20.6 billion pounds of soybean oil was reported to have been produced in the US in 2008, with 15.2 billion pounds or roughly three-quarters of the total supplies used for edible oil consumption [American Soybean Association, 2009]. This implies a surplus soybean oil supply of approximately 5.4 billion pounds whereas, the 700 million gallons of biodiesel produced in the same year will have required 5.3 billion pounds of oil feedstock. Edible oil demands are expected to continue increasing in the future due to increasing population; hence the surplus supply will likewise decrease. Therefore, a disadvantage to the use of soybean oil are growing concerns about food security and rising food costs due to the utilization of feedstocks normally used for food production to biofuels production instead to cater to the rising demands of the biofuels industry (food vs. fuel issue). Crop oil supplies are also limited by planting and harvesting seasons and face the risk of supply interruptions and variations in lipid quality due to location, season, disease, pests, weather conditions, and climate change [National Renewable Energy Laboratory, 2004]. To overcome these limitations, and to make biodiesel more cost-competitive with petroleum diesel, it is important to explore low-cost, nonfood-based lipid feedstocks that are readily available all-year round. Previous studies have evaluated the use of non-edible oil sources such as *Jathropa curcas* [Foidl, et al., 1996], lard [Lee,

et al., 2002], beef tallow [Nelson and Schrock, 2006], and waste cooking oil [Kulkarni and Dalai, 2006] as possible biodiesel feedstock sources. Another potential biodiesel feedstock that meets these criteria is municipal sewage sludge.

Municipal Sewage Sludge as Novel Biodiesel Feedstock

Municipal sewage sludges are gaining considerable attention in the United States and in the world as a potential source of abundant low-cost lipid feedstock for biodiesel production [Kargbo, 2010]. Sewage sludges are solid residues produced during the wastewater treatment process and may contain a significant lipid fraction consisting of adsorbed oils and fats as well as phospholipids contained in the cell membranes of microbial cells [Boocock, et al., 1992; Rittman and McCarty, 2001; Reveille, et al., 2003; Jarde, et al., 2005]. Municipal wastewater treatment plants in the United States produce approximately 7 - 8 million dry tons of sludge annually according to estimates by the US Environmental Protection Agency [U.S. EPA, 1999] and this represents an untapped resource of feedstock for biofuels production. This amount is still expected to increase in the future due to increasing urbanization and industrialization resulting in population growth in urban areas. As of 2008, around 14,780 municipal wastewater treatment facilities were in operation in the United States treating a combined flow of 32.3 billion gallons of wastewater daily [U.S. EPA, 2008]. The majority of these treatment plants employ the activated sludge process which produces significant amounts of sewage sludge as a by-product.

The Activated Sludge Process

The activated sludge process is currently the most widely used technology for municipal and industrial wastewater treatment [Yan, et al., 2007]. It involves the degradation of organic pollutants in the wastewater that constitutes its biochemical oxygen demand (BOD) through aerobic cultivation of the indigenous microorganisms in the wastewater. The microbial community in most municipal wastewaters is a mixed population containing a wide variety of species of bacteria, virus, protozoa, fungi, metazoa, and algae. Among these groups, heterotrophic bacteria mostly belonging to the genera *Pseudomonas, Arthrobacter, Comamonas, Lophomonas, Zooglea, Sphaerotillus, Azobacter, Chormobacterium, Achromobacter, Flavobacterium, Bacillus,* and *Nocardia* are the ones primarily involved in the degradation of organic pollutants in the wastewater [Rittman and McCarty, 2001].

As shown in Figure 1.5, a typical wastewater treatment plant employing the activated sludge system consists of a primary settling tank, aeration tank, and secondary clarifier with a solids recycle and wasting line where two distinct types of sewage sludges, the primary and secondary or activated sludge, are produced [Rittman and McCarty, 2001]. Influent wastewater first enters the treatment plant and undergoes screening, grit removal, and primary clarification. The solids separated from the wastewater during primary clarification are collectively called primary sludge, which consists of floating grease, fecal matter, fibers, and other bulk solids that were not removed during screening. The clarified wastewater influent is then passed through the

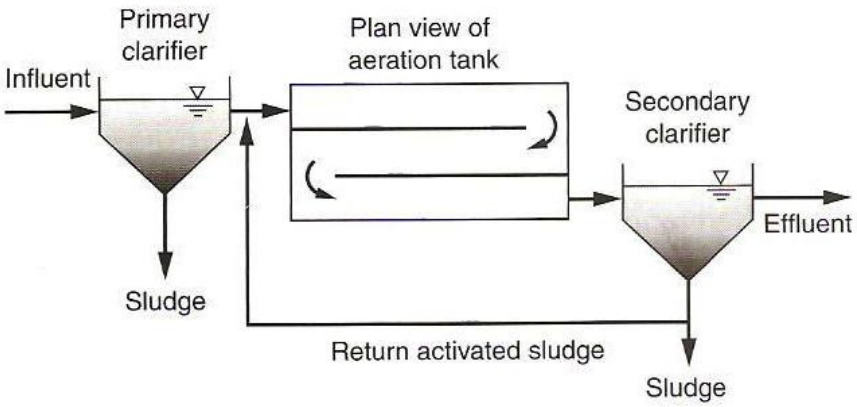

Figure 1.5: Schematic flow diagram of a plug-flow activated sludge process [Tchobanoglous, et al., 2003].

aeration tank or aerobic bioreactor to allow for the cultivation of the indigenous heterotrophic bacteria in the wastewater using the existing levels of organic compounds as carbon and energy source. At the same time, microbial aggregates consisting of live and dead microbial debris and organic suspended solids are produced and are subsequently separated from the wastewater through a secondary clarifier or settling tank. The solids that settle out in the secondary clarifier are what are collectively referred to as *activated sludge.* Part of the activated sludge stream is recycled back to the aeration tank at flow rates typically 50-75 % of the average wastewater flow rate to maintain a sufficient concentration of microorganisms required for a certain degree of treatment; whereas the remainder is wasted and combined with the primary sludge for further treatment and stabilization by aerobic or anaerobic digestion prior to disposal [Tchobanoglous, et al., 2003]. The most common sludge disposal methods for stabilized sludge include incineration, land application, and landfill disposal. However, these disposal practices may result in harmful emissions that contain dioxins and heavy metals

and into the accumulation of heavy metals and toxic organic compounds in soils and groundwater. A viable alternative to these disposal methods and mitigate their negative environmental impacts is to utilize the sludge as a lipid feedstock for biodiesel production given its significant lipid fraction and abundant supply.

Current Status of Lipids/Biodiesel from Sewage Sludge

Despite the obvious advantages, investigating the potential of lipid extraction and/or biodiesel production from sewage sludge has been limited to a few studies. Initial research involving extraction and fractionation of lipids from sewage sludge found a significant amount of lipids suitable for biodiesel production in terms of its fatty acid composition [Boocock, et al., 1992; Boocock, et al., 1992; Konar, et al., 1994; Reveille, et al., 2003; Jarde, et al., 2005]. Studies that involved the actual production of biodiesel from sewage sludge were fairly recent [Dufreche, et al., 2007; Mondala, et al., 2009; Revellame, et al., 2010] and have shown biodiesel yields of 14.5 and between 2-5 % (w/w dry sludge) from primary and activated sludges, respectively using sequential lipid extraction and/or transesterification and *in situ* transesterification. A comprehensive cost estimate which included capital investment costs in addition to production costs put the break even price of sewage sludge biodiesel at $3.23 per gallon assuming a 10 % (w/w dry sludge) biodiesel yield [Mondala, et al., 2009]. Additionally, the fraction of the cost associated with the feedstock was also reduced to 53 % as opposed to 70-85 % when soybean oil is used. These values are desirable compared with cost estimates for soy and yellow grease biodiesel shown in Table 1.1, which do not include capital costs. The major challenge therefore is to make sewage sludge more cost-competitive with

conventional crop oils and animal fats and to further reduce the cost below the $3.00 per gallon mark.

One alternative to accomplish this goal, it is necessary to increase the lipid content of sewage sludge that could be used to produce more biodiesel. Based on initial economic estimates made in a previous paper [Mondala, et al., 2009], it was found that, increasing the biodiesel yield from sewage sludge to 20 % could significantly reduce the cost per gallon of sludge biodiesel to $2.63. Since the lipid content of primary sludge is mainly a result of external factors that are beyond the plant operator's control (i.e., the amounts of oils, fats, and grease dumped into the sewers), it is of interest in this study to increase the lipid content of the microorganisms found in activated sludge in order to suit biofuel production requirements. A potential solution is to apply microbial cultivation techniques that would trigger the biosynthesis of lipidic storage materials within the microbial cells as opposed to cellular multiplication or production of non lipid cellular materials. This phenomenon has been observed in so-called *oleaginous* microorganisms.

Microbial Lipids as Potential Biodiesel Feedstock

The production of microbial lipids, or single cell oils, has been known and studied for over 125 years, with the primary purpose of supplementing edible oils and fats for human consumption. Oleaginous microorganisms are defined as bacteria, yeast, fungi, and algae species capable of accumulating 20-80 % of their biomass as lipids under stress exerted by the limitation of a key nutrient (usually nitrogen) relative to an excess supply of the carbon source [Ratledge, 2005]. Table 1.2 shows a list of representative strains

Table 1.2: Lipid accumulation by different oleaginous microorganisms.

Species	Oil yield (% w/w)	Reference
Microalgae		
Chlorella vulgaris	40	[Illman, et al., 2000]
Botryococcus braunii	21	[Zhila, et al., 2005]
Yeast		
Lipomyces starkeyi	20.4	[Liu, et al., 2000]
Cryptococcus curvatus	37.1 g/L	[Mainul, et al., 1996]
Rhodotorula glutinis	61	
Fungi		
Mucor circinelloides	25	[Wynn, et al., 2001]
Mortierella alpina	40	[Wynn, et al., 2001]
Bacteria		
Rhodococcus opacus	87	[Alvarez and Steinbuchel, 2002]
Pseudomonas aeruginosa	38	[De Andres, et al., 1991]

from different microbial groups that have been known to accumulate large amounts of stored lipids. A generalized explanation as to how these microorganisms accumulate oils is shown in Figure 1.6, wherein during the cultivation process at the time the nitrogen source is depleted and there is a surplus of the carbon source remaining in the culture, the microorganisms utilize the latter in the formation of storage lipid globules as a form of energy storage material in response to an environmental stress (depletion of nitrogen source). However, this explanation is shallow at best, as sequences of biochemical reactions that vary among prokaryotes and eukaryotes occur as a result of nitrogen limitation leading into microbial oil synthesis. The types of storage lipids produced also

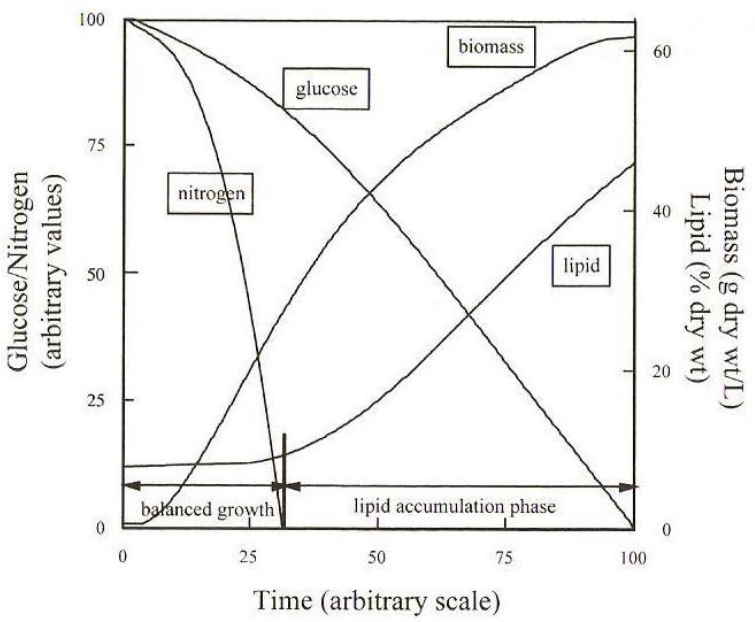

Figure 1.6: Idealized representation of the process of lipid accumulation in oleaginous microorganisms [Ratledge, 2005].

vary between prokaryotes and eukaryotes, as eukaryotes such as yeasts, fungi, and algae synthesize polyunsaturated fatty acid TAG similar to vegetable oil [Losel, 1988; Rattray, 1988; Wood, 1988]. On the other hand, most prokaryotic bacteria tend to manufacture specialized lipids such as polyhydroxyalkanoates (PHAs), glycolipids, lipoproteins, and wax esters [Makula, et al., 1975; O'Leary and Wilkinson, 1988; Wilkinson, 1988; Anderson and Dawes, 1990], although TAG accumulation has been reported in a few bacterial strains to the actinomycetes group such as species of *Mycobacterium, Streptomyces, Rhodococcus,* and *Nocardia* [Brennan, 1988; Alvarez and Steinbuchel, 2002]. A more detailed discussion of the biochemistry of lipid accumulation in oleaginous microorganisms will be provided in the literature review sections.

It was only until recently that microbial oils have been considered as feedstocks for biodiesel production [Dai, et al., 2007; Liu and Zhao, 2007; Li, et al., 2008; Zhu, et al., 2008; Easterling, et al., 2009; Gouveia and Oliveira, 2009; Meng, et al., 2009; Vicente, et al., 2009]. The use of microbial oils for biodiesel production is thought to be more advantageous over vegetable oils and animal fats because of its short life cycle; less labor requirements for production; minimal influence by location, season, and climate; and ease of process scale-up [Li and Wang, 1997].

Lipid Accumulation in Activated Sludge Microbiota

Most of the researches conducted on microbial lipid production have utilized pure cultures of microorganisms. The utilization of mixed cultures such as activated sludge is expected to be more economically favorable than pure culture fermentations since bioreactor sterilization could be considered unnecessary and organic material and nutrients in wastewater can be considered to have a negative cost [Bengtsson, et al., 2008]. Previous studies have indicated the ability of certain members of the activated sludge microbial communities to accumulate cellular storage products such as polyhydroxyalkanoates (PHA), under excess carbon and nutrient-limited conditions in aerobic bioreactors as a reserve source of carbon and energy for survival during stress conditions [Reddy, et al., 2008]. In some cases, activated sludge can also exhibit significant PHA storage capacity under alternating high and low organic loadings or feast and famine conditions in wastewater [Bengtsson, et al., 2008]. Overall, the results of these studies imply the significant influence of wastewater treatment plant conditions on the microbial composition and metabolic activities of the activated sludge microbial

consortium. Population shifts within the activated sludge microbiota may also result from stress conditions such as increasing or decreasing the organic loading of the influent wastewater towards specific microbial groups such as the case of PHA-producing bacteria. The same principle could then be applied in the desire to enhance the lipid content of activated sludge microorganisms for increased biodiesel yield, which to our knowledge has not been attempted before.

Based on these concepts, an innovative strategy for increasing the lipid content of municipal sewage activated sludge was investigated in this study. Figure 1.7 shows the proposed WWTP configuration, where a lipid accumulation and extraction process is installed in a conventional activated sludge process. A portion of the waste activated sludge generated in the primary aeration tank will be used as inocula for cultivation in another similarly-constructed aeration tank designated as the lipid accumulation chamber. Conventional activated sludge bioreactors typically operate under low carbon and nitrogen conditions; hence to theoretically increase the lipid content of activated sludge microorganisms, the lipid accumulation chamber will operate under a high carbon loading and nitrogen-limited conditions (high C:N ratio). Part of the primary-treated wastewater stream will also be diverted into the lipid accumulation chamber and supplemented with nutrients and sugars for use as the cultivation medium. The generated sludge biomass with high oil content will then be settled, dewatered, and subjected to lipid extraction procedures. This novel approach in wastewater utilization is advantageous due to the large volumes of wastewater, which contains carbon, nitrogen, phosphorus, and other nutrients required for microbial growth, generated daily in the United States amounting to around 33 billion gallons per day [U.S. EPA, 2008].

Wastewater then could serve as an excellent cultivation media for microorganisms due to its nutrient content. Wastewater microorganisms will be able to produce high-value products such as lipids for biodiesel production. Most of the initial studies involving oleaginous microorganisms used glucose as the carbon source. However, in order to reduce costs and maintain environmental sustainability, sugars derived from the hydrolysis of low-cost waste lignocellulose biomass are considered as an alternative carbon and energy source for the aerobic cultivation and lipid production of activated sludge microorganisms.

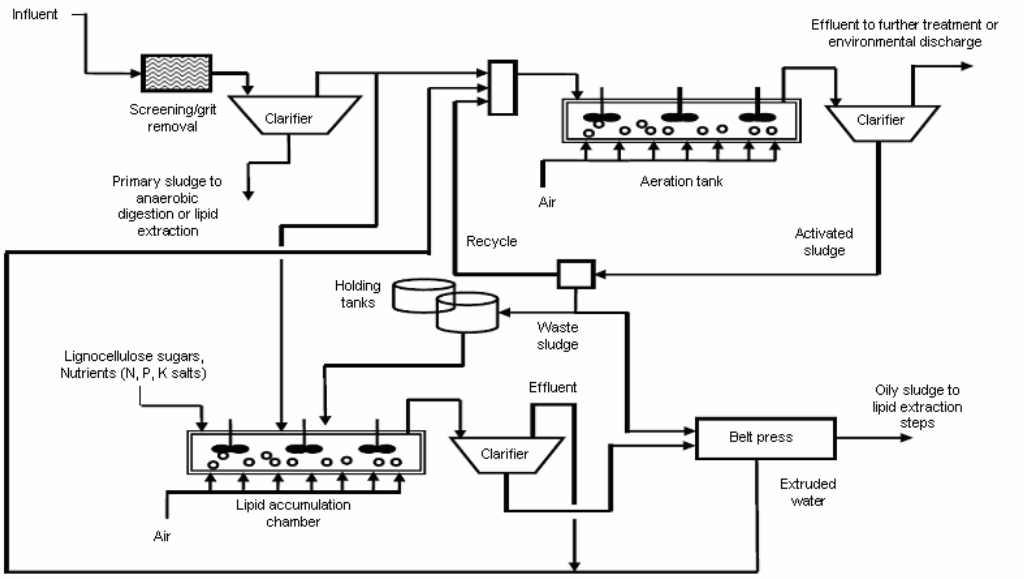

Figure 1.7: Proposed municipal wastewater treatment plant concept for the enhancement of lipid and biodiesel yields from sewage sludge.

Lignocellulose as Substrate for Microbial Lipid Production

Introduction to Lignocellulose

Lignocellulose biomass is a biopolymer composed mainly of: (1) Cellulose, which is a linear polymer of D-glucose units linked by 1,4-β-D-glycosidic bonds; (2) Hemicellulose, which is a heterogeneous polymer of pentose sugars such as xylose and arabinose; hexose sugars such as mannose, glucose, and galactose; and uronic acids; and (3) Lignin, which is a mainly a macromolecule composed of aromatic and phenolic units [Zaldivar, et al., 2001]. Figure 1.8 shows the molecular structures of these three main components. It can be seen that there is an abundance of sugar residues that can be utilized for fermentation processes; however the complexity of its macromolecular structure renders this difficult. Prior to being used as fermentation substrates by microorganisms, lignocellulose biomass materials need to undergo pretreatment and hydrolysis. These include physical methods such as hot water treatment, steam pressure, steam explosion, and supercritical CO_2 explosion; chemical methods such as acid- or base hydrolysis, treatment with organic solvents and water, or enzymatic hydrolysis; or a combination of these methods [Claassen, et al., 1999].

Figure 1.9 shows the relative percentages of its main components and the potential degradation/hydrolysis products of each fraction, which includes hexose sugars such as glucose, mannose, and galactose; and pentose sugars such as xylose and arabinose, both of which are liberated via degradation of the cellulose and hemicellulose components of lignocellulose. These free sugars can then be more readily utilized by microorganisms in fermentation processes. In addition to sugars, several degradation by-

product compounds are also produced during hydrolysis. These compounds include sugar degradation products such as furfural from xylose, and 5-hydoxymethylfurfural from glucose; organic acid such as acetic acid from the acetyl groups, formic acid from xylose oxidation, and levulinic acid from glucose oxidation; and lignin degradation products such as vanillin, syringaldehyde, and 4-hydroxybenzaldehyde [Chen, et al., 2009].

The composition of lignocellulose hydrolyzates in terms of sugars and degradation products depends heavily on the type of biomass used as well as the type and conditions of pretreatment and hydrolysis as shown in Table 1.3. In most lignocellulose hydrolyzates, xylose concentrations are higher than glucose since hemicelluloses are easier to degrade than cellulose. Increasing the severity (concentration of acid coupled with residence time) of the hydrolysis reaction could increase glucose yield but at the same time increase the concentration of the degradation products. Acetic acid and furans (furfural and 5-hydroxymethylfurfural) are also the most commonly produced degradation by-products, while lignin-derived substances (phenolic compounds) are normally found in concentrations well below 0.1 mM. As it will be discussed in later chapters, these compounds have been found to exert inhibitory effects on the growth and metabolism of microorganisms such as bioethanol-producing yeasts [Chung and Lee, 1985; Boyer, et al., 1992; Taherzadeh, et al., 1997; Palmqvist, et al., 1999; Zaldivar and Ingram, 1999; Keating, et al., 2006; Wikandari, et al., 2010], and more recently on oleaginous microorganisms [Chen, et al., 2009; Hu, et al., 2009; Huang, et al., 2009]. In addition to determining the effects of the inhibitory effects of lignocellulose degradation by-products, the potential of utilizing pentose sugars such as xylose as carbon and energy source instead of glucose has also been investigated due to the fact that xylose usually

occurs in hydrolyzates at relatively higher concentrations than glucose at less severe hydrolysis conditions. The use of xylose for bioethanol production by yeasts [Hahn-Hagerdal, et al., 2007] has been considered as well as in the production of microbial lipids [Evans and Ratledge, 1983; Dai, et al., 2007; Kong, et al., 2007; Zhao, et al., 2008].

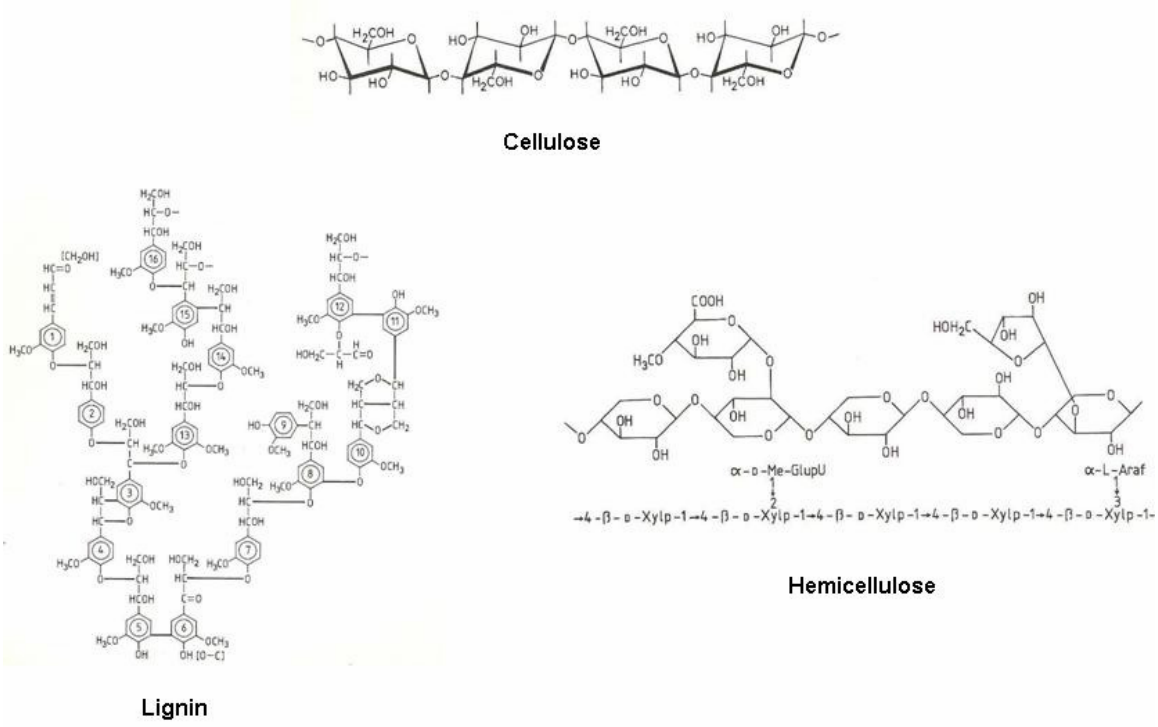

Figure 1.8: Molecular structures of cellulose, hemicellulose, and lignin [Fengel and Wegener, 1984]

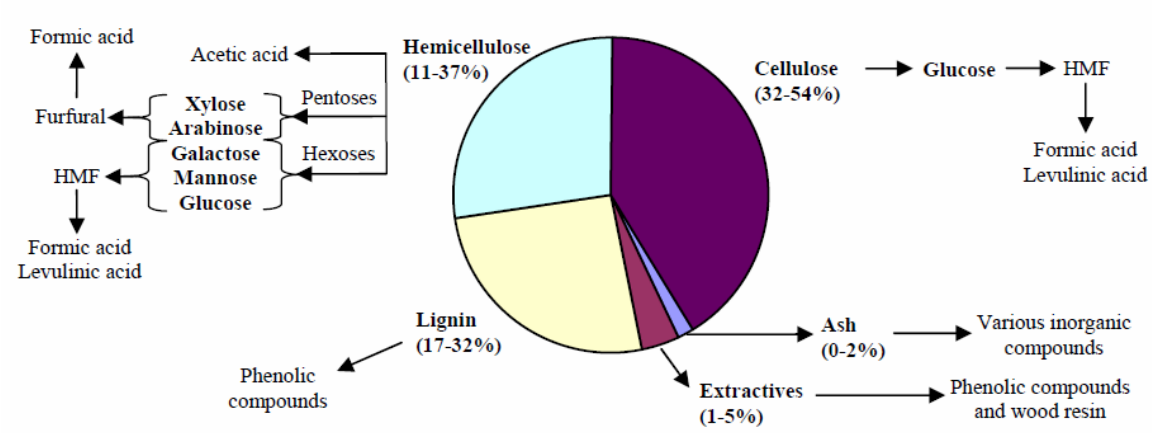

Figure 1.9: Composition of lignocellulosic materials and their potential degradation products [Taherzadeh and Karimi, 2007].

Table 1.3 Concentration (g/L) of hydrolysis products of some lignocellulose biomass.

Component	Sugarcane bagasse[1]	Spruce residue[2]	Corn stover[3]
Glucose	2.6	19.15	6.27
Xylose	49.5	7.25	24.96
Mannose	-	15.88	†
Galactose	-	3.25	†
Arabinose	4.5	1.42	†
Fructose	-	-	†
Sucrose	-	-	†
Cellobiose	-	-	†
Acetic acid	4.5	2.8	6.09
Furfural	0.01	0.95	0.63
5-hydroxymethylfurfural	0.09	1.34	0.76

[1]Using 100 mg H_2SO_4/g solids at 140 °C, 20 min [Carvalho, et al., 2004].
[2]Two-stage acid hydrolysis using 5g/L H_2SO_4, 30 % (w/w) solids [Nilsson, et al., 2001].
[3]Average values based on H_2SO_4 concentration, 0.5-1.41 % w/w; temperature, 165- 183 °C; residence time, 3-12 min; and solids loading, 20 % w/w [Schell, et al., 2003; Agbogbo and Wagner, 2007].
†Not reported.

Current Status of Lignocellulose Biomass

Lignocellulose biomass presents an abundant and renewable resource for biofuels production that has not been extensively utilized as fermentation substrates. It has been estimated that lignocellulose accounts for nearly 50 % of all the biomass in the world, which is approximately 10-50 billion dry tons [Claassen, et al., 1999]. Examples of lignocellulose biomass materials that are being investigated as fermentation substrates for biofuel applications are agricultural wastes such as wheat straw, corn stover, and sugarcane bagasse; pulp and paper wastes; forestry residues; energy crops such as switchgrass and bermuda grass; and municipal solid wastes such as used paper, cardboard, yard trash, and discarded wood products [Zaldivar, et al., 2001; Saha, 2004]. In the United States, the total annual production of agricultural crop residues was estimated to be 1.3 million tons [Lal, 2004]. Furthermore, corn stover production in the U.S. was estimated to 82 million dry tons based on the annual corn production data [Kadam and McMillan, 2003].

Due to its abundance, non-food origin and uses, and low cost, lignocellulose biomass has been largely tapped to replace food crops such sugarcane and corn grains and starch as the major feedstocks for the production of bioethanol [Zaldivar, et al., 2001]. Numerous researches have been conducted to optimize lignocellulose pretreatment and hydrolysis conditions to maximize sugar yield and minimize degradation by-products yield, including hydrolyzate detoxification [Taherzadeh, et al., 1997; Palmqvist, et al., 1999; Carvalho, et al., 2004; Agbogbo and Wagner, 2007; Jensen, et al., 2008]. Other studies have investigated the improvement of lignocellulose fermentation processes [Taherzadeh, et al., 1999a; Nilsson, et al., 2001; Petersson and Liden, 2007], screening of

microbial strains tolerant to inhibitory degradation by-products [Keating, et al., 2006; Chen, et al., 2009], and genetic and metabolic engineering of microorganisms [Zaldivar, et al., 2001]. However, studies on the utilization of lignocellulose biomass hydrolyzate as substrates for oleaginous microorganisms under the stress and inhibition applied by lignocellulose degradation by-products are very limited; much less the use of these substrates by activated sludge microorganisms for oil production which has yet to be studied.

CHAPTER II

RESEARCH OBJECTIVES

Statement of the Problem

The main motivation for this work was to improve the value and cost-competitiveness of municipal sewage sludge as a source of feedstock lipids for biodiesel production by increasing its intracellular lipid content, especially its saponifiable fraction. A microbiological approach was taken in the attempt to solve this problem, specifically the utilization of the microbial community in municipal sewage activated sludge for the production of large amounts of microbial lipids via aerobic fermentation. In the desire to minimize production costs and maintain environmental sustainability, the use of lignocellulose biomass hydrolyzates as the carbon and energy source for the activated sludge microorganisms was proposed. However, previous studies utilizing lignocellulose hydrolyzates in fermentations indicated anti-microbial and inhibition effects on the growth and metabolism of microorganisms that are fed the hydrolyzate; hence their effects on activated sludge microorganisms must also be considered.

In attempting to solve this problem, the following constraints were set:

1. The aerobic fermentation process must be performed with minimal environmental controls in order to clearly observe the natural response of the activated sludge

microbiota as it would if the process were to be applied large scale municipal wastewater treatment plants;

2. Nutrients such as nitrogen and phosphorus required for bacterial growth will originate solely from wastewater media;
3. Activated sludge inocula must not undergo any prior culture enrichment process, and must be added to the culture as is; and
4. No prior detoxification of the lignocellulose hydrolyzate must be made. The hydrolyzate must contain the degradation by-products in actual concentration levels that result from pretreatment or hydrolysis. Hence, additional costs for substrate processing can be avoided.

Hypothesis

The guiding hypothesis formulated for this work was aerobic cultivation of activated sludge microorganisms in wastewater under the stress condition of high carbon-to-nitrogen ratio and substrate loading result into the production of sludge biomass with significantly higher lipid content and biodiesel yield than raw activated sludge. By supplementing the wastewater with a sufficiently high amount of sugars, excess carbon and nitrogen-limited conditions conducive for the shift in microbial population in activated sludge towards lipid-producers or the activation of enzymes involved in lipid biosynthesis within the existing microorganisms in the sludge will be established. Initially, glucose was used as the substrate due to its extensive use in numerous microbial lipid studies and also due to the fact that it is the major precursor of glycolysis and other important biochemical pathways related to lipid biosynthesis. Hexose (i.e., glucose) and

pentose (i.e., xylose) sugar mixtures obtained via lignocellulose biomass degradation will also be utilized by the activated sludge microorganisms for enhanced oil accumulation, and this could lead to a reduction in costs of the lipid product. Additionally, activated sludge microbiota would be able to tolerate the presence of degradation by-products (inhibitors) present in lignocellulose hydrolyzate along with sugars either through co-utilization or detoxification. Furfural and acetic acid were chosen as representative inhibitory compounds due to their high abundance relative to other degradation by-products and the extensive amount of literature regarding their inhibitory mechanisms and effects on pure cultures of ethanol- and oil-producing yeasts and bacteria. It is envisioned that this research will provide fundamental knowledge on the response of the activated sludge microbiota in terms of cell growth, lipid accumulation, substrate utilization, and microbial diversity when subjected to manipulated conditions of C:N ratio and carbon loading in aerobic bioreactors. Additionally, this research is expected to generate kinetic data in terms of growth, lipid production, and substrate utilization rates, as well as substrate affinity and inhibition constants that will be necessary for large-scale process engineering and equipment design for incorporation in existing municipal wastewater treatment plant configurations.

Goals and Objectives

The overall goal of this research was to determine the feasibility of applying an aerobic fermentation process with activated sludge microbial communities utilizing lignocellulose hydrolyzate as carbon and energy source for the enhancement of lipid and biodiesel yields from municipal sewage sludges. This overall goal has been further divided into three specific objectives:

Specific Objective 1: Evaluation of activated sludge microbiota for lipid accumulation via fermentation of glucose

The capability of activated sludge microorganisms for oil accumulation was first evaluated via batch aerobic cultivation experiments using glucose as the sole carbon and energy source. Glucose was initially used as the substrate due to its extensive use in fermentation studies and its being the precursor in glycolysis and other important biochemical pathways involved in growth and metabolism of microorganisms. Experiments were conducted to determine the effect of the initial carbon-to-nitrogen ratio (C:N) and substrate loading on sludge biomass production and cellular lipid content. This was done to determine the optimum C:N ratio and glucose loading for maximum lipid production by activated sludge microorganisms and to generate kinetic data and mathematical model parameter values on cell growth, lipid accumulation, and sugar consumption using glucose as the sole carbon and energy source. The kinetic model parameters that were of interest were the maximum specific growth rate and lipid yield with respect to biomass and sugar consumption. The product lipids were then characterized in terms of its saponifiable fraction and fatty acid profile to determine

applicability for biodiesel production. These data were used as a baseline for comparison with activated sludge fermentations that utilized lignocellulose hydrolysis products. Results of the initial glucose fermentation experiments with activated sludge microorganisms can be found in Chapter VI which is preceded by a discussion of fermentation kinetic modeling theory in Chapter V.

Specific Objective 2: Evaluation of lignocellulose hydrolyzate as carbon and energy source for lipid accumulation by activated sludge microbiota

In addition to glucose fermentation, the ability of activated sludge microorganisms to utilize lignocellulose hydrolyzate containing pentose sugars and degradation by-products was assessed. Batch activated sludge cultures were fed with artificially-prepared mixture of lignocellulose hydrolysis products containing the following representative compounds: glucose for hexose sugars, xylose for pentose sugars, and acetic acid and furfural for degradation by-products. An artificial mixture was chosen over an actual biomass hydrolyzate in order to have a uniform substrate composition. Moreover, these compounds were chosen for their relatively higher reported concentrations in most lignocellulose biomass hydrolysis studies. First, experiments were conducted to investigate the effects of acetic acid and furfural on sludge lipid content, saponifiable fractions, fatty acid composition, and fermentation kinetics of activated sludge microbiota individually and in binary mixtures with experimental low and high levels and relative to control runs (no inhibitor). The results of this study can be found in Chapter VII. Experiments were also conducted to determine the effect and kinetics of hexose and pentose sugar co-fermentation using glucose and xylose, and the findings can be found in Chapter VIII. The effect of different fermentation modes namely batch, fed-

batch, semi-continuous, and continuous utilizing the artificial lignocellulose hydrolyzate as substrate was also studied with the objective of attaining a maximum lipid yield and sugar conversion to lipids and the results are presented in Chapter IX.

Specific Objective 3: Compositional analysis of activated sludge microbial community applied in lipid accumulation process

The variation in the composition of activated sludge microbial community as it was applied in fermentation processes for lipid accumulation was also studied. Using DNA extraction and 16S rRNA sequence analysis techniques, the identities and relative abundance of specific bacterial groups at different time points in the fermentation processes were obtained. The results were correlated with fermentation kinetic data in order to identify possible oil-producing microbial groups in activated sludge for future isolation and enrichment. The findings of this study are presented in Chapter X.

For all the chapters in this document corresponding to the different phases of the study, a general experimental procedure and analytical protocol was implemented as discussed in Chapter IV (Materials and Methods). However, specific experimental designs were used for each chapter depending on the objective/s it sought to satisfy.

CHAPTER III

LITERATURE REVIEW

Lipid Production by Oleaginous Microorganisms

Lipid Types and Composition

Under conditions of stress particularly starvation conditions, certain microorganisms respond by producing some type of energy storage materials such as lipids to be used for their continued growth and metabolism until favorable conditions have been restored. One example is oleaginous microorganisms. Triacyglycerols (TAG) is known to be the principal form in which lipid is accumulated in oleaginous yeasts under the stress of nitrogen-limitation, while other lipid classes such as phospholipids comprise less than 10 % of the oil produced [Davies and Holdsworth, 1992]. In oleaginous fungi such as *Mucor cicinelloides* however, free fatty acids and phospholipids comprise 32 and 21 % of the total lipids, respectively as opposed to TAG, which comprised around 14 % [Vicente, et al., 2009]. Many algal species have also been shown to accumulate substantial amounts of neutral lipids (20-50 % w/w), majority of which is TAG [Hu, et al., 2008].

On the other hand, many prokaryotes (bacteria) synthesize polymeric lipid, such as polyhydroxyalkanoates (PHA) under nutrient starvation conditions, whereas accumulation of wax esters and TAG accumulation are limited to a few bacteria [Alvarez

and Steinbuchel, 2002]. Wax esters as energy storage compounds were speculated to be widespread in bacteria belonging to the genus *Acinetobacter* while TAG biosynthesis has been detected only in aerobic heterotrophic bacteria and cyanobacteria, specifically the actinomycetes group including the genera *Streptomyces, Nocardia, Rhodococcus, Mycobacterium, Dietzia,* or *Gordionia.* To date, *Rhodococcus opacus* is the only bacteria in its native form shown in literature that is able to accumulate more than 20 % of its biomass as lipids, producing as high as 87 % (w/w) lipids containing TAG [Alvarez, et al., 1996]. However the extensive body of knowledge already available regarding the expressions of genes in fatty acid synthesis makes it relatively easy to apply genetic and metabolic engineering to modify bacterial performance in oil accumulation [Li, et al., 2008]. For instance, there is a report on direct fatty acid ester synthesis by a metabolically engineered *E. coli* using renewable carbon sources [Kalscheuer, et al., 2006].

Table 3.1 shows the relative fatty acid compositions of lipids extracted from various oleaginous microorganisms in comparison with animal (tallow) and plant (soybean) oil sources. In all the oleaginous microorganism types, the majority of fatty acids synthesized have chain lengths that range from C_{16} to C_{18}. Palmitic (C16:0) and oleic (C18:1) acids constitute the majority of these fatty acids among the representative yeast, fungi, and bacterial strains. These are similar to tallow and soybean oil, with the exception of linoleic acid (C18:2) in soybean oil, which constitutes about half of the fatty acids. On the other hand in the representative algae, linoleic (C18:2) and linolenic (C18:3) levels match or even surpass those of oleic acid.

Table 3.1: Relative fatty acid composition of oils from different sources, % of total fatty acids.

Source	Fatty acids						
	C16:0	C16:1	C18:0	C18:1	C18:2	C18:3	Others
Yeasts[a]							
Lipomyces starkeyi	33	4.8	4.7	55.1	1.6	-	-
Rhodotorula glutinis	18	1	6	60	12	2	-
Rhodosporidium toruloides	24.3	1.1	7.7	54.6	2.1	-	-
Fungi[b]							
Mucor circinelloides	20	2.3	2	37	14.3	18.5	2
Bacteria[c]							
Rhodococcus opacus	16.8	5.9	2.8	73.8	-	-	-
Algae							
Botryococcus braunii[c]	19.1	0.9	4.8	24.4	8.4	19.0	15.4
Chlorella sorokiniana[d]	40	4.0	-	5	36	23	32
Tallow[e]	26	3.5	19.5	40	4.5	-	3
Soybean oil[f]	11.8	-	4	25	55.4	3.8	Tr

(-): Not detected or measured. Tr: Trace.
[a][Li, et al., 2008].
[b][Vicente, et al., 2009]
[c][Zhila, et al., 2005].
[d][Patterson, 1970]
[e][Alvarez and Steinbuchel, 2002].
[f][Ferrari, et al., 2005].

Biochemistry of Lipid Biosynthesis

A common intrinsic requirement for lipid accumulation to occur in all oleaginous microorganism types (yeasts, fungi, bacteria) is an excess of carbon over a limiting nutrient, usually nitrogen. In batch cultures, there will be an initial period of cell proliferation in the presence of sufficient nitrogen. This is then followed by an increase in lipid content and cessation of cell growth initiated by exhaustion of the limiting nutrient. The excess carbon supply is used to accumulate lipids for carbon and energy storage. It

has also been observed that oleaginous microorganisms can mobilize the stored lipids as a carbon source should nitrogen becomes available again in the media [Holdsworth and Ratledge, 1988]. However, nitrogen depletion is only a trigger for the underlying cascade of biochemical reactions leading to lipid biosynthesis, which is discussed in this section. Although other lipid classes (i.e. phospholipids) that can also be utilized to produce biodiesel are also produced by these microorganisms, this discussion will be limited to the series of biochemical events that lead to the biosynthetic pathways of fatty acids and triacylglycerols (TAG). These biochemical pathways will not be discussed here in detail and for more specific information regarding enzyme structures, functions, and reaction mechanisms, the reader is referred to any standard college biochemistry textbook for consultation.

Eukaryotes

The following discussion outlines the possible biochemical mechanisms leading to fatty acid and TAG biosynthesis in eukaryotes (i.e. yeasts, fungi, and algae) as described by previous papers [Davies and Holdsworth, 1992; Wynn, et al., 2001; Ratledge, 2002; Ratledge and Wynn, 2002; Hu, et al., 2008]. Fatty acid and TAG synthesis has been established as a cytosolic process employing acetyl-coenzyme-A (acetyl-CoA) as the key intermediate and occurs in the following steps: (1) intermediate metabolism to produce cytosolic acetyl-CoA; (2) fatty acid biosynthesis; (3) formation of glycerol intermediates; and (4) sequential esterification of the glycerol moiety with fatty acyl residues [Davies and Holdsworth, 1992; Alvarez and Steinbuchel, 2002].

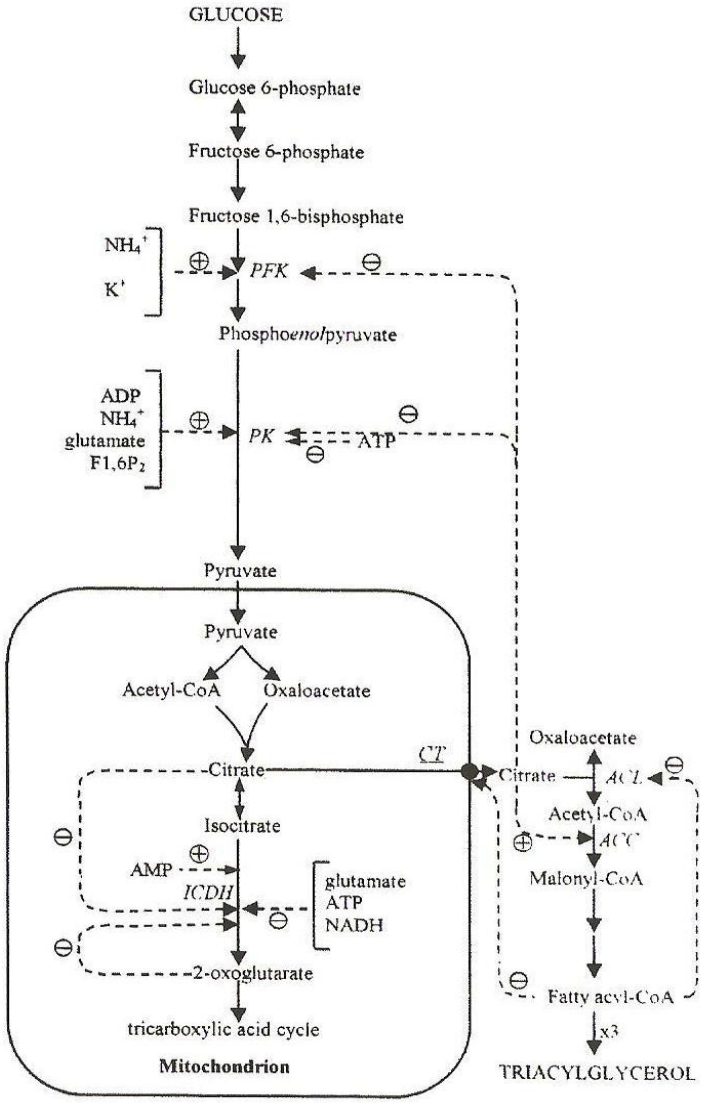

Figure 3.1: Outline of the main sequence of events leading to lipid accumulation in oleaginous yeasts and molds [Ratledge and Wynn, 2002].

The acetyl-CoA building blocks needed for TAG biosynthesis originate mainly from glycolysis (Figure 3.1) and pentose phosphate pathway, which produce pyruvate and release them in the cytosol. Pyruvate is then converted to acetyl-CoA via acylation of coenzyme-A in the pyruvate decarboxylation process:

$$\text{pyruvate} + \text{NAD}^+ + \text{CoA-SH} \xrightarrow[\text{dehydrogenase}]{\text{pyruvate}} \text{acetyl CoA} + \text{CO}_2 + \text{NADH} + \text{H}^+ \qquad (3.1)$$

The acetyl CoA produced either enters the TCA cycle or is transported in the form of acetyl carnitine via mediation by the enzyme carnitine acetyl transferase to the cytosol for fatty acid synthesis.

It has been understood that nitrogen limitation is the main trigger for lipid accumulation and this initiates a sequence of biochemical events as shown in Figure 3.1. Nitrogen source depletion in the media causes the reduction of intracellular NH_4^+, which is an activator of the phosphofructokinase (PFK) enzyme in glycolysis. This leads to a reduced carbon flux in the glycolytic pathway, which will limit adenosine triphosphate (ATP) production and reduce the energy charge within the cell, resulting into the activation of the AMP deaminase. The AMP deaminase then converts AMP into inosine monophosphate (IMP) and ammonium probably to provide an emergency source of nitrogen for the cells:

$$AMP \xrightarrow{\text{AMP deaminase}} IMP + NH_4^+ \qquad (3.2)$$

The drop in AMP concentration then leads to a decrease in NAD^+:isocitrate dehydrogenase (ICDH) activity due to the fact that this enzyme's activity is completely dependent on AMP. Loss of this activity leads to a build-up of isocitrate, which equilibrates with citrate via the aconitase enzyme, thus enabling citrate to accumulate in the mitochondrion. The citrate is then transported back to the cytosol via a stoichiometric exchange of citrate in the mitochondrion and malate in the cytosol mediated by a specific tricarboxylate carrier. The malate that is transported into the cytosol is thought to be converted back to pyruvate via the action of malic enzyme, thereby generating nicotinamide adenine dinucleotide phospate (NADPH) for use in fatty acid synthesis.

Although malic enzyme occurs in a wide range of oleaginous and non-oleaginous fungi and yeasts it is considered an essential enzyme for lipid biosynthesis, being an absolute requirement for fatty acid biosynthesis as the sole source of NADPH for the action of the fatty acid synthase (FAS) enzyme [Ratledge, 2002]. Perhaps the most important factor that delineates oleaginous and non-oleaginous microorganisms is the presence of the ATP:citrate lyase enzyme in the former. The ATP:citrate lyase (ACL) enzyme is a cytosolic enzyme whose action yields an increased cytosolic pool of acetyl-CoA precursors for enhanced fatty acid and TAG biosynthesis [Davies and Holdsworth, 1992; Ratledge and Wynn, 2002].

De novo fatty acid biosynthesis occurs through the sequential catalysis of the two enzyme systems mentioned above: acetyl-CoA carboxylase (ACC) and fatty acid synthetase (FAS) [Schweizer, 1989]. The priming reaction for fatty acid synthesis is catalyzed by ACC as summarized in the reaction:

$$\text{Acetyl-CoA} + HCO_3^- + \text{ATP} \xrightarrow{\text{ACC}} \text{Malonyl-CoA} + P_i \qquad (3.3)$$

Biosynthesis of long-chain fatty acids from acetyl-CoA and malonyl-CoA is catalyzed by the FAS multi-enzyme complex. In most organisms, palmitate is the major fatty acid produced from which all other long-chain fatty acids, including unsaturated, hydroxy acids, and longer-chain acids are derived. The overall reaction for the biosynthesis of palmitate is:

$$\begin{aligned} &\text{Acetyl-CoA} + 7\text{Malonyl-CoA} + 14\text{NADPH} + 14H^+ \\ &\qquad\qquad \downarrow FAS \\ &\text{Palmitate} + 8\text{CoA-SH} + 7CO_2 + 6H_2O + 14\text{NADP}^+ \end{aligned} \qquad (3.4)$$

Although majority of studies investigating TAG biosynthesis in yeasts involve non-oleaginous strains such as *Saccharomyces cerevisiae,* there have been a few reports that TAG biosynthesis in both oleaginous and non-oleaginous strains occur via the α-glycerol phosphate pathway [Davies and Holdsworth, 1992]. As shown in Figure 3.2, this involves two sequential acylation of α-glycerol phosphate (more commonly known as derived from glycerol to yield phosphatidic acid (PA), which is considered to be the key precursor to TAG biosynthesis. The biochemical pathways for glycerol biosynthesis in microbial cells have been described extensively in previous studies and most college biochemistry textbooks, hence is not discussed here. Figure 3.2 also shows that PA can also be formed via direct acylation of dihydroxyacetone phosphate (DHAP). The PA is then converted to DAG via phosphatidic acid phosphatase (PAP)-catalyzed dephosphorylation. Diacylglycerol is then converted to TAG via catalysis by the diacylglycerol acyltransferase (DAGAT) enzyme. In all these steps, fatty acids (in the form of fatty acyl-CoA) derived from *de novo* synthesis are incorporated into the intermediates leading to TAG.

Bacteria

As mentioned earlier, biosynthesis and accumulation of fatty acids and TAG in bacteria under N-limited conditions has been detected only in some aerobic heterotrophs and cyanobacteria. The few papers that deal with bacterial TAG accumulation contends that the process follows similar biochemical pathways (Figure 3.1 and 3.2) as with oleaginous yeasts and fungi [Alvarez and Steinbuchel, 2002]. TAG accumulation was shown to occur mostly in the stationary growth phase, since during the exponential phase,

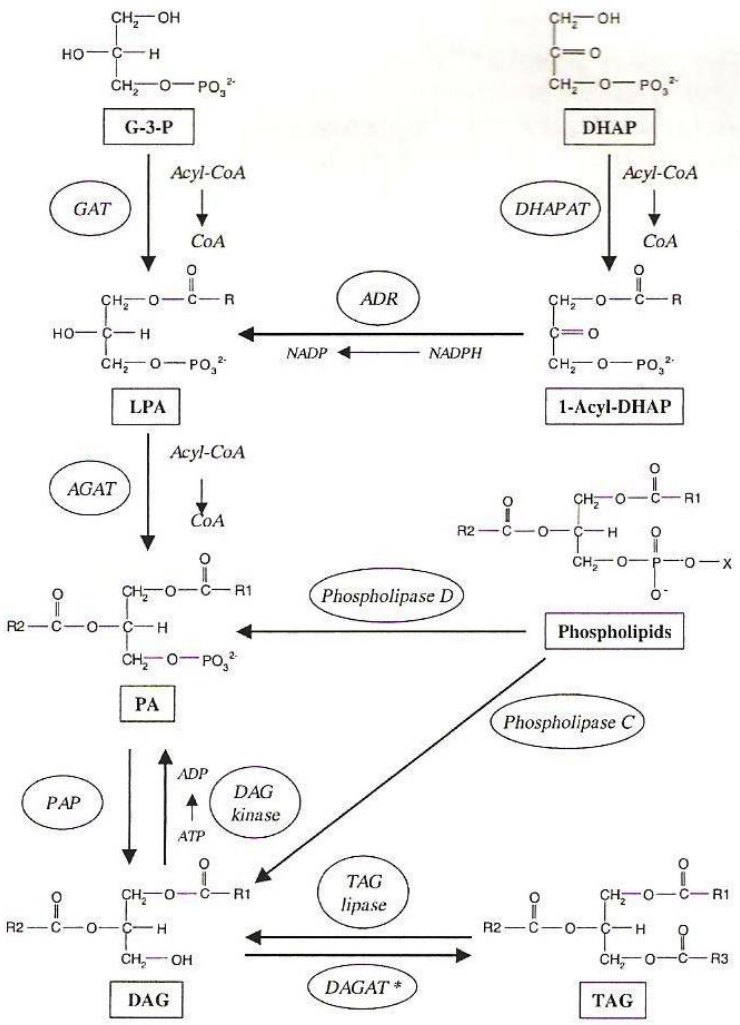

Figure 3.2: Biochemical pathways leading to triacylglycerol (TAG) biosynthesis in *Saccharomyces cerevisiae* [Sorger and Daum, 2003].

the synthesized fatty acids are probably used mostly for the synthesis of phospholipids, which are essential for cell proliferation [Alvarez, et al., 2000]. It has been shown that diacylglycerol acyltransferase (DAGAT) is the primary enzyme responsible for the switch from phospholipid to TAG biosynthesis and its activity has been reported to increase five-fold during the stationary phase as opposed to the exponential phase and

decreased in older cultures concomitant with the increase in TAG hydrolase activity [Olukoshi and Packter, 1994].

A notable situation with regards to storage lipid formation in bacteria is the simultaneous accumulation of PHA and TAG as observed in *Rhodococcus ruber* and similar species [Alvarez, et al., 2000]. Accumulation of PHA occurs during the exponential growth phase even in the presence of ammonium and reaches a maximum when the cells have consumed the nitrogen source completely. Subsequently, TAG biosynthesis and accumulation happens, wherein in this stage, PHA and TAG biosynthesis pathways compete for the common precursors acetyl-CoA and propionyl-CoA, which are used in the late stationary phase preferentially for TAG production.

Effect of Process Conditions

Carbon Source

The type and concentration of organic compounds, which provide sources of carbon, nitrogen (usually in the form of ammonium ions), and other nutrients in cultivation media has been repeatedly shown to influence lipid contents and composition in oleaginous microorganisms. Research on the effects of various carbon sources ranging from pure sugars to food processing wastes and lignocellulose biomass have been particularly important due to the substrate's major contribution to microbial oil production costs and the desire to enhance the cost-competitiveness of microbial oils for biodiesel feedstock uses by using renewable carbon sources.

Glucose is perhaps the most widely used and studied substrate for most microbial fermentations, including oil production from oleaginous microorganisms. Glucose can be

utilized rapidly and efficiently by most oleaginous yeasts through the glycolytic pathway. Theoretical calculations indicated that 33 g of lipids can be produced from 100 g of glucose, assuming that glucose is not used for the synthesis of other cellular materials. However, in actual practice fat coefficients rarely exceed 22 g/100 g glucose [Ratledge, 1982]. Numerous studies suggest that the efficiency of glucose conversion to lipids relative to other sugars is dependent upon microbial type and strains. In batch cultures of the yeast *Candida curvata* utilizing a pool of carbohydrates consisting of glucose, sucrose, lactose, xylose, and ethanol, it has been found that use of lactose resulted in the highest biomass yield (12.5 g/L and 42.2 g/g substrate utilized) whilst xylose was favorable for maximum lipid production (47.6 % cell dry weight and 17.4 g/g substrate utilized) [Evans and Ratledge, 1983]. In continuous cultures using the same yeast, the use of lactose resulted into maximum biomass (18 g/L and 60 g/100 g substrate) and lipid (31 % cell dry weight and 18.6 g/100 g substrate) yields at a dilution rate of 0.04/h. Similar results were obtained from the fungi *Cunninghamella echinulata* and *Mortierella isabelina*, wherein glucose favored the maximum production of mycelial mass (15 g/L for *C. echinulata* and 27 g/L for *M. isabelina*) while xylose induced the maximum accumulation of lipids (65.5 % for *C. echinulata* and 57.7 % for *M. isabelina* in mycelial dry mass basis) [Fakas, et al., 2009]. In addition to these, co-fermentation of glucose and xylose proved to be beneficial for lipid accumulation of the yeast *Lipomyces starkeyi*, which reached a maximum lipid content of 61 % w/w dry cell mass [Zhao, et al., 2008].

Aside from simple sugars, complex carbohydrates such as starch have been utilized for growth and lipid accumulation by oleaginous yeasts such as *L. starkeyi,* which produced a lipid yield of 24 % w/w dry biomass [Guerzoni, et al., 1985], and a

mixed culture of *Saccharomyces fibuliger* and *Rhodosporidium toruloides*, which has been grown in starch with a maximum lipid productivity of 0.28 g/L·h [Dostalek, 1986]. However, these studies required the acid or enzymatic (amylase) hydrolysis of starch. Other complex sugar sources that have been investigated: Whey, which contains 5 % sugars that is mostly lactose and nitrogen and mineral components, making is appropriate for substrate use without further nutrient supplementation [Ykema, et al., 1989]; and molasses, which contains around 50 % fermentable sugars that is mostly sucrose [Woodbine, 1959].

Alkanes and crude oil fractions have also been utilized as sole carbon sources for microbial lipid accumulation, such as in study involving a yeast *Candida* sp that utilized an alkane mixture (22% dodecane, 48 % tetardecane, 28 % tetradecane) achieved biomass and fatty acid yields of 60 and 21 g/L, respectively [Ratledge, 1968]. The use of alkanes was also found to have a greater influence on the fatty acyl composition of the microbial lipids produced by *Candida* sp. than with sugars. At the end of the lipid accumulation phase, 54 % of the total fatty acids produced during cultivation with the alkane mixture were shorter in chain length than palmitate (C16:0), whereas with glucose, less than 2 % were short chain fatty acids.

In addition to these, low cost carbon sources for microbial lipid production have been investigated. Some examples include crude glycerol obtained as a by-product of biodiesel production [Meesters, et al., 1996; Fakas, et al., 2009], sweet potato processing wastes [Du, et al., 2007], and pretreated sewage sludges [Angerbauer, et al., 2008]. Apart from these supposedly cheap carbon sources, much attention has been given to the utilization of lignocellulose biomass as a source of fermentable sugars for use by lipid-

accumulating microorganisms. A more detailed discussion on lignocellulose biomass utilization for microbial oil production is provided in a later section.

Carbon-to-Nitrogen Ratio

The carbon-to-nitrogen ratio (C:N) of the cultivation media appears to be the most important factor affecting storage lipid accumulation in oleaginous microorganisms. Batch fermentation processes involving these microorganisms generally involves two phases: a growth phase, and a lipid-accumulating phase, which is triggered by the exhaustion of the nitrogen source. Hence, a high C:N (mass or mole) ratio, wherein the amount of carbon source supplied is greater than the stoichiometric amount relative to the concentration of the nitrogen source, is a major prerequisite in formulating the media to be used for these processes to produce maximum lipid. As an example, we use the following overall reaction for the production of new microbial cell, represented as $C_5H_7NO_2$ from organic matter represented by glucose ($C_6H_{12}O_6$) assuming that the carbon source is used solely for the production of new cells and energy, and nitrogen is the only nutrient source [Tchobanoglous, et al., 2003]:

$$3C_6H_{12}O_6 + 8O_2 + 2NH_3 \xrightarrow{\text{microorganisms}} 2C_5H_7NO_2 + 8CO_2 + 14H_2O \qquad (3.5)$$

From the above reaction, the stoichiometric C:N (mass) ratio is calculated as 7.7. Hence, at C:N ratios higher than this theoretical value, the carbon source is in excess and at a given reaction rate, the nitrogen source will be depleted sooner than the carbon source. The excess carbon is then utilized for storage lipid production according to the biochemical reactions described earlier. The concentration of the limiting nutrient (nitrogen) will determine the quantity of biomass produced while the concentration of the

excess carbon source will largely determine the amount of oil accumulated. However, it is important to note that the carbon source is not only used for cell growth but also for energy and cell maintenance.

Throughout years of extensive research, it has been found that oleaginous microorganisms only accumulate storage lipids at media C:N ratios above 20:1 and optimum levels are generally between 30:1 and 80:1; the most common value used being 40:1 [Davies and Holdsworth, 1992]. A notable exception was the yeast *Cryptococcus terricolus,* which was found to accumulate lipids even at low C:N ratios < 20:1 [Pederson, 1962]. A previous study concluded that increasing the C:N ratio of the media led to higher fat coefficients, defined as g fat produced/100 g of glucose consumed, in the oleaginous yeast *Rhodotorula gracilis* CFR-I [Sattur and Karanth, 1989a]. Fat coefficients of 21 % at C:N ratio of 267:1 as opposed to 1.6 % at C:N ratio 18.3:1 were reported, although no indications were made regarding the actual lipid content values (% dry weight) of the yeast cell biomass generated. In determining the optimum C:N ratio for lipid accumulation, the authors of the study considered the effect of C:N ratio on biomass yield and sugar utilization. The unusually high fat coefficients reported at the higher C:N ratios (> 200:1) was found to be a residual effect of the low sugar utilization levels. Sugar utilization levels were higher (≥ 98 %) at low C:N ratios while at high C:N ratios (> 100:1), sugar utilization levels dropped to a minimum of 40 %. At very high C:N ratios above a critical or optimum level, the nitrogen supply is too low, which could have led to low sugar utilization with consequently low biomass and lipid yields [Sattur and Karanth, 1989c]. The data also suggest that the variation in fat coefficient with C:N

ratio was also dependent on the initial sugar concentration, hence its effects needed to be considered when optimizing the initial media conditions.

Substrate Loading

Further investigations conducted by Sattur and Karanth found that the initial sugar loading, when compounded with C:N ratio exerts an significant effect on lipid production by the oleaginous yeast *Rhodotorula gracilis* CFR-I [Sattur and Karanth, 1989c]. At different glucose concentrations, the trends in biomass yield (Figure 3.3), sugar utilization (Figure 3.4), and fat coefficient (Figure 3.5) with C:N ratio exhibited similar patters but pointed to different optimum conditions. As shown in Figure 3.3, biomass production increased with increasing glucose concentration and the optimum C:N ratio was found to be around 70:1, beyond which biomass yield decreased gradually with increasing C:N ratio. Sugar utilization trends (Figure 3.4) were also similar in that in all glucose concentrations investigated, the percentage of sugar utilized decreased with increasing C:N ratio. However, the range of C:N ratios in which sugar utilization levels are high (≥ 98 %) covers a wider range of up to 120:1 at the highest initial glucose concentration tested (90 g/L). The fat coefficient trends (Figure 3.5) at each glucose concentration investigated showed an increase up to a maximum before decreasing, giving optimum C:N ratios of around 60:1 and 100:1 at 30 and 60 g/L glucose

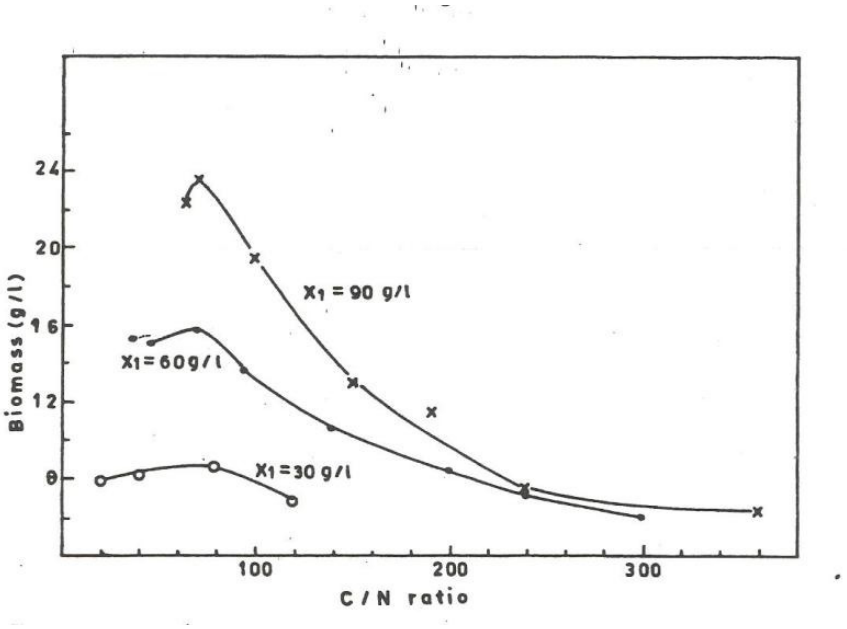

Figure 3.3: Effect of C:N ratio on biomass yield of *Rhodotorula gracilis* CFR-I at different glucose concentrations [Sattur and Karanth, 1989c].

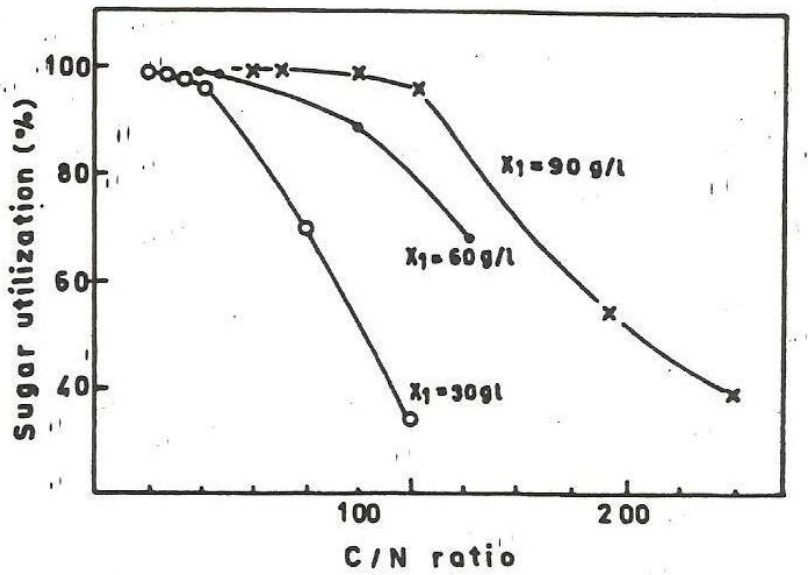

Figure 3.4: Effect of C:N ratio on sugar utilization of *Rhodotorula gracilis* CFR-I at different glucose concentrations [Sattur and Karanth, 1989c].

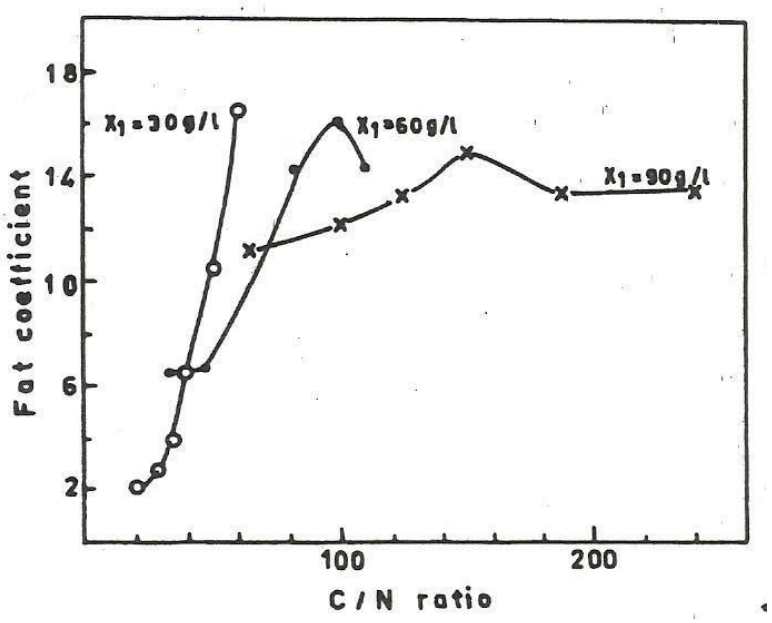

Figure 3.5: Effect of C:N ratio on fat coefficient of *Rhodotorula gracilis* CFR-I at different glucose concentrations [Sattur and Karanth, 1989c].

concentration, respectively, whereas a saturation fat coefficient was observed at 90 g/L glucose concentration. Based on these observations, glucose concentrations 60 g/L and below may be more beneficial in terms of maximizing the fat coefficient.

Nitrogen Source

Next to the carbon and energy source, the type of nitrogen source has the most profound effect on the lipid content and composition of oleaginous microorganisms and has attracted some attention from researchers on microbial lipid production. The study conducted by Evans and Ratledge [1984] found that the use organic nitrogen sources (i.e. glutamate, urea, and arginine) resulted into lipid contents above 50 % (w/w) in batch cultures of the yeast *Rhodosporidium toruloides,* compared to 18 % (w/w) when an

inorganic nitrogen source, NH_4Cl was used. The increased lipid production with organic nitrogen sources in batch cultures, specifically glutamine, has been attributed to the build-up of citrate in the yeast cells [Evans and Ratledge, 1984]. Citrate, as it has been stated in the earlier section, plays an important role in the biochemical reactions leading to lipid biosynthesis. The effect of using organic versus inorganic nitrogen sources on lipid accumulation however, was not observed in fermenter-scale cultures [Moreton, 1988], where it has been speculated that in shake flasks, organic nitrogen sources provided additional buffering capacity to maintain the pH at optimal levels for growth. The effect of the ratio of organic (yeast extract) to the inorganic (ammonium nitrate) nitrogen source has also been investigated; however only a minimal increase in biomass and decrease in fat coefficient with increasing organic N/inorganic N were observed [Sattur and Karanth, 1989b].

pH

Previous investigations on the effect of pH on growth and lipid accumulation of oleaginous microorganisms mainly focused on yeasts, whereas those of bacteria are extremely rare. It has been shown previously that most oleaginous microorganisms were able to grow over a wide range of pH, as demonstrated by the yeast *Candida* sp. 107 over a pH range of 3.5-7.5 [Ratledge, 1968] and *Apiotrichum curvatum* between pH 3.45 and 5.7 [Davies, 1988]. However, the research by Kessel [1968] concluded that biomass growth of *Rhodotorula gracilis* was reduced as the pH of the media was lowered; and although the maximum total lipid and total fatty acids produced remained the same, the rate of lipid and fatty acid production at nitrogen exhaustion was significantly higher at

lower pH. The same study also found significant changes in the fatty acid composition due to changes in the pH value, specifically the average ratio of unsaturated to saturated fatty acids, which fell from 3.54 at pH 6.0 to 2.74 at pH 3.0; although the concentration of polyunsaturated fatty acids increased from 26 % at pH 6.0 to 39 % at pH 3.0 since the concentration of saturated fatty acids also increased accordingly [Kessell, 1968]. The overall increase in unsaturation was then attributed to oleic acid, which has been found to increase with increasing pH in *Aspergillus nidulans* [Singh and Walker, 1956].

Temperature

In addition to pH, the cultivation temperature has been mostly studied for its effect on microbial lipid accumulation, focusing mainly on lipid unsaturation and were prompted by the knowledge that lipids, particularly microbial phospholipids, undergo a phase transition from crystalline to liquid-crystalline over the temperature range in which microorganisms in general are able to grow [Rose, 1989]. Overall, an increase in temperature reduces the lipid yield form oleaginous yeast biomass, as in the case of *Rhodotorula gracilis,* which was reduced from 62 to 52 % (w/w) as the temperature was increased from 27 to 35°C [Enebo and Iwamoto, 1966]. Biomass and lipid yields (g/kg substrate) by the yeast *Apiotrichum curvatum* were also reduced from 24.8 and 9.36, respectively at 30°C to 16.5 and 6.64 at 35°C with an accompanying reduction in substrate utilization [Davies, 1988]. The published findings also reported a general increase in fatty acid unsaturation in oleaginous yeasts as the growth temperature is lowered, and vice versa. For example, Enebo and Iwamoto [1966] reported significant increases in the concentration of the unsaturated fatty acids oleate (C18:1), linoleate

(C18:2), and linolenate (C18:3) in *Rhodotorula gracilis* with decreasing temperature, while the saturated fatty acids remained unchanged. Similar findings have also been observed for the yeast *C. lipolytica*, which showed increased linoleic acid content at 10°C relative to 25°C [Ferrante and Kates, 1986]. On the other hand, the decrease in unsaturated fatty acids (palmitoleate, C16:1 and oleate, C18:1) in *E. coli* ML 30 phospholipids with increasing temperature was accompanied by an increase in the unsaturated fatty acid palmitate (C16:0). All of these studies attribute the increase in unsaturated fatty acid content with decreasing temperature to a compensatory or homeostatic mechanism commonly referred to as homeoviscous adaptation, with the objective of maintaining cell membrane fluidity at low temperatures [Rose, 1989].

These findings point to the importance of the cultivation temperature as an important factor in controlling the fatty acid profile of microbial oils to suit specific requirements such as in biofuels production. In batch cultures however, temperature changes could also affect the microbial growth rate and the dissolved oxygen level of the culture. Hence their effects on lipid production are discussed in the next sections.

Dissolved Oxygen

In most fermentation processes involving oleaginous microorganisms, the maximum cell density is usually determined by the rate of oxygen transfer to the culture [Ratledge and Hall, 1977]. Most studies employed an aeration rate of 1.0 volume of air per volume medium per minute (vvm) and at times conducted fermentation experiments with stepwise increases in the agitation rate [Ratledge, 1968] to increase oxygen transfer and maintain a dissolved oxygen level above a critical value required for maximum

aerobic cell growth. However, it was found that during the lipid accumulation phase in which the nitrogen level in the medium has been exhausted, oxygen demands dropped dramatically, which has been anticipated as fat is essentially chemically reduced and requires no oxygen for its synthesis from malonyl-CoA [Ratledge and Hall, 1977].

Similar to growth temperature, numerous researchers have investigated the effect of oxygen levels on the fatty acid profile of oleaginous yeasts. Significant alterations to the fatty acid profile of the obligate aerobe yeast *Rhodotorula gracilis* with decreasing dissolved oxygen levels were reported; specifically, increases in stearate (C18:0) and oleate (C18:1) levels, decreases in linoleate (C18:2) and linolenate (C18:3) levels, and a decrease in palmitate (C16:0) proportional to the stearate increase [Choi, et al., 1982]. However, findings from other researches indicated that oxygen level effects on fatty acid profile could be strain dependent. For instance, with the yeast *Candida* 107, no significant changes in fatty acid profile were observed at low aeration rates (0.05 vvm) [Hall and Ratledge, 1977]. It was also demonstrated previously that much lower oxygen flow rates (< 3 mmol O_2 per L per h) were required to induce a change in the fatty acid profile of the yeast *Apiotrichum curvatum*, specifically a reduction in oleic acid (55 to 41 %) and linolenic acid (9 to 3 %) [Davies, et al., 1990]. However, the negative effects of operating at these low aeration conditions are decreased oil content and increased fermentation time.

The underlying theory behind the effect of oxygen levels on fatty profile (increased unsaturation with decreasing oxygen level, and vice versa) has been attributed to the oxygenase-catalyzed desaturation of saturated fatty acids (i.e., the introduction of a double bond into the fatty acid chain), which requires NADPH and molecular oxygen

[Rose, 1989; Davies and Holdsworth, 1992]. Hence, and increased aeration rate would increase the supply of oxygen that could be used to drive the oxgenase-catalyzed desaturation of saturated fatty acids, and vice versa.

Fermentation Modes

Although high C:N ratios have been shown to increase lipid content in percent by dry weight of microbial biomass in most batch cultures, the resulting total biomass concentrations are usually low due to low nitrogen levels. The unusually high fat coefficients or lipid yields based on the amount of glucose consumed were probably due to low utilization rates brought about by the low cell densities. A more realistic expression of lipid output by oleaginous cultures is by reporting the mass of lipids produced per volume of media (g/L), hence the lipid contents need to be factored in with the biomass concentration. Studies have been conducted in evaluating different fermentation modes with the aim of increasing biomass concentrations prior to lipid accumulation, enhance lipid production rates, and reduce substrate inhibition due to high initial carbon source loadings required in batch cultures [Li, et al., 2007].

The use of a fed-batch fermentation mode (with discontinuous feeding) has been investigated previously by a number of studies with good results [Yamaguchi, et al., 1983; Pan, et al., 1986; Ykema, et al., 1988; Meesters, et al., 1996; Li, et al., 2007]. Pan et al. [1986] reported a final cellular lipid content of 40 % (w/w) in *Rhodotorula glutinis* via fed-batch cultures using a high sugar media (600 g/L glucose). Cell densities as high as 153 g/L for *Lipomyces starkeyi* [Yamaguchi, et al., 1983], 91.4 g/L for *Candida curvatus* fed with whey permeate [Ykema, et al., 1988], and 118 g/L from *Candida*

curvatus fed with glycerol [Meesters, et al., 1996]. The resulting lipid contents were 54 % (w/w) for *L. starkeyi,* 33 % (w/w) for *C. curvatus* in whey, and 25 % (w/w) for *C. curvatus* in glycerol. However, these studies involved a simultaneous batch feeding of the carbon and nitrogen source, which could have produced an unfavorable C:N ratio for lipid accumulation. A two-stage fed batch culture was employed previously for the yeast *Rhodosporidium toruloides* Y4 using glucose, which involved an initial batch culture with nutrient-rich media, followed by a discontinuous feeding phase with only the carbon source [Li, et al., 2007]. A high biomass densities, cellular lipid contents, and overall lipid productivities of 151.5 g/L, 48 % (w/w), and 0.12 g/L·h, respectively were obtained in flask cultures while 106 g/L, 67.5 % (w/w), and 0.54 g/ L·h, respectively were obtained in fermenter cultures.

Relatively few studies involving the use of continuous cultures for the cultivation of lipid-accumulating microorganisms have been found. The series of studies conducted by the group of Ratledge is perhaps the most recognizable and provided elegant results regarding the use of single- or two-stage chemostats for the growth and lipid accumulation of the oleaginous yeast *Candida* 107 [Gill, et al., 1977; Hall and Ratledge, 1977; Ratledge and Hall, 1977]. Similar to fed batch cultures, the continuous experiments that they conducted involved an initial batch culture in nutrient-rich media for 24 h to achieve maximal biomass density, followed by continuous feeding of nutrient-limited media for lipid accumulation. The growth rate of *Candida* 107 was kept considerably less than the maximum during the oil accumulation phase to achieve similar yields as with the batch culture. This was through the adjustment of the dilution rate (D), which is considered to be the reciprocal of the culture residence time, the specific growth rate of

the microorganism (μ) was controlled to achieve a certain level since at steady state in continuous cultures, D (h^{-1}) is equal to μ (h^{-1}) [Shuler and Kargi, 2002]. For *Candida* 107, it was found that the optimum dilution rate in a single stage continuous culture for maximal lipid accumulation (40 % by wt., 22 g of lipid per 100 g glucose consumed) was 0.06/h [Gill, et al., 1977]. The fatty acid composition of the lipid also remained unchanged over many weeks under steady state conditions; hence the use of a continuous process is advantageous when a uniform product composition is desired. The same group also tested a two-stage continuous process, which involves an initial batch culture for 24 h in nutrient-rich media in one fermenter followed by the transfer of the entire culture into a second fermenter where the nutrient-limited media was continuously fed into. However this complicated set-up offered no practical advantages over the single state continuous culture, since the maximum lipid yield (28 % by wt.) and lipid coefficient (14 g of lipid per 100 g of glucose) were considerably less than the latter [Hall and Ratledge, 1977].

Fermentation of Lignocellulose Hydrolyzate

In recent years, much attention has been given to the use of lignocellulose biomass as cheap non-food based fermentation substrates for biofuel production, specifically bioethanol [Taherzadeh, et al., 1997; Taherzadeh, et al., 1999a; Zaldivar, et al., 2001; Taherzadeh and Karimi, 2007], and more recently for oil production by oleaginous microorganisms for biodiesel feedstock oil production [Dai, et al., 2007; Chen, et al., 2009; Hu, et al., 2009; Huang, et al., 2009]. The majority of the studies focused mainly on pentose sugar fermentations and elucidating the effects of

lignocellulose hydrolysis by-products such as furans (e.g. furfural and 5-hydroxymethylfurfural), organic acids (acetic and formic acids), and phenolic compounds (vanillin, hydroxymethoxybenzaldehyde) on the fermentative performance of biofuel-associated microorganisms. These studies involved fermentation process optimizations, biomass hydrolysis optimization, and genetic and metabolic engineering of microorganisms with pentose sugar utilization capability and increased tolerance towards certain lignocellulose degradation by-products, which have been found to exert inhibitory effects on the growth and metabolism of most microorganisms constitute the whole body of research devoted to the full utilization of this abundant and untapped resource for the production of biofuels.

Pentose Sugar Utilization

The complete utilization of lignocellulose hydrolyzate sugars is considered to be one of the requirements for the economic competitiveness of biomass-based alternative fuels such as bioethanol [Galbe and Zacchi, 2002] and more recently, for the production of lipid biodiesel feedstocks by oleaginous microorganisms [Li, et al., 2008]. This means that all types of hexose as well as pentose sugars derived from the cellulose and hemicellulose fractions of lignocellulose must be utilized and converted by microorganisms into valuable products efficiently with a high yield and high productivity [Taherzadeh and Karimi, 2007]. Dilute acid hydrolysis is the most commonly used and studied lignocelulose pretreatment and/or hydrolysis method due to its effectiveness and low cost [Lu, et al., 2007; Taherzadeh and Karimi, 2007]. This process can effectively solubilize hemicellulose into monomeric hexose and pentose sugars and soluble

oligomers better than it degrades cellulose due to the fact that chemical bonds in hemicelluloses are weaker than those in cellulose. Also, most dilute acid hydrolysis processes are usually performed under mild temperature conditions to prevent the formation of degradation by-products. Hence, the resulting liquor, or hydrolyzate usually contains larger amounts of pentose sugars, which is mostly xylose, than hexose sugars such as glucose [Lu, et al., 2007]. This is mostly the case in hydrolyzates obtained from many hardwood hemicelluloses [Taherzadeh, et al., 1997]. Therefore, there is an increasing interest in the use of xylose as the sole carbon source or as a co-substrate with other sugars such as glucose in microbial fermentations.

The biochemical pathways involved in xylose metabolism (Figure 3.6) are different in enteric bacteria and yeast [Zaldivar, et al., 2001]. In bacteria, a xylose isomerase (XI) converts xylose to xylulose. In yeasts, xylose is converted into xylitol and subsequently to xylulose in reactions catalized by xylose reductase (XR) and xylitol dehydrogenase (XH), respectively with NADPH and NAD^+ acting as cofactors. The xylulose produced is then phosphorylated to form xylulose-5-phosphate (D-Xylu5P) and metabolized through the pentose phosphate pathway. The pentose phosphate pathway generates reducing equivalents in the form of NADPH needed for fatty acid biosynthesis (Eq. 3.4) and also the intermediates glyceraldehyde-3-phosphate (G-3-P) and fructose-6-phosphate, which are utilized in glycolysis for the production of pyruvate. Pyruvate is

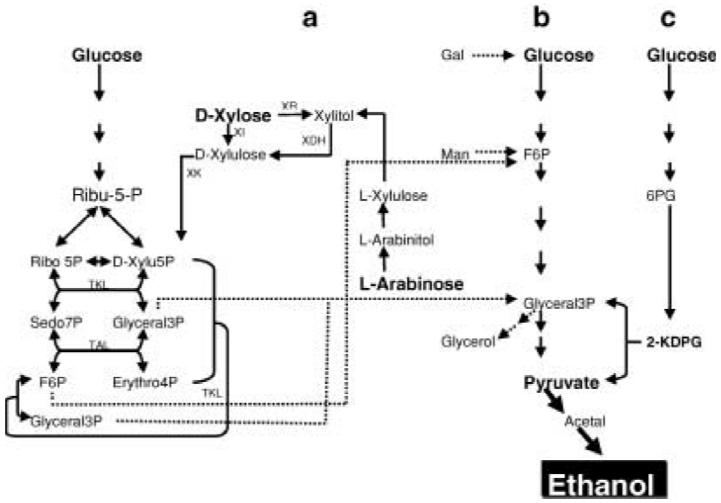

Figure 3.6: Overview of possible metabolic pathways of xylose utilization for the production of ethanol: (a) Pentose phosphate pathway, (b) glycolysis, and (c) Entner-Doudoroff pathway [Zaldivar, et al., 2001].

then used to produce the acetyl-CoA building blocks needed in the fatty acid and TAG biosynthetic pathways as described in earlier sections.

Although xylose is the most abundant sugar in the hemicellulose fraction of biomass, it considered to be the most difficult to ferment efficiently to ethanol [Olsson and Hahn-Hagerdal, 1993]. For instance, the most widely used microorganism in ethanol production, *Saccharomyces cerevisiae* lacks the genes encoded for xylose reductase (XR) and xylitol dehydrogenase (XH) enzymes, hence cannot utilize xylose [Taherzadeh and Karimi, 2007]. In spite of this, many wild type ethanol-producing microorganisms capable of fermenting xylose have been found, among them yeasts such as *Pichia stipitis, Pachysolen tannophilus,* and *Candida shehatae* and bacteria *Clostridium*

thermosaccharolyticum, and *Thermoanaerobacter ethanolicticus* [Olsson and Hahn-Hagerdal, 1993]. Genetic and metabolic engineering methods have been applied mostly to *S. cerevisiae, Zymomonas mobilis,* and *Escherichia coli* to incorporate the genes required for pentose utilization, specifically the genes that allow the expression of the XR and XH enzymes for ethanol production [Zaldivar, et al., 2001].

Despite the abundance of xylose in lignocellulose biomass hydrolyzates, it has been seldom used as substrate for microbial oil production, thus no conclusion can yet be drawn about its conversion threshold [Fakas, et al., 2009]. The theoretical fat coefficient on xylose is similar to that of glucose (34 %) assuming that xylose conversion to lipids occurred via the phosphoketolase-catalyzed reaction in the pentose phosphate pathway [Ratledge, 1988]. More recently, the xylose utilization capabilities of a few naturally-occurring oleaginous microorganisms have been investigated. As described earlier, the yeasts *Candida curvata, Rhodotorula glutinis,* and *Lipomyces starkeyi* and the fungi *Cunninghamella echinulata* and *Mortierella isabelina* have all been shown to utilize xylose by itself or as a co-substrate with glucose for lipid accumulation with excellent results [Evans and Ratledge, 1983; Zhao, et al., 2008; Fakas, et al., 2009]. Various oleaginous yeasts have also been screened previously using xylose as sole carbon source in nitrogen-limited batch cultures and results showed that strains belonging to the species *Lipomyces starkeyi* produced high amounts of total biomass (21 g/L) containing 20 % lipids by weight while strains belonging to the genera *Rhodosporidium, Trichosporon,* and *Rhodotorula* produced lower quantities of total biomass (4.2 to 7.2 g/L) and lipids (4 to 20 %) with a maximum fat coefficient of 11 % [Li, et al., 2005].

Effect of Inhibitory Compounds

Another requirement for the efficient use of lignocellulose as potential fermentation substrates for microbial oil production is the ability of oleaginous microorganisms to withstand the potential inhibitory effects of a number of lignocellulose hydrolysis by-products [Hahn-Hagerdal, et al., 2007; Taherzadeh and Karimi, 2007]. A schematic showing the origins of inhibitory compounds produced during the dilute acid hydrolysis of lignocellulose is shown in Figure 3.7. Based on this figure, the various inhibitory compounds can be grouped into three major groups:

(1) Furans such as furfural, from xylose degradation, and 5-hydroxymethylfurfural (5-HMF) from glucose degradation;

(2) Organic acids such as acetic acid from the decomposition of acetylated sugars in hemicellulose, formic acid from xylose and furfural oxidation, and levulinic acid from glucose and 5-HMF oxidation; and

(3) Phenolic/aromatic compounds such as vanillin and syringaldehyde obtained form the partial breakdown of lignin.

Hydrolysis conditions such temperature, reaction time, and acid concentration influence the generation of these inhibitory compounds their relative proportions in the resulting hydrolyzate [Palmqvist and Hahn-Hagerdal, 2000]. The influence of these parameters are combined into a single reaction coordinate called the combined severity (CS) [Chum, et al., 1990]. Generally in most hydrolysis reactions, maximum yields of hemicellulose-derived sugars such as xylose and mannose are obtained at CS levels lower than that required for maximum glucose yield. Increasing the CS further could result in the degradation of fermentable hemicellulose sugars and glucose to HMF and furfural,

which in turn were degraded to formic acid and levulinic acid. The fermentability of the hydrolyzate drastically decreased at CS levels where furfural and HMF started to accumulate. In most cases, the toxicity of an actual hydrolyzate differs substantially from that of a synthetic mixture of model compounds with the same concentration of inhibitory substances, which leads to the assumption that a combination of the action of several of these compounds, even in trace concentrations, is the reason behind an observed inhibition [Clark and Mackie, 1984; Taherzadeh, et al., 1999a].

Among the numerous lignocellulose degradation products identified, furfural and acetic acid are present in relatively high concentrations in most hydrolyzates and are extensively studied for their inhibitory effects on microbial fermentations involved in the production of high value chemicals such as ethanol [Chung and Lee, 1985; Boyer, et al., 1992; Taherzadeh, et al., 1997; Taherzadeh, et al., 1997; Palmqvist, et al., 1999; Zaldivar and Ingram, 1999; Galbe and Zacchi, 2002; Keating, et al., 2006; Agbogbo and Wagner, 2007; Wikandari, et al., 2010], xylitol [Felipe, et al., 1996; Converti, et al., 2000; Carvalho, et al., 2004], and more recently biodiesel feedstock lipids [Chen, et al., 2009; Hu, et al., 2009; Huang, et al., 2009].

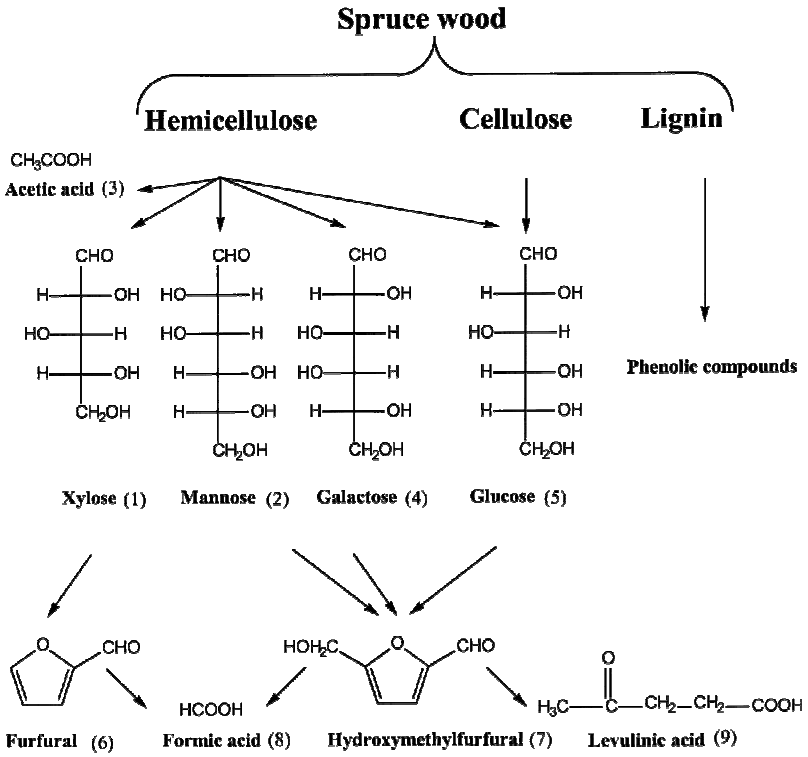

Figure 3.7: Reactions occurring during hydrolysis of lignocellulosic biomass [Palmqvist and Hahn-Hagerdal, 2000].

Inhibition by Acetic Acid

Acetic acid is typically the most abundant organic acid found in lignocellulose hydrolyzates obtained via the cleavage of the acetyl groups from hemicelluloses such as acetylxylan during mild pretreatment conditions [Zaldivar and Ingram, 1999; Diaz, et al., 2009]. In addition, acetic acid is also a by-product of fermentation [Oura, 1977], hence its initial and intermediate levels during fermentations do not depend solely on the severity of the lignocellulose hydrolysis reaction. Numerous studies have reported the inhibitory effects of acetic acid or organic acids in general on the growth and metabolism of enteric

bacteria and yeasts for bioethanol production. Biomass yields from *S. cerevisiae* decreased by 45 % at 3.3 g/L of acetic acid loading compared with no acetic acid [Taherzadeh, et al., 1997]. However, in spite of lower biomass yields, ethanol production was found to be 20 % higher with acetic acid than without it in the media. Similarly, acetic acid has been shown to indirectly inhibit ethanol production by *Escherichia coli* LY01 primarily by inhibiting cell growth rather than directly inhibiting the central pathways for glycolysis and energy generation [Zaldivar and Ingram, 1999], as concentrations of acetic acid that inhibited growth by 80 % either stimulated or caused modest inhibition of ethanol production from xylose. The same results were also found for the ethanologenic yeasts *Saccharomyces cerevisiae* ATCC 96581 and *Candida shehatae* NJ 23, wherein acetic acid levels up to 9 g/L stimulated ethanol yields and volumetric ethanol production rate [Palmqvist, et al., 1999]. However, other studies reported concentration ranges of acetic acid that stimulated ethanol production, beyond which ethanol yields and productivity declined. Acetic acid levels of up to 15 g/L have been shown to cause a markedly lower ethanol yields, despite little effect on sugar consumption rates [Keating, et al., 2006].

More recently, acetic acid effects on lipid accumulation by oleaginous microorganisms have been reported [Chen, et al., 2009; Hu, et al., 2009]. Hu and coworkers [2009] reported that acetic acid levels up to 70 mM (4.2 g/L) had negligible inhibitory effects on lipid production of the oleaginous yeast *Rhodosporidum toruloides;* and at 120 mM acetate loading, the lipid content of the yeast actually reached 68 % by dry biomass. This was probably due to the fact that acetate (the dissociated form of acetic acid) can be readily utilized as a carbon source by microorganisms [Zaldivar and Ingram,

1999], such as in the case of *R. toruloides,* which probably utilized acetate to produce acetyl-CoA, which are building blocks for fatty acid biosynthesis. An added effect is the increase in the C:N ratio of the media due to the contribution of acetate such that the lipid accumulation process was greatly augmented [Hu, et al., 2009]. Another study found that the oleaginous yeast *Trichosporon cutaneum* 2.1374 was the most adapted strain towards acetic acid, and can still grow in media containing 5 g/L acetic acid [Chen, et al., 2009].

It was generally understood that the inhibitory effect of acetic acid in microbial fermentations is related to the hydrophobicity of its undissociated or protonated form [Thomas, et al., 2002]. In aqueous solution, acetic acid dissociates into acetate according to the reaction:

$$\underset{\text{Acetic acid}}{CH_3COOH} + H_2O \longrightarrow \underset{\text{Acetate}}{CH_3COO^-} + H_3O^+ \qquad (3.6)$$

Due to its hydrophobicity, the protonated acetic acid can diffuse through the cell membranes of microorganisms and dissociate in the cytosol, this decreasing the intracellular pH thus inhibiting cell growth [Gottschalk, 1987; Palmqvist and Hahn-Hagerdal, 2000]. Hence, the pH of the culture is an important variable in fermentations involving organic acids such as acetic acid, as it has been shown previously that increasing the initial pH of the culture above the pKa of acetic acid (4.75 at 25°C) to 6, 7 and 8 reduced the toxicity of organic acids by reducing the concentration of the protonated/undissociated acid while increasing the concentration of the dissociated form [Zaldivar and Ingram, 1999]. The presence of acetic acid has also been found to increase the minimum allowable pH for growth in *Saccharomuces cerevisiae* cultures to near the pKa for acetic acid [Taherzadeh, et al., 1997]. In the absence of acetic acid, it was

possible to grow the yeasts at a pH as low as 2.5 whereas with an acetic acid loading of 10 g/L, the minimum allowable pH for growth was increased to 4.5.

The two mechanisms that have been proposed to explain the inhibitory effects of weak acids such as acetic acid in microbial fermentation are uncoupling and intracellular anion accumulation [Russell, 1992]. The uncoupling theory states that in order to maintain a neutral intracellular pH to combat the inflow of undissociated acids into the cytoplasm, protons are pumped across the cell membrane by the action of the plasma membrane ATPase at the expense of ATP hydrolysis. This increases the ATP requirement for cell maintenance at the expense of cell biomass production and at even higher extracellular acid concentrations above the critical level, the proton pumping capacity of the cell is exhausted resulting in the depletion of ATP, dissipation of the proton motive force, and uncontrolled acidification of the cytoplasm [Verduyn, et al., 1990a]. However, the theory regarding the dissipation of the proton motive force due to high extracellular acid concentrations has been questioned since each molecule of undissociated acid transferred across the plasma membrane leads to the import of only one proton [Russell, 1992] while synthetic uncouplers such as dinitrophenol can move across the plasma membrane in both dissociated and protonated forms to cause a high rate of proton transfer [Palmqvist and Hahn-Hagerdal, 2000b]. Hence an alternative theory of intracellular anion accumulation was proposed, which suggests that the toxicity of the weak acid is due to its anionic (dissociated) form. The anionic acid form is captured in the cell and the undissociated acid diffuses through the cell membrane to attain equilibrium [Rottenberg, 1979]. Since the equilibrium concentration of the undissociated acid is a function of pH, the extent of intracellular anion accumulation will

be a function of the pH gradient across the cell membrane. Low extracellular pH levels have also been shown to increase the intracellular anionic acid concentration in *S. cerevisiae* as the yeast attempts to maintain a neutral intracellular pH [Russell, 1992]. In addition to these, the presence of acetic acid has also been shown to negatively affect the activity of glycolytic enzymes, specifically the enolase enzyme, due to both internal acidification and direct interference of the acid [Pampuhla and Loureiro-Dias, 1990].

Inhibition by Furfural

Furfural, along with 5-hydrolymethylfurfural (HMF), are usually the only furans present in significant amounts in most lignocellulose hydrolyzates [Taherzadeh, et al., 1997a]. Since furfural is the primary decomposition product from pentoses and therefore likely to be present in hydrolyzates, the effect of furfural on fermentation by yeasts such as *Saccharomyces cerevisiae* to ethanol has been the subject of numerous investigations.

Most of the previous researches have shown furfural to be a potent inhibitor in anaerobic microbial fermentation of glucose to ethanol. It has been found that furfural concentrations on the order of 1 g/L already have negative effects on yeast viability, specific growth rate, sugar consumption and volumetric fermentation rate of ethanol-producing yeasts such as *S. cerevisiae* [Banerjee, et al., 1981; Chung and Lee, 1985; Boyer, et al., 1992; Keating, et al., 2006] and *Pichia stipitis* [Weigert, et al., 1988; Agbogbo and Wagner, 2007; Diaz, et al., 2009]. Among these factors, cell growth has been shown to be more sensitive to the presence of furfural than is the production of ethanol from glucose [Palmqvist, et al., 1999]. The immediate effect of adding furfural into an exponentially-growing culture of *S. cerevisiae* was a rapid decrease in the CO_2

evolution rate (around 35 % within the first five minutes) followed by a more gradual decrease. Furfural was also found to inhibit aerobic fermentation process such as xylitol (for artificial sweeteners) production by the yeast *Candida guilliermondii* by reducing the maximum specific xylitol productivity by more than 50 % at 0.7 g/L furfural compared to a control set-up [Converti, et al., 2000]. Furfural concentrations as low as 1 mM also exhibited a significant inhibitory effect on the aerobic growth and lipid accumulation of the oleaginous yeast *Rhodosporidum toruloides* Y4, which exhibited a 41 % decrease in glucose consumption, 45.5 % reduction in biomass production, and 26.5 % decrease in lipid yields compared with a control set-up [Hu, et al., 2009]. Numerous oleaginous yeast strains (*Trichosporon cutaneum, Rhodotorula glutinis, Lipomyces starkeyi,* and *Rhodosporidium toruloides*) were previously screened for tolerance to furfural in the range of 0 to 1 g/L, and in all the species tested exhibited little or no cell growth [Chen, et al., 2009]. Similar to ethanol-producing yeasts, it was discovered furfural had a greater inhibitory effect on the total biomass production than on lipid accumulation [Hu, et al., 2009]. In spite of this, relatively few studies can be found regarding the furfural inhibition on oleaginous microorganisms as opposed to ethanologenic yeasts as this research topic is considered to be relatively new.

The proposed mechanism of furfural inhibition, specifically on bioethanol production by yeasts which is basically an anaerobic process, is its inhibition *in vitro* of several important glycolytic enzymes such as hexokinase, aldolase, phosphofructokinase, and triosephosphate dehydrogenase, as well as pyruvate decarboxylase and alcohol dehydrogenase for the production of ethanol from pyruvate [Banerjee, et al., 1981; Modig, et al., 2002]. Additionally, ethanol producing yeasts have also been found to

metabolize furfural to less inhibitory compounds, consisting mostly of furfuryl alcohol, which accounts for 70 % of the initial furfural concentration [Diaz de Villegas, et al., 1992]. Minor products such as furoic acid (less than 1 % conversion) [Diaz de Villegas, et al., 1992; Taherzadeh, et al., 2000b], furoin, and furil (traces) [Morimoto, et al., 1969] have also been detected. After complete exhaustion of furfural, some of the furfuryl alcohol formed are then converted to furoic acid. Most of the studies mentioned reported appreciable biomass growth once furfural has been completely converted to by-products, which led to the generalization that furfuryl alcohol and furoic acid are less toxic than furfural and that the microbial conversion process is essentially a natural detoxification response by the microorganisms. In contrast, it was reported that furfural and furfuryl alcohol exerted roughly the same amount of inhibition on the oleaginous yeast *R. toruloides* Y4 (45 % reduction of biomass yield at 1 mM concentration for each), while furoic acid had a slightly lower inhibitory effect (31.7 % reduction of biomass yield at 1 mM) [Hu, et al., 2009]

Furfural degradation rates were reported to be faster in exponentially-growing cells (0.6 g g^{-1} h^{-1}) as opposed to cultures in the stationary phase (0.07 g g^{-1} h^{-1}) when glucose has been depleted, hence emphasizing the dependence of furfural reduction of active glycolysis [Taherzadeh, et al., 1999b]. It was also stated that high furfural levels causes the inhibition of the enzymes downstream of pyruvate namely pyruvate decarboxylase and aldehyde dehydrogenase (ADH), and this could in turn lead to the build-up of pyruvate and feedback inhibition of glycolysis. Additionally, the reduction of furfural to furfuryl alcohol is catalyzed by ADH, and therefore may compete with the reduction of acetaldehyde, which is also catalyzed by ADH. This may result in a reduced

glycolytic capacity and glucose flux into biomass and ethanol biosynthesis, leading to low biomass yields and ethanol productivity [Taherzadeh, et al., 1999b; Modig, et al., 2002]. Biomass synthesis is thought to be the main source of surplus NADH resulting to glycerol formation during anaerobic conditions [Verduyn, et al., 1990b], hence one might expect glycerol formation to decrease due to the reduction of biomass. However, it was found that glycerol yield increased instead after introduction of furfural, hence it was hypothesized that furfural reduction partially replaced glycerol formation as a way to regenerate NAD^+ [Horvath, et al., 2003]. To investigate inhibition effects outside of the glycolytic pathway, *S. cerevisiae* was also grown on the non-fermentable carbon substrates ethanol and acetic acid, which likewise resulted in a strong inhibition of cell growth until complete conversion of furfural to furfuryl alcohol and furoic acid has occurred [Taherzadeh, et al., 2000].

On the other hand, only a few studies have described the mechanisms of furfural inhibition under aerobic conditions as opposed to anaerobic fermentations such as bioethanol production. These studies are important in postulating the possible furfural inhibition mechanisms in aerobic fermentations such as xylitol and microbial lipid accumulation by oleaginous microorganisms. According to a study by Taherzadeh and colleagues [1999], similar inhibitory effects of furfural (decreased specific growth rate and ethanol productivity) were observed for both anaerobic and aerobic cultures of *S. cerevisiae* [Taherzadeh, et al., 1999b]. The presence of oxygen in aerobic fermentations with *S. cerevisiae* was also found to have no significant effects on the conversion rates, identities and yields of furfural degradation products. In contrast, the study by Horvath et al. [2003] reported that furoic acid was the only furfural degradation product detected in

the aerobic chemostat culture of *S. cerevisiae* [Horvath, et al., 2003] as opposed to furfuryl alcohol and the newly-discovered condensation product of furfural and pyruvate, 3-(2-furfuryl)-2-hydroxy-2-methyl-3-oxo-propanoic acid or FHMOPA in anaerobic cultures [Taherzadeh, et al., 1999b]. In that study, flux distribution analysis (Figure 3.8) revealed that during respiratory growth in furfural-free conditions, cell biomass was the major product of carbon metabolism, the pentose phosphate pathway was very active in providing NADH and precursors for biosynthesis, glycolysis provided precursors and pyruvate, and the tricarboxylic acid (TCA) cycle was also highly active. The addition of furfural decreased the specific rates of glycolysis, TCA cycle, and respiration and decreased the biomass yields based on ATP. Furfural was reduced to furoic acid using NAD^+ as cofactor and the NADH generated in this reaction accounted for 27 % of additional NADH respired; with the rest originating from the action of glyceraldehyde dehydrogenases and the TCA cycle. Overall, under aerobic conditions, a shift to respirofermentative metabolism occurs when the furfural degradation capacity of the culture is exceeded, leading to a decrease in biomass yield.

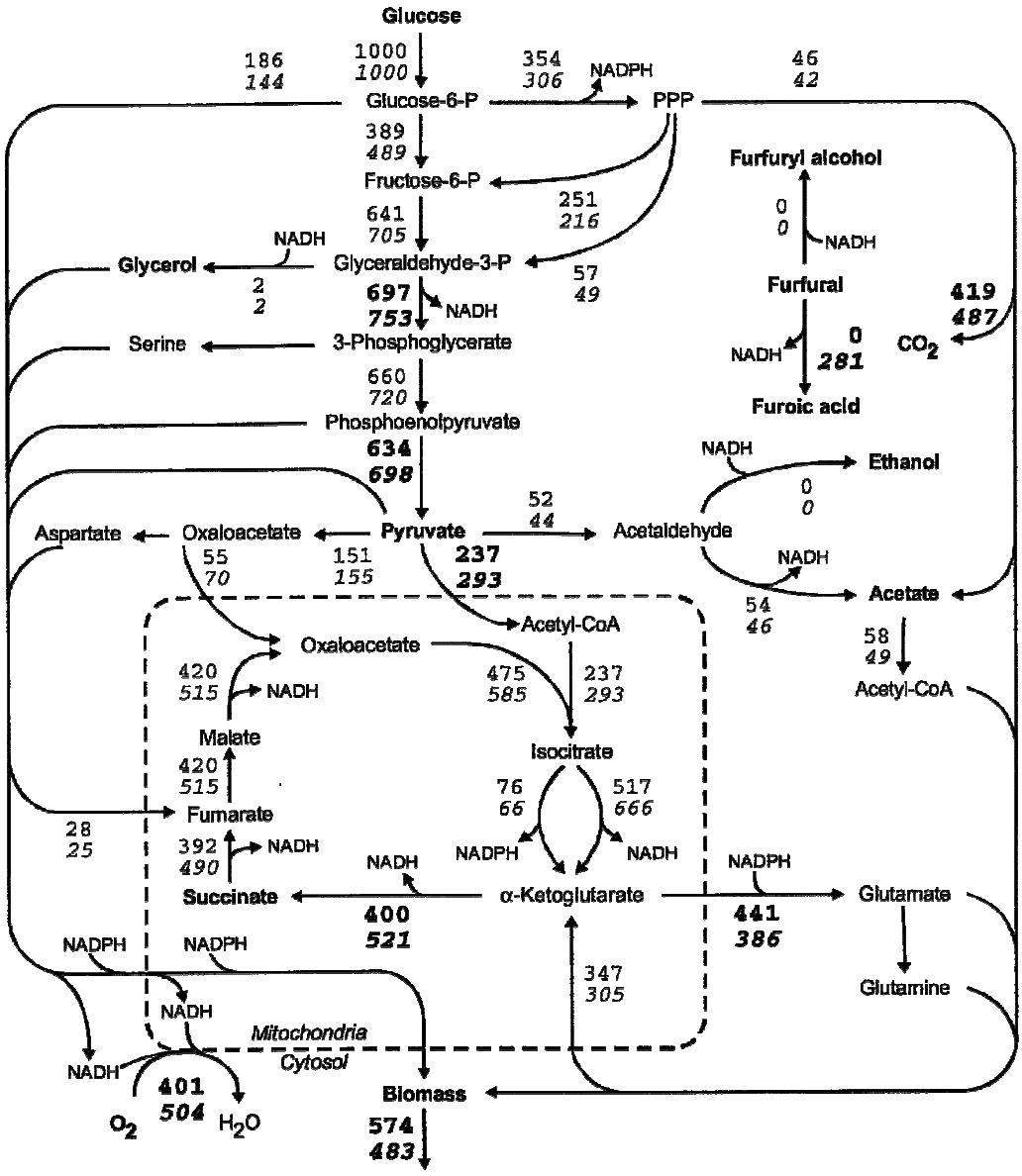

Figure 3.8: Flux distribution during respiratory growth of *Saccharomyces cerevisiae* obtained at furfural-free (top values) and in the presence of 2.25 g/L furfural (bottom values in italics). Values are in millimoles per mole glucose [Horvath, et al., 2003].

Previous studies on the effects of another furan lignocellulose derivative, HMF, showed that it was not as severely toxic to *S. cerevisae* as furfural [Taherzadeh, et al., 2000c]. This is in line with the observation that the *in vitro* inhibition of the enzymes pyruvate dehydrogenase and aldehyde dehydrogenase is lower by HMF than by furfural. Moreover, it was reported that the conversion rate of HMF is much slower that that of furfural, probably due to lower membrane permeability, thus causing a longer lag-phase in growth [Larsson, et al., 1998]. It was found the main conversion product of HMF is 5-hydroxymethyl furfuryl alcohol, which suggests similar inhibition mechanisms for HMF and furfural [Taherzadeh, et al., 2000c]

Interaction Effects of Furfural and Acetic Acid

In addition to studying the individual effects of inhibitory compounds such as furfural and acetic acid, several studies have also been conducted dealing with synthetic mixtures of these two compounds and other known lignocellulose degradation by-products in order to better simulate the fermentation of an actual biomass hydrolyzate mixture. Previously, acetic acid (10 g/L) and furfural (3 g/L) was shown to have an interactive negative effect on the specific growth rate (μ) of two ethanologenic yeasts, *Saccharomyces cerevisiae* ATCC 96581 and *Candida shehatae* NJ 23 [Palmqvist, et al., 1999]. The existence of an interaction effect between these two inhibitors means that the observed decrease μ was greater than the sum of the decreases in μ caused by the individual compounds [Myers and Montgomery, 1991]. On the other hand, the effect of furfural-acetic mixtures on ethanol productivity was found to be solely additive. Similar results were obtained from the ethanologenic yeast *Pichia stipitis*, wherein acetic acid

and furfural binary mixtures produced a total growth inhibition of the yeast [Diaz, et al., 2009]. In the case of lipid accumulation by *Rhodosporidium toruloides*, the inhibitory effect of furfural-acetic acid mixture was not tested; however, it was reported that binary mixtures containing HMF, vanillin, syringaldehyde, p-hydroxybenzaldehyde (PHB), and furfural all exhibited strong synergistic or interactive inhibitory effects on both cell growth and lipid accumulation [Hu, et al., 2009].

Utilization Strategies

Detoxification

As discussed in the previous sections, biomass and ethanol or lipid yields obtained during fermentation of lignocellulosic hydrolyzates are usually decreased due to the presence of inhibiting compounds. Various methods have been proposed with the objectives of removing inhibitor compounds to improve the fermentability and composition of the hydrolyzates [Palmqvist and Hahn-Hagerdal, 2000a]. Detoxification methods, which can be physical, chemical, or biological, have been employed to remove specific inhibitors from lignocellulose hydrolyzates. Physical detoxification methods include: (1) Vacuum evaporation of the volatile fraction of the hydrolyzate followed by dilution of the remaining non-volatile residue, which led to the reduction in acetic acid, furfural, and vanillin levels by 54, 100, and 29 %, respectively in willow hemicellulose hydrolyzate [Wilson, et al., 1989; Palmqvist, et al., 1996]; (2) solvent extraction using diethyl ether at pH 2 or ethyl acetate to separate organic acids, furans, and phenolics from the aqueous hydrolyzate mixture [Clark and Mackie, 1984]; and (3) adsorption of

inhibitory compounds on activated carbon or other adsorbent material [Huang, et al., 2009]

A commonly-used chemical detoxification method for lignocellulose hydrolyzates is alkali treatment via addition of $Ca(OH)_2$, termed as "overliming", in order to increase the pH to 9-10 followed by readjustment of pH to 5.5 with H_2SO_4, which has been reportedly used as early as 1945 [Leonard and Hajny, 1945; Palmqvist and Hahn-Hagerdal, 2000a]. The detoxifying effect of this method was attributed to the precipitation of toxic compounds and instability of some of the inhibitors at alkaline pH [Palmqvist and Hahn-Hagerdal, 2000a]. Indeed, ethanol yields and productivity have been found to improve following fermentation of alkali-treated spruce hydrolyzates [Palmqvist, et al., 1998]. Pretreatment of a dilute acid hydrolyzate of spruce via adjustment of pH to 10 using NaOH and $Ca(OH)_2$ has also been reported to reduce the concentrations of Hibbert's ketones by 22 to 30 % and HMF and furfural levels by 20 % [Palmqvist and Hahn-Hagerdal, 2000a]. A combination of overliming and sulfite treatment (0.1 % sodium sulfite at 90°C for 30 min) for the detoxification of a willow hydrolyzate has also been shown to enhance the utilization rate of xylose and reduce the fermentation time by a factor of three by a recombinant *Escherichia coli* for ethanol production [Olsson, et al., 1995]. Similar results were obtained previously by Van Zyl and co-workers [1988] for the pretreatment of sugarcane bagasse hydrolyzate with KOH (pH 10) followed by readjustment of pH to 6.5 with HCl and addition of 1 % sodium sulfite at room temperature prior to fermentation by *Pichia stipitis* [Van Zyl, et al., 1988]

Combinations of physical and chemical detoxification methods for lignocellulose hydrolyzates have been applied as well with good results. Hydrolyzates of corn stover

[Agbogbo and Wagner, 2007] and olive tree cuttings [Diaz, et al., 2009] were utilized as fermentation substrate for ethanol production by the yeast *Pichia stipitis* with prior dilutions and detoxification via overliming and/or activated charcoal treatment. In both cases, the ethanol yields obtained were in the range of 0.35-0.44 grams per grams total sugar (glucose + xylose). However, the hydrolyzates produced required pretreatment in order to match ethanol yields found in synthetic hydrolyzate mixtures. Similarly for microbial lipid production by the oleaginous yeast *Trichosporon fermentans*, fermentation of rice straw hydrolyzate obtained via dilute sulfuric acid treatment without prior detoxification gave poor lipid yields of approximately 1.7 g/L, which was considerably lower than using pure glucose (13.6 g/L) or xylose (9.9 g/L) as sole carbon sources [Huang, et al., 2009]. Fermentation of the hydrolyzate following dilution, overliming, concentration via vacuum evaporation, and adsorption using Amberlite XAD-4 significantly improved the total biomass (28.6 g/L), lipid content (40 % w/w), and lipid yield (11.5 g/L).

Biological detoxification methods were reported previously involving treatment of lignocellulose hydrolyzates with peroxidase and laccase enzymes from the lignolytic fungus *Trametes versicolor* for the oxidative polymerization of low molecular weight phenolic compounds, thereby increasing the maximum ethanol yield from a hemicellulose hydrolyzate of willow by a factor of two to three [Jonsson, et al., 1998]. Furthermore, the filamentous soft-rot fungus *Trichoderma reesei* has also been reported to degrade inhibitors such as acetic acid, furfural, and benzoic acid from willow hemicellulose hydrolyzates, resulting in a three-fold increase in ethanol productivity and four-fold increase in ethanol yield [Palmqvist, et al., 1997].

Fermentation Techniques

The use of appropriate fermentation conditions and configuration can be used alternately or in conjunction with the detoxification methods in order to decrease the levels of inhibitory compounds and improve the fermentability of lignocellulose hydrolyzates; however equipment and process costs must be evaluated with respect to product yield and productivity. The use of high-level yeast inocula has been suggested as means of overcoming toxicity in batch cultures which ferment acid hydrolyzates, based on the premise that furfural can be taken up and converted faster in the presence of a higher concentration of yeast cells [Chung and Lee, 1985]. Fermentation runs with high initial biomass concentrations (5 to 25 g/L) have been shown to increase the productivity and reduce the pH sensitivity of ethanologenic yeasts [Ghose and Tyagi, 1979; Palmqvist, et al., 1996]. However, the specific growth rate and cell viability have been reported to decrease with increasing inoculum size, and at very high initial cell densities, no net increase and cell biomass concentration was detected [Ghose and Tyagi, 1979].

The use of a fed-batch configuration for the fermentation of undetoxified lignocellulose hydrolzyates has also been reported recently [Taherzadeh, et al., 1999a; Taherzadeh, et al., 2000b; Nilsson, et al., 2001; Petersson and Liden, 2007]. Initial substrate concentrations are usually high in batch processes; hence for the fermentation of lignocellulose hydrolyzates, the concentrations of inhibitor compounds are likewise high, causing inhibition in cell growth and product formation. As alternative to detoxification and high-level inocula seeding, discontinuous feeding of hydrolyzates in lower amounts or addition of hydrolyzates at a constant low feeding rate into a culture could be used to significantly reduce the concentration of inhibitors and allow the microbial cells to

degrade these compounds *in situ* [Taherzadeh and Karimi, 2007]. Complete utilization of glucose and mannose sugars in spruce and birch hydrolyzates containing high levels of furfural (2.2 and 5.7 g/L, respectively) and HMF (7.3 and 2.4 g/L, respectively), along with 90 % and 40-70 % degradation of furfural and acetic acid, respectively without prior detoxification have been reported [Taherzadeh, et al., 1999a]. However, adjustment of substrate feeding rates to optimum levels were required to avoid the termination of cell growth and product formation due to dilution of the culture and build-up of inhibitor compounds at very high feeding rates, and low cell growth and productivity due to very low feeding rates [Taherzadeh, et al., 1999a; Taherzadeh, et al., 2000b; Nilsson, et al., 2001]. On the other hand, relatively few studies on the successful use of continuous fermentation mode of lignocellulose hydrolyzates have been found due to its major disadvantages such as its toxicity, which results into cell washout at high dilution rates leading to low cell biomass concentrations and ethanol productivity; as well as low conversion rates of inhibitors at low dilution rates due to the decreased specific growth rate [Taherzadeh and Karimi, 2007]. However, several studies recently employed cell retention techniques such as cell immobilization in calcium alginate and cell recirculation by filtration or sedimentation [Talebnia and Taherzadeh, 2006; Brandberg, et al., 2007]; and flocculation and encapsulation [Talebnia and Taherzadeh, 2006; Brandberg, et al., 2007]. The findings of these papers indicated that cell recirculation improved hexose conversion from 76 % to 94 % while cell immobilization via flocculation or encapsulation improved the tolerance and stability of ethanol productivity even at higher dilution rates ($> 0.30\ h^{-1}$) and increased the microorganisms' capacity for *in situ* detoxification.

As of the time of writing this document, no reports on the application of fed-batch or continuous fermentation of hydrolyzates for lipid accumulation in oleaginous microorganisms have yet to be found in literature, although similar results are to be expected.

Adaptation and Genetic Engineering of Microorganisms

Another alternative approach to lignocellulose hydrolyzate detoxification is the cultivation of microorganisms in the presence of toxic compounds in fermentation cultures to induce tolerance and adaptability; followed by isolation of these tolerant microorganisms from the next generation of cells derived from the original culture [Taherzadeh and Karimi, 2007]. Previous publications have reported improved fermentation rates, pentose sugar utilization, and tolerance to organic acids, furans, and phenolic compounds found mostly in undetoxified lignocellulosic hydrolyzates by adapted microbial strains such as *Saccharomyces cerevisiae* on sugarcane bagasse hydrolyzate [Martin, et al., 2007], *Pichia stipitis* on corncob hydrolyzate [Amartey and Jeffries, 1996], and *P. stipitis* on aspen and red oak hydrolyzates [Olsson and Hahn-Hagerdal, 1996]. However, a better understanding of the genetic mechanisms and biochemical pathways responsible for inhibitor response is needed to allow the development of genetically engineered novel strains that could withstand the adverse effects of inhibitory compounds generated from lignocellulose biomass pretreatment [Liu, et al., 2004].

The biochemical and genetic modes of microbial tolerance to organic acids (i.e. acetic acid) and furans (i.e. furfural) was outlined recently [Mills, et al., 2009]. As it was

discussed in an earlier section, organic acids such as acetic acid inhibit cellular growth and metabolism by increasing the intracellular pH due the transport of the undissociated acid across the plasma membrane [Gottschalk, 1987; Palmqvist and Hahn-Hagerdal, 2000]. Bacteria such as *E. coli* have been known to sense and regulate intracellular pH and acid tolerance has been shown to improve by50-fold by exposure to moderately low pH (5.0) before exposure to very low pH levels (3.0-3.5) [Goodson and Rowbury, 1989]. A proposed mechanism for the acid tolerance naturally seen in acidophiles involves the presence of an amino acid (glutamate or arginine) decarboxylase coupled with an antiporter that exports the decarboxylated product and imports the amino acid used across the plasma membrane The effect of this transport is the simultaneous transport of one intracellular proton across the cell membrane, thus raising the pH of the cell for continued growth and survival [Lin, et al., 1995]. It has been known that the *rpoS* regulon is induced by exposure to weak acids and its response leads to higher survival rates in low pH, oxidative stress and heat stress [Arnold, et al., 2001]. However, its response is supplemented by other sigma factors and various regulatory proteins in order to express the genes associated with decarboxylase and antiporter required for acid tolerance [Ma, et al., 2003].

In addition to the biochemical mechanisms of furfural inhibition described in an earlier section, furfural has been known to cause DNA damage specifically single strand breaks in sequence sites with three or more adenine or thymine bases [Hadi and Shahabuddin, 1989]. In spite of this, some cells have been shown to repair DNA damaged by furfural via a *polA*-mediated DNA repair pathway [Khan and Hadi, 1994]. Extensive studies done on the adaptability of ethanologenic *E.coli* recently found that

silencing the *yqhD* and *dkgA* genes, which encode for products with low affinities for NADPH allowed the mutant strain to concurrently grow and reduce furfural to less toxic products such as furfuryl alcohol and furoic acid [Miller, et al., 2009]. Further it was found that overexpression of the gene *zwf1*, which is one of several genes encoding for pentose phosphate pathway enzymes, allowed *Saccharomyces cerevisiae* to grow at furfural concentrations that are normally toxic [Gorsich, et al., 2006]. This section serves only to provide a summary of the underlying genetic mechanisms for developing tolerance towards inhibitory substances from biomass hydrolyzates that are used as bases for genetic engineering of specific microbial strains, which is beyond the scope of this study. For more specifics, the reader is referred to the citations previously mentioned.

Population Dynamics of Activated Sludge Microbial Communities

At present, most modern municipal and industrial wastewater treatment processes such as the activated sludge process depend primarily on the composition and activity of the communities of microorganisms (i.e., microbial consortia, microbiota) in activated sludge or biofilms for carbon and nutrient removal from sewage [Wagner and Loy, 2002; Yan, et al., 2007]. In contrast, the presence of certain microbial species and population shifts within the activated sludge/biofilm microbial community resulting from changes in prevailing weather conditions, influent wastewater loading and composition, and treatment plant operating conditions may cause operation problems such as poor sludge settling, compaction, foaming, and dewatering [Chipasa and Medrzycka, 2000; Wagner and Loy, 2002; Nielsen, et al., 2004]. Hence analysis of the composition and variations

brought about by changes in environmental conditions of activated sludge microbial communities are of great interest.

Thorough knowledge of the ecology of the microbial communities is required to reveal factors influencing the efficiency and stability of biological treatment processes and to develop promising strategies for improved process performance [Wagner and Loy, 2002]. Traditional methods of analyzing microbial communities in municipal wastewaters include light microscopy or cultivation-dependent techniques wherein identification of microorganisms were based on shape (e.g., rod, coccus), cell wall type (e.g., gram-negative or gram-positive), and hosts of biochemical tests (e.g., oxidase-positive, oxidase-negative) [Yan, et al., 2007]. However, most of the microbial groups and species in sludge cannot be cultured in nutrient media; therefore, molecular methods independent of cultivation have been employed. These include total bacteria measurements by 4',6-diamidino-2-phenylindone (DAPI) staining, determination of the bioactive (i.e., living) fraction of the total bacteria via fluoresence *in situ* hybridization (FISH) with oligonucleotide staining probes, or determination of the fraction of bacteria that is able to uptake radioactive substances by microautoradiography (MAR) [Nielsen and Nielsen, 2002; Yan, et al., 2007]. However, more recent studies employ a systematic approach based on the nucleotide sequence of ribonucleic acid (RNA) found in the 16S subunit of the ribosome (16S rRNA), wherein classification and identification of microorganisms is based on sequences of four nucleotide bases namely; adenine (A), cytosine (C), guanine (G), and uracil (U) [Agbogbo and Wagner, 2007; Yan, et al., 2007]. The 16S rRNA in prokaryotes was chosen because it is present in large quantities in all cells, it is easy to purify, and it tends to change only slowly over long periods of

evolutionary time, which means it could be applied to study the relationships of very distantly related organisms [Karp, 2008]. The so-called full-cycle rRNA approach based on the 16S rRNA method involves extraction of nucleic acids from the sludge biomass followed by amplification of the 16S rDNA (rRNA) gene via polymerase chain reactions (PCR), construction of 16S rRNA clone libraries, and identification of microorganisms by using databases such as the Ribosomal Data Project [Yan, et al., 2007; Cole, et al., 2008].

Based on 16S rRNA gene library analysis, several general microbial diversity surveys of activated sludge and biofilm systems have been reported and summarized in a recent paper [Wagner and Loy, 2002]. In most of the reported 16S rRNA sequences, those affiliated with *Beta-, Alpha-,* and *Gammaproteobacteria, Bacteriodetes,* and *Actinobacter* were the most frequently retrieved [Snaidr, et al., 1997]. Specific microbial groups and strains responsible for enhanced biological phosphorus removal (*Acinetobacter*, *Rhodocyclus*); nitrogen removal (*Nitrosomonas europaea, Nitrobacter* spp.); PHA production (*Rhodopseudomonas palustris* and *Blastochloris sulfoviridis*), and filamentous bacteria (*Nostocoida limicola, Microthrix parvicella*) have also been identified [Snaidr, et al., 1997; Yan, et al., 2007].

Furthermore, several previous studies have reported population shifts in activated sludge microbial communities due to variations in environmental conditions and plant operating conditions. Operating temperatures in WWTPs are primarily influenced by seasons and prevailing weather conditions and it was found previously that Actinomycetes were isolated only during the summer months whereas *E. coli* strains constitute the majority of the *Enterobacteriaceae* group [Mehandjiyska, 1995]. Shock

loading of salts (NaCl) also affected the protozoan and ciliate groups in activated sludge, wherein *Vorticella* spp. and *Opercularia articulate* resisted higher salt dosages better than the other members of the group [Salvado, et al., 2001]. At times, population shifts caused by modifications in wastewater treatment conditions have been taken advantage of in amending problems that negatively affect the performance of wastewater treatment unit processes and also to improve the effectiveness and efficiencies of the said treatment processes. For instance, the addition of a synthetic polymer as solution to filamentous bulking problem in activated sludge systems has also been shown to cause a population shift in the activated sludge microbiota by inhibiting the growth of some predominant bacteria and floc-formers such as *Pseudomonas vesicularis* and *Brevibacterium acetylicum* and the domination of bacteria that were previously constituted the minority in sludge such as *Aeromonas hydrophila* [Juang and Chiou, 2007]. Similar results on the shift of population structure for higher protists (i.e., protozoa and nematodes) in activated sludge before and after synthetic polymer addition were also observed. A high wastewater pH (8.0) has been shown to improve the performance of an enhanced biological phosphorus removal (EBPR) process by favoring the dominance of polyphosphate-accumulating bacteria (*Accumulibacter*) over glycogen-accumulating bacteria (*Competibacter*), thus improving the phosphorus removal efficiency of the process [Oehmen, et al., 2005]. Moreover, an increase in hydraulic retention times (HRT) and addition of an organic carbon substrate (acetate) [Nogueira, et al., 2002], and increase in influent C:N ratios [Okabe, et al., 1996] were found to inhibit the growth of nitrifying bacteria (i.e., *Proteobacteria* belonging to *Nitrospira* group) in biofilm reactors, hence negatively affecting the performance of nitrification process.

These results could implicate similar dynamics in the microbial population of activated sludge when subjected to conditions that are known to be favorable for the growth of oil-accumulating microorganisms. As of the time of writing, no research has yet been found relating the composition of microbial consortia such as activated sludge with the lipid content. The results that could be generated in doing this could pinpoint potential high lipid-accumulating members of the activated sludge microbiota in order that they may be isolated for pure culture fermentations or that the aerobic bioreactor conditions may be optimized for the proliferation of such microorganisms for maximal oil yields from activated sludge.

CHAPTER IV

MATERIALS AND METHODS

This chapter provides a general description of the materials, experimental procedures, and analytical methods used throughout this study. The specific details of the procedures, fermentation conditions, and experimental design are discussed in the succeeding chapters.

Source of Microorganisms

Return activated sludges obtained from the Hilliard Fletcher Wastewater Treatment Plant in Tuscaloosa, AL, which operates an activated sludge biological treatment process, were used as inocula for the fermentation experiments. The samples were stored in 1 L polyethylene bottles with a small headspace provided. These were then transported under ice to the Renewable Fuels and Chemicals Laboratory (RFCL) at Mississippi State University. Upon arrival, the sludge samples were transferred into a 5 L jar and acclimated by aeration at room temperature prior to the fermentation experiments as shown in Figure 4.1.

Figure 4.1: Return activated sludge used in this study.

Synthetic Wastewater Media

A synthetic wastewater shown in Table 4.1 based on the formulation described elsewhere [Ghosh and LaPara, 2004] was used as fermentation medium for the municipal sewage sludge microorganisms in order to simulate the nutrient composition of a typical primary-treated municipal wastewater stream. The recipe was modified for the purpose of this study by the addition of sugars (glucose and/or xylose), and increases in the levels of ammonium sulfate and monobasic and dibasic potassium phosphate levels to provide appropriate levels of carbon, nitrogen, and phosphorus sources for microbial cell growth. Initial sugar and ammonium sulfate concentrations were set according to the experimental designs specified in each chapter. Additionally, the synthetic wastewater medium was supplemented with a trace mineral solution based on Wolfe's mineral

Table 4.1: Modified synthetic wastewater medium formulation [Ghosh and LaPara, 2004].

Component	Concentration (g/L dH_2O)
Sugar	Variable
$(NH_4)_2SO_4$	Variable
Gelatin	0.15
Starch	0.07
Yeast extract	0.07
Casamino acids	0.01
KH_2PO_4	1.50
NaH_2PO_4	1.00
Trace Mineral Supplement	5 mL/L

Table 4.2: Trace mineral supplement used for the synthetic wastewater medium based on Wolfe's formulation [ATCC, 2002].

Component	Concentration (g/L dH_2O)
EDTA	0.5
$MgSO_4 \cdot 7H_2O$	3.0
$MnSO_4 \cdot H_2O$	0.5
NaCl	1.0
$FeSO_4 \cdot 7H_2O$	0.1
$CaCl_2$ anhydrous	0.1
$ZnSO_4 \cdot 7H_2O$	0.1
$CuSO_4 \cdot 5H_2O$	0.01

solution [ATCC, 2002]. All media components were obtained as laboratory- and ACS-grade from Fisher Scientific (Pittsburgh, PA, USA) and used as received.

Fermenter/Bioreactor Set-Up

The fermentation experiments were conducted using a set of three BioFlo® 310 Fermeter/Bioreactors manufactured by New Brunswick Scientific, Inc (Edison, NJ, USA) shown in Figure 4.2. The system consists of one master control unit (Unit 1 located in the middle) and two utility units (Units 2 and 3) located on either side of the master control unit. The utility units are connected and controlled by the master control unit via an

Figure 4.2: BioFlo 310 Fermenters/Bioreactors. LEFT: Set-up showing the master control unit with the VGA touch-screen display in the middle and two utility units on either side. RIGHT: Close-up image of one fermentation unit vessel (New Brunswick Scientific Co., Edison, NJ, USA).

RS232/422 communication port interface. The BioFlo® 310 is a fully-equipped fermentation and cell culture system that can be employed for batch or continuous culture with microprocessor control of pH, dissolved oxygen, agitation, temperature, pump feed, harvesting, antifoam, and vessel level. Each unit consists of the following major components [New Brunswick Scientific Co., 2007]:

- The bioreactor vessel, which has a total volume of 5 L and designed for a maximum working volume of 3.5 L, consisting of a stainless steel head plate, a thick-walled flanged glass tube vessel body, and a detachable stainless steel jacketed bottom-dished head for the circulation of temperature-controlled water. Ports in the headplate are provided for, but are not limited to inoculation, acid and base addition, thermowell for a resistance temperature detector (RTD) probe, foam/level probe, sparger, harvest tube, sampling port, exhaust condenser,

dissolved oxygen probe, and pH probe. The agitation drive bearing housing is also located in the headplate.

- The agitation system, which consists of a removable agitation servo motor attached on top of the bearing housing and connected to the agitation shaft via multi-jaw coupling. The motor provides an agitation speed range of 20 to 1200 RPM and a PID control loop holds the setting to within ±1 RPM.
- The control systems cabinet, which houses the electronic circuitry for controlling aeration, pH, dissolved oxygen, antifoam, addition pumps, and vessel level; as well as three built-in constant speed peristaltic pumps for media and substrate additions and/or culture harvesting, and a water pump and heating element for temperature control. The control system parameters are displayed and controlled through a 15" touch-screen VGA monitor, which is located in the master controller unit in the middle used to control the utility units.

The pH of the media was monitored by a gel-filled pH probe and the dissolved oxygen was monitored by a polarographic DO electrode. The temperature was controlled automatically within the range of 5 to 80 °C (±0.1 °C) using the RTD submerged in the thermowell, which triggers the built-in water pump, solenoid valve, and heating element to supply either hot or cooling water to the fementer jacket as needed. Up to four types of gases, including air, nitrogen, carbon dioxide, and oxygen, can be introduced into the culture through the ring sparger inside the vessel. Gas flow rates were controlled automatically by any of four thermal mass flow controllers for each of the four available gas lines, according to the values set via the master control unit touchscreen display.

General Fermentation Protocols

An overall scheme of the fermentation experiments and analyses conducted in this research is shown in Figure 4.3. This scheme was implemented in all of the experiments conducted in Chapters VI to X. However, more details of the specific experimental designs for each phase of the study are discussed in each of these chapters. The following discussion details the general procedure for the fermentation experiments.

The synthetic wastewater medium was prepared by weighing the required amounts for a 3-L volume of the media. The main carbon source (glucose and/or xylose) was dissolved in 2 L of deionized water and transferred into the bioreactor vessel. The vessel and its contents were then sterilized using an Amsco Century® SG-120 Autoclave (Steris Corp., Mentor, OH, USA) shown in Figure 4.4 at 121 °C and 20 psig for 15 minutes. The nutrient components were dissolved in 400 mL of deionized water in a separate container and sterilized in the autoclave. The sugars were sterilized separately from the nutrients in order to prevent caramelization of the media due to the formation of growth inhibitory glucose degradation products such as aldehydes and dicarbonyl compounds, known as the browning or Maillard reaction [Ingram, 1959]. After sterilization and cooling to room temperature, the nutrient solution was transferred aseptically into the fermenter vessel and combined with the sugars. Calibration of the pH and dissolved oxygen probes were conducted following manufacturer's instructions before and after sterilization. The temperature was set at 25 °C (± 0.1 °C) and the initial pH of the media was set to 6.5 using sterile 1 M H_2SO_4 or1 M NaOH solution.

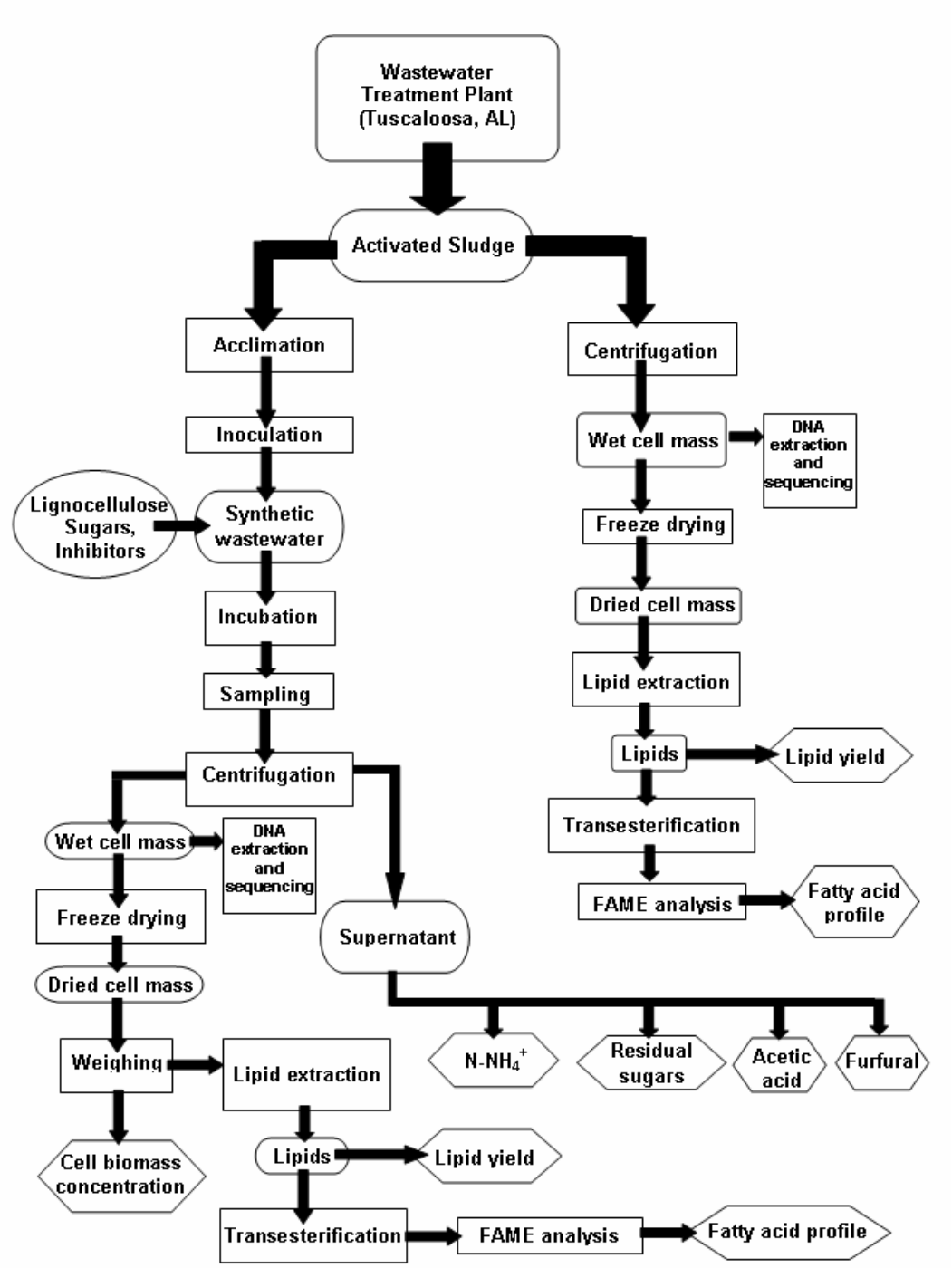

Figure 4.3: Schematic diagram showing the overall experimental plan of this study.

Figure 4.4: Amsco Century SG-120 Laboratory Autoclave/Sterilizer (Steris Corp., Mentor, OH, USA).

After temperature and pH adjustment and aeration of the media to approximately 100 % saturation, the media was inoculated with 20 % (v/v) of activated sludge by aseptically transferring a 600-mL volume of the acclimated activated sludge into the sterile media to a total culture volume of 3 L. Air passed through 0.45-µm HEPA-vent filters (Whatman Inc., Piscataway, NJ, USA) was supplied at a constant rate of 1 L of air/L media/min. Agitation was set at 300 RPM at 0 to 24 h, 400 RPM at 24 to 48 h, and 500 RPM from 48 h up to the end of the experiment. Foaming was controlled by the automatic addition of a 1:10 dilution of a non oil, silicone-based Antifoam 204 concentrate (Sigma Aldrich, St. Louis, MO, USA). The culture was incubated for seven days unless specified otherwise, and duplicate 30-mL samples of the fermentation broth were obtained at specific time intervals and stored in tared DNAse- and RNAse-free 50-mL Corning® plastic centrifuge tubes (Fisher Scientific, Pittsburgh, PA, USA).

Analytical Methods

Cell Biomass Concentration

The cell biomass concentration of the fermentation broth was determined gravimetrically as the dry mass per volume of the culture. The samples were centrifuged at 3,400 × *g* for 20 min using a Sorvall® ST 40 Centrifuge (Thermo Fisher Scientific, Waltham, MA, USA) shown in Figure 4.5. The supernatant were decanted into separate vials and set aside and stored in a freezer for further analysis. The cell pellets were washed twice with 0.85 % (w/v) NaCl and stored in a -80°C freezer (Revco) overnight. The frozen cell pellets were then lyophilized (freeze-dried) using a Freezone® 6 Bulk Tray Freeze Dryer (Labconco Corp., Kansas City, MO, USA) shown in Figure 4.6 for at

least 24 h. After the freeze-drying step, the Corning tubes containing the dried cell masses were weighed using a Pinnacle series analytical balance (Denver Instrument, Bohemia, NY, USA) having a sensitivity of up to 0.01 mg (Figure 4.7). The balance was calibrated internally approximately every 20 weight measurements and dry cell masses were obtained by difference.

Lipid Extraction

The lipid content of the harvested cells was determined by using a modification of the extraction method of Bligh and Dyer [Bligh and Dyer, 1959]. It was found through examination of the chloroform-methanol-water ternary diagram that optimum lipid extraction could be achieved when homogenized tissue samples are mixed with a mixture of chloroform, methanol, and water at a volume ratio of 1:2:0.8, which yields a monophasic solution. The lipid extract was then isolated by diluting the resulting homogenate with water and chloroform to a volume ratio of 2:2:1.8 chlorofrom:methanol:water and centrifuging the mixture, resulting in a heterogeneous mixture containing the following phases: the chloroform layer at the bottom, the cell pellets in the middle, and the methanol/aqueous layer at the top. The chloroform layer theoretically should contain the lipids while the non-lipids are left behind in the methanol-water layer.

For this study, approximately 200 mg of the freeze-dried (Figure 4.8a) and pulverized cell pellets were transferred into a 50-mL glass centrifuge tube. To the dried cell pellets, 5 mL of deionized water, 12.5 mL methanol, and 6.25 mL of chloroform

Figure 4.5: Sorvall ST 40 centrifuge (Thermo Fisher Scientific, Waltham, PA, USA).

Figure 4.6: Freezone 6 bulk tray freeze-dryer used for the dehydration of cell biomass for cell dry mass determination prior to lipid extraction (Labconco Corp., Kansas City, MO, USA).

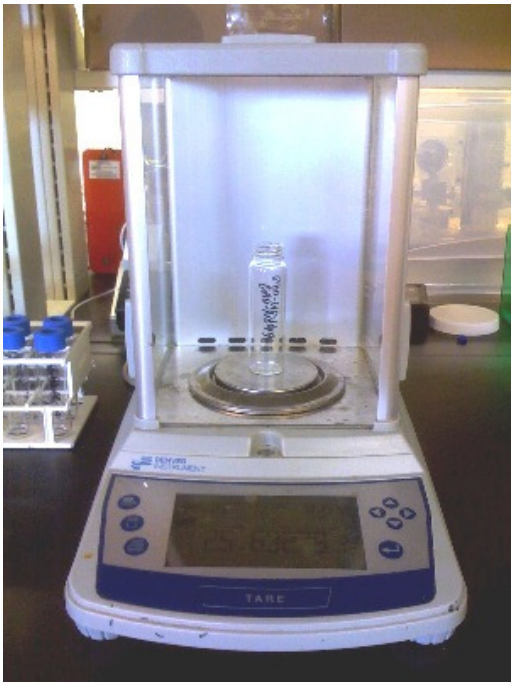

Figure 4.7: Analytical balance used for gravimetric determinations of biomass and lipids in this study (Denver Instrument, Bohemia, NY, USA).

were added to obtain a monophasic mixture. The mixture was then vortex-mixed for 10 minutes, after which an additional 6.25 mL of chloroform and 6.25 mL of deionized water was added to it resulting into the biphasic mixture. The biphasic mixture was then centrifuged at 3,400 × *g* for 20 min using Sorvall® ST 40 Centrifuge (Thermo Fisher Scientific, Waltham, MA, USA), after which three distinct phases (water-methanol, cells, and chloroform) were clearly seen (Figure 4.8b). The bottom chloroform layer was then carefully withdrawn using a long-tipped Pasteur pipette by stabbing through the aqueous and biomass layers while applying positive pressure on the aspirator bulb and then releasing the bulb once the pipette tip has reached the bottom chloroform layer. The chloroform extracts were then passed through another Pasteur pipette that was tightly packed with a plug of glass wool in order to filter out moisture and biomass debris and

collected into tared glass vials. These steps were repeated once more and the combined chloroform extracts were evaporated to dryness using a Turbovap® LV concentrator (Caliper Life Sciences, Hopkinton, MA, USA) operating at a water bath temperature of 52°C and nitrogen pressure of 10-15 psi (Figure 4.9). The vials containing the dried residues shown in Figure 4.8c were then weighed using the analytical balance and the mass of the residue, assumed to be the total lipids from the dried biomass, was obtained by difference.

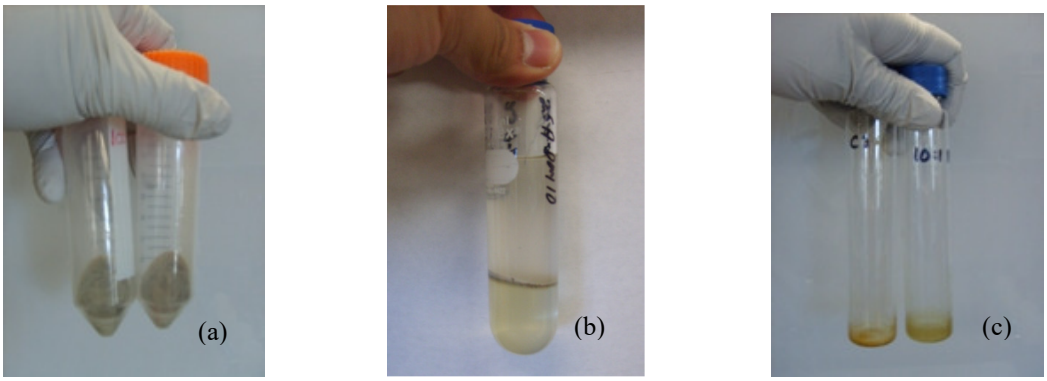

Figure 4.8: Various stages during the extraction of lipids from activated sludge biomass using the modified Bligh and Dyer method: (a) lyophilized biomass used for the extraction; (b) three-phase mixture obtained after second adjustment of $CHCl_3$:CH_3OH:H_2O volume ratios and centrifugation; and (c) dried lipid extract residue obtained after evaporation of chloroform.

Figure 4.9: Turbovap LC concentrator used for recovery of lipid extracts. LEFT: Exterior image. RIGHT: Interior image showing the arrangement of the vials containing the chloroform extracts and the gas flow needles (Caliper Life Sciences, Hopkinton, MA, USA).

Conversion of Lipids to Fatty Acid Methyl Esters (FAMEs)

The lipid residues obtained via Bligh and Dyer extraction method were then converted into their fatty acid methyl ester derivative to facilitate the analysis of its fatty acid composition and saponifiable fraction using the following transesterification procedure based on the method of Christie [Christie, 2003]. To the dried lipid residue in the glass vial, 2 mL of a 2 % (v/v) sulfuric acid in methanol solution was added. The mixture was then vortex mixed well and incubated at 60°C (± 1°C) for two hours in an Isotemp 110 water bath incubator (Fisher Scientific, Pittsburgh, PA, USA) in order to ensure complete derivatization of the lipid samples. After the two-hour reaction time has elapsed, the mixture was cooled to room temperature and quenched with 5 mL of a 3 % $NaHCO_3$ and 5 % NaCl (v/v) aqueous solution. Then, 2 mL of Optima-grade toluene (Fisher Chemical, Pittsburgh, PA, USA) containing 200 ng/µL of the internal standard 1,3-dichlorobenzene and 100 ng/µL of butylated hydroxyltoluene (BHT) (Sigma Aldrich,

St. Louis, MO, USA) was added to the quenched mixture. The mixture was then vortex-mixed well and allowed to stand in order to separate the toluene and aqueous layers. The top toluene layer was withdrawn using a long-tipped Pasteur pipette and transferred into an 8-mL amber glass vial containing a pinch (≈ 0.5 g) of anhydrous sodium sulfate to remove any remaining water in the toluene layer. The extraction step was repeated once in order to ensure maximum recovery of the methyl esters in the mixture. The toluene extracts were combined into the glass vial with the anhydrous sodium sulfate. The dried toluene extracts were then withdrawn and transferred into another 8-mL amber vial after standing overnight and then diluted into a 1:4 volume ratio using the toluene containing the internal standard and BHT described previously. The diluted samples were then transferred into 2-mL autosampler vials (Fisher Scientific, Pittsburgh, PA, USA) for analysis by gas chromatography.

FAME Analysis by Gas Chromatography

The fatty acid composition and saponifiable fraction (i.e., the sum of fatty acid methyl ester derivatives) of the lipid extracts were analyzed via gas chromatographic analysis of the methyl ester derivatives of the fatty acids contained in the lipid samples. Since these methyl esters were considerably volatile at 300 °C, a gas chromatographic analysis with flame ionization detection (FID) was employed. A schematic diagram of a typical gas chromatograph is shown in Figure 4.10. In this method, the liquid or gas sample is vaporized upon introduction into the instrument via an injector, which is

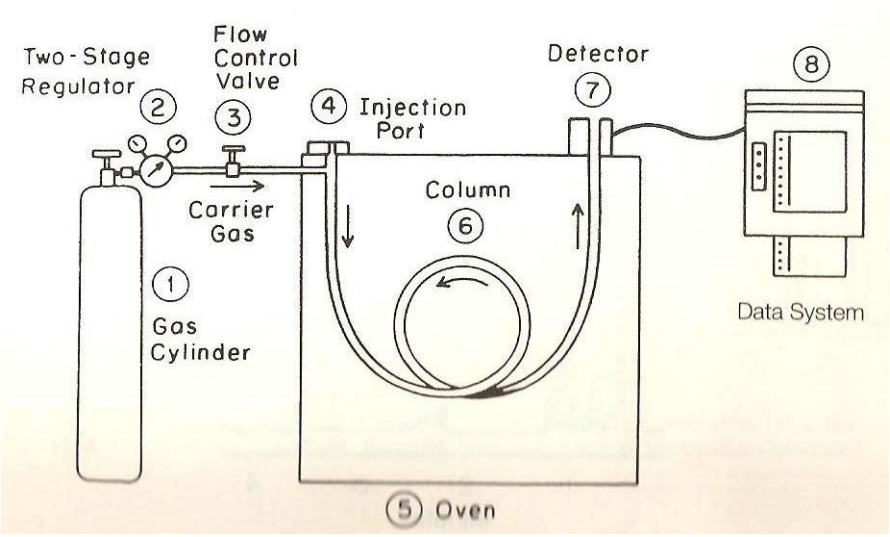

Figure 4.10: Schematic diagram of a typical gas chromatograph [McNair and Miller, 1998].

typically heated from 200-300 °C, which is high enough to vaporize most compounds rapidly. The vaporized sample is then carried by a high purity inert carrier gas such as helium or nitrogen (*mobile phase*) through an analytical column containing the *stationary phase*. These columns are typically wall-coated open tubular (WCOT) in construction with the stationary phase coating the inner wall of the capillary column [Christie, 2003]. The sample then partitions between the mobile and stationary phases based on their solubilities at a given temperature and their components (*analytes* or *solute*) are separated from one another based on their relative vapor pressures and affinities for the stationary phase, as represented by the parameter called the *distribution constant* K_C:

$$K_C = \frac{[A]_S}{[A]_M} \tag{4.1}$$

which is defined as the concentration of the analyte or solute in the stationary phase divided by its concentration in the mobile phase [McNair and Miller, 1998]. Based on this premise, an analyte A with a higher affinity (i.e., stronger Van der Waals forces) toward the stationary phase, hence higher K_C will have a greater distribution in the stationary phase, and as a consequence it spends longer time (*retention time*) in the stationary phase than another analyte B with less affinity and K_C toward the stationary phase in the column. Therefore analyte B is carried out or *elutes* from the column faster than analyte A. Eventually all analytes leave the column and pass through a *detector* which produces a signal called *chromatogram*, which represents the separation attained among the analytes as signal peaks in given sample.

The column is housed in an oven, which also controls the column temperature. In most applications such as in samples with analytes having a wide range of boiling points (BP), temperature programming as opposed to isothermal condition is the most popular and widely used [McNair and Miller, 1998]. The effect of column temperatures in the separation of analytes in a sample is summarized as follows: At low temperatures, the vapor pressures of the analytes are low, hence they move slowly through the column leading to longer analysis times; however there is better *resolution*, or higher degree of separation between adjacent peaks. On the other hand, higher temperatures result into decreased retention times; therefore shorter analyses times, but at the expense of reduced resolution. Therefore, in a sample containing components having a wide range of boiling temperatures, the temperature of the oven, hence the column, can be programmed such that it starts at a low level (i.e., 50°C) to allow the separation of the low BP components, after which the temperature is programmed to increase at a specific rate (i.e., 8°C/min) up

to a temperature higher than the first isothermal value (i.e., 250°C). The effect of increasing the temperature is that it decreases K_C of the higher BP analytes remaining in the column so that they elute at a faster rate.

The analytes exiting the column are then passed through the detector, which produces an electrical signal in response to the presence of a specific compound. The FID can be used for virtually all organic compounds, has a high sensitivity and stability, low volume, fast response time, and a linear response over a very wide range of concentrations [Christie, 2003]. The detector operates by detecting the ions that are generated by the combustion of the organic compounds as they elute from the column in a diffusion flame of hydrogen and air. The ions are then passed through a cylindrical collector electrode that is placed just above the hydrogen-air flame wherein a potential is applied across it. The ion current produced as the ions are passed through the potential is then measured, the signal current amplified and recorded, and the response is matched with signals produced from specific compounds for identification and quantification.

In this study, an Agilent 6890N Gas Chromatograph (Agilent Technologies, Palo Alto, CA, USA) equipped with a flame ionization detector (FID) and a Restek 11023 Stabilawax DA 30 m × 0.25 mm ID capillary column with a 0.25-µm film thickness was used (Figure 4.11). Two microliters of the sample were injected by means of an autosampler into an injector operating at a constant temperature of 260 °C in splitless mode. Ultra high purity grade helium (Nexair, Memphis, TN, USA) at 40 psi flowing at

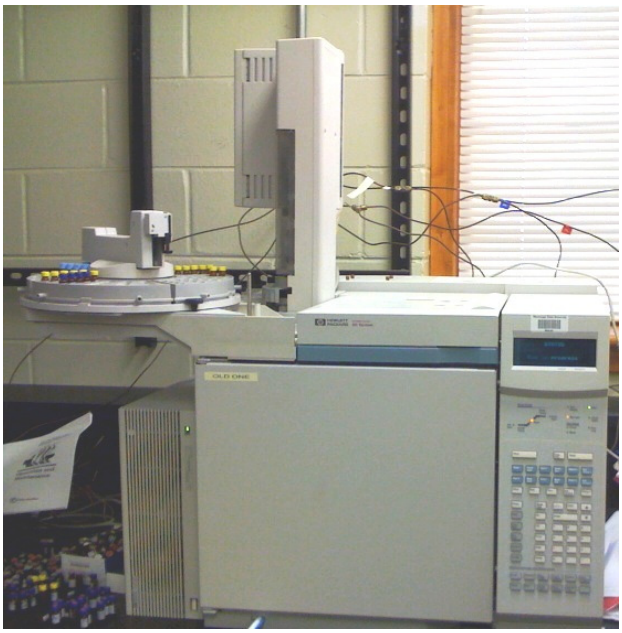

Figure 4.11: The Agilent 6890N gas chromatograph equipped with a flame ionization detector (GC-FID) and autosampler used for FAME analysis (Agilent Technologies, Palo Ato, CA, USA).

53.5 mL/min was used as the carrier gas. The oven temperature was programmed to start at 50 °C for 2 minutes, and then ramped to 250 °C at 10 °C/min where it remained constant for 13 minutes. The detector temperature is set at 260 °C and 40 mL/min of compressed dry air and 400 mL/min of ultra high purity hydrogen (Nexair, Memphis, TN, USA) was used to produce the flame in the FID. The gas chromatograph was calibrated using five dilution levels of a FAME mix standard solution containing C_8 to C_{24} methyl esters (Sigma Aldrich, St. Louis, MO, USA). The compounds were calibrated according to their relative response factors with respect to the internal standard, 1,3-dichlorobenzene. The relative response factor is given as:

$$f_X = f_{IS} \times \left(\frac{A_{IS}}{A_X} \right) \times \left(\frac{w_X}{w_{IS}} \right) \qquad (4.2),$$

where f_X is the relative response factor of the calibrated or unknown compound, f_{IS} is the response factor of the internal standard and was arbitrarily assigned the value of 1.00, (A_{IS}/A_X) is the area ratio of the internal standard to the calibrated compound, and (w_X/w_{IS}) is the weight ratio of the calibrated compound to the internal standard [McNair and Miller, 1998]. Rearranging Equation 4.2 leads to the equation:

$$\left(\frac{A_X}{A_{IS}}\right) = \frac{1}{f_X}\left(\frac{w_X}{w_{IS}}\right) \qquad (4.3),$$

which is the linear response equation used for the calibration obtained by plotting the area ratios versus the amount ratios at five dilution levels for the specific compound to get the slope, which is the reciprocal of the relative response factor.

A list of the fatty acid methyl esters calibrated for quantification by the instrument with their corresponding average retention times and relative response factors are shown in Table 4.3. Analyte peaks in the samples were identified by matching their retention times within a retention window of ± 2 % of the retention time of the calibrated FAMEs and quantified using Equation (4.3). The peak responses for unidentified peaks were quantified based on the response factor of palmitic acid (C16:0) since its response factor represents the median value among the calibrated FAMEs. Blank and midpoint calibration standards were injected along with the samples during each sequence run to ensure consistency of compound resolution and retention times and baseline detector responses.

Table 4.3: Calibration parameters of standard FAMEs used for gas chromatographic analysis of activated sludge lipid extracts.

Compound	Formula	Retention Time (min)	Relative Response Factor	Coefficient of determination, R^2
Octanoic AME	C8:0	7.579	0.88	0.99997
1,3-dichrolobenzene†	$C_6H_4Cl_2$	7.924	1.00	N/A
Decanoic AME	C10:0	10.026	0.79	0.99996
Lauric AME	C12:0	12.324	0.75	0.99996
Myristic AME	C14:0	14.436	0.71	0.99996
Palmitic AME	C16:0	16.38	0.69	0.99997
Palmitoleic AME	C16:1	16.617	0.70	0.99995
Stearic AME	C18:0	18.17	0.68	0.99996
Oleic AME	C18:1	18.34	0.65	0.99993
Linoleic AME	C18:2	18.737	0.70	0.99997
Linolenic AME	C18:3	19.281	0.71	0.99998
Arachidic AME	C20:0	19.83	0.68	0.99997
Behenic AME	C22:0	21.379	0.70	0.99997
Erucic AME	C22:1	21.545	0.67	0.99998
Lignoceric AME	C24:0	22.926	0.72	0.99998

†Internal standard.

Determination of Residual Sugars by YSI Analyzer

The supernatant samples were analyzed for residual levels of two sugars, namely glucose and xylose using a YSI 2700 Select Biochemistry Analyzer shown in Figure 4.12 (YSI Inc. Life Sciences, Yellow Springs, OH, USA). The instrument consists of a main unit which houses the buffer, calibrator solution, and waste reservoirs; buffer, calibrator, and sipper pumps; sipper arm assembly, and the sample chamber with two attached sensor probes; as well as an LCD display, numeric keypad, and a printer. A model 2710 Turntable is attached to the main unit for automated sampling and the whole unit is controlled via an RS232/422 communications interface using the LabView™ data-logging software. The analyzer is configured with dual probes containing glucose oxidase and pyranose oxidase membranes for the simultaneous analysis of glucose and xylose

Figure 4.12: YSI 2700 Biochemistry Analyzer used for residual glucose and xylose analysis (YSI Inc. Life Sciences, Yellow Springs, OH, USA). LEFT: Exterior image showing the attached 2710 Turntable. RIGHT: Interior image of the main unit.

concentrations, respectively in complex matrices such as fermentation cultures of lignocellulose hydrolyzates [YSI Inc., 2008]. These membranes allow for rapid (approx. 2 min) specific glucose measurements in the range of 0.05 to 9.00 g/L and xylose measurements in the range of 0.5 to 30.0 g/L in undiluted samples by measuring the current of the sample in nanoamperes (nA). Calibration is performed automatically by the instrument using commercially-available standard 2.50 g/L glucose (YSI 2776) and 20.0 g/L xylose (YSI 2767) calibrator solutions. Linearity standard solutions for glucose, 9.00 g/L (YSI 1531) and xylose, 30.0 g/L (YSI 2768) are also used to test the linearity of the instrument response.

The samples were prepared by diluting 1 mL of the fermentation broth supernatant sample with 3 mL commercially available phosphate buffer (YSI 2357) in a glass test tube. The resulting mixture was then vortex-mixed and the test tube was placed into the turntable. Thirteen microliters of the diluted sample was then aspirated from the

test tube by the motorized sipper arm assembly and transferred into the sample chamber, and is diluted with the buffer solution and mixed with the built-in stir bar inside the sample chamber. The amount of sugars in the sample was then measured using the two probes with the specific membranes for glucose and xylose measurements. Each probe contains a sliver and platinum electrode and is fitted with a three-layer membrane containing the immobilized enzymes in the middle layer. The face of the probe, covered with the membrane, is situated in a buffer-filled sample chamber into which the samples are injected. The analyte (sugars) in the sample then diffuses through the membrane and upon contact with the immobilized enzyme, undergoes rapid oxidation to produce hydrogen peroxide. For glucose, the reaction is given as:

$$\beta - \text{D-glucose} + O_2 \xrightarrow{\text{Gluc oxidase}} \text{glucono-}\delta\text{-lactone} + H_2O_2 \qquad (4.4)$$

The hydrogen peroxide (H_2O_2) is oxidized in the platinum anode to yield electrons:

$$H_2O_2 \xrightarrow{\text{Pt anode}} 2H^+ + O_2 + 2e^- \qquad (4.5)$$

A dynamic equilibrium is achieved when the rate of H_2O_2 production and the rate at which H_2O_2 leaves the immobilized enzyme layer are constant and is indicated by a steady state response. The electron flow is linearly proportional to the steady state H_2O_2 concentration, and therefore the concentration of the substrate [YSI Inc., 2000].

Determination of Residual Ammonium-Nitrogen by Ion Chromatography

Analysis of the residual ammonium-nitrogen (NH_4^+) was conducted to monitor the nitrogen levels for cell growth and metabolism, and to determine the point of nitrogen limitation, which theoretically signals the start of the lipid accumulation phase. Ion chromatography (IC) or ion-exchange chromatography was first developed by the Dow

Physical Research Lab (now Dionex) in the early 1950s in order to replace the numerous wet chemistry methods for different inorganic ions with a single chromatographic procedure [Michalski, 2006; Dionex Corp., 2010]. Ion chromatography (IC) is based on the separation of ions or polar molecules based on their charge properties and interaction with chemically-bound ions having an opposite charge [Haddad and Jackson, 1990]. A schematic diagram of a typical modern IC system utilizing suppressed conductivity detection is shown in Figure 4.13. Samples containing the analyte ions are carried by the mobile phase called the *eluent*, whose role is to compete with solute ions for the fixed ions in the stationary phase and to separate the mixture of solute ions into well-defined peaks [Haddad and Jackson, 1990]. Eluents used for both suppressed and non-suppressed IC may include aromatic and aliphatic carboxylic acids and salts, sulfonic acid and salts, and potassium hydroxide for anion separations; and inorganic acids, organic bases, and complexing eluents for cation separations. The stationary phases used in IC are typically ion-exchange resins with charged functional groups such as sulfonic acid $\left(\text{-}SO_3^-H^+\right)$, carboxylic acid $\left(\text{-}COO^-H^+\right)$, and phosphonic acid $\left(\text{-}PO_3H^-H^+\right)$ for cation exchangers; and primary $\left(\text{-}NH_3^+OH^-\right)$, secondary $\left(\text{-}NH_2^+(CH_3)^+OH^-\right)$, tertiary $\left(\text{-}NH^+(CH_3)_2^+OH^-\right)$, and quaternary $\left(\text{-}NH(CH_3)_3^+OH^-\right)$amines for anion exchangers [Haddad and Jackson, 1990].

The proper choice of the eluent depends on the on selectivity coefficient $K_{A,E}$. For an ion-exchange process involving *y* moles of the solute ion A^{x-} exchanging with *x* moles of the competing (eluent) ion E^{y-}:

$$yA_r^{x-} + xE_m^{y-} \qquad yA_m^{x-} + xE_r^{y-} \tag{4.6},$$

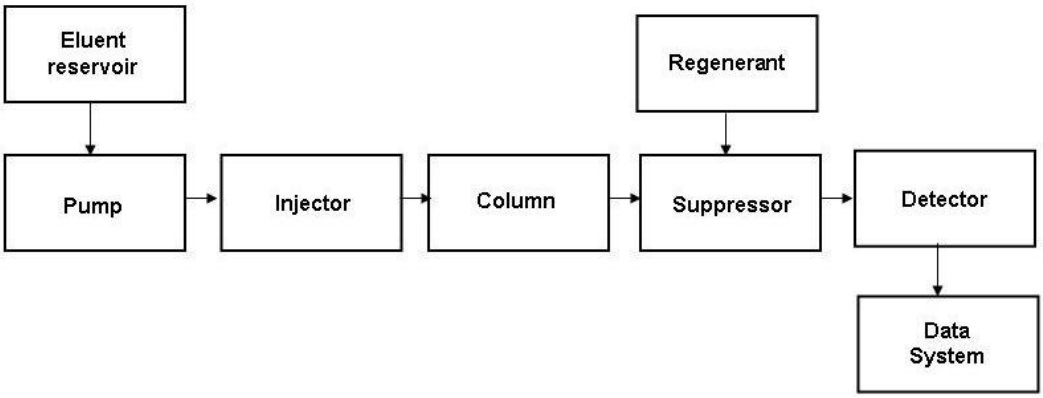

Figure 4.13: Block diagram of an ion chromatograph with suppressed conductivity detection [Haddad and Jackson, 1990].

Figure 4.14: ICS-3000 ion chromatograph used for residual ammonium analysis (Dionex Corp., Sunnyvale , CA, USA).

the selectivity coefficient $K_{A,E}$ is given by:

$$K_{A,E} = \frac{\left[A_r^{x-}\right]^y \left[E_m^{y-}\right]^x}{\left[A_m^{x-}\right]^y \left[E_r^{y-}\right]^x} \quad (4.7).$$

where the subscripts *m* and *r* refer to the mobile (or eluent) and resin (or stationary) phases, respectively. At $K_{A,E}$ values greater than unity, the stationary phase will contain a higher concentration of the analyte ion A^{x-} that the eluent (mobile phase), hence has a higher selectivity towards A^{x-} than E^{y-} and vice versa. A higher selectivity implies a longer retention time for the analyte ion and hence, longer analyses times. Therefore, suitable eluent is one which provides a value of $K_{A,E}$ which leads to an appropriate degree of retention for the solute ion [Haddad and Jackson, 1990]. In addition to the nature of the eluent, separations according to selectivity and retention times can also be controlled by adjusting the concentration of the competing ion as well as the pH of the eluent. The mobile phase containing the analyte eluting from the column then passes through a device called *suppressor* where the conductivity of the eluent is neutralized by electrolysis without affecting the conductivity of the analyte in order to provide a lower baseline for the subsequent detection of the analytes using a conductivity detector. The conductivity detector then measures the conductivity of the eluent and the analytes are identified based on their retention times and quantified by correlating the detector response with the concentration of the analyte in the solution.

For this study, the samples were analyzed using an isocratic IC method as follows: Supernatants obtained earlier via centrifugation of fermentation broth samples

were pretreated by passing 20 mL of the sample through a C_{18} SepPak Cartridge (Waters Corp., Millford, MA, USA) that was preconditioned with 5 mL of Optima grade methanol (Fisher Scientific, Pittsburgh, PA, USA) and 5 mL of ASTM Type II deionized water with an 18-mΩ-cm resistivity, in order to remove hydrophobic organics in the sample that may shorten the service life of the analytical and guard columns [Dionex Corp., 2008]. The eluent from the cartridges were then collected, diluted to a 1:20 volume ratio with ASTM Type II deionized water, filtered through 0.45-µm syringe filters (Millipore, Billerica, MA, USA), and transferred into autosampler polyvials. Twenty-five microliters of the diluted sample was injected by means of the AS40 Autosampler into an ICS-3000 Dual System Ion Chromatograph shown in Figure 4.14 (Sunnyvale, CA, USA) equipped with an IonPac CS16 cation exchange analytical column (250 × 5 mm ID) containing carboxylic acid functional groups immobilized in cation exchange resins and CG16 guard column (50 × 5 mm ID) operating at 30°C. A 38 mM methanesulfonic acid (MSA) solution generated on site using the eluent generator module and flowing at the rate of 1.0 mL/min was used as the eluent, producing a total background pressure ≥ 2300 psi. The CSRS 300 suppressor current was set at 100 mA and the total analysis time was 10 min. The instrument was calibrated using five dilution levels of commercially available six-cation Standard Mix (PN 040187) manufactured by Dionex (Sunnyvale, CA, USA). The average elution time for the ammonium peak is approximately 10 minutes.

Analysis of Acetic Acid and Furfural by Gas Chromatography

Residual concentrations of acetic acid and furfural in the culture were measured using solvent extraction and subsequent analysis of the extracts by gas chromatography with flame ionization detection (GC-FID) based on a method described previously [Thomann and Hill, 1986]. Fermentation broth supernatant samples were transferred (0.5 mL) in microcentrifuge tubes, into which 1 mL of Optima® grade chloroform (Fisher Scientific, Pittsburgh, PA, USA) containing 1 g/L of hexanoic acid (Sigma Aldrich, St. Louis, MO, USA), and 0.5 g of NaCl was added. The contents were then mixed by inverting the tubes 18 times in 10 s, after which the tubes are centrifuged at 13,400 × *g* for 30 s using a Model 5415D Microcentrifuge (Eppendorf NA, Hauppauge, NY, USA) shown in Figure 4.15. After centrifugation, the bottom (chloroform) layer was withdrawn using a long-tipped Pasteur pipette and transferred into an autosampler vial with glass inserts. The samples were then analyzed using an Agilent 6890N Gas Chromatograph (Agilent Technologies, Palo Alto, CA, USA) equipped with a flame ionization detector (FID) and a Restek 11023 Stabilawax DA 30 m × 0.25 mm ID capillary column with a 0.25-µm film thickness was used (Figure 4.16). Two microliters of the sample were injected by means of an autosampler into an injector operating at a constant temperature of 250 °C in splitless mode. Ultra high purity grade helium (Nexair, Memphis, TN, USA) at 40 psi flowing at 53.5 mL/min was used as the carrier gas. The oven temperature was programmed to start at 50 °C for 2 minutes, and then ramped to 250 °C at 10 °C/min where it remained constant for 13 minutes. The detector temperature is set at 300 °C and 40 mL/min of compressed dry air and 400 mL/min of ultra high purity grade hydrogen

Figure 4.15: Eppendorf 5415 D microcentrifuge used in this study (Eppendorf NA, Hauppauge, NY, USA).

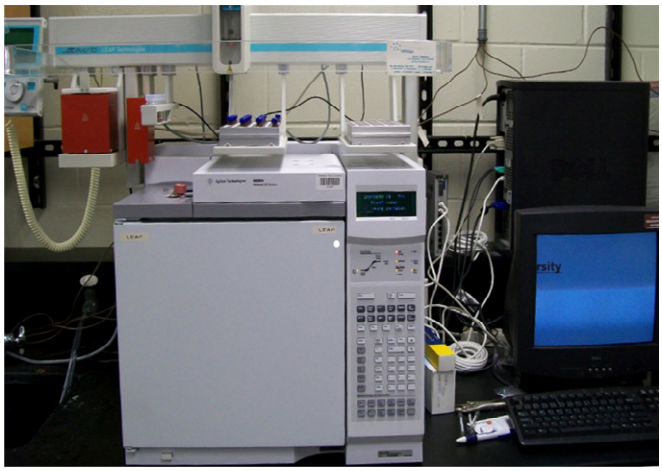

Figure 4.16: Agilent 6890N gas chromatograph used for acetic acid and furfural analysis.

(Nexair, Memphis, TN, USA) was used to produce the flame in the FID. The syringe needle was rinsed with acetone in between sample injections to avoid precipitation and blockage in the syringe needles. The instrument was calibrated using a standard solution containing known amounts of acetic acid and furfural based on the response factor of the internal standard hexanoic acid. The average retention times of acetic acid, furfural, and hexanoic acid were found to be at 10.5, 11, and 15.3 min, respectively.

Analysis of Activated Sludge Microbial Communities by 16S rRNA Sequencing

Analysis of composition activated sludge microbial communities before and after fermentation of sugars for microbial lipid production was performed using sequence analysis of 16S rRNA gene clone libraries via a full cycle rRNA approach. The so-called full-cycle rRNA approach based on the 16S rRNA method involves extraction of nucleic acids from the sludge biomass followed by amplification of the 16S rDNA (rRNA) gene via polymerase chain reactions (PCR), construction of 16S rRNA clone libraries, and identification of microorganisms by using databases such as the Ribosomal Data Project [Yan, et al., 2007; Cole, et al., 2008].

Grab samples of raw activated sludge (n = 10) and temporal fermentation broth samples (n=10) in activated sludge cultures grown under low and high C:N ratios using glucose were collected in sterile 2.0-mL RNAase- and DNAse-free polypropylene microcentrifuge tubes. The samples were then centrifuged at 13,400 × *g* for 5 min using a Model 5415D Microcentrifuge (Eppendorf NA, Hauppauge, NY, USA) shown previously in Figure 4.15. The supernatants were decanted and discarded and the biomass pellets

were stored in a -80°C freezer until further processing and were subsequently sent to the the U.S. Environmental Protection Agency (EPA), National Risk Management Research Laboratory in Cincinnati, OH, USA for DNA extraction, amplification, and cloning. These were conducted by the group of J.W. Santo Domingo, Ph.D. according to the following protocols: DNA was extracted from the biomass using PowerSoil® DNA isolation kits (Mo Bio Laboratories, Inc., Carlsbad, CA, USA) following the manufacturer's instructions. The DNA extracts were stored in new sterile microcentrifuge tubes at -20°C until further processing.

Polymerase chain reaction (PCR) assays on the DNA extracts obtained from raw and cultured sludge biomass were conducted in order to amplify the 16S rRNA gene fragments in the samples. This technique is widely used for the amplification of specific DNA fragments with out the need for bacterial cells. It employs a heat-stable DNA polymerase called *Taq* polymerase, originally obtained from *Thermus aquaticus*, a bacterium that grows in hot springs at temperature above 90 °C [Karp, 2008]. Various protocols of PCR have been developed and conducted since its inception in 1983 by Kary Mullis of Cetus Corporation [Karp, 2008]; however the simplest protocol involves mixing a sample of DNA with an aliquot of *Taq* polymerase and deoxyribonucleotides along with a large excess of two short synthetic DNA fragments or oligonucleotides that are complementary to DNA sequences at the 3' ends of the region of DNA to be amplified. These oligonucleotides serve as *primers* into which the nucleotides are added during the replication steps. The mixture is then heated (95 °C) to allow the DNA molecules in the sample to separate into their two component strands, after which it was cooled to around 60 °C to allow the primers to hybridize the strands of the target DNA.

The temperature is then raised to around 72 °C to allow the polymerase to add nucleotides to the 3' end of the primer. As the polymerase extends the primer, it selectively copies the target DNA to form new complementary DNA strands. This temperature cycle is repeated several times, each time doubling the amount of the specific DNA region that is flanked by the bound primers. In this process, billions of copies of the DNA region can be generated in a matter of hours using a machine called a *thermal cycler* that automatically changes the temperature of the reaction mixture to allow each step of the cycle to take place [Karp, 2008].

In this study, four dilutions (by volume 1:1, 1:10, 1:20, and 1:50) of the DNA extracts were prepared and mixed with 25 µL of PCR solution containing the following reagents: 18 µL of UltraPure water; 2.5 µL of Ex *Taq* 10×buffer, 20 mM Mg^{2+} (Takara Bio Inc., Shiga, Japan); 2 µL of Ex *Taq* deoxynucleoside triphosphate (dNTP) 2.5 mM mixture (Takara Bio Inc., Shiga, Japan); 0.125 µL Ex *Taq* DNA polymerase, and 0.5 µL each of the forward (8F) and reverse (787R) universal bacterial 16S rRNA gene-targeted primers. Reactions were conducted on a DNA Engine Tetrad 2 Thermal Cycler equipped with four Alpha Unit 96-well reaction modules (Bio-Rad Laboratories, Hercules, CA, USA) shown in Figure 4.17 using the following temperature program: 94 °C for 5 min followed by 35 cycles of 94 °C for 20 s, 58 °C for 20 s, and 72 °C for 30 s, and a final extension step consisting of 72 °C for 5 min. To test for the presence of extraneous DNA contamination that may have been introduced during laboratory procedures, extraction blanks (n =8) were included in the PCR assays. The amplification products were visualized using 1 % agarose gels (Amresco, Solon, OH, USA) and GelSTAR nucleic acid stain (Cambrex Bioscience, East Rutherford, NJ, USA). Images of the PCR products

(Figure 4.18) were photographed under UV light using a Kodak EDAS 290 Camera (Eastman Kodak Co. Image Sensor Solutions, Rochester, NY, USA).

Clone libraries were developed for activated sludge DNA samples prior to the treatments (t=0) and for each of the treatments at days 3 and 7 of cultivation. DNA cloning is often used to produce DNA *libraries,* which are basically collections of cloned DNA fragments for later use in DNA sequencing. The PCR amplification products were purified using a QIAquick PCR purification kit according to manufacturer's instructions (Qiagen, Valencia, CA, USA). Representative purified PCR samples were cloned into pCR®4-TOPO vector as described in the user manual (Invitrogen, Carlsbad, CA, USA). Individual *Escherichia coli* clones were subcultured into 300 µL of commercially-available Luria broth containing 50 µg/mL ampicillin and screened for inserts using M13 PCR. The clones were then submitted to the Children's Hospital DNA Core Facility (Cincinnati, OH, USA) for sequencing using Big Dye sequencing chemistry (Applied Biosystems, Foster City, CA), M13 forward and reverse primers, and a Prism 3730XL DNA Analyzer. The sequences were manually verified and cleaned using the Sequencher 4.7 software (Gene Codes, Ann Arbor, MI). The generated 16S rRNA sequences were then classified and the relative abundance of microbial groups were determined using the LIBCompare on-line computer software available online at http://rdp.cme.msu.edu/ [Cole, et al., 2008].

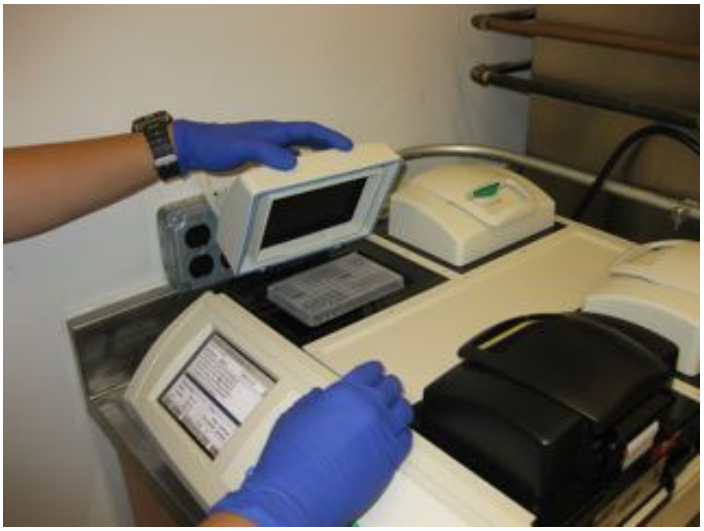

Figure 4.17: DNA Engine Tetrad 2 Thermal Cycler equipped with four Alpha Unit 96-well reaction modules (Bio-Rad Laboratories, Hercules, CA, USA).

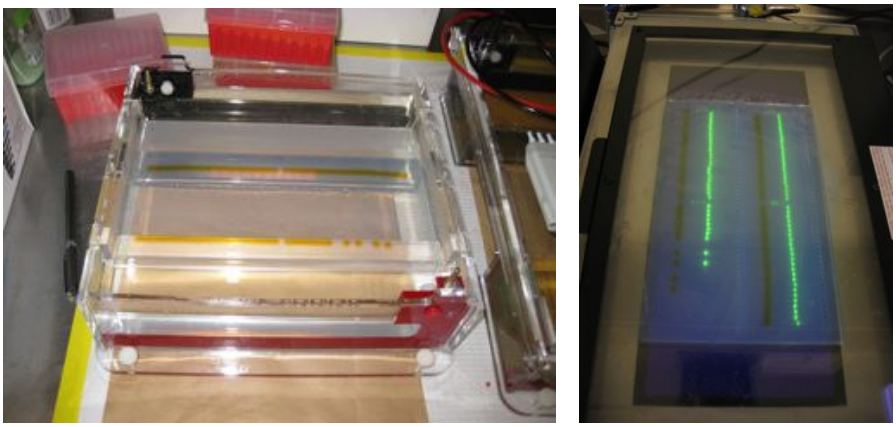

Figure 4.18: Left: PCR amplification products of activated sludge DNA extracts in 1% agarose electrophoresis gel. Right: Products imaged under UV light.

CHAPTER V

FERMENTATION KINETICS MODELING THEORY

Analysis of the kinetics of oil accumulation by activated sludge was conducted with the following objectives: (1) To develop mathematical models that accurately describe the behavior of activated sludge microbial communities in lipid production cultures in batch, fed-batch, and continuous bioreactors; and (2) to obtain estimates of kinetic model parameters needed for process and bioreactor design and scale-up. The following texts describe the proposed kinetic models and the modeling theory in each of the fermentation modes investigated.

Batch Fermentation

The batch fermentation mode involves a microbial culture supplied with an initial charge of medium that is not altered by further nutrient addition or removal, and is therefore the simplest and widely used in both the laboratory and in industry [Shuler and Kargi, 2002]. Initially, the mathematical model for batch fermentation kinetics of activated sludge microorganisms in an aerobic lipid accumulation cultures was developed based on three target processes: cell growth represented by non lipid biomass biosynthesis, lipid accumulation, and sugar utilization. The following modeling approach was widely used specifically in fermentations for the production of biomass-associated

products such as xanthan gum [Klimek and Ollis, 1980; Weiss and Ollis, 1980]; the biopolymer hyaluronic acid or HA [Don and Shoparwe, 2010]; and microbial lipids from oleaginous yeast *Rhodotorulla gracilis* CFR-1 [Karanth and Sattur, 1991; Sattur and Karanth, 1991]. Based on microorganism behavior and transient characteristics common to batch processes such as microbial growth, variations in sugar concentration, and accumulation of metabolic products, a set of modeling hypotheses was formulated for each for target processes.

Microbial growth

Microbial growth is a considered to be a complex process affected by various factors in the physiochemical environment of microorganisms such at temperature, pH, and the amount of available substrate and nutrients in the growth medium and is a result of both change in cell size and replication [Shuler and Kargi, 2002]. Microorganisms can grow under a variety of environmental conditions and extract the substrate and nutrients from the medium and convert them into biological compounds or for energy production. As a result, the total mass of microbial biomass increases with time and the rate of microbial growth is expressed as

$$\frac{dX}{dt} = \mu_{\text{net}} X \tag{5.1}$$

where μ_{net} is the net *specific growth rate* (h^{-1}), which is analogous to a first-order reaction rate constant in chemical processes. Integrating Equation 5.1 leads to

$$X = X_0 e^{\mu_{\text{net}} t} \tag{5.2}$$

where X and X_0 are the cell biomass concentrations (g/L) at any time t and at $t = 0$, respectively. The relationship between the specific growth rate and the initial substrate concentration in the medium often assumes a form of saturation kinetics, which implies growth inhibition due to the presence of high amounts of substrate (substrate-limited growth). Assuming that microbial growth is dependent only on a single species S, and that endogenous metabolism or cell death is negligible compared to the growth rate, the growth kinetics can be described by the Monod equation

$$\mu_{\text{net}} = \mu_g = \frac{\mu_{\max} S}{K_S + S} \tag{5.3}$$

where S is the initial substrate concentration (g/L) in the medium, K_S is the *saturation constant* or *half velocity constant* (g/L) equal to the concentration of the rate-limiting substrate when the specific growth rate is equal to one-half of the maximum, and $\mu_{\max}$ is the maximum specific growth rate (h^{-1}) when $S >>> K_S$. The Monod equation is analogous to the Langmuir-Hinshelwood kinetics in traditional chemical kinetics or Michaelis-Menten kinetics for enzyme reactions. The parameters $\mu_{\max}$ and K_S may be evaluated via the double reciprocal or Lineweaver-Burke plot by taking the reciprocal of both sides of Equation 5.3:

$$\frac{1}{\mu_g} = \frac{X}{r_g} = \frac{K_S}{\mu_{\max}} \frac{1}{S} + \frac{1}{\mu_{\max}} \tag{5.4}$$

where $r_g = dX/dt$. Values of the growth rate are calculated by using the polynomial method and then X/r_g is plotted against $1/S$. By linear regression, the slope $K_S / \mu_{\max}$ and y-intercept $1/\mu_{\max}$ are obtained and used to calculate $\mu_{\max}$ and K_S [Fogler, 2006].

However, Equations 5.1 - 5.4 have limited utility for the kinetic analysis of fermentation systems such as EPS and microbial lipid production because these equations are only valid for the exponential growth phase whereas the major part of the fermentation involving lipid accumulation and a considerable portion of the biomass increase occurs during the stationary phase [Sattur and Karanth, 1991]. Hence, it was desired to have a kinetic expression for biomass that is valid for the entire course of the fermentation process at the same time should describe the substrate/media inhibition effect towards microbial growth.

Similar to the previous studies mentioned that involved products that are produced as fractions of the total biomass, the Logistic equation was used to characterize microbial growth in terms of the carrying capacity of the culture independent of the substrate concentration. The Logistic equation is given as:

$$\frac{dX}{dt} = \mu_{max} X(t)\left(1 - \frac{X(t)}{X_{max}}\right) \tag{5.5}$$

where X is the biomass concentration (g/L) in the fermentation broth at any time t (h), μ_{max} is the maximum specific growth rate (h^{-1}), X_{max} is the maximum biomass concentration attainable corresponding to the maximum carrying capacity (g/L), and $\left[1-(X/X_{max})\right]$ represents the unused carrying capacity. However, in order to distinguish between biomass growth and lipid accumulation and the possible separation of these processes, the non lipid biomass data, which is the difference between the total biomass and the lipid concentrations, were used as values of X in the model [Sattur and Karanth, 1991]. Assuming that at $t = 0$, $X = X_0$, Equation 5.4 can be integrated as:

$$\ln\frac{X}{X_{\max}-X}=\mu_{\max}t+\ln\frac{X_0}{X_{\max}-X_0} \tag{5.6}$$

Rearranging Equation 5.6 gives:

$$X=\frac{X_0e^{\mu_{\max}t}}{1-\frac{X_0}{X_{\max}}\left(1-e^{\mu_{\max}t}\right)} \tag{5.7}$$

The maximum specific growth rate ($\mu_{\max}$) was estimated using the rearranged form of Equation 5.7 given as:

$$\mu_{\max}t=\ln\frac{X}{X_{\max}-X}-\ln\frac{X_0}{X_{\max}-X_0} \tag{5.8}$$

A plot of $\ln\left[X/\left(X_{\max}-X\right)\right]$ vs. t gave a straight line with a slope of $\mu_{\max}$.

$X_{\max}$ was obtained from the experimental data of non lipid biomass with fermentation time. From the intercept of the straight line, the initial viable inoculum size was also calculated from:

$$X_0=\frac{X_{\max}}{e^{-y_i}+1} \tag{5.9}$$

where $-y_i$ is the intercept of the straight line in the y-axis.

Lipid Accumulation

Since the lipids of interest in this study are theoretically contained within the microbial cell (i.e., intracellular lipids), it was assumed that the biosynthesis of lipids by activated sludge microorganisms occurred via two processes: growth-associated lipid production resulting from cell replication and non growth-associated lipid production

resulting from the increase in the fraction of lipidic material within each microbial cell relative to the non lipids. Based on these hypotheses, lipid accumulation was described using the Leudeking-Piret equation

$$q_P = m\mu_g + n \tag{5.10}$$

where q_P is the specific rate of lipid (P) production (h^{-1}) equal to $\left(dP/dt\right)/X$. For the estimation of the parameters m and n, the Monod rate law (Equation 5.3) can be incorporated into Equation 5.10. Taking the reciprocal of the resulting equation leads to

$$\frac{X}{r_P} = \frac{K_S}{m\mu_{\max}}\frac{1}{S} + \frac{1}{m\mu_{\max}} + \frac{1}{n} \tag{5.11}$$

where $r_P = dP/dt$. Similar to biomass growth, values of the lipid production rate are calculated by using the polynomial method and then X/r_P is plotted against $1/S$. By linear regression, the slope $K_S/m\mu_{\max}$ and y-intercept $1/m\mu_{\max} + 1/n$ are obtained and used to calculate m and n using the estimates of $\mu_{\max}$ and K_S obtained previously [Fogler, 2006]

For evaluation of the parameters m and n using the Logistic rate law approach for non lipid biomass growth, Equation 5.10 can be expressed alternately as Equation 5.12 using Equation 5.1 for μ_g where the rate of lipid production is a function of the instantaneous non lipid biomass concentration, X, and the growth rate dX/dt based on the non lipid biomass in a linear fashion:

$$\frac{dP}{dt} = q_P X = nX + m\mu_g X = nX + m\frac{dX}{dt} \tag{5.12}$$

In Equation 5.12, P is the lipid concentration (g/L) in the fermentation broth at any time t (h), and m and n are empirical constants that may be used to describe growth and non growth-associated product formation, respectively. Based on this, generalizations were made on whether lipid accumulation in activated sludge microbiota is growth-associated or non-growth associated based on the relative magnitudes of m and n, which are empirical constants that may vary with the fermentation conditions. The constant n was estimated from lipid production rate (dP/dt) data at the stationary phase wherein $dX/dt \approx 0$, such as:

$$n = \frac{(dP/dt)_{stat}}{X_{max}} \tag{5.13}$$

By incorporating the Logistic equation for the prediction of non lipid biomass in Equations 5.5 and 5.7 and assuming that at $t = 0$, $P = P_0$, Equation 5.11 was integrated to yield:

$$P = P_0 + m(X - X_0) + n\frac{X_{max}}{\mu_{max}}\left[\mu_{max} t + \ln(X/X_0)\right] \tag{5.14}$$

The parameter m was estimated by plotting $P - P_0 - n\frac{X_{max}}{\mu_{max}}\left[\mu_{max} t + \ln(X/X_0)\right]$ vs. $(X - X_0)$ to give a straight line with a slope equal to m.

Substrate Consumption

Substrate utilization by the activated sludge microbiota was also modeled by a Leudeking-Piret equation (Eq. 5.15) where the rate of substrate (sugar) utilization is

expressed as a function of three sink terms: the instantaneous non lipid biomass growth, lipid formation rate, and cell maintenance:

$$-\frac{dS}{dt} = \frac{1}{Y_{X/S}}\frac{dX}{dt} + \frac{1}{Y_{P/S}}\frac{dP}{dt} + k_e X \tag{5.15}$$

where S is the residual glucose concentration (g/L) in the fermentation broth at any time t (h); $Y_{X/S}$ and $Y_{P/S}$ are to the non lipid biomass and lipid yield coefficients (g/g substrate consumed), respectively; and k_e is the maintenance coefficient (g/g·h). $Y_{X/S}$ and $Y_{P/S}$ are assumed to be fractional yields and are given as

$$Y_{X/S} = \frac{X - X_0}{S_0 - S} \tag{5.16}$$

and

$$Y_{P/S} = \frac{P - P_0}{S_0 - S} \tag{5.17}$$

Alternately, Equation (5.15) can be written as:

$$-\frac{dS}{dt} = \alpha\frac{dX}{dt} + \beta X \tag{5.18}$$

where:

$$\alpha = \left(\frac{1}{Y_{X/S}} + \frac{m}{Y_{P/S}}\right) \tag{5.19}$$

and

$$\beta = \left(\frac{n}{Y_{P/S}} + k_e\right) \tag{5.20}$$

Similarly, Equation 5.18 was integrated by incorporating the Logistic equation for the prediction of non lipid biomass and assuming that at $t = 0$, $S = S_0$ to yield the analytical solution:

$$S = S_0 - \beta \frac{X_{\max}}{\mu_{\max}} \left[\mu_{\max} t + \ln\left(X_0 / X \right) \right] - \alpha \left(X - X_0 \right) \tag{5.21}$$

The parameter β was estimated from substrate utilization rate at the stationary phase the stationary phase wherein $dX/dt \approx 0$, such as:

$$\beta = \frac{-\left(dS/dt \right)_{\text{stat}}}{\mathrm{X}_{\max}} \tag{5.22}$$

The parameter α was estimated by plotting $S_0 - S - \beta \frac{X_{\max}}{\mu_{\max}} \left[\mu_{\max} t + \ln\left(X / X_0 \right) \right]$ vs. $\left(X - X_0 \right)$ to give a straight line with a slope equal to α.

Fed-Batch Fermentation

In the fed-batch fermentation, nutrients and substrate are supplied into the culture either by intermittent or shock feeding (discontinuous fed-batch mode) or continuous feeding (semicontinuous mode) while the culture is harvested discontinuously as shown in Figure 5.1. This fermentation mode has been used to overcome substrate inhibition or catabolite repression by intermittent addition to maintain a low substrate concentration and improve productivity [Shuler and Kargi, 2002]. It can also be applied in cases wherein the substrate contains inhibitory compounds such as lignocellulose hydrolyzates such that intermittent addition of the substrate could improve the rate of *in situ* degradation of toxic compounds by the microorganisms [Taherzadeh and Karimi, 2007].

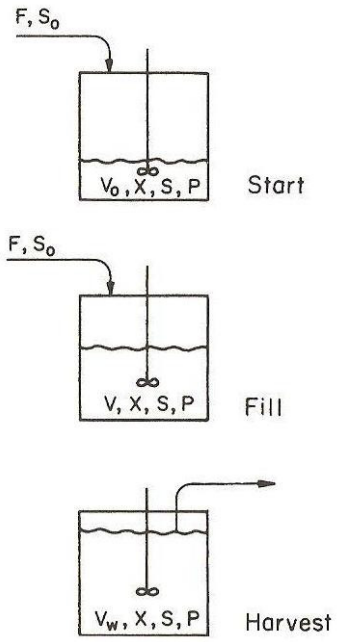

Figure 5.1: Schematic of a fed-batch culture [Shuler and Kargi, 2002].

The discontinuous fed-batch culture usually involves an initial batch culture with an initial charge of nutrients and substrate. Successive additions of fresh media are made when the residual substrate concentration in the culture has been depleted or has reached a limiting level in order to re-establish the substrate concentration back to the initial level in the first batch stage or to another specified level. Therefore, the culture time span between each successive feeding can be treated as individual batch cultures and then analyzed using batch fermentation kinetic equations. On the other hand, the semicontinuous fermentation mode usually involves an initial batch culture (initiation stage) followed by continuous addition of fresh media (processing stage) until a limiting culture volume is reached, after which a volume of the culture is harvested continuously (harvesting stage). In some cases though, the initiation stage also involves a continuous

addition of media as shown in Figure 5.1. The process can then be repeated in multiple cycles and hence referred to as a cyclic fed batch mode.

Similarly, the batch initiation stage preceding a semicontinuous fermentation process can be analyzed using batch fermentation kinetics. The design equations for the actual semicontinuous culture stages (processing and harvesting) include a rate expression for the change in culture volume caused by media addition and culture harvesting:

$$\frac{dV}{dt} = F \tag{5.23}$$

where V is the culture volume (L) at any time t and F is the feed or harvest flow rate (L/h). Integrating Equation 5.23 leads to

$$V = V_0 + Ft \tag{5.24}$$

The non lipid biomass concentration in the vessel at any time t can be expressed as the ratio of the total non lipid biomass X^t (g) and the volume V (L):

$$X = \frac{X^t}{V} \tag{5.25}$$

Hence, the rate of change in non lipid biomass concentration is obtained by differentiating Equation 5.25 to obtain

$$\frac{dX}{dt} = \frac{V\left(dX^t/dt\right) - X^t\left(dV/dt\right)}{V^2} \tag{5.26}$$

By Equation 5.23 and since $dX^t/dt = \mu_{\text{net}} X^t$, Equation 5.26 is reduced to

$$\frac{dX}{dt} = \left(\mu_{\text{net}} - D\right) X \tag{5.27}$$

where D is the dilution rate (h^{-1}) equal to F/V and is also the reciprocal of the residence time. If maintenance energy due to endogenous metabolism and cell death can be neglected, the net specific growth rate μ_{net} can be expressed as the Monod rate law (Equation 5.3). Applying a mass balance on the rate-limiting substrate without maintenance energy gives

$$\frac{dS}{dt} = DS_0 - DS - \frac{\mu_{net} X}{Y_{X/S}} - \frac{q_P X}{Y_{P/S}} \tag{5.28}$$

where S_0 and S are the concentrations of substrate in the feeding solution and in the culture, respectively (g/L). During the processing stage, $DS = 0$ while at the harvesting stage $DS_0 = 0$. Similarly, the rate of product (lipid) formation can be expressed by applying a mass balance of lipids around the fermenter

$$\frac{dP}{dt} = q_P X - DP \tag{5.29}$$

where q_P is given by Equation 5.10.

Continuous Fermentation

In batch cultures, environmental conditions changes continually with time since growth, product formation, and substrate utilization cease after certain time intervals. On the other hand, growth and product formation can be sustained for prolonged periods in continuous cultures wherein fresh nutrient medium is continually supplied to a perfectly mixed stirred tank reactor called a *chemostat* shown in Figure 5.2 at the same time products and cells are withdrawn continuously from the culture [Shuler and Kargi, 2002]. A mass balance on the non lipid biomass concentration around the chemostat gives

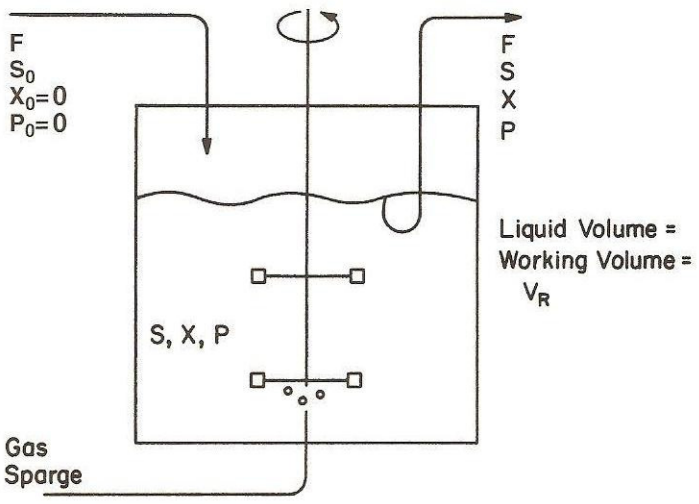

Figure 5.2: Schematic of a chemostat [Shuler and Kargi, 2002]

$$V\frac{dX}{dt} = FX_0 - FX + V\mu_g X - Vk_d X \tag{5.30}$$

where k_d is the endogenous or death rate constant (h^{-1}). Rearranging Equation 5.30 and $D = F/V$ leads to

$$\frac{dX}{dt} = DX_0 + \left(\mu_g - k_d - D\right)X \tag{5.31}$$

If the feed medium is sterile ($X_0 = 0$), and if endogenous metabolism or cell death rate is negligible compared to the growth rate ($k_d << \mu_g$), Equation 5.31 can be reduced to Equation 5.27 given earlier for the fed batch culture. At steady state where $dX/dt \approx 0$, Equation 5.31 is reduced to

$$\mu_g = D \tag{5.32}$$

which implies that cells are removes at a rate equal to their growth rate. The Monod equation (Equation 5.3) can be substituted into Equation 5.32 to give an expression for the steady-state limiting substrate concentration

$$S = \frac{K_S D}{\mu_{\max} - D} \tag{5.33}$$

At D values greater than $\mu_{\max}$, the cells in the culture cannot multiply quickly enough to maintain a viable cell concentration and is therefore *washed out.* Therefore, the expression for the critical D above which washout occurs is obtained by rearranging Equation 5.33 as

$$D_{\text{washout}} = \frac{\mu_{\max} S_0}{K_S - S_0} \tag{5.34}$$

where S_0 is the concentration of the substrate in the feed to the chemostat.

A mass balance on the carbon substrate around the chemostat in the absence of endogenous metabolism yields

$$V\frac{dS}{dt} = FS_0 - FS - V\frac{\mu_g X}{Y_{X/S}} - V\frac{q_P X}{Y_{P/S}} \tag{5.35}$$

where S_0 and S are the feed and effluent substrate concentrations (g/L). At steady state condition where $dS/dt \approx 0$, and by Equations 5.32 and 5.34, Equation 5.35 can be rearranged as

$$X = Y_{X/S}\left(S_0 - \frac{K_S D}{\mu_{\max} - D}\right) \tag{5.36}.$$

By multiplying both sides of Equation 5.36 with D, differentiating with respect to D and setting the derivative equal to zero, an expression for the optimum dilution rate that maximizes productivity can be derived as

$$D_{\text{opt}} = \mu_{\max}\left(1 - \sqrt{\frac{K_S}{K_S + S_0}}\right) \tag{5.37}$$

Graphically, the optimum and critical D values can be determined by plotting cell production rate (DX), and cell (X) and substrate concentrations (S) versus D as shown in Figure 5.3. The optimum dilution rate corresponds to D at which the peak of the cell production rate curve occurs, above which cell production decreases. The point of zero cell production at the other end of the DX curve is the critical D above which washout occurs. Furthermore, the rate of product (lipid) formation can also be expressed by applying a material balance of the lipid product around the chemostat:

$$V\frac{dP}{dt} = FP_0 - FP + Vq_P X \tag{5.38}$$

where P_0 and P are the feed and effluent lipid concentrations, respectively and q_P is given by Equation 5.10. For a sterile feed $P_0 = 0$ and with $D = F/V$, Equation 5.38 reduces to

$$\frac{dP}{dt} = nX + m\mu_g X - DP \tag{5.39}$$

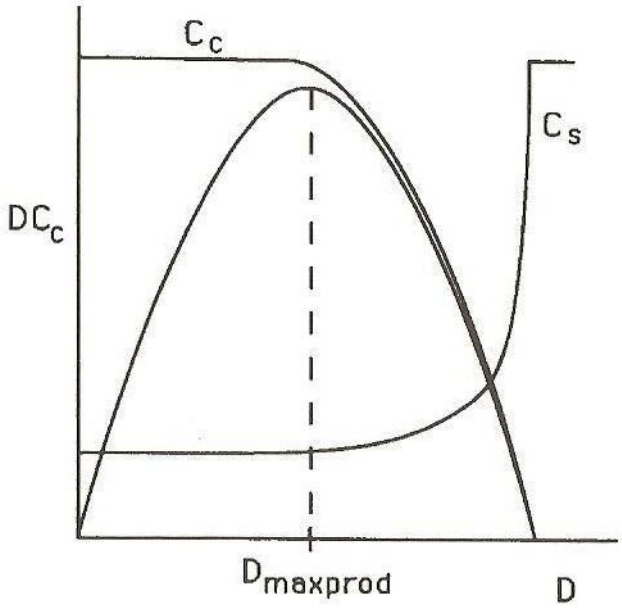

Figure 5.3: Cell concentration and production rate as a function of dilution rate for the determination of D_{opt} and $D_{washout}$ [Shuler and Kargi, 2002]

Summary of Modeling Algorithm

In summary, the procedure for modeling the fermentation kinetics of activated sludge involving non lipid biomass growth, lipid accumulation, and sugar consumption to obtain values of the important kinetic parameters for the fermentation experiments are as follows:

(1) Initial estimates of the kinetic parameters for the Logistic and Luedeking-Piret models were obtained by linear regression of the linearized forms of the rate equations. For non lipid biomass growth, μ_{max} was estimated by linear regression of Equation 5.8 with the experimental non lipid biomass concentration data with cultivation time. For lipid accumulation, n was estimated using Equation 5.13 and m was estimated via linear regression of

Equation 5.14 with the experimental lipid concentration data with cultivation time. For substrate consumption, β was estimated using Equation 5.22 and α was estimated via linear regression of Equation 5.21 with the experimental substrate consumption data with cultivation time.

(2) Using the initial estimates obtained via the method mentioned in (1), the kinetic parameter values were optimized by iterative nonlinear least-squares regression of Equation 5.7 for non lipid biomass growth, Equation 5.14 for lipid accumulation, and Equation 5.21 for substrate consumption via the Levenberg-Marquardt algorithm of the Polymath® Professional 6.1 software (CACHE Corp., USA), which minimized the sum of squares of the errors (i.e. the difference between the actual value of the dependent variable and the calculated value of the dependent variable from the model expression).

(3) The optimized parameter values obtained in step (2) were then incorporated into the rate expressions for non lipid biomass growth (Equation 5.5), lipid accumulation (Equation 5.12), and substrate consumption (Equation 5.18) to obtain simulated profiles of these variables with fermentation time using the Runge-Kutta-Fehlberg (RK45) algorithm of the ordinary differential equations program of Polymath® Professional 6.1 (CACHE Corp., USA).

(4) The validity and performance of the model with the three rate equations were evaluated by calculating the coefficient of determination R^2:

$$R^2 = 1 - \frac{\sum_i^n \left(y_i - y_p \right)^2}{\sum_i^n \left(y_i - \bar{y_i} \right)^2} \tag{5.40}$$

where y_i and y_p are the experimental data and model simulations, respectively.

This procedure was used to obtain values of the kinetic parameters and R^2 used to interpret the data in Chapters VI, VII, and VIII. On the other hand, parameter estimation in Chapter IX for fed batch and continuous fermentations were done only by linear regression of the Lineweaver-Burke plots of the Monod equation for growth.

CHAPTER VI

EVALUATION OF LIPID ACCUMULATION BY ACTIVATED SLUDGE MICROORGANISMS: EFFECT OF C:N RATIO AND GLUCOSE LOADING

Introduction

In this initial phase of the study, the potential for enhancing lipid production and biodiesel yields from municipal sewage activated sludge via fermentation of lignocellulose biomass hydrolyzates was investigated. Activated sludge microbial communities and their constituents were evaluated for oleaginicity (i.e., increase in cellular lipid content due to nitrogen limitation) via a batch fermentation process utilizing glucose as the sole carbon source. Two variables describing substrate and nutrient availability conditions in fermentation media, the initial carbon-to-nitrogen ratio (C:N) and initial substrate loading in mass per volume of media, have been identified in previous studies as the primary factors that influence the accumulation of microbial lipids by oleaginous microorganisms (see Chapter III). Numerous studies have experimentally confirmed the theory that in a fermentation culture formulated in such a way that the nutrient (i.e., nitrogen) source is depleted with an excess of the carbon source still in the culture, then a series of biochemical events would trigger the diversion of the excess carbon toward the formation of storage lipids which are mainly triacylglycerols (TAG).

These storage lipids combined with the phospholipids comprising microbial cell membranes would constitute the available lipids that could be extracted and in turn converted to biodiesel. Hence, in order to assess the ability of activated sludge microbiota in increasing its biomass lipid content for use in biofuels production, activated sludge was cultivated in batch bioreactors with varying levels of initial C:N ratio and substrate loading according to the general fermentation protocols described in Chapter IV. The bioreactor cultures were then analyzed for biomass and lipid yields using the methods described in Chapter IV to evaluate their performance and potential for large-scale biodiesel feedstock lipids production.

Methodology

Glucose and ammonium sulfate were used as the carbon and nitrogen sources, respectively and were supplied into the synthetic wastewater media in concentrations according to the experimental design shown in Table 6.1. In this one-factor-at-a-time approach, the initial C:N ratio (10:1 – 70:1) was varied while the initial glucose loading was kept constant (60 g/L) in the first three treatments (1-3); whereas in treatments (3-5) the initial glucose loading was varied (20 – 60 g/L) while the C:N ratio was kept constant (70:1). Treatments belonging to each subset were tested in fermentation runs using the set of three BioFlo 310 Fermenter/Bioreactors (New Brunswick Scientific, Edison, NJ, USA) and the same grab samples of activated sludge following the general fermentation protocols described in Chapter IV.

Table 6.1: Experimental design used to determine the effect of C:N ratio and glucose loading on lipid accumulation by activated sludge.

Treatment	C:N mass ratio	Glucose loading (g/L)	Ammonium sulfate (g/L)
1	10:1	60	11.3
2	40:1	60	2.8
3	70:1	60	1.6
4	70:1	40	1.1
5	70:1	20	0.5

Four replicate experiments for each subset of the overall experimental design were conducted at most 1-2 weeks apart to minimize the variability of activated sludge characteristics such as biomass concentration, initial lipid content, and composition of the microbial population. Fermentation broth and biomass samples were analyzed according to the methods described in Chapter IV. The proposed mathematical model for the batch fermentation described in Chapter V was fitted into the fermentation data and estimates of the kinetic parameters were obtained using the algorithm described also in Chapter V.

Results and Discussion

Effect of C:N Ratio

The effect of C:N ratio on the fermentation profiles of activated sludge microorganisms grown in glucose-supplied synthetic wastewater are shown in Figs. 6.1 – 6.5 . In these charts, the error bars represented the standard deviation of the four replicate runs. As shown in Fig. 6.1, an increase in the C:N ratio results in a decrease in the total biomass yield of activated sludge. Since the initial glucose supply was constant, the

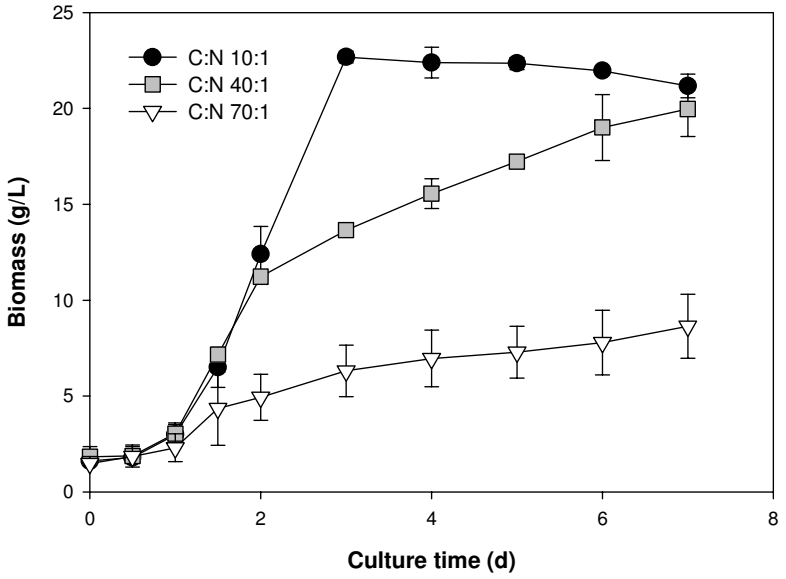

Figure 6.1: Effect of C:N ratio on biomass production by activated sludge cultures at constant glucose loading (60 g/L).

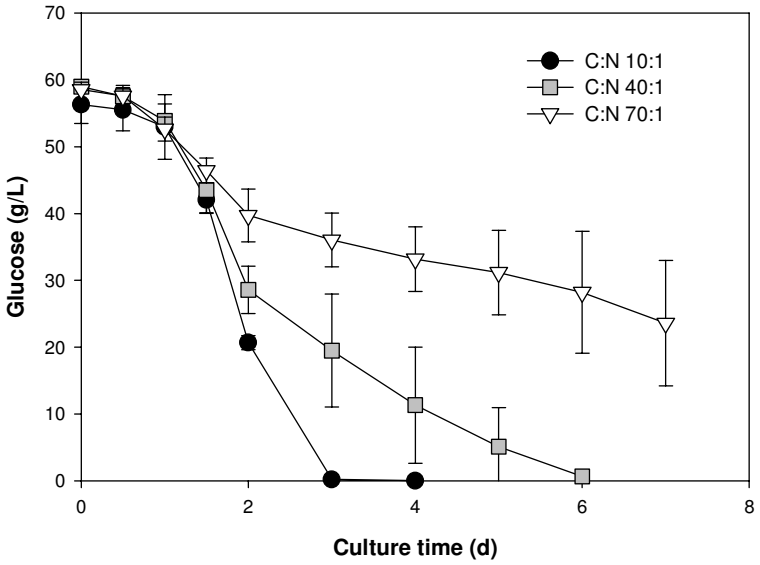

Figure 6.2: Effect of C:N ratio on glucose consumption by activated sludge cultures at constant glucose loading (60 g/L).

increased biomass yield at C:N 10:1 and 40:1 compared to C:N 70:1 was affected primarily by the higher initial amounts of NH_4^+-N in the medium. A lag phase was observed during the first 24 h of fermentation in all C:N ratios investigated, after which the duration of the exponential phases and the observed cell growth rates differed significantly. At the C:N 10:1 culture, the exponential growth phase occurred between days one to three of fermentation at a significantly higher rate than C:N 40:1 and 70:1 to reach the highest attained biomass concentration among all the treatments. The biomass concentration then started its gradual decline due to the depletion of glucose at after 3 d as shown in Fig. 6.2 despite having approximately 2 g/L residual NH_4^+-N in the fermentation broth shown in Fig. 6.3. The observed glucose consumption profiles (Fig. 6.2) indicated similar glucose utilization rates and patterns for all three C:N ratios tested during the first 36 h of fermentation corresponding to the lag phase. From thereon, the glucose uptake rate increased with decreasing C:N ratio probably due to the higher concentration of microbial cell biomass consuming the available glucose as substrate for growth and maintenance at lower C:N ratios. Glucose was fully consumed after 3 d at C:N 10:1 and 6 d at C:N 40:1 while approximately one-third remained at C:N 70:1 after 7 d. This could also indicate some substrate inhibition due to the high glucose residual relative to microbial cell concentration or the lower glucose uptake rate due to very low nitrogen levels in the culture. Furthermore, at higher C:N ratios (40:1 and 70:1), the duration of the exponential phases was shorter (1-2 d) and was still followed by a gradual increase in the total biomass. In these C:N ratios, residual NH_4^+-N levels in the culture

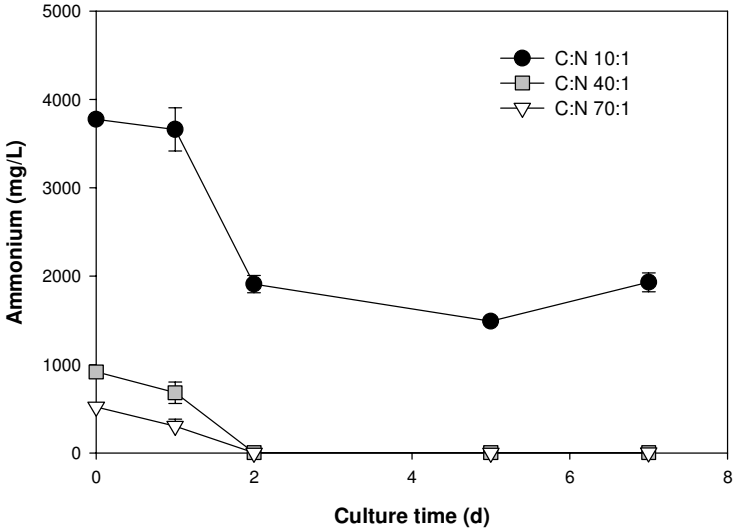

Figure 6.3: Effect of C:N ratio on ammonium-nitrogen consumption by activated sludge cultures at constant glucose loading (60 g/L).

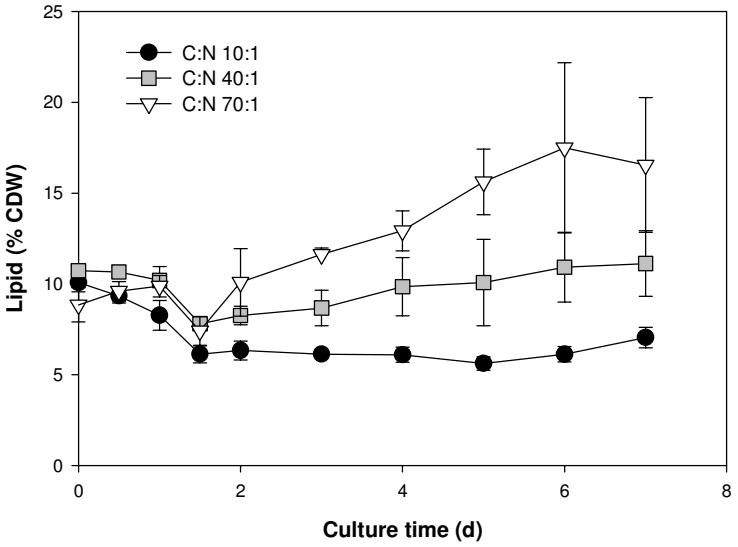

Figure 6.4: Effect of C:N ratio on lipid accumulation by activated sludge cultures at constant glucose loading (60 g/L). CDW: cell dry weight.

were found to be negligible after 2 d (Fig. 6.3), hence the observed increase in total biomass could be attributed to the increase in the lipid fraction.

The observed gravimetric lipid content (% CDW) profiles indicate an initial reduction in the lipid content of the activated sludge coinciding with the lag phase (Fig. 6.4), perhaps being mobilized as an initial carbon source for the synthesis of enzymes for subsequent utilization of glucose by activated sludge microorganisms. Subsequently at C:N 40:1, the lipid content appeared to increase gradually at the onset of the exponential phase but returned only to its initial level. At C:N 10:1, the lipid content of the sludge biomass did not increase and stayed constant at approximately 7 % CDW. The only significant increase in the lipid content was observed at C:N ratio 70:1, in which a maximum lipid content of 17 % CDW was achieved from 10 % CDW initially in raw activated sludge. Although this result implies a 70 % increase in the amount of extractable lipids in the activated sludge biomass, this value is still relatively lower than most oleaginous microorganisms, which by definition should have a minimum of 20 % lipids by weight [Ratledge, 2005]. In all the fermentation runs, the culture pH was not controlled, causing a rapid decline from 6.5 to around 2.5 during the exponential phase and possibly an inhibitory effect on both biomass and lipid production as previously reported [Davies, 1988]. However, despite having no significant enhancement in its gravimetric lipid content, activated sludge grown at C:N ratio 40:1 showed higher volumetric lipid yields (g lipid per L of fermentation broth) as shown in Fig. 6.5 due to the higher total biomass production at this treatment compared with C:N ratio 70:1. The same was observed initially at C:N 10:1 up to day three but started its decline along with

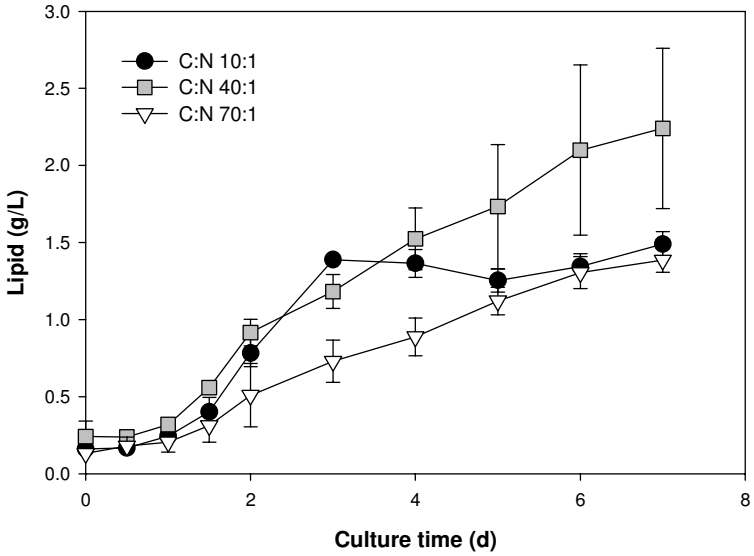

Figure 6.5: Effect of C:N ratio on lipid production by activated sludge cultures at constant glucose loading (60 g/L).

the onset of the stationary phase. On the other hand, volumetric lipid yields in C:N 70:1-grown activated sludge exhibited an increasing trend compared to the lower C:N ratios; albeit at lower levels than C:N 40:1 despite having higher gravimetric lipid contents due to the lower biomass production.

The maximum attained gravimetric yield from activated sludge (17 % CDW) were significantly lower than that obtained from the oleaginous yeast *Rhodotorula gracilis* (approximately 60 % CDW) under similar conditions (C:N ratio 70:1, 60 g/L glucose loading). This was most likely due to the fact that activated sludge is a consortium of numerous microbial species as opposed to pure cultures of *R. gracilis.* The microorganisms in the consortium may be engaged in predator-prey relationships which

could result in the consumption of some of the lipid-rich cells by other microorganisms; or other unknown mechanisms that resulted into the observed net lipid content of sludge.

Effect of Glucose Loading

The effect of initial glucose loading was investigated and the generated fermentation profiles for biomass production, lipid accumulation, and glucose consumption are shown in Figs. 6.6 – 6.10. Similarly, the error bars in the charts represent the standard deviation of the four replicate runs. At the initial glucose loadings of 40 and 60 g/L, the biomass concentration increased continuously and the lag, exponential, and stationary phases were not statistically different from each other in the growth curves (Fig. 6.6). Both treatments resulted in similar maximum biomass yields, with slightly higher levels at the 40 g/L treatment. At a glucose loading of 20 g/L however, the lag and exponential phases occurred during 0 to 2 d and 2 to 3 d of fermentation, respectively, followed by a very distinct stationary phase from day three onwards, wherein the biomass levels remained constant at the maximum biomass concentration attained (≈ 4 g/L). Glucose consumption profiles (Fig. 6.7) were very similar for the three initial glucose levels investigated. Furthermore, an increase in the initial glucose loading led to longer times needed for 100 % sugar utilization. Similarly, ammonium-nitrogen levels (Fig. 6.8) were depleted after 1 d for 20 g/L glucose loading and after 2 d at 40 and 60 g/L glucose loading. Gravimetric lipid yield profiles (Fig. 6.9) were also similar for all three treatments. The highest increase in gravimetric lipid content relative to the raw activated sludge lipid content was observed at 60 g/L glucose

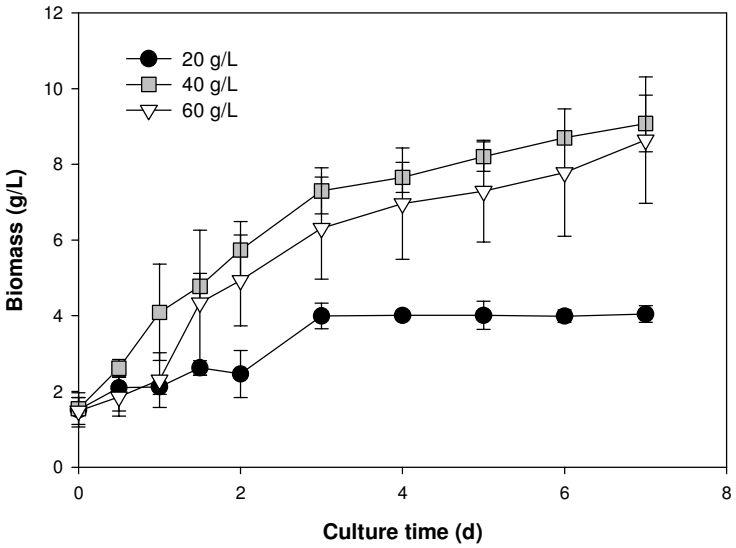

Figure 6.6: Effect of initial glucose loading on biomass production by activated sludge cultures at constant C:N ratio (70:1).

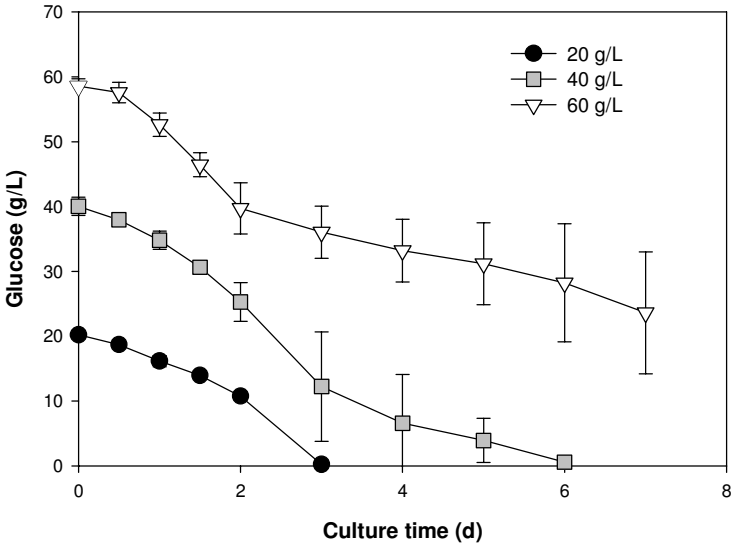

Figure 6.7: Effect of initial glucose loading on glucose consumption by activated sludge cultures at constant C:N ratio (70:1).

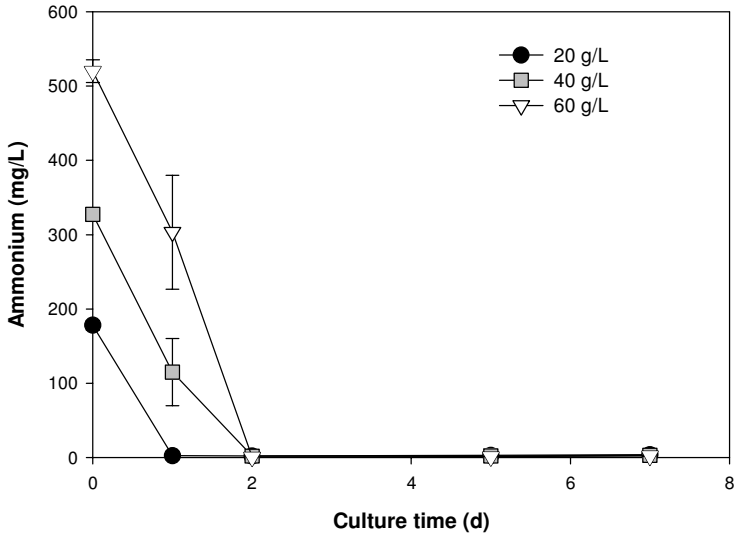

Figure 6.8: Effect of initial glucose loading on ammonium-nitrogen consumption by activated sludge cultures at constant C:N ratio (70:1).

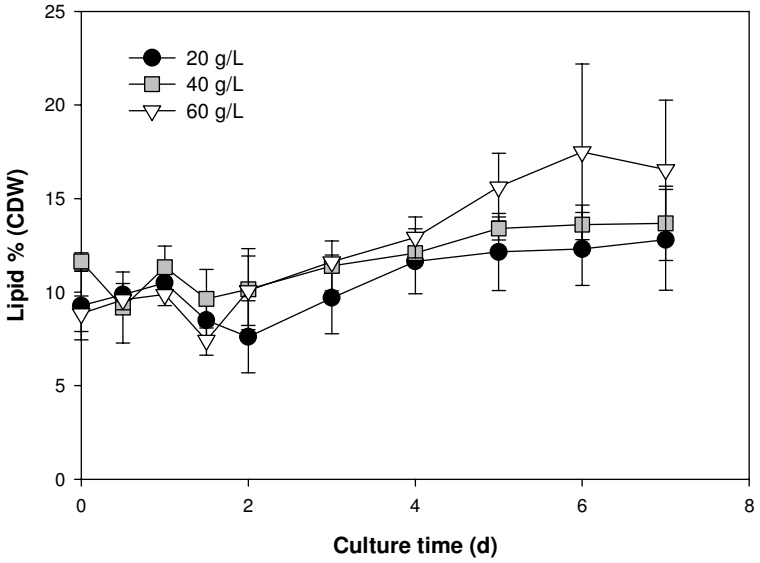

Figure 6.9: Effect of initial glucose loading on lipid accumulation by activated sludge cultures at constant C:N ratio (70:1).CDW: cell dry weight.

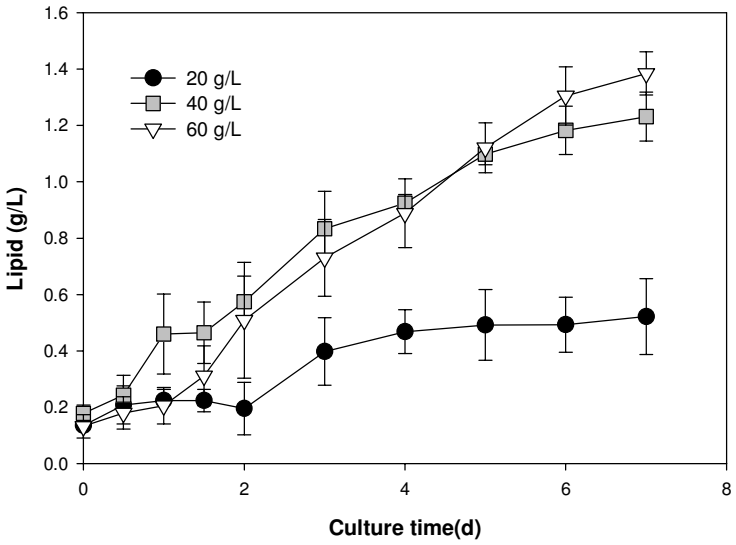

Figure 6.10: Effect of initial glucose loading on lipid production by activated sludge cultures at constant C:N ratio (70:1).

loading (approximately 17 % CDW), whereas only slight increases were observed at the 20 and 40 g/L treatments. However, the volumetric lipid yields (Fig. 6.10) at 40 and 60 g/L showed very similar trends and values as an affect of the slightly higher biomass yields at 40 g/L glucose loading. At 20 g/L glucose loading, lipid concentrations in the culture reached a plateau value (≈ 0.4 g/L) after 3 d of cultivation due to the cessation of biomass production.

Fermentation Kinetics

Table 6.2 shows a summary of the kinetic parameter estimates from the proposed mathematical model. Knowing that activated sludge consists of microbial communities, these parameters were assumed to be the average or bulk value for the microbial community as a whole. Further, biomass growth parameters were based on the non lipid

Table 6.2: Parameter estimates for the proposed kinetic model for non lipid biomass, lipid, and glucose consumption.

Parameters	C:N ratio				
	10:1	40:1	70:1	70:1	70:1
	Glucose loading (g/L)				
	60	60	60	40	20
Non lipid biomass					
μ_{max} (h^{-1})	0.0998	0.0516	0.0455	0.0428	0.0337
X_0 (g/L)	0.241	1.41	1.15	1.66	1.33
X_{max} (g/L)*	21.3 (3)	17.7 (7)	7.26 (7)	7.58 (7)	3.66 (3)
R^2	0.990	0.974	0.959	0.989	0.920
Lipid accumulation					
m (g/g)	0.051	0.0657	0.0797	0.105	0.0993
n (g/g·h)	9.35×10^{-5}	4.88×10^{-4}	9.77×10^{-5}	4.54×10^{-4}	3.54×10^{-4}
P_{max} (g/L)*	1.49 (3)	2.2 (7)	1.41 (7)	1.24 (7)	0.537 (7)
R^2	0.994	0.997	0.997	0.998	0.987
Glucose consumption					
α (g/g)	2.54	3.49	5.03	4.08	6.29
β (g/g·h)	8.19×10^{-3}	2.49×10^{-3}	4.83×10^{-4}	1.87×10^{-2}	3.92×10^{-2}
$Y_{X/S}$ Overall (g/g)	0.354	0.274	0.167	0.166	0.113
$Y_{X/S}$ Growth Phase (g/g)	0.388	0.284	0.162	0.268	0.166
$Y_{X/S}$ Lipid Phase (g/g)	0.320	0.261	0.181	0.108	0.101
$Y_{P/S}$ Overall (g/g)	0.024	0.034	0.038	0.027	0.020
$Y_{P/S}$ Growth Phase (g/g)	0.026	0.023	0.019	0.029	0.022
$Y_{P/S}$ Lipid Phase (g/g)	0.024	0.054	0.063	0.026	0.019
R^2	0.990	0.987	0.975	0.978	0.912

*Values in parenthesis indicate fermentation time elapsed (d) when maximum value was attained.

biomass data, calculated via the difference between the total biomass and the lipid concentrations at any time in order to more clearly distinguish cell growth from lipid production. As shown in the table, the Logistic equation parameters maximum specific growth rate, μ_{max}, and maximum predicted non lipid biomass concentration representing the carrying capacity of the culture at the specified conditions, X_{max}, decreased with increasing C:N ratio most probably due to the reduced nitrogen supply needed for synthesis of cellular materials at high C:N ratios. The relatively high μ_{max} at C:N ratio

10:1 is also reflected by the observation that X_{max} was attained early in the fermentation process (3 d) during the transition from the exponential to the stationary growth phase.

In terms of lipid accumulation, the maximum volumetric lipid yield attained (P_{max}) was highest at C:N ratio 40, with no significant difference between C:N ratios 10:1 and 70:1. This suggests that the overall volumetric lipid yields may have been influenced more by cell multiplication and total biomass increase than the actual increase in cellular lipid content. The relative magnitudes of the empirical constants of the Leudeking-Piret equation for lipid accumulation *m* and *n* were also indicative of this apparent trend, since in all C:N ratios investigated, $m > n$. This means that lipid production by activated sludge microbiota was mixed growth-associated with greater contributions from the growth-associated lipid production term [Karanth and Sattur, 1991]. The yield coefficients for non lipid biomass ($Y_{X/S}$) and lipids ($Y_{P/S}$) were also calculated during the growth and lipid accumulation phases wherein the growth phase corresponded to the fermentation time span during which nitrogen (as ammonium) was still present in the culture, whilst the lipid accumulation phase covers the fermentation time span starting at the time of ammonium-nitrogen depletion up to the time of glucose depletion (when applicable). As shown in Table 6.2, the $Y_{X/S}$ and $Y_{P/S}$ values were close during the growth and lipid accumulation phases at C:N ratio 10:1; whereas at C:N ratios 40:1 and 70:1, $Y_{P/S}$ values during the lipid accumulation phase were higher than those during the growth phase, which is further evidence of lipid accumulation during the said condition at the onset of nitrogen depletion in the medium.

With respect to initial glucose loading, μ_{max} and X_{max} values were similar at 40 and 60 g/L initial glucose loading, as it was also seen in their respective biomass growth

profiles, while values of the said parameters for 20 g/L initial glucose loading were the lowest obtained among all treatments (including those at varying C:N ratio), due to the very low initial level of nitrogen in the media required to establish a high C:N ratio with a relatively low initial glucose loading. Furthermore, P_{max} also increased with increasing initial glucose loading. Lipid production was also found to be mixed growth-associated with a greater influence exerted by cell multiplication ($m > n$) for all glucose loadings. From these observations, it is evident that at C:N ratio 70:1, glucose loadings of 40 or 60 g/L were more favorable for enhancing both biomass yield and gravimetric lipid content, which has a combined influence in the resulting volumetric lipid yield. $Y_{P/S}$ during the lipid accumulation phase was also found to increase with increasing glucose loading due to the presence of more substrate for lipid production. Similarly designed experiments involving the oleaginous yeast *Rhodotorula gracilis* [Karanth and Sattur, 1991; Sattur and Karanth, 1991] showed relatively lower μ_{max} values and comparable overall $Y_{X/S}$ and X_{max} estimates for activated sludge. However, at similar experimental conditions (C:N 70, 60 g/L glucose), P_{max} and $Y_{P/S}$ for cultured activated sludge (1.41 g/L, 0.038 g/g glucose overall, 0.067 g/g glucose at stationary phase) were lower than the values obtained from *R. gracilis* (11.60 $g \cdot L^{-1}$, 0.19 g/g glucose overall).

Based on the kinetic parameters that were considered, it is apparent that in order to attain maximum lipid yields in terms mass per volume of media and mass per mass of glucose consumed, the production of non lipid biomass needs to be enhanced as well as to provide sufficient cellular vehicles that contain the accumulated lipids. Based on the results, the combination of C:N ratio 40:1 and 60 g/L glucose loading produced higher

volumetric lipid yields in a batch cultivation as shown in the higher overall $Y_{X/S}$ and a $Y_{P/S,}$ which is comparable to C:N 70:1.

Model Validation

To test the reliability of the proposed models for non lipid biomass production, lipid accumulation, and glucose utilization of activated sludge, the nonlinear regression-estimated parameters (Table 6.2) were used to simulate the model with the 4th/5th order Runge-Kutta method. Experimental and simulated values were compared in representative plots (Fig. 6.11) from C:N ratio 70:1, 60 g/L glucose loading treatment. Coefficients of determination (R^2) values were also calculated for each treatment (Table 6.2) and in all cases, R^2 values were greater that 0.90. Some limitations of the proposed model that may account for the 10 % difference could be the assumption by the logistic model that no endogenous metabolism or degradation of cellular material occurs hence only saturation levels are reported from the stationary phase up to $t = \infty$ [Shuler and Kargi, 2002]. The Leudeking-Piret model predictions for lipid production also failed to predict slight decreases in the lipid concentration particularly at C:N ratio 10:1 as a result of endogenous utilization of the stored lipids for cell maintenance due to depletion of the primary carbon source (glucose) [Karanth and Sattur, 1991]. As a result, it would be useful to incorporate cell death phase kinetics and degradation of storage lipids as an endogenous carbon source in future models.

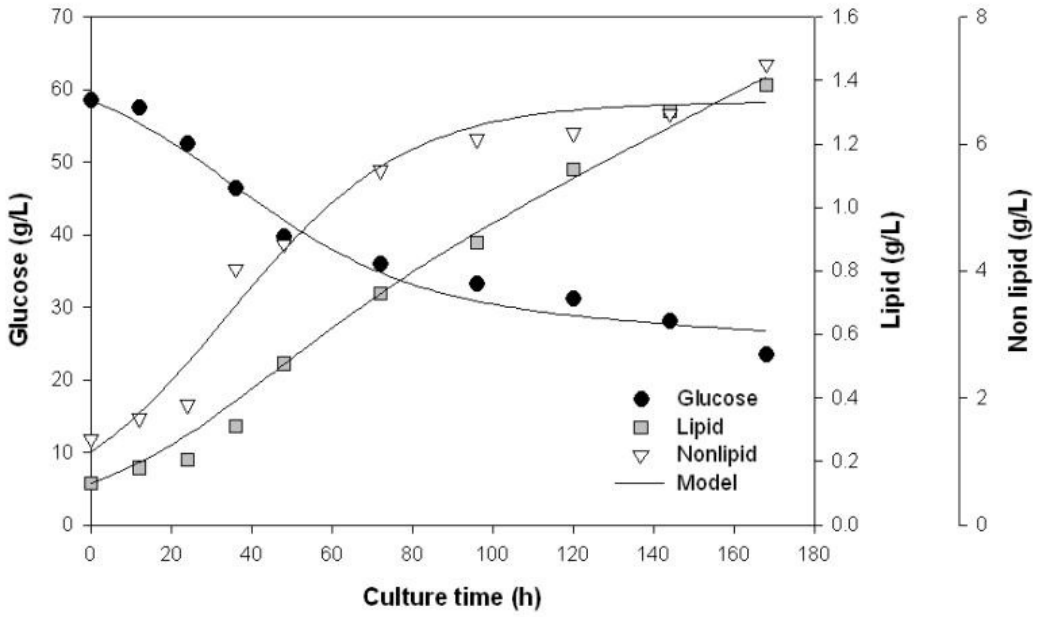

Figure 6.11: Model testing for non lipid biomass production, lipid accumulation, and glucose utilization at C:N ratio 70:1 and 60 g/L glucose loading.

Lipid Analysis

Results obtained via GC-FID analysis of the lipids extracted from glucose-grown activated sludge indicated that the saponifiable fraction of the lipid extracts, which represents the total fatty acid methyl ester (FAMEs) or biodiesel yield, increased proportionally and exhibited the same trend with the total gravimetric lipid yield with respect to fermentation time for all the treatments investigated. Overall, the saponifiable lipids constituted 50-60 % (CDW) of the total extracts in all the treatments investigated, compared to only 25 % (CDW) in raw activated sludge, suggesting an increase in viability of the sludge lipid extracts for biofuel feedstock application (Figs. 6.12 and 6.13). The highest saponifiable lipid yield (10.2 ± 2.5 % CDW) was obtained at C:N

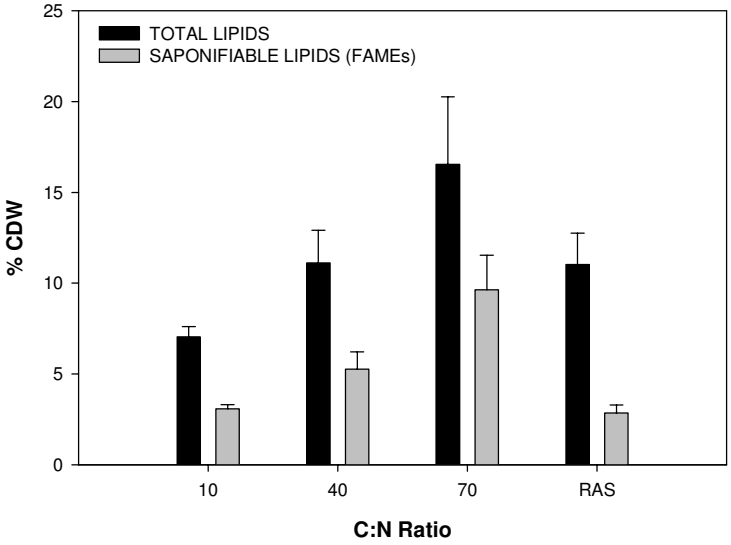

Figure 6.12: Maximum yields of total and saponifiable lipids from cultured activated sludge at varying initial C:N ratios and 60 g/L glucose loading. RAS: Raw activated sludge.

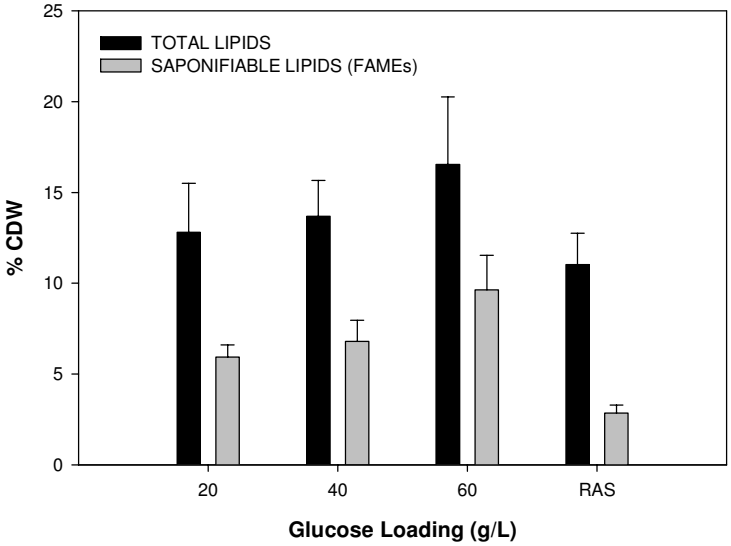

Figure 6.13: Maximum yields of total and saponifiable lipids from cultured activated sludge at varying initial glucose loading and C:N ratio 70:1. RAS: Raw activated sludge.

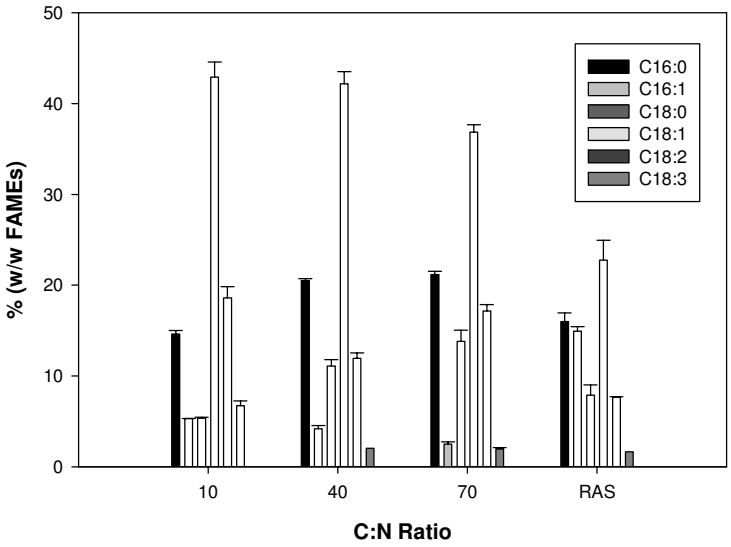

Figure 6.14: Fatty acid profiles of cultured activated sludge lipid extracts at different initial C:N ratios and 60 g/L glucose loading. RAS: Raw activated sludge.

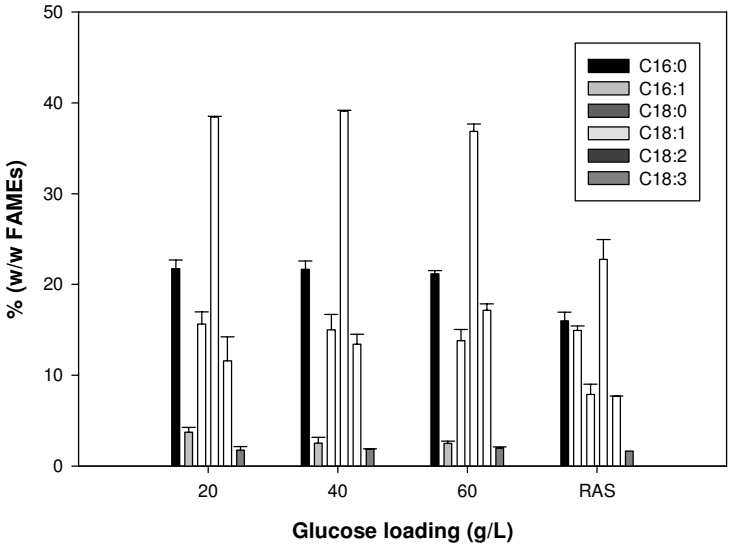

Figure 6.15: Fatty acid profiles of cultured activated sludge lipid extracts at different initial glucose loadings and C:N ratio 70:1. RAS: Raw activated sludge.

ratio 70:1 and 60 g/L glucose loading after 6 d of fermentation and corresponded to a total lipid extract yield of 17 % CDW compared to 2.8 % CDW biodiesel and 10 % CDW total lipids from raw activated sludge.

The major fatty acyl residues in activated sludge oil affected by glucose-fed aerobic fermentation were palmitic (C16:0), palmitoleic (C16:1), stearic (C18:0), oleic (C18:1), linoleic (C18:2), and linolenic (C18:3) acids (Figs. 6.14 and 6.15). For raw activated sludge oil, majority of the fatty acids consisted of unsaturated fatty acids oleate (22 %) and palmitoleate (14.9 %) followed closely by the saturated fatty acid palmitate (16 %), plus about 25 % of unclassified residues. After 7 d of aerobic cultivation in glucose, the proportion of unsaturated fatty acids in activated sludge increased to approximately 70 % in all the treatments investigated and the percentage of unclassified FAMEs was reduced to an average of 5 %. The majority of the unsaturated fatty acids in glucose-grown activated sludge were composed of oleic acid, whose levels were on average nearly twice those from raw activated sludge (i.e. 40 vs. 22.8 %). Different trends have also been observed for each type of fatty acyl residue as an effect of varying initial C:N ratio and glucose loading. Palmitic and stearic acid levels generally increased with increasing initial C:N ratio, with slightly higher levels at lower initial glucose loadings. On the other hand, levels of the unsaturated fatty acids palmitoleate, oleate, linoleate, and linolenate generally decreased slightly with increasing C:N ratio and remained fairly constant with changing initial glucose loading. Regardless of C:N ratio or glucose loading, oleic acid was found to be the dominant fatty acyl residue (38 – 43 %) in glucose-grown activated sludge. The enhanced unsaturated fatty acid concentration due to oleic acid relative to the saturated fatty acids (mostly palmitic acid) in glucose- and/or

xylose-grown activated sludge was comparable with a target soybean oil composition to produce biodiesel with improved cold flow, ignition quality (cetane number), oxidative stability, and presumably reduced nitrogen oxide emissions due to very low levels of linolenic acid (C18:3) and is a significant improvement compared with biodiesel obtained from raw activated sludge [Bringe, 2005].

Conclusion

In this chapter, the potential of lipid accumulation by activated sludge microbial communities was evaluated in order to assess the viability of enhancing lipid and biodiesel yields from municipal sewage activated sludge via fermentation of lignocellulose sugars. Results showed that increasing the initial C:N ratio and glucose loading in activated sludge bioreactors yielded activated sludge biomass with enhanced gravimetric lipid and biodiesel yields, indicating possible oleaginicity among members of the activated sludge community. A maximum gravimetric lipid yield of 17 % (CDW) with a corresponding biodiesel yield of 10 % (CDW) was obtained at initial C:N ratio 70:1 and glucose loading of 60 g/L. These values are significantly higher than those obtained in raw activated sludge (10 % CDW total lipids, 2.8 % CDW biodiesel yield). The kinetic parameters obtained following mathematical modeling of the fermentation process using the proposed modeling approach added further evidences to this observed phenomenon. The bulk maximum specific growth rate of the activated sludge microbiota decreased with increasing initial C:N ratio due to the limitation of nitrogen needed for non lipid biomass production at high C:N ratios. Lipid yield coefficients were higher during the lipid accumulation phase than during the growth phase at C:N ratios 40:1 and

70:1, indicating that majority of lipid biosynthesis occurred during the absence of nitrogen in the media. However, lipid production in activated sludge microbiota was mixed growth-associated with total biomass production exerting a greater influence than actual increases in the lipid contents of individual cells. Indeed, volumetric lipid yields were highest at C:N ratio 40:1 than C:N ratio 70:1 due to a higher total biomass yield in the former. Hence, for process optimization of batch aerobic fermentation of glucose using activated sludge, non lipid biomass yields need to be considered in addition to gravimetric lipid yields. The resulting fatty acid profiles indicated that lipids derived from activated sludge grown aerobically in glucose-containing synthetic wastewater medium consisting mainly of C_{16} and C_{18} fatty acids is suitable for the production of biodiesel with improved properties.

CHAPTER VII

EFFECT OF LIGNOCELLULOSE DEGRADATION BY-PRODUCTS (ACETIC ACID AND FURFURAL) ON LIPID ACCUMULATION BY ACTIVATED SLUDGE MICROBIOTA

Introduction

In the previous chapter, it has been shown that activated sludge microorganisms were able to accumulate additional storage lipids under high C:N ratio (70:1) and glucose loading (60 g/L). The net result was an enhanced lipid content for improved biodiesel yield from sludge biomass. However, to justify the economic competitiveness of the process in the large scale the activated sludge microorganisms should have high growth rates on wide varieties of substrates and utilize cheap raw materials, and at the same time the lipid products should meet fatty acid profile (carbon number) required for biodiesel (C_{16}-C_{18}). In addition to using municipal wastewater influent as media and nutrient source, the use of lignocellulose biomass as opposed to pure sugars (glucose) has been considered. Furthermore, lignocellulosic biomass must undergo hydrolysis to release the fermentable hexose and pentose sugars (mostly glucose and xylose, respectively) liberated from the polymeric structures of the cellulose and hemicellulose components of lignocellulose. In addition to sugars, other degradation by-products, mainly furfural and acetic acid are also produced during hydrolysis. As discussed in earlier sections,

numerous studies on lignocellulose utilization for biofuels (bioethanol or lipids) have found these compounds to exert inhibitory effects on the growth and metabolism of microorganisms. In most cases, pretreatment of lignocellulose hydrolyzates by physical and chemical detoxification methods have been suggested to reduce the levels of inhibitors and to enhance their fermentability. However, such processes may add to the production cost of microbial lipids from activated sludge; hence in this part of the study, it was of interest to determine the effect of two representative inhibitory compounds, furfural and acetic acid, on the growth and lipid production of activated sludge microorganisms utilizing glucose in aerobic bioreactors. Fermentation kinetic parameters were obtained to evaluate the performance of activated sludge microorganisms in the presence of inhibitors relative to a control setup with glucose as sole carbon source. The results obtained hereunto were used to assess inhibitor tolerance and whether or not detoxification steps are necessary prior to fermentation of lignocellulose hydrolyzate.

Methodology

Following the general fermentation protocols described previously in Chapter IV, batch fermentation experiments were conducted using a constant initial glucose loading of 60 g/L and C:N ratio of 70:1 as these were found to be the best conditions for enhancing the lipid content of activated sludge in Chapter VI. Ammonium sulfate was supplied as the nitrogen source at 1.62 g/L. Furfural and acetic acid were supplied individually and in binary mixtures in the amounts shown in Table 7.1. Control runs with no inhibitors (glucose as sole C carbon source) were conducted alongside the high and low inhibitor level treatments to ensure the same initial characteristics of the activated

sludge prior to the fermentation runs. Four replicate experiments were conducted within 1-2 weeks apart to minimize the variability of the initial activated sludge characteristics. Batch fermentation experiments were conducted for seven days and fermentation broth samples were processed and analyzed according to the procedures described in Chapter IV. The fermentation profiles obtained from this study were normalized relative to the initial levels of biomass and lipids and were presented alongside the average normalized fermentation profiles of the control runs in order to account for some variations in initial characteristics of the sludge inocula. Kinetic analysis of the fermentation data was conducted according to the proposed model and solution algorithm discussed in Chapter V. The calculated kinetic parameters from experiments on individual inhibitors and mixtures are provided in Tables 7.2 and 7.3, respectively.

Table 7.1: Experimental design used to determine the effect of inhibitors on lipid accumulation by activated sludge.

Treatment	Furfural (g/L)	Acetic Acid (g/L)
Lo Furfural	0.5	0
Hi Furfural	1.5	0
Lo Acetic acid	0	2
Hi Acetic Acid	0	10
Lo Furfurual Lo Acetic acid	0.5	2
Hi Furfural Hi Acetic acid	1.5	10
Control (No inhibitor)	0	0

Table 7.2: Kinetic parameter estimates for the Logistic and Leudeking-Piret models for treatment runs involving individual inhibitors.

Parameter estimates	Inhibitor Concentration (g/L)				
	0 (Control)	Furfural		Acetic acid	
		0.5	1.5	2	10
Non lipid biomass					
μ_{max} (h^{-1})	0.027	0.0125	-	0.0286	0.0303
X_0 (g/L)	5.54	6.23	-	5.05	4.21
X_{max} (g/L)	12.9	11.85	-	8.09	16.6
R^2	0.912	0.848	-	0.931	0.956
Lipid					
m (g/g)	0.150	0.106	-	0.112	0.0912
n (g/g·h)	82.0×10^{-5}	56.2×10^{-5}	-	15.8×10^{-5}	3.23×10^{-5}
Maximum Lipid Content (% CDW)	18	15.3	10.3	12.5	10.2
P_{max} (g/L)	2.67	2.07	-	1.15	1.65
R^2	0.955	0.800	-	0.9	0.806
Glucose					
α (g/g)	1.39	4.14	41.7	2.75	5.10
β (g/g·h)	0.041	0.0309	0.215	0.0933	0.0091
k_e (g/g·h)	0.019	0.007	0.043	0.079	0.007
$Y_{X/S}$ Overall (g/g)	0.0957	0.0621	-	0.0463	0.166
$Y_{X/S}$ Growth Phase (g/g)	0.228	0.101	-	0.171	0.111
$Y_{X/S}$ Lipid Phase (g/g)	0.0506	-	-	0.207	0.147
$Y_{P/S}$ Overall (g/g)	0.0383	0.0237	-	0.0114	0.0204
$Y_{P/S}$ Growth Phase (g/g)	0.0558	0.0175	-	0.0216	0.0186
$Y_{P/S}$ Lipid Phase (g/g)	0.0331	0.0255	-	0.0099	0.0096
R^2	0.943	0.955	0.759	0.969	0.973

Results and Discussion

Effect of Furfural

The effects of furfural on the fermentation profiles of activated sludge microorganisms in aerobic bioreactors with glucose as sole carbon source are shown in Figures 7.1 -7.7 while the estimated kinetic parameters are shown in Table 7.2. The error bars in the charts represent the standard deviations of the four replicate runs. In general, biomass growth was inhibited by the presence of furfural (Fig. 7.1) even at levels as low as 0.5 g/L. Biomass growth trends were similar in the absence of furfural (control) and at a furfural level of 0.5 g/L. Initial biomass degradation was observed during the lag phase in both cases and the exponential phases began after 24 h of cultivation. However, the relative biomass increase observed at 0.5 g/L furfural was significantly lower than in the absence of furfural. As seen in Table 7.2, maximum specific growth rate (μ_{max}), maximum predicted non lipid biomass concentration (X_{max}), and overall non lipid biomass yield coefficient ($Y_{X/S}$) were reduced by 54, 8, and 35 %, respectively by the addition of 0.5 g/L furfural. Cultivation at 1.5 g/L furfural was characterized by a prolonged lag phase that extended until the end of the fermentation run (7 d), indicating a severe inhibition of biomass growth in activated sludge. No measurable increase in biomass relative to the initial value was observed at this furfural level hence model fitting with the fermentation data failed and no kinetic parameters were obtained.

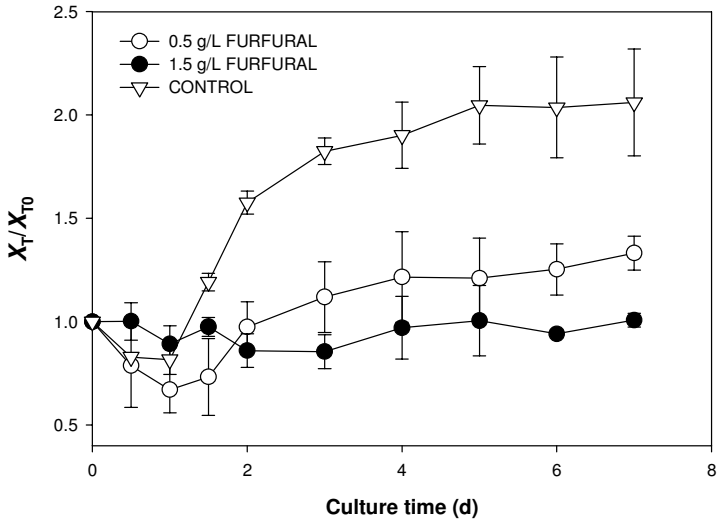

Figure 7.1: Effect of furfural on relative biomass production in glucose-fed activated sludge cultures.

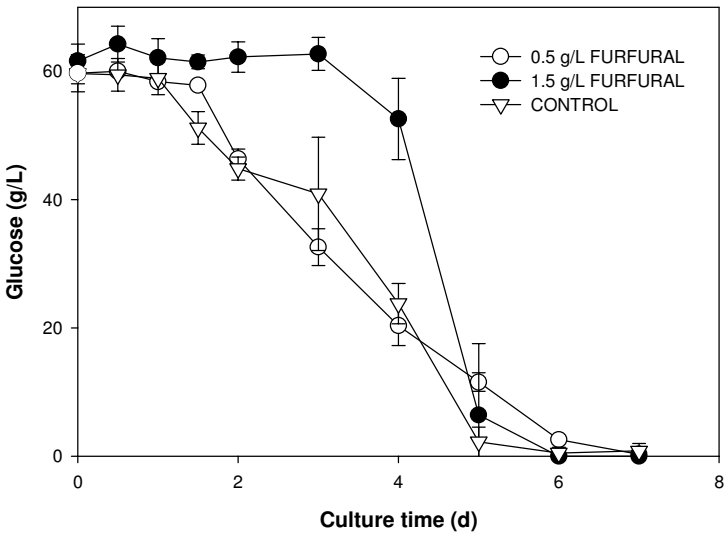

Figure 7.2: Effect of furfural on glucose utilization in glucose-fed activated sludge cultures.

Glucose utilization profiles (Fig. 7.2) were similar at the control and 0.5 g/L furfural runs, with roughly the same overall glucose uptake rates. With the addition of 0.5 g/L furfural a short lag period (0 – 24 h) in glucose uptake was observed before the glucose uptake rate increased coinciding with the onset of the exponential growth phase. On the other hand, the addition of 1.5 g/L furfural resulted in an extended lag period in glucose uptake (0 – 3 d), indicating significant inhibition in glucose utilization. It was only until after 3 d of cultivation when an increased rate of glucose uptake was observed. In all three treatments, majority of the initial glucose supply (> 90 %) was utilized after 5 d of cultivation. As shown in Figs. 7.3 and 7.4, the initial lag in glucose uptake could be attributed to the sequential consumption of glucose and furfural by the activated sludge microbiota. In both treatments, furfural was initially consumed by the microorganisms and the lag phases in glucose uptake coincided with the cultivation time span used to reduce the furfural concentration to less than 20 % of the initial levels. This phenomenon could perhaps be indicative of the natural furfural detoxification mechanism previously seen in ethanologenic and oleaginous yeasts wherein furfural was converted to the supposedly less toxic compounds furfuryl alcohol and furoic acid [Diaz de Villegas, et al., 1992; Hu, et al., 2009]. Moreover, the ammonium-nitrogen consumption profile (Fig. 7.5) also followed the same trend. The overall nitrogen consumption rate was highest with no furfural followed by 0.5 g/L furfural treatment. In both treatments, nitrogen levels were depleted after 2 d of fermentation whist at 1.5 g/L furfural addition, nitrogen levels were not depleted until after 5 d of cultivation. The extended lag phases in biomass

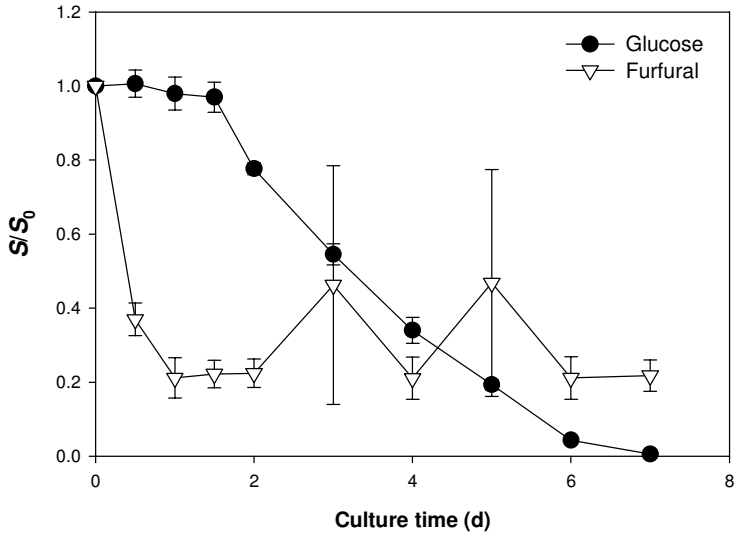

Figure 7.3: Time profiles of substrate utilization at 0.5 g/L initial furfural loading in glucose-fed activated sludge cultures.

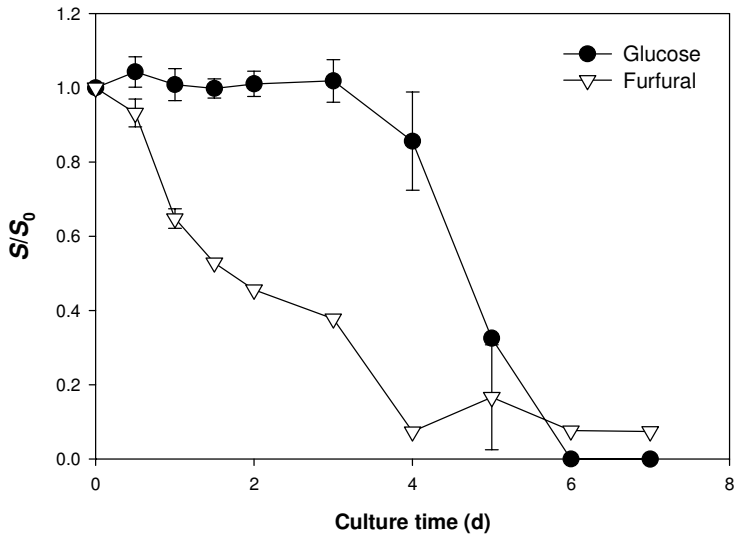

Figure 7.4: Time profiles of substrate utilization at 1.5 g/L initial furfural loading in glucose-fed activated sludge cultures.

growth and glucose consumption could be attributed to the inhibition of several enzymes involved in glycolysis and TCA cycle thus reducing the specific rates of these as discussed in Chapter III [Horvath, et al., 2003]. Further, the conversion of furfural to supposedly less toxic substances are also catalyzed by enzymes downstream pyruvate namely pyruvate decarboxylase and aldehyde dehydrogenase ADH, the latter of the two being also used for the reduction of acetaldehyde [Banerjee, et al., 1981]. Based on the results that were obtained in this study, the consumption of furfural appeared to be the favored process initially in the fermentation, once it was depleted, glucose consumption rates increased and biomass growth was observed. Therefore, it could be possible that ADH was preferentially utilized for furfural degradation leading to acetaldehyde build-up, which has been suggested as responsible for the observed lag phase [Palmqvist, et al., 1999].

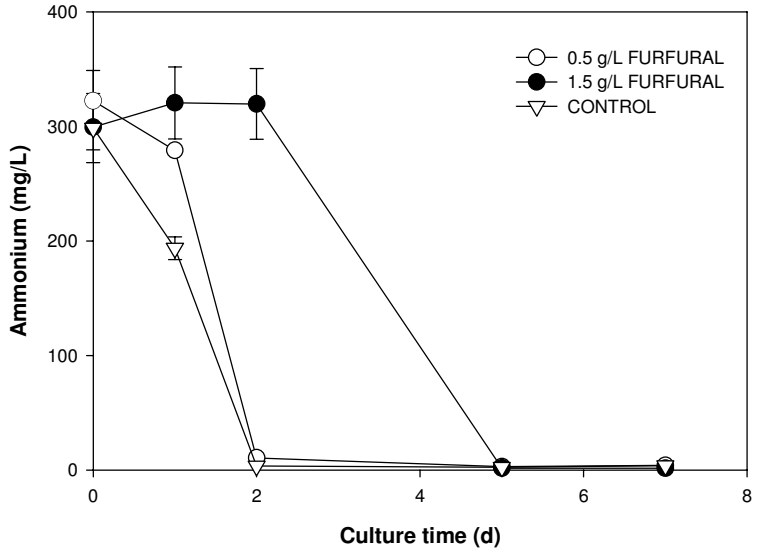

Figure 7.5: Effect of furfural on ammonium-nitrogen utilization in glucose-fed activated sludge cultures.

Lipid production by activated sludge was also severely inhibited by the addition of furfural as shown in Figs. 7.6 and 7.7. As shown in Fig. 7.6, the variation in gravimetric lipid yield observed at both levels of furfural addition involved an initial reduction followed by a gradual increase. The increase in the gravimetric lipid content relative to the initial lipid content in raw activated sludge (7.4 ± 1.1 % CDW) for the fermentation runs with added furfural were much lower than the increases in lipid content observed during control run. Compared with the control run, in which the activated sludge lipid content increased to a maximum of 18 % CDW, the addition of 0.5 g/L and 1.5 g/L furfural in the fermentation medium resulted in maximum lipid contents of 15.3 % and 10.3 % CDW, respectively, which were higher than that in raw activated sludge as well. The maximum volumetric lipid yield ($P_{\max}$) and overall lipid yield coefficient ($Y_{P/S}$) were reduced by 22 and 38 %, respectively at the 0.5 g/L furfural treatment (2.07 g/L and 0.024 g/g) compared with the control run (2.67 g/L and 0.038 g/g) whereas due to the severe inhibition in biomass growth resulting from the addition of 1.5 g/L furfural, no significant increase in volumetric lipid yield relative to the initial level was observed which even led to a negative lipid yield coefficient. The observed reduction of lipid and biomass yields in the presence of furfural despite the full utilization of glucose could be attributed to sugar consumption for cell maintenance. As shown in Table 7.2, the value of the maintenance coefficient term (k_e) was higher in the presence of 1.5 g/L furfural (0.043 g/g·h) than in the absence of furfural (0.019 g/g·h) although k_e at 0.5 g/L furfural level (0.007 g/g·h) was found to be slightly lower than that from the control setup.

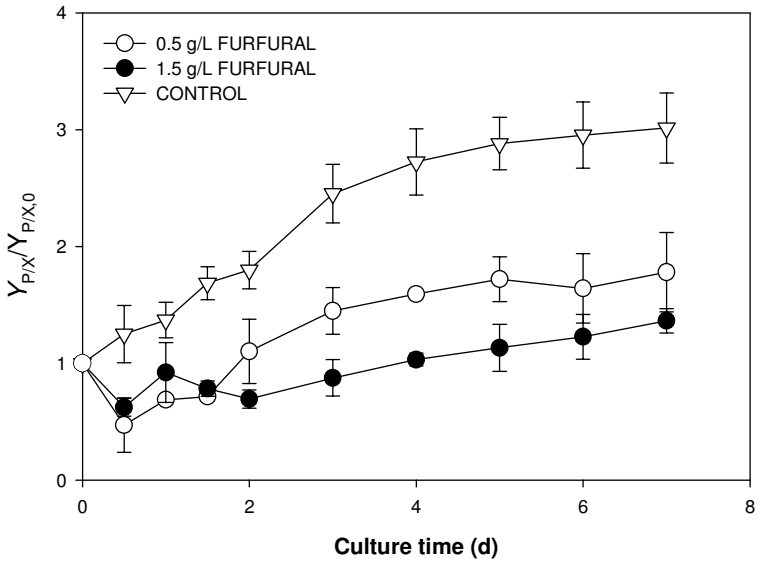

Figure 7.6: Effect of furfural on relative lipid yield (% dry biomass) in glucose-fed activated sludge cultures.

.

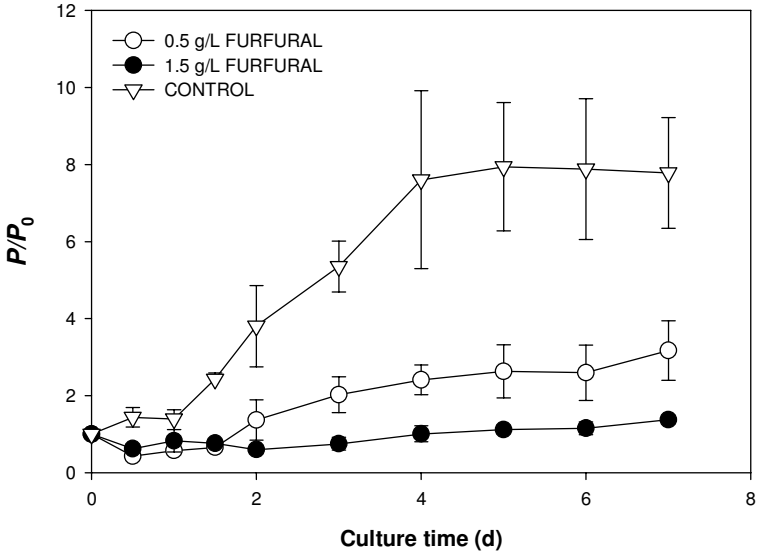

Figure 7.7: Effect of furfural on relative lipid concentration in glucose-fed activated sludge cultures.

In previous investigations, furfural levels as low as 1 mM (0.09 g/L) was found to have a drastic inhibitory effect on the oleaginous yeast *Rhodosporidium toruloides,* which led to reduction of glucose consumption, biomass yield, and lipid content by 41.1 %, 45.5, and 26.5 %, respectively [Hu, et al., 2009]. Compared with this data, cultivation of activated sludge in the presence of 0.5 g/L furfural resulted in 8 and 22 % reductions in biomass and lipid contents, respectively. Glucose was also fully consumed by activated sludge and furfural levels were reduced significantly as well. In addition, screening experiments conducted by Chen and colleagues [2009] obtained biomass and lipid concentrations in the culture, gravimetric lipid contents, and lipid yield coefficients for some oleaginous yeast strains at similar initial furfural concentrations similar to this study. Based on the results, the activated sludge cultures dosed with 0.5 g/L furfural produced higher maximum total biomass yields (12.7 ± 0.9 g/L) than the oleaginous yeasts *Trichosporon cutaneum 2.1374* (2.94 g/L), *Lipomyces starkeyi 2.1390* (5.41 g/L), and *Rhodotorula glutinis 2.107* (7.42 g/L). The final cellular lipid content (% CDW) of glucose-grown activated sludge were (12.7 ± 0.9 g/L) was relatively lower than *T. cutaneum 2.1374* (42.5 %CDW) and *L. starkeyi 2.1390* (30.3 % CDW) but higher than *R. glutinis 2.107* (5.51 %). With the exception of *T. cutaneum 2.1374* ($Y_{P/S}$ = 0.123 g/g), the overall lipid yield coefficient obtained with activated sludge at 0.5 g/L furfural dose (0.062 g/g) was comparable with *L. starkeyi 2.1390* (0.093 g/g) and greater than *R. glutinis 2.107* (0.021 g/g). Overall, these data suggest that activated sludge microorganisms could have better tolerance against relatively low furfural levels in the order of 0.5 g/L in fermentation media than some pure oleaginous yeast strains.

Effect of Acetate/Acetic Acid

The resulting fermentation profiles following fermentation of glucose in synthetic wastewater medium supplemented with acetic acid are shown in Figs. 7.8 – 7.14 and the estimated kinetic parameters are shown in Table 7.2. Likewise, the error bars in the charts represent the standard deviation of four replicate runs. Unlike furfural, the presence of acetic acid appeared to improve biomass growth by activated sludge microorganisms as shown in Fig. 7.8. The duration of the lag phase was shorter (12 h) with added 2 g/L acetic acid, whereas the lag phases in the control and 10 g/L acetic acid runs were slightly longer (24 h). However, the maximum total biomass concentration attained during the stationary phase in the 2 g/L acetic acid run (9.24 ± 0.37 g/L) were approximately 35 % lower than that attained in the control run (15.1 ± 2.6 g/L). The resulting overall non lipid kinetic parameters $Y_{X/S}$ and $X_{\max}$ values shown in Table 7.2 in the 2 g/L acetic acid run (0.046 g/g, 8.09 g/L) were also found to be around 52 and 37 % lower, respectively than $Y_{X/S}$ and $X_{\max}$ obtained with the control run (0.096 g/g, 12.9 g/L), indicating inhibition of biomass growth at this low acetic acid level. On the other hand, at the same initial glucose and nitrogen levels, biomass production was found to be significantly enhanced by the addition of 10 g/L acetic acid leading to a maximum total biomass production of 16.8 ± 0.9 g/L, which is higher than in the control run (15.1 ± 2.6 g/L). Overall glucose conversion to non lipid biomass was also enhanced by approximately 73 % and $X_{\max}$ was increased by around 39 % with the addition of 10 g/L acetic acid (0.17 g/g and 16.6 g/L, respectively) compared with the absence of acetic acid (0.096 g/g and 12.9 g/L). Further,

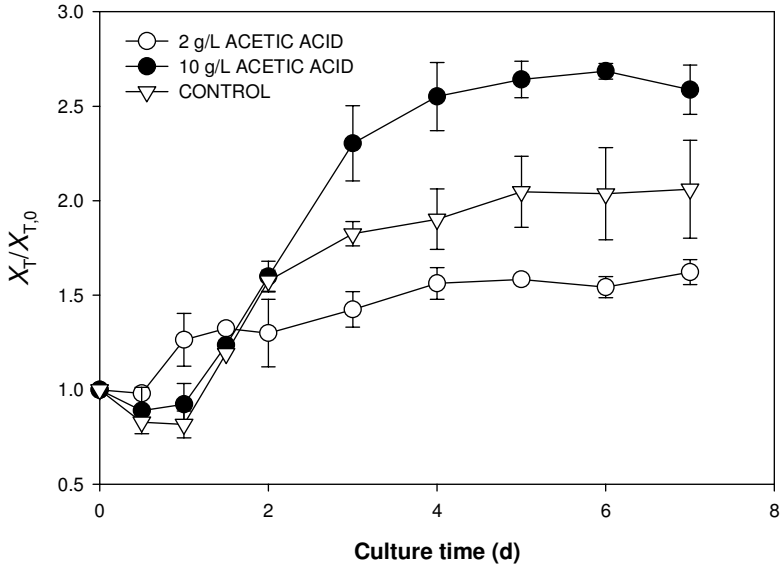

Figure 7.8: Effect of acetic acid on relative biomass production in glucose-fed activated sludge cultures.

calculated values of μ_{max} were similar between the control (0.027 h^{-1}) and the 2 g/L acetic acid run (0.029 h^{-1}) and was highest at the 10 g/L acetic acid run (0.03 h^{-1}).

The enhanced biomass production could be attributed to the fact that in the experiments performed, the initial pH of the media was set to 6.5 after acetic acid addition; hence it can be assumed that the compound is present mostly as acetate. As discussed in previous studies, the inhibitory effect of acetic acid was mostly attributed to the undissociated acid diffusing through the cell membranes and causing inhibition via reduction of intracellular pH [Gottschalk, 1987; Palmqvist and Hahn-Hagerdal, 2000], whereas the dissociated acid (acetate) could have been utilized as an additional carbon source for biomass production in excess levels such as in the 10 g/L acetic acid treatment level [Hu, et al., 2009].

The pH response of the cultures could have played a role in the observed biomass yields in the presence of acetic acid. As opposed to the control runs in which the pH dropped rapidly from 6.5 to 2.0 – 2.5 during the exponential phase and stayed constant from thereon, the pH of the culture with the 2 g/L acetic treatment run dropped more gradually from 6.5 to around 2.5 – 3.0 during the exponential and stationary growth phases. In the medium without or with relatively small initial acetic acid levels, the decrease in pH during fermentation observed was mostly attributed to the formation of carbonic acid (H_2CO_3) from the CO_2 produced by the microorganisms [Liden, et al., 1993]. In addition to this, acetic acid could also be a fermentation by-product that could contribute to the decrease in the pH of the culture. In the 2 g/L acetic acid treatment run, the low pH of the culture caused the acetic acid to remain in its undissociated form, causing the inhibition of cell growth late in the fermentation run. On the other hand, the pH response of the activated sludge culture dosed with 10 g/L acetic acid was characterized by an initial decrease from 6.5 to around 5.5 during the exponential phase (24 – 36 h) followed by an increase in the pH of up to 8.8 – 10.5. This pH increase has also been observed previously on the ethanologenic yeast *Pichia stipitis* and has been attributed to the reduction in levels of the undissociated acetic acid, which exists in equilibrium with the acetate form. By virtue of Lé Chatelier's principle, consumption of the acetate caused a corresponding decrease in the acetic acid and hydronium (H_3O^+) concentration, causing the increase in pH. Although carbonic acid production from CO_2 and possible endogenous acetic acid production could have also occurred simultaneously with the consumption of acetate/acetic acid, the latter process appeared to be more dominant, causing the net effect of pH increase.

As shown in Fig. 7.9, glucose consumption rates in the presence of acetic acid/acetate were found to be faster than in the control runs unlike in the fermentation runs with furfural. The lag period in glucose uptake observed in the control run was slightly longer than the acetic acid treatments. However, the average glucose consumption rates during the exponential phase in the presence of 2 g/L (0.79 g/L·h) and 10 g/L acetic acid (0.73 g/L·h) were higher than that in the control run (0.35 g/L·h). Glucose was fully consumed after only 3 d with the addition of 2 g/L acetic acid. However, despite the higher initial glucose uptake rates at 10 g/L acetic acid compared with the control run, the glucose uptake rate decreased gradually in the former treatment and 100 % glucose utilization was achieved after 5 d in both cases. Acetic acid uptake rate was also slightly higher than the glucose uptake rate in the 2 g/L acetic acid (Fig. 7.10) treatment run whereas both substrate consumption rates were similar with the addition of 10 g/L acetic acid (Fig. 7.11). These relatively higher rates of glucose consumption could be attributed to the utilization of glucose for the production of additional ATP by the ATP synthase enzyme complex located in the plasma membrane. The ATP production is coupled with the pumping protons out of the cytoplasm across the cell membrane to combat the decrease in intracellular pH brought by the diffusion of the undissociated acetic acid into the cell [Verduyn, et al., 1990a]. The added ATP production increased the requirement for glucose for cell maintenance in addition to those

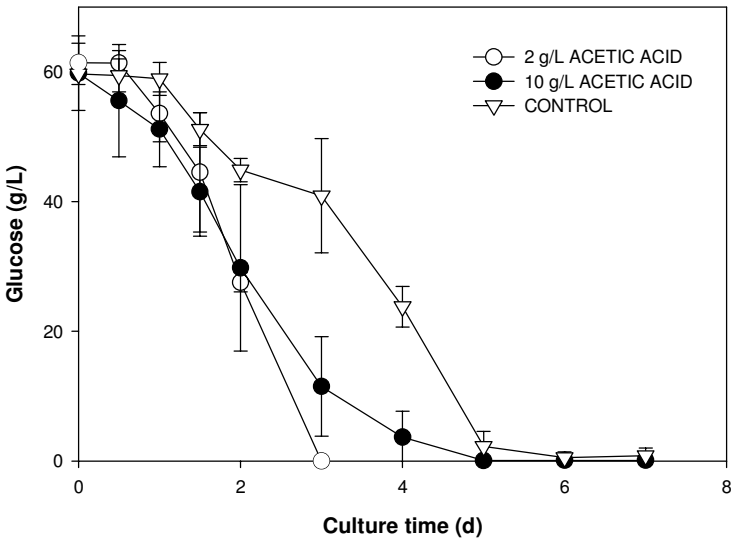

Figure 7.9: Effect of acetic acid on glucose utilization in glucose-fed activated sludge cultures.

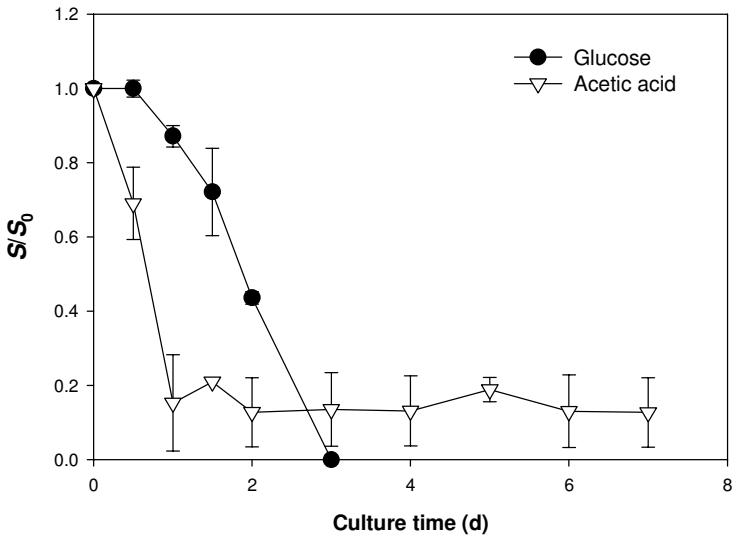

Figure 7.10: Time profiles of substrate utilization at 2 g/L initial acetic acid loading in glucose-fed activated sludge cultures.

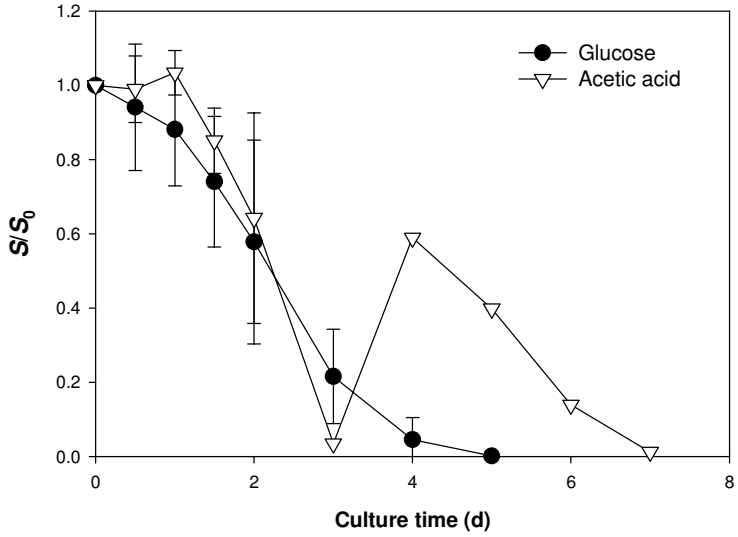

Figure 7.11: Time profiles of substrate utilization at 10 g/L initial acetic acid loading in glucose-fed activated sludge cultures.

converted to biomass and lipids, hence the increased rate. This is reflected in the k_e value obtained at the 2 g/L acetic acid treatment run (0.079 g/g·h), which is relatively higher than k_e obtained in the control run (0.019 g/g·h). On the other hand, the k_e value obtained from the 10 g/L acetic acid treatment run (0.007 g/g·h), which was much lower than the in the control run could further imply minimal inhibition by reduced levels of undissociated acid, given that final pH levels were above neutral unlike in the 2 g/L acetic acid run. Furthermore, this apparent similarity of glucose and acetic acid consumption rate could be also attributed to the fact that both glucose and acetic acid/acetate (which could be converted to acetyl-CoA) are intermediates of the glycoltic pathway; hence no additional pathways and therefore lag periods are necessary for the consumption of acetate. It should be noted that the substrate utilization parameters

presented here were based only on glucose; whereas the possible utilization of acetate in the medium may need to be considered in the total biomass yield obtained. Furthermore, the observed increase in acetic acid level after 4 d at the 10 g/L acetic acid treatment run could be an effect of endogenous production of acetic acid by some members of the activated sludge microbiota. The ammonium-nitrogen consumption profiles in Fig. 7.12 shows that nitrogen uptake rates were highest with the addition of 2 g/L acetic acid followed by the control run, leading to nitrogen depletion after 24 and 48 h of fermentation, respectively. This trend reflected that of the biomass production (Fig. 7.8) wherein the exponential growth phase started earlier at the 2 g/L acetic acid treatment run causing the initially higher biomass concentration, hence the nitrogen supply was consumed more quickly. Ammonium-nitrogen uptake rates at the 10 g/L acetic acid run were found to be much slower initially, despite similar biomass growth trends between 24 and 48 h of cultivation after which nitrogen levels were depleted as well. The added biomass weight level could then be attributed to the increase in the lipid fraction of the total biomass.

As opposed to the observed enhancement in biomass production due to acetic acid, lipid production was inhibited in both acetic acid levels tested. As shown in Fig. 7.13, cellular lipid contents (% CDW) of activated sludge grown in the presence of acetic acid increased by no more than 50 % of the initial value in raw activated sludge, as opposed to the control run with no acetic acid supplied wherein the lipid content of activated sludge biomass generated after 7 d (17.8 ± 2.8 % CDW) was thrice that of the initial value (5.4 ± 1.0 % CDW). Different trends were observed between the two levels

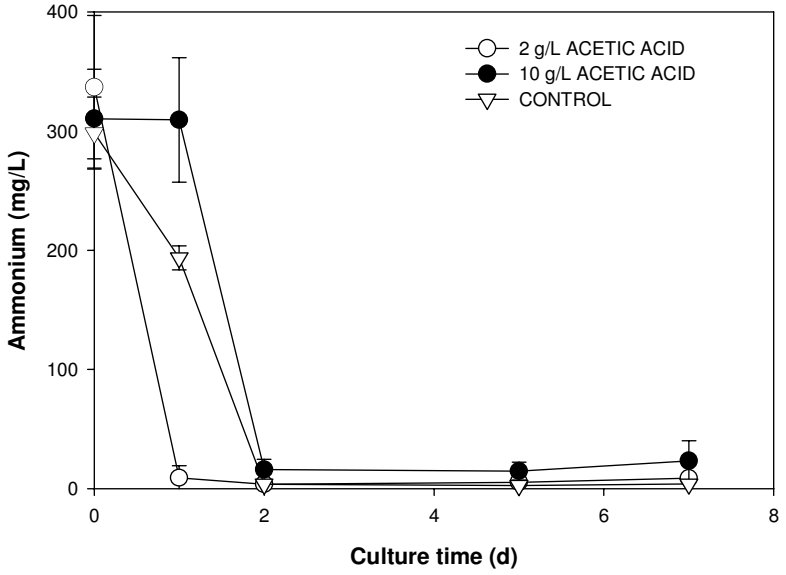

Figure 7.12: Effect of acetic acid on ammonium-nitrogen utilization in glucose-fed activated sludge cultures.

of acetic acid investigated. With the addition of 2 g/L acetic acid in the activated sludge culture, biomass lipid contents increased gradually to reach the maximum of 12.5 ± 0.7 % (CDW) after 7 d; whilst at the 10 g/L acetic acid treatment run, biomass lipid content jumped from 7 to 9 % (CDW) between 36 to 48 h of fermentation and gradually increased to a maximum level of 10.2 ± 4.3 % (CDW) after 5 d, after which it decreased. It is interesting to note that this observed decrease in lipid content at 10 g/L initial acetic acid loading roughly coincided with the sudden increase in acetic acid (undissociated) concentration day four of fermentation (Fig. 7.11) and the reduction in the biomass production rate Fig. 7.8) after 4 d of cultivation. It is probable that due to the increased demand for ATP production in order to maintain a neutral intracellular pH, majority of the glucose is used for this purpose. After glucose depletion at 5 d, the activated sludge

microorganisms might have proceeded to utilize the stored lipids as a carbon source for this purpose. Overall lipid yield coefficients ($Y_{P/S}$) shown in Table 7.2 were also reduced by 70 % and 47 % with the addition of 2 and 10 g/L acetic acid in the media, respectively and majority of the lipid production occurred during the growth phase due to the higher $Y_{P/S}$ during this phase as opposed to the lipid accumulation phase. Lipid accumulation was also influenced more by instantaneous biomass growth since $m > n$ in all cases. The lipid concentration profiles (Fig. 7.14), which describe the net effect of total biomass yield and gravimetric lipid content, showed similar trends with the gravimetric lipid yield profiles (Fig. 7.13). The maximum lipid concentrations attained in the culture with 2 and 10 g/L acetic acid loadings were reduced by 57 % (1.2 g/L) and 38 % (1.7 g/L), respectively compared to the control run (2.67 g/L).

Overall, the results obtained regarding the effect of acetic acid on activated sludge were similar with experiments on the oleaginous yeast *Trichosporon cutaneum 2.1374*, wherein the maximum cell mass obtained at the fermentation run with 5 g/L acetic acid added to the initial medium (3.68 g/L) was greater than that without acetic acid (2.75 g/L) [Chen, et al., 2009]. Unlike the activated sludge however, lipid accumulation in *T. cutaneum* was even slightly improved with the addition of 5 g/L acetic acid (1.12 g/L) compared with no acetic acid (1.09 g/L). Similar levels of acetic acid (4.2 – 7.2 g/L initial loading) were also found to have a little effect on lipid production in *Rhodosporidium toruloides Y4,* in which lipid contents reached as high as 68 % by mass [Hu, et al., 2009]. In these cases, the high concentration of acetate led to an increase in C:N ratio such that lipid accumulation was further enhanced.

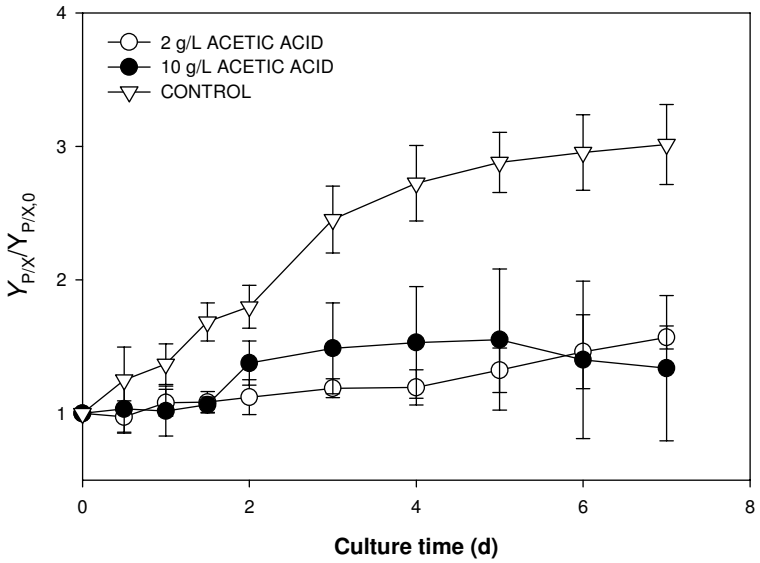

Figure 7.13: Effect of acetic acid on relative lipid yield (% dry biomass) in glucose-fed activated sludge cultures.

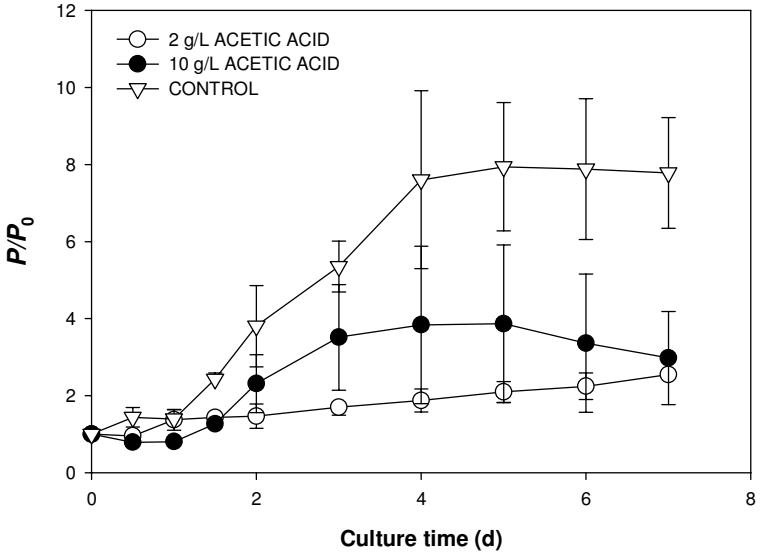

Figure 7.14: Effect of acetic acid on relative lipid concentration in glucose-fed activated sludge cultures.

Effect of Furfural and Acetic Acid Combinations

Further experiments were conducted using combinations of furfural and acetic acid to investigate any interaction between these two inhibitors. The resulting fermentation profiles are shown in Figs. 7.15 – 7.21 and the calculated kinetic parameters specific for these experiments and the corresponding control runs are summarized in Table 7.3. Combinations of low furfural (0.5 g/L)/low acetic acid (2 g/L) and high furfural (1.5 g/L)/high acetic acid (10 g/L) were tested. In terms of biomass growth, Fig. 7.15 shows complex patterns between the two treatments investigated relative to the control run. The biomass growth pattern at the control runs conducted alongside the treatment runs can be described by a short lag phase (0 -12 h) followed by a gradual increase in the total biomass concentration up to 8.64 ± 1.67 g/L. At the low furfural/low acetic acid treatment, the lag phase occurred within 24 h of cultivation time followed by the exponential phase from day one to three in which the total biomass increased approximately six-fold from 1.26 ± 0.11 g/L to 8.11 ± 1.50 g/L. As a result, the calculated values of the μ_{max} and X_{max} at this treatment (0.058 h^{-1} and 8.27 g/L) were higher than the control run (0.046 h^{-1} and 7.26 g/L). On the other hand, cell biomass growth at combination of 1.5 g/L furfural and 10 g/L acetic acid was characterized by a prolonged lag phase spanning up to 3 d followed by growth at a higher rate in the exponential phase to a maximum of 14.1 ± 0.6 g/L, which is almost ten-fold the initial biomass concentration. However, due to the longer lag phase, the calculated overall μ_{max} for this treatment (0.044 h^{-1}) was only slightly lower than that in the control run (0.046 h^{-1}). Compared with the control run, overall non lipid biomass yields ($Y_{X/S}$) based

Table 7.3: Kinetic parameter estimates for the Logistic and Leudeking-Piret models for treatment runs involving mixed inhibitors.

Parameters	Inhibitor Concentration (g/L)		
	0 (Control)	Combined Furfural/Acetic acid	
		0.5/2	1.5/10
Non lipid biomass			
μ_{max} (h^{-1})	0.0455	0.0583	0.0441
X_0 (g/L)	1.15	0.79	0.12
X_{max} (g/L)	7.26	8.27	14.5
R^2	0.959	0.966	0.980
Lipid			
m (g/g)	0.0797	0.0655	0.0393
n (g/g·h)	9.77×10^{-5}	1.51×10^{-5}	9.20×10^{-5}
Final Lipid Content (% CDW)	18	6.0	3.5
P_{max} (g/L)	1.41	0.64	0.77
R^2	0.997	0.973	0.898
Glucose			
α (g/g)	5.03	0.253	3.32
β (g/g·h)	4.83×10^{-4}	0.124	0.0184
k_e (g/g·h)	0.006	0.122	0.011
$Y_{X/S}$ Overall (g/g)	0.167	0.141	0.218
$Y_{X/S}$ Growth Phase (g/g)	0.162	0.136	0.208
$Y_{X/S}$ Lipid Phase (g/g)	0.181	0.240	0.0511
$Y_{P/S}$ Overall (g/g)	0.038	0.0094	0.013
$Y_{P/S}$ Growth Phase (g/g)	0.019	0.0094	0.0102
$Y_{P/S}$ Lipid Phase (g/g)	0.063	0.0095	0.0033
R^2	0.975	0.901	0.992

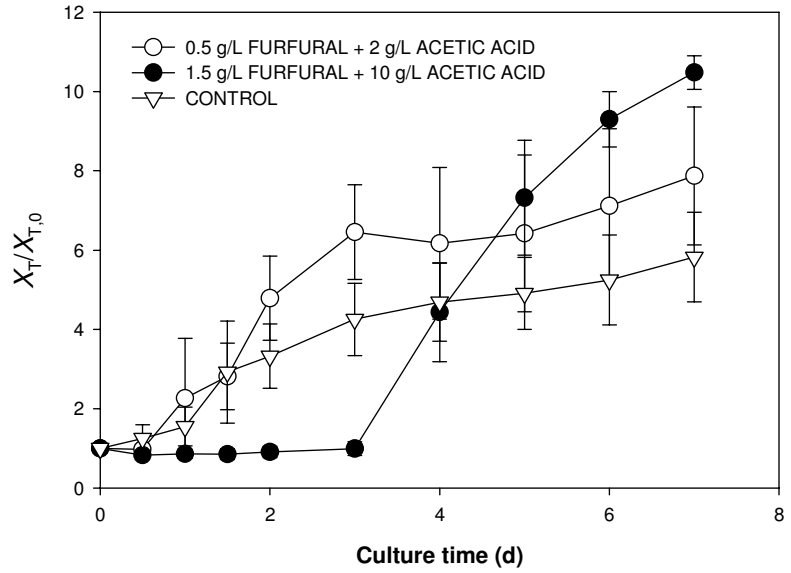

Figure 7.15: Interaction effect of furfural/acetic acid combinations on relative biomass production in glucose-fed activated sludge cultures.

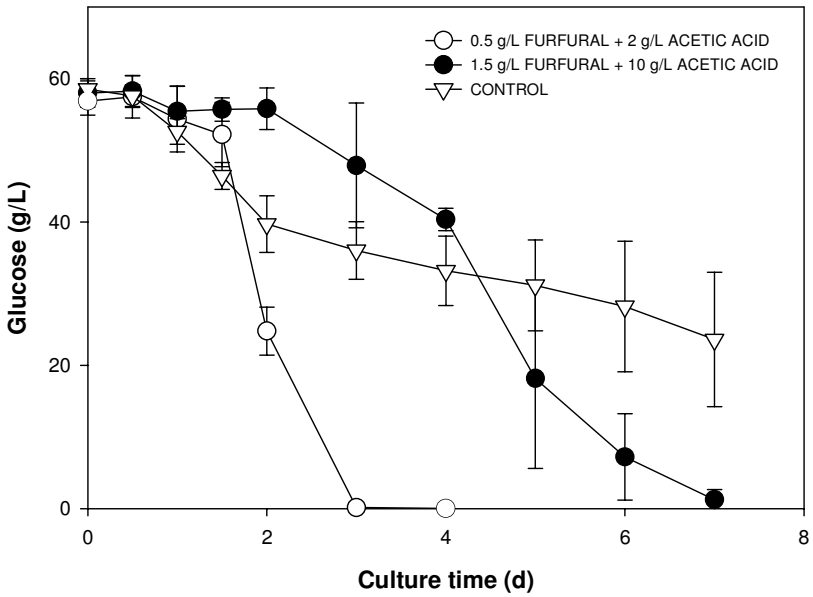

Figure 7.16: Interaction effect of furfural/acetic acid combinations on glucose utilization in glucose-fed activated sludge cultures.

on glucose consumed was lower at the low furfural/low acetic acid treatment run (0.141 g/g) but higher at the high furfural/high acetic acid run (0.218 g/g).

As shown in Fig. 7.16, the glucose consumption profiles could be correlated to the biomass growth patterns previously discussed. In all cases, the lag periods in glucose uptake coincided with lag phases in biomass growth. Increased rates of glucose uptake were observed along with the exponential growth phases. These observed lag period in glucose consumption could also be further explained by the degradation patterns of acetic acid and furfural shown in Figs. 7.17 and 7.18. Whereas the effect of furfural is an initial lag in glucose uptake as shown earlier (Figs. 7.3 and 7.4) while the effect of acetic acid is an increased rate in glucose uptake (Figs. 7.10 and 7.11), the combined effect of furfural and acetic acid in glucose uptake appears to be additive. Consumption of the three carbon sources was found to be sequential, with furfural being consumed first by the activated sludge microorganisms probably for conversion to the less toxic furfuryl alcohol and furoic acid. After only 10 to 20 % of the initial furfural concentration remained, acetic acid and glucose consumption rates started to increase since glucose is consumed for the production of ATP needed for counteracting the decrease in intracellular pH caused by acetic acid. In both treatments, some increases in acetic acid concentrations were observed possibly due to acetic acid production by some members of the activated sludge microbiota. This could be the case in the high furfural/high acetic acid run, wherein the lag phase in glucose uptake caused by furfural degradation caused the acetic acid levels to spike up to 20 % higher than the initial concentration after which degradation occurred

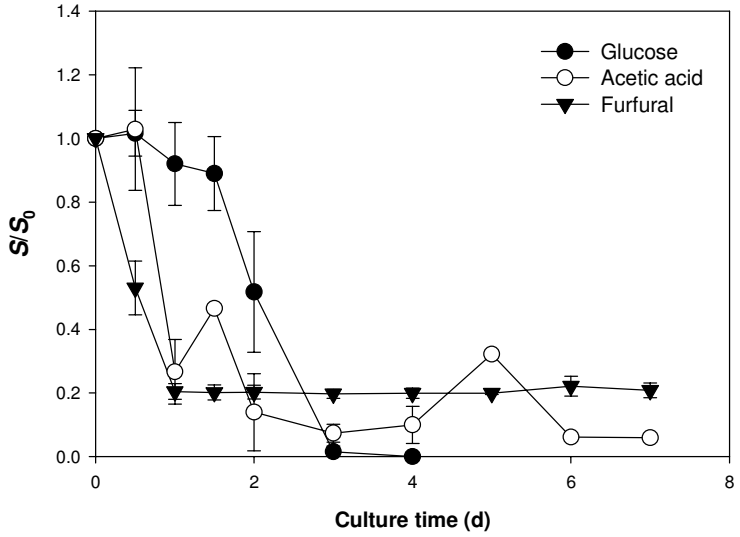

Figure 7.17: Time profiles of substrate utilization at low furfural (0.5 g/L) and low acetic acid (2 g/L) loading in glucose-fed activated sludge cultures.

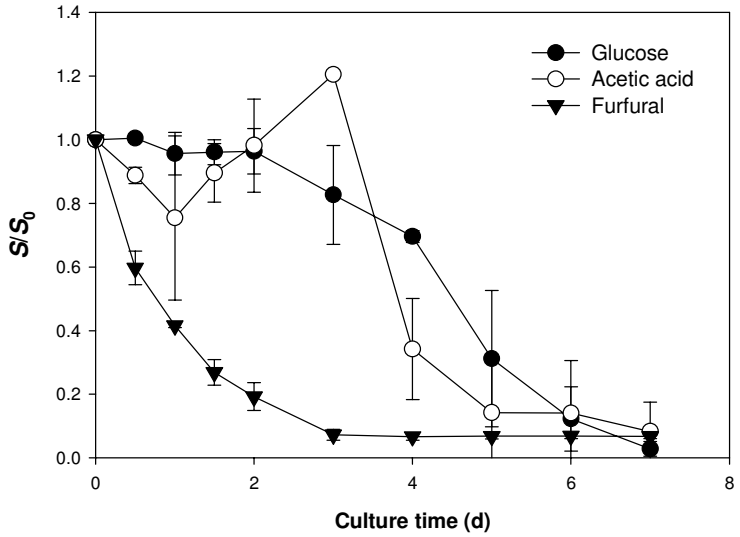

Figure 7.18: Time profiles of substrate utilization at high furfural (1.5 g/L) and high acetic acid (10 g/L) loading in glucose-fed activated sludge cultures.

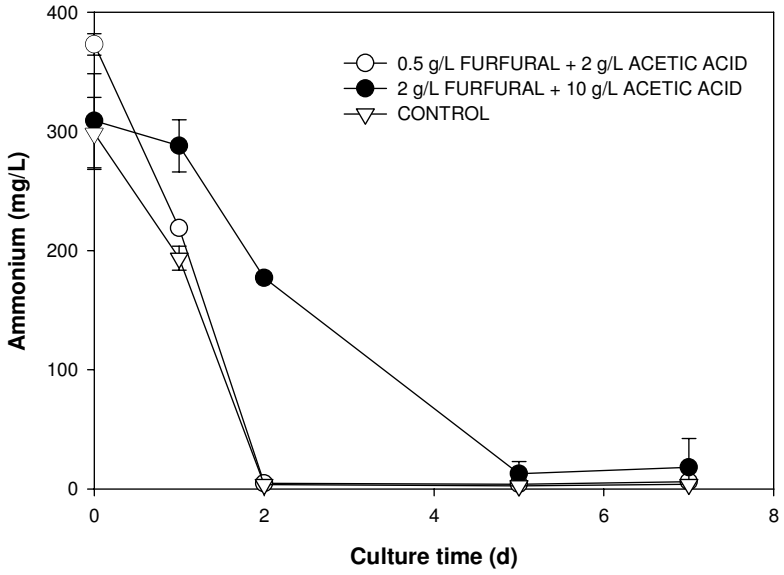

Figure 7.19: Interaction effect of furfural/acetic acid combinations on ammonium-nitrogen utilization in glucose-fed activated sludge cultures.

when furfural levels were sufficiently low. As a result, maintenance coefficient (k_e) values were higher at the treatments than in the control run (Table 7.3). Similarly, the effect of furfural/acetic acid combinations on ammonium nitrogen utilization appears to be additive as well as shown in Fig. 7.19. The lag period in nitrogen consumption at the 1.5 g/L furfural and 10 g/L acetic acid combination was attributed to inhibition due to high levels of furfural and acetic acid observed individually whereas the faster nitrogen consumption rate at the combination of low furfural (0.5 g/L) and low acetic acid (2 g/L) were also observed in the fermentation runs involving the individual inhibitors at the same levels.

As shown in Fig. 7.20, lipid accumulation was inhibited at the 0.5 g/L furfural + 2 g/L acetic acid run, where biomass lipid contents remained constant at the initial level in

raw activated sludge (7.5 ± 1.7 % CDW). On the other hand, the cellular lipid content increased to a maximum of 10 -11 % (CDW) initially at the 1.5 g/L furfural + 10 g/L acetic acid run from days one to three of cultivation, after which it decreased significantly to less than 4 % CDW. This phenomenon could be correlated to the observed sudden increase in biomass growth and glucose consumption after furfural levels have been sufficiently reduced to low levels. In spite of this, Fig. 7.21 shows that volumetric lipid yields increased with fermentation time even with the addition of furfural/acetic acid mixtures, which could be an effect of the enhanced total biomass production observed previously. Moreover, overall lipid yields ($Y_{P/S}$) were 75 and 66 % lower at the 0.5 g/L furfural + 2 g/L acetic acid (0.009 g/g) and 1.5 g/L furfural + 10 g/L acetic acid (0.013 g/g) treatment runs, respectively than the control run (0.038 g/g). Maximum predicted lipid concentrations were also reduced by 55 and 45 % at the 0.5 g/L furfural + 2 g/L acetic acid (0.64 g/L) and 1.5 g/L furfural + 10 g/L acetic acid (0.77 g/L) treatment runs, respectively relative to the control run (1.41 g/L).

As mentioned in a previous paper, if the sum of the relative reductions in kinetic parameters obtained from single inhibitor fermentations (based on the corresponding control run) is equal or close to those obtained from experiments with mixed inhibitors, the inhibition of the two inhibitors was defined as additive; while if the experimental data exceeded the calculated one, the inhibition was defined as synergistic [Hu, et al., 2009]. Based on the values of $Y_{P/S}$ and $X_{\max}$ obtained in this study, the relative percent

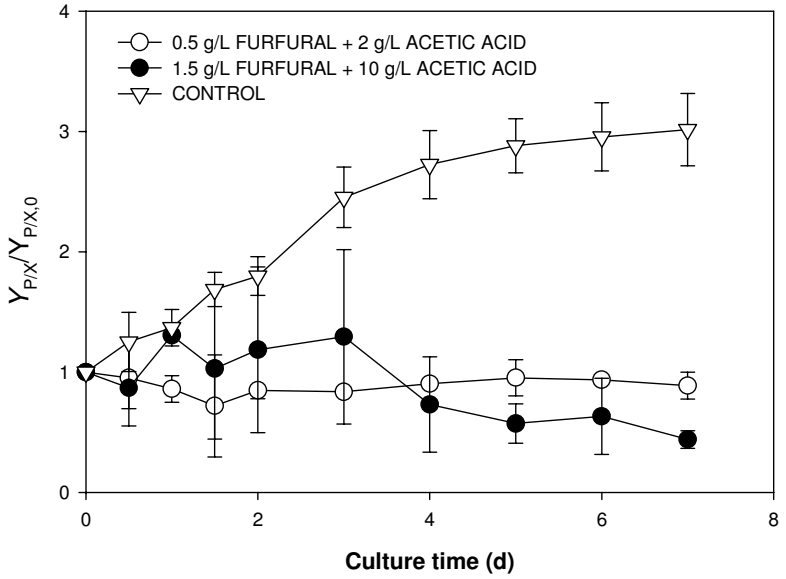

Figure 7.20: Interaction effect of furfural/acetic acid combinations on relative lipid yield (% dry biomass) in glucose-fed activated sludge cultures.

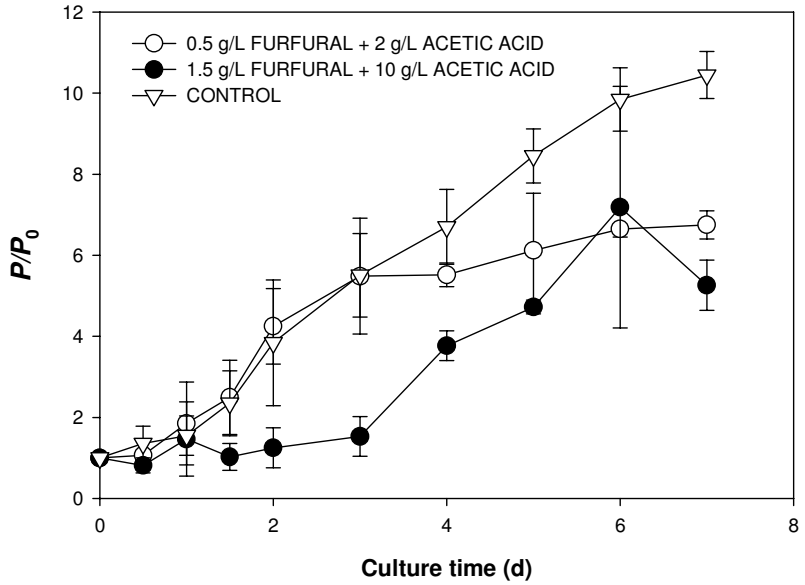

Figure 7.21: Interaction effect of furfural/acetic acid combinations on relative lipid concentration in glucose-fed activated sludge cultures.

reductions obtained from mixed inhibitor experiments were found to be much less than the sum of the percent reductions obtained from single inhibitor fermentation experiments, which implies neither an additive nor synergistic inhibitory effect. Instead, the inhibitory effects of furfural on total biomass and lipid production was probably counteracted with the stimulatory effect of acetate on total biomass production (which affects the volumetric lipid yield) to produce the net effect reduction in the values of $Y_{P/S}$ and $X_{\max}$ relative to the control run.

Lipid Analysis

The lipid extracts from the activated sludge biomass generated after cultivation under different levels and combinations of furfural and acetic acid were transesterified and characterized via GC-FID analysis. The relative proportions of the total lipid extracts and the saponifiable fractions in the total biomass at their final values (after 7 d) from the different treatments investigated are shown in Figs. 7.22 – 7.24, whereas the final fatty acid profiles of the lipid extracts from the different treatments are shown in Figs. 7.25 – 7.27. After 7 d of cultivation the total lipid extract yield in the absence of inhibitors was higher than those obtained with the addition of furfural and acetic acid. Also, the saponifiable fraction of the lipid extract, or those converted to methyl esters (biodiesel) consistently accounted for approximately 50 – 60 % of the total lipid extract regardless of treatment levels investigated compared to that in raw activated sludge (25 %). In all the treatments investigated, saponifiable fractions constitute around 25 % of the total lipids during the lag periods of growth and substrate consumption, after which levels increased

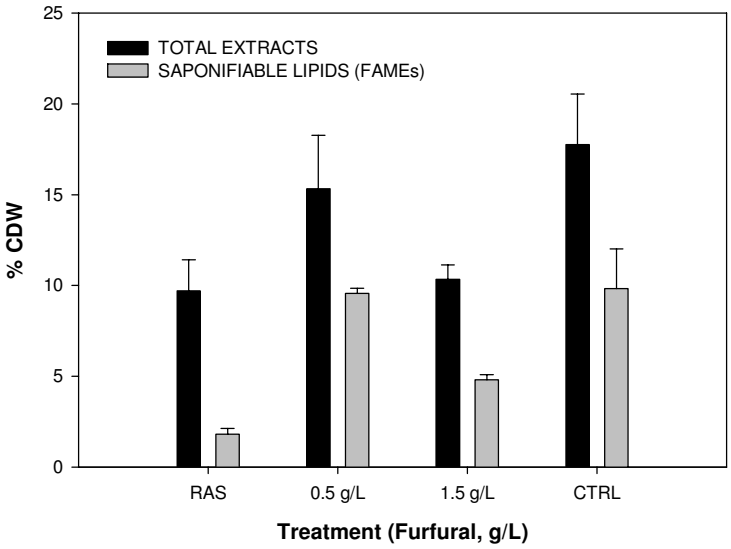

Figure 7.22: Effect of furfural on total and saponifiable lipid yields from glucose-grown activated sludge. RAS: raw activated sludge.

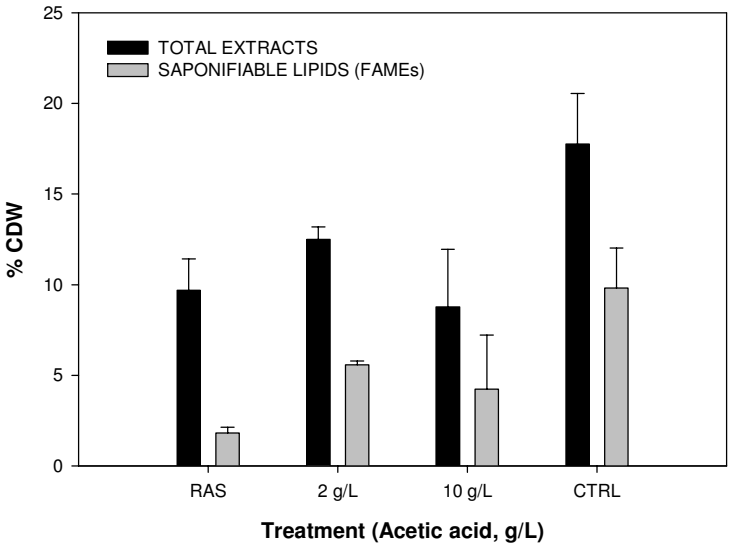

Figure 7.23: Effect of acetic acid on total and saponifiable lipid yields from glucose-grown activated sludge. RAS: raw activated sludge.

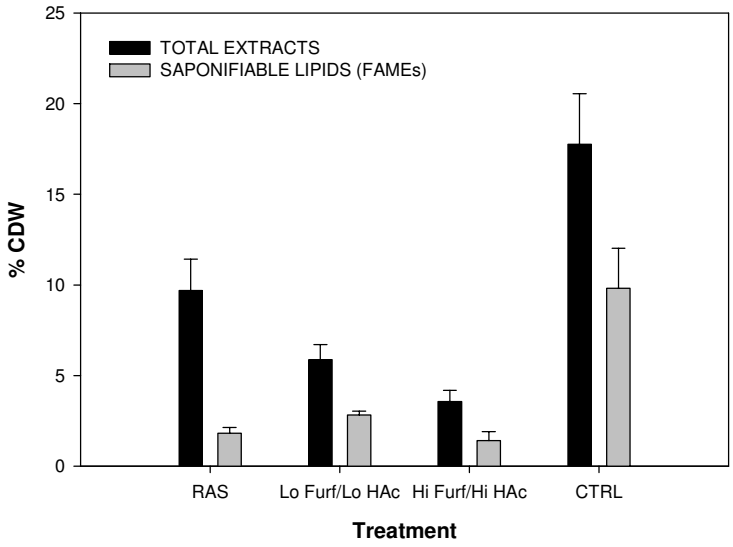

Figure 7.24: Effect of furfural/acetic acid combinations on total and saponifiable lipid yields from glucose-grown activated sludge. Lo Furf = 0.5 g/L, Hi Furf = 1.5 g/L. Lo HAc = 2 g/L, Hi HAc = 10 g/L. RAS: Raw activated sludge.

to 50 -60 % once growth and glucose consumption rates have increased. The maximum saponifiable lipid (i.e., biodiesel) yield attained in the presence of inhibitors was 9.7 % CDW, which is very close to that obtained in the control run (10 % CDW). However, due to the severe biomass growth inhibition caused by furfural, this increase in the saponifiable fraction seemed insignificant due to the very low resulting volumetric yields.

In terms of the fatty acid distribution of the lipid extracts, Figs. 7.25 – 7.27 shows that among the major fatty acyl residues (C_{16} - C_{18}) investigated, oleic acid (C18:1) was found to be the dominant fatty acid residue in the cultivated activated sludge, constituting around 35 – 40 % of the total FAMEs compared with around 25 % in raw activated sludge, and was slightly lower than that obtained in the control run (approximately 40-45 %) in all the inhibitor concentrations and combinations investigated. The increase in oleic

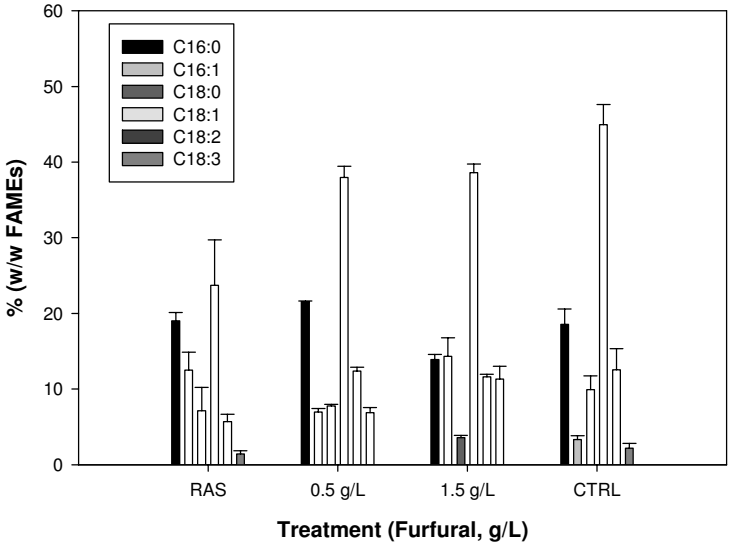

Figure 7.25: Fatty acid profiles of cultured activated sludge lipid extracts at different furfural loadings.

acid contributed heavily to the increase in unsaturated fatty acid levels in the activated sludge lipids, while the proportion of saturated fatty acids remained fairly constant, majority of which is palmitic acid (C16:0). Similar results were observed in the oleaginous yeast *Rhodosporidium toruloides,* wherein oleic acid was likewise the major fatty acid (40 – 53 % of total fatty acids) regardless of the identity and concentration of the inhibitor. Next to oleic acid, palmitic (C16:0) and linoleic (C18:2) acids were also present in significant levels Palmitic acid levels were essentially the same with raw and glucose-grown activated sludge (18 – 20 %) while in all the treatments, linoleic acid levels increased from around 5 % in raw sludge to 13% in glucose-grown activated sludge. The fatty acid profile obtained in this study were similar to plant oils, hence lipid produced by activated sludge microorganisms from lignocellulose hydrolyzate is of great potential as biodiesel feedstock. [Liu and Zhao, 2007].

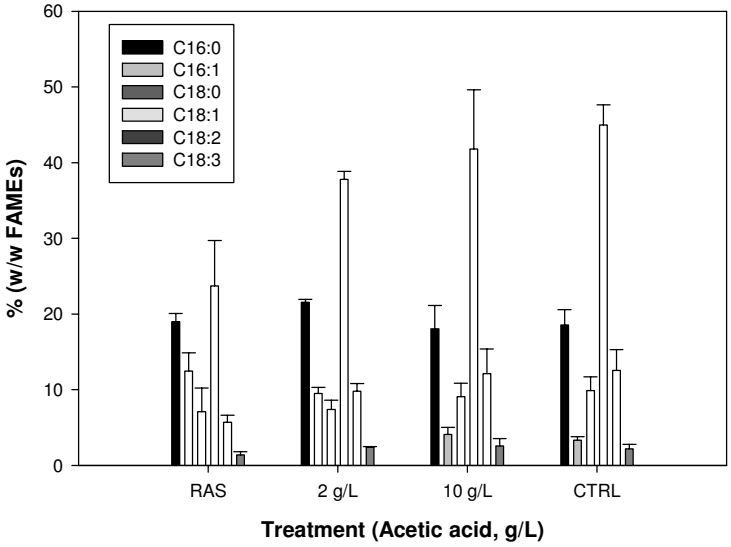

Figure 7.26: Fatty acid profiles of cultured activated sludge lipid extracts at different acetic acid loadings.

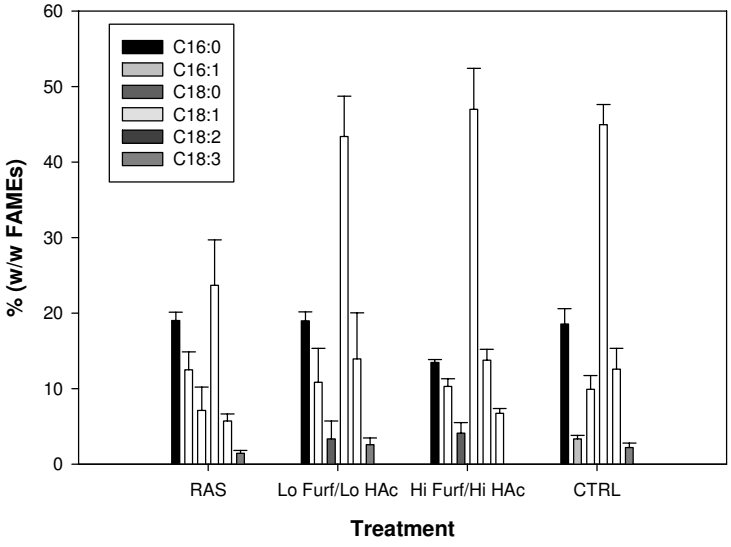

Figure 7.27: Fatty acid profiles of cultured activated sludge lipid extracts at different furfural/acetic acid mixture loadings. Lo Furf = 0.5 g/L, Hi Furf = 1.5 g/L. Lo HAc = 2 g/L, Hi HAc = 10 g/L.

Conclusion

Effective utilization of lignocellulose biomass in fermentative processes in biofuels production requires pretreatment and hydrolysis to release the fermentable sugars, which is accompanied by the formation of degradation by-products with known toxic properties. Hence, tolerance of microorganisms towards these compounds is required for the successful application of these waste biomass materials for the production of high value products such as biofuels. The results obtained from this phase of the study indicated that the presence of the lignocellulose hydrolysis by-products furfural and acetic acid in aerobic cultures of activated sludge with glucose as the sole carbon source affected the fermentation process related to biomass growth, lipid accumulation, and glucose consumption by activated sludge microorganisms. Overall, the presence of furfural in the activated sludge cultures caused significant inhibition in total biomass growth, lipid accumulation, and initially, glucose consumption rates due to the assumed conversion of furfural to supposedly less toxic compounds such as furfuryl alcohol and furoic acid for cell maintenance. On the other hand, the presence of acetic acid, particularly in high levels in the order of 10 g/L caused an enhancement in biomass growth in activated sludge most likely due to the utilization of acetate as an additional carbon source. However, intracellular lipid accumulation was reduced in the presence of acetic acid, and the observed higher rates of glucose consumption was attributed to the production of ATP catalyzed ATP synthase enzyme to drive the proton pump across microbial cell membranes in order to maintain intracellular pH close to neutral and maintain cell viability. Combinations of furfural and acetic acid exhibited additive effects resembling a stepwise detoxification process in which furfural was

degraded initially followed by a sudden increase in acetic acid and glucose uptake, presumably for the maintenance of intracellular pH to neutrality. Biomass production and glucose uptake were inhibited initially as long as furfural was still present in the culture, after which biomass growth exceeded those observed in the control run. However, lipid accumulation was inhibited presumably due to the effect of the residual acetic acid in the culture. Although the resulting gravimetric lipid yields were lower in the presence of the acetic acid/furfural mixtures, volumetric lipids yields (g/L) showed increasing trends with fermentation time due to the significant biomass growth. Analysis of the activated lipid extracts indicated that the presence of inhibitors have negligible effect on the saponifiable lipid fraction (with respect to the total lipid extract yield, % CDW) and fatty acid distribution. Similar with fermentation runs with no inhibitors, biodiesel (FAME) yields from the total extracts were consistent at 50 -60 % (w/w total extracts) while oleic acid was found to be the most dominant fatty acid in the lipids.

Based on these findings, further investigations will be necessary in order to reduce the inhibitory effects exhibited by both furfural and acetic acid, two of the most commonly found inhibitor compounds in lignocellulose hydrolyzates, on the fermentation of sugars by activated sludge microorganisms for lipid and biodiesel yield enhancement. While physical and chemical detoxification methods are in common practice, adaptation methods to select for tolerant members of the activated sludge microbiota and fermentation techniques designed to minimize inhibitor compound dosings should be considered as well.

CHAPTER VIII

EFFECT OF GLUCOSE AND XYLOSE CO-FERMENTATION ON LIPID PRODUCTION BY ACTIVATED SLUDGE MICROBIOTA

Introduction

The results obtained from the initial phase of this study found that activated sludge microorganisms were able to accumulate additional amounts of lipids suitable for biodiesel production in aerobic bioreactor cultures operated under high C:N ratio and glucose loading. With the aim of reducing lipid production costs due to substrate, lignocellulose-based pentose and hexose sugars obtained via hydrolysis of waste biomass materials have been considered as alternative carbon sources for microbial fermentations for the production of lipids. In Chapter VII, it has been shown that the inhibitor compounds furfural and acetic acid, which are by-products of hydrolysis of biomass to release fermentable sugars, exerted inhibitory effects on lipid biosynthesis by activated sludge microorganisms; although enhancements in biomass growth have been attributed to acetic acid. As most traditional fermentation processes in biofuels application use starch-based raw materials containing mostly glucose, effective co-fermentation of pentose (e.g., xylose and arabinose) and hexose (e.g., glucose, mannose, galactose) sugars are currently not well-established [Zhao, et al., 2008]. In this chapter, the effects

of co-fermentation of xylose and glucose on lipid accumulation by activated sludge microorganisms were investigated. Xylose and glucose were chosen as representative pentose and hexose sugars, respectively due to their relative high abundance in most lignocellulose biomass hydrolyzates. It was expected that effective co-fermentation of pentose and hexose sugars will significantly improve the overall economics of microbial lipid accumulation due to the full utilization of all sugar components of low cost raw materials such as waste lignocellulose biomass.

Methodology

Following the general batch fermentation protocols described in Chapter IV, batch fermentation experiments were conducted using an initial total sugar loading of 60 g/L and C:N ratio of 70:1. Ammonium sulfate was supplied as the nitrogen source at 1.62 g/L. Glucose and xylose were supplied individually and in binary mixtures according to the experimental design shown in Table 8.1. Four replicate experiments were conducted 1-2 weeks apart to minimize the variability of the initial activated sludge characteristics. Batch fermentation experiments were performed for seven days and fermentation broth samples were processed and analyzed according to the procedures described in Chapter IV. The fermentation profiles obtained from this study were normalized relative to the initial levels and were presented alongside the average fermentation profiles of the control run (i.e., glucose as sole carbon source) in order to account for some variations in initial characteristics of the sludge inocula between grab activated sludge samples obtained from the wastewater treatment plant at different times. Kinetic analysis of the

batch fermentation data was conducted according to the proposed model and solution algorithm discussed in Chapter V.

Results and Discussion

Fermentation Profiles and Kinetics

The resulting fermentation profiles of activated sludge microorganisms cultivated in glucose, xylose, and glucose/xylose mixtures are shown in Figs. 8.1-8.7 and the kinetic parameter estimates are summarized in Table 8.2. As shown in Fig. 8.1, the normalized biomass production showed similar trends and levels of total biomass yield; although, in the treatments with xylose as sole carbon source and 1:2 mass ratio of glucose to xylose, the lag phase was followed by a continuously increasing trend in biomass production with no stationary phase. On the other hand, stationary growth phases were observed in the treatment runs with glucose as sole carbon source and 2:1 mass ratio of glucose to xylose. Values of the maximum specific growth rate (μ_{max}) were also roughly similar among the treatments investigated with the exception of 2:1 glucose-to-xylose ratio (0.034 h^{-1}), which was slightly higher than the other three treatments. However, the highest maximum attained total biomass concentration and maximum predicted non lipid biomass yield (X_{max}) was obtained using glucose as sole carbon source at 15.1 and 12.9 g/L, respectively.

Table 8.1: Experimental design used to determine the effect of glucose/xylose co-fermentation on lipid accumulation by activated sludge.

Treatment	Glucose (g/L)	Xylose (g/L)
Glucose (Control)	60	-
Xylose	-	60
2:1 Glucose:Xylose	40	20
1:2 Glucose:Xylose	20	40

Table 8.2: Kinetic parameter estimates for the Logistic and Leudeking-Piret models for glucose and xylose co-fermentation. Total sugars = 60 g/L.

Parameters	Treatment			
	Glucose	Xylose	2:1* Glu:Xyl	1:2 Glu:Xyl
Non lipid biomass				
μ_{max} (h^{-1})	0.027	0.024	0.034	0.028
X_0 (g/L)	5.54	2.98	3.35	2.97
X_{max} (g/L)	12.9	12.2	11.7	11.1
R^2	0.912	0.980	0.930	0.797
Lipid				
m (g/g)	0.150	0.058	0.104	0.091
n (g/g·h)	82.0×10^{-5}	1.6×10^{-3}	7.3×10^{-4}	4.9×10^{-4}
Maximum Lipid Content (% CDW)	17.8	21.5	14.9	11.7
P_{max} (g/L)	2.67	3.09	2.16	1.49
R^2	0.955	0.973	0.964	0.981
Total Sugars				
α (g/g)	1.39	0.741	1.72	0.838
β (g/g·h)	0.041	0.031	0.023	0.029
k_e (g/g·h)	0.019	0.0053	0.0068	0.015
Maximum Glucose Uptake Rate g/(L·h)	17.1	-	13.4	11.4
Maximum Xylose Uptake Rate g/(L·h)	-	9.11	3.82	6.68
% Glucose Utilized	100	-	71	100
% Xylose Utilized	-	75	27	41
$Y_{X/S}$ Overall (g/g)	0.0957	0.189	0.197	0.201
$Y_{X/S}$ Growth Phase (g/g)	0.228	0.269	0.239	0.227
$Y_{X/S}$ Lipid Phase (g/g)	0.0506	0.165	0.161	0.185
$Y_{P/S}$ Overall (g/g)	0.0383	0.064	0.044	0.035
$Y_{P/S}$ Growth Phase (g/g)	0.0558	0.035	0.035	0.030
$Y_{P/S}$ Lipid Phase (g/g)	0.0331	0.072	0.052	0.037
R^2	0.943	0.965	0.827	0.981

In terms of sugar utilization, glucose consumption rates were found to be generally higher than xylose consumption rates as shown in Figs. 8.2 and 8.3 in which each sugar was supplied individually as sole carbon sources. Furthermore, Table 8.2 shows that the maximum glucose and xylose uptake rates obtained in these treatments were 17.1 and 9.11 g/(L·h), respectively. Also, while glucose was fully consumed by the activated sludge microorganisms after 5 d of fermentation, approximately 25 % of the initial xylose supply remained. The observed sugar consumption profiles in fermentation run using glucose/xylose mixtures shown in Figs. 8.4 and 8.5 implies a sequential consumption pattern wherein glucose is consumed initially followed by xylose. As shown in Fig. 8.4 wherein the substrate used was a 2:1 mass ratio of glucose-to-xylose, glucose was rapidly consumed by the activated sludge by approximately 55 % of the initial level within the first three days of cultivation corresponding whereas the initial xylose supply was reduced by only 12 %. The instantaneous glucose consumption rate already reached near the maximum level (12.8 g/L) after 24 h of fermentation corresponding to a 34 % reduction of the initial glucose supply while at this time, the instantaneous xylose consumption rate was still much lower at 0.8 g/(L·h) resulting into only a 5 % consumption of the initial xylose supply. The xylose consumption rate then increased to its maximum at 3.82 g/(L·h) after 36 h at the same time the maximum glucose uptake rate of 13.4 g/(L·h) was achieved. Overall, 71 % of the initial glucose and 27 % of initial xylose were consumed; resulting into residual glucose and xylose levels of 10.8 and 16.7 g/L, respectively after 7 d of fermentation. On the other hand, where xylose is supplied in excess of glucose (1:2 glucose/xylose mixture), glucose was 96 % consumed within the

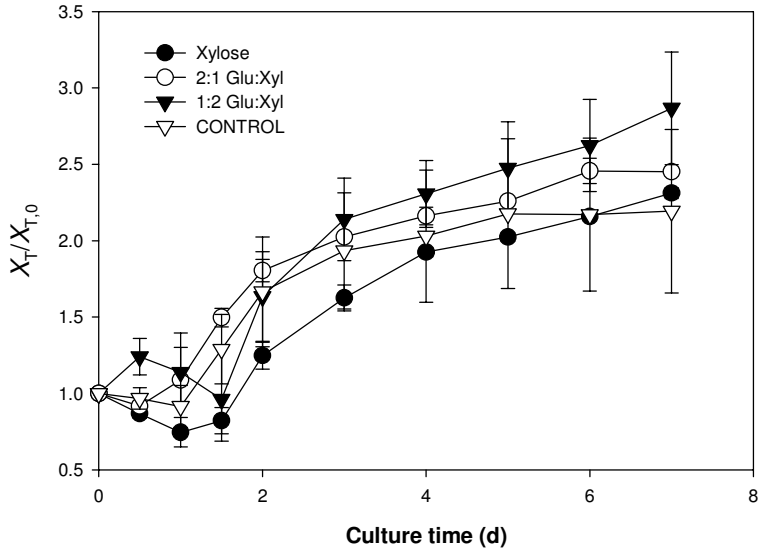

Figure 8.1: Effect of glucose and xylose co-fermentation on relative biomass production by activated sludge microbiota.

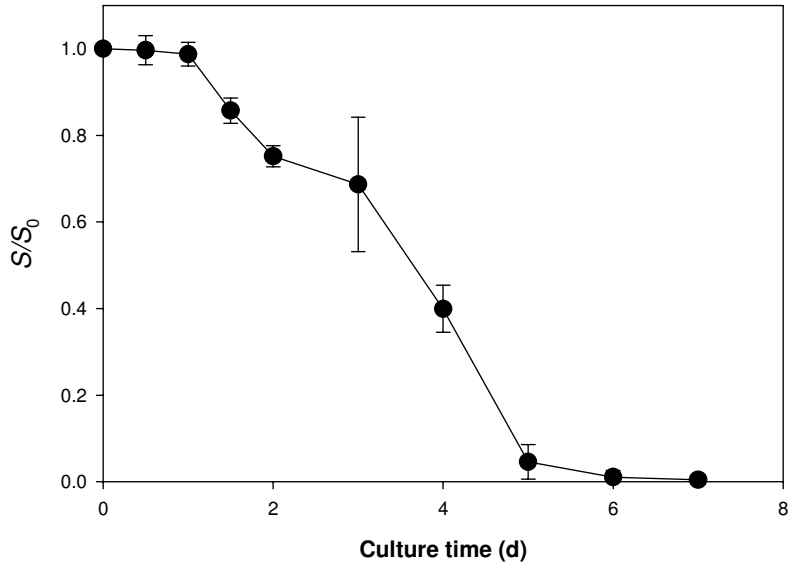

Figure 8.2: Sugar consumption profile in activated sludge culture using glucose as sole carbon source. Initial concentration: 60 g/L.

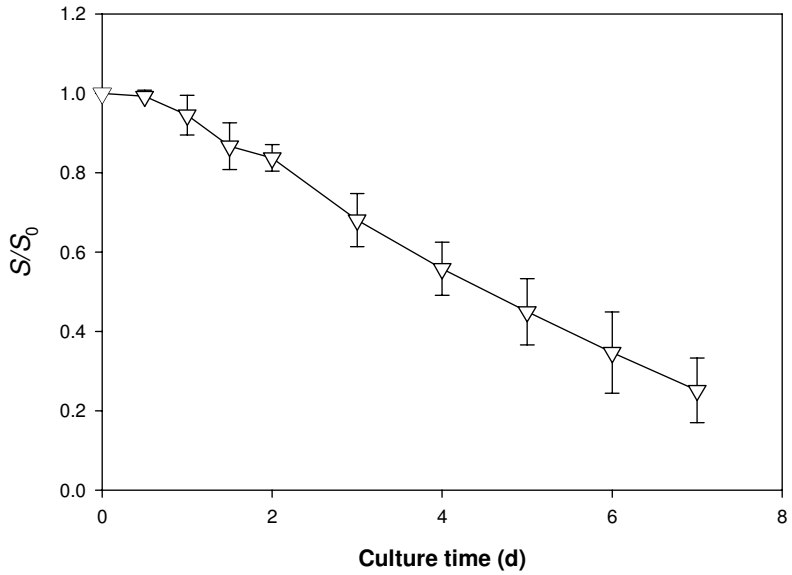

Figure 8.3: Sugar consumption profile in activated sludge culture using xylose as sole carbon source. Initial concentration: 60 g/L.

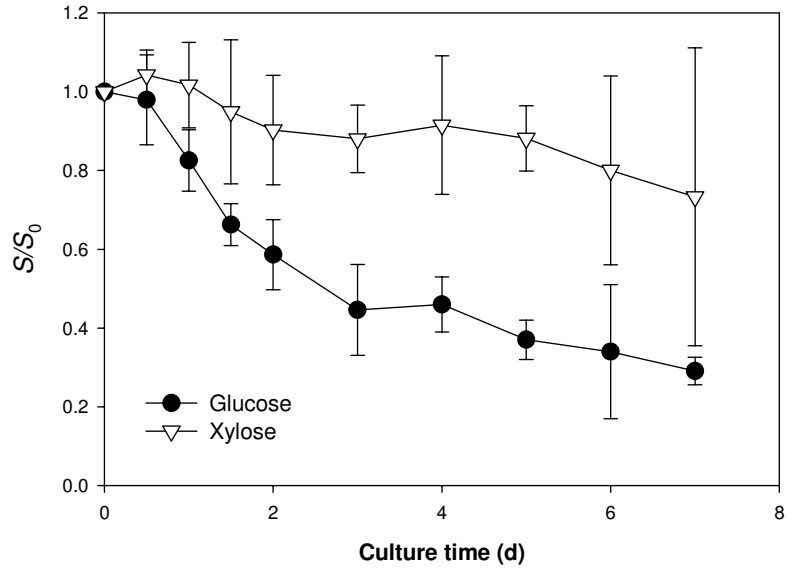

Figure 8.4: Sugar consumption profile in activated sludge culture using 2:1 mass ratio of glucose-to-xylose. Total sugar concentration: 60 g/L.

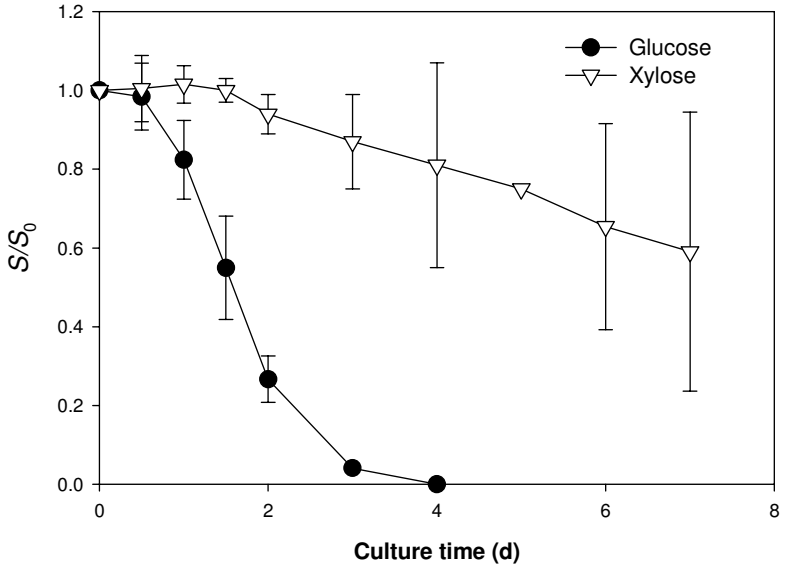

Figure 8.5: Sugar consumption profile in activated sludge culture using 1:2 mass ratio of glucose-to-xylose. Total sugar concentration: 60 g/L.

first 3 d of fermentation and the maximum instantaneous glucose uptake rate of 11.4 g/L·h was obtained at 2 d of fermentation. However, only around 4 % xylose utilization was observed during the same time span (0 - 3 d) and the overall glucose and xylose uptake rates were 6.44 and 0.93 g/(L·h), respectively. After 3 d of cultivation wherein glucose was fully consumed, the xylose consumption rate increased drastically, reaching its maximum level (6.68 g/L·h) after 6 d of fermentation and resulting into an overall xylose utilization of 41 %. The observed xylose consumption rates were lower than the glucose consumption rates probably due to the additional biochemical steps needed for xylose utilization by microorganisms. Furthermore, since significant amounts of xylose remained unconsumed, the overall non lipid biomass yields $Y_{X/S}$ based on the total amount of sugars in the treatments with xylose either as sole carbon source (0.19 g/g) or

in 2:1 (0.20 g/g) and 1:2 (0.20 g/g) glucose-to-xylose mass ratio mixtures were higher compared to that with glucose as sole carbon source (0.096 g/g) as seen in Table 8.2; although the former produced slightly lower maximum biomass concentrations.

As shown in Fig. 8.6 for all treatments, ammonium-nitrogen levels were exhausted from the culture after 2 d of fermentation, theoretically signaling the onset of lipid accumulation. Indeed, the normalized biomass lipid contents in the treatment runs using xylose started to increase within 36 to 48 h of fermentation after an initial degradation observed in the initial stages of the fermentation (Fig. 8.7) while the fermentation run with glucose as sole carbon source increased continuously from the start until the end of the fermentation run. The calculated $Y_{X/S}$ and $Y_{P/S}$ values for the different treatments in Table 8.2 also showed higher $Y_{X/S}$ in the growth phase than in the lipid production phase, and higher $Y_{P/S}$ values in the lipid phase than in the growth phase (except with glucose as sole carbon source), indicating the diversion of a greater fraction of the total sugars for lipid production at the later stages of the fermentation process when nitrogen has been exhausted from the culture. Although the normalized lipid contents obtained from the treatments runs containing xylose were relatively smaller than those obtained from pure glucose, Table 8.2 also shows that the highest maximum lipid content of activated sludge was obtained using pure xylose (21.5 % CDW) compared with pure glucose (17.8 % CDW). Maximum lipid contents obtained using glucose/xylose mixtures were lower at 14.9 and 11.7 % CDW from 2:1 and 1:2 glucose-to-xylose mass ratios, respectively than when using pure glucose and xylose individually. Moreover, the volumetric lipid yield trends illustrated in Fig. 8.8 showed similar profiles with total biomass production using pure xylose producing a higher maximum lipid

concentration of 3.09 g/L compared with pure glucose, which was 2.67 g/L. In glucose/xylose mixtures however, the higher proportion of glucose seemed to favor the production of lipids, as shown in Table 8.2 where $P_{\max}$ values are 2.16 and 1.49 g/L for 2:1 and 1:2 glucose/xylose mixtures, respectively. Also, the highest overall lipid yield coefficient $Y_{P/S}$ was obtained using xylose as sole carbon source (0.064 g/g) compared with pure glucose (0.038 g/g). The lipid yield coefficient was slightly higher when glucose dominant mixture (2:1) was used as carbon source at 0.044 g/g, than when the xylose dominant mixture (1:2) was used (0.035 g/g). The resulting lipid contents and

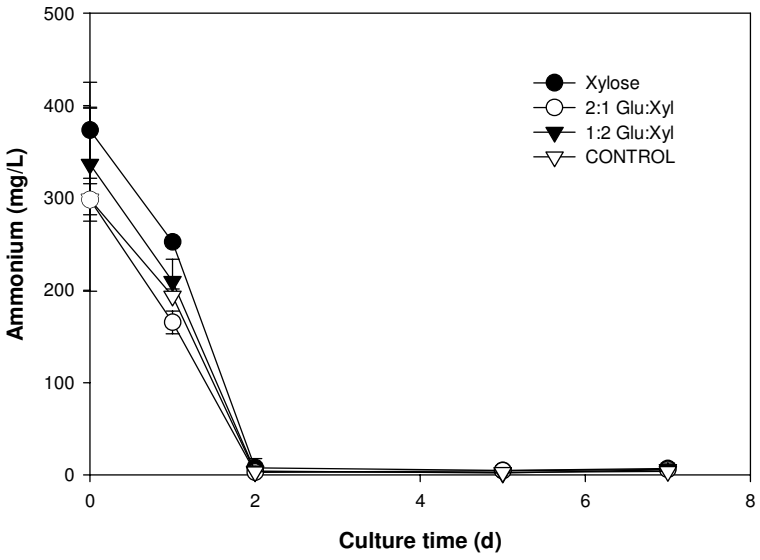

Figure 8.6: Effect of glucose and xylose co-fermentation on ammonium-nitrogen consumption of activated sludge microbiota.

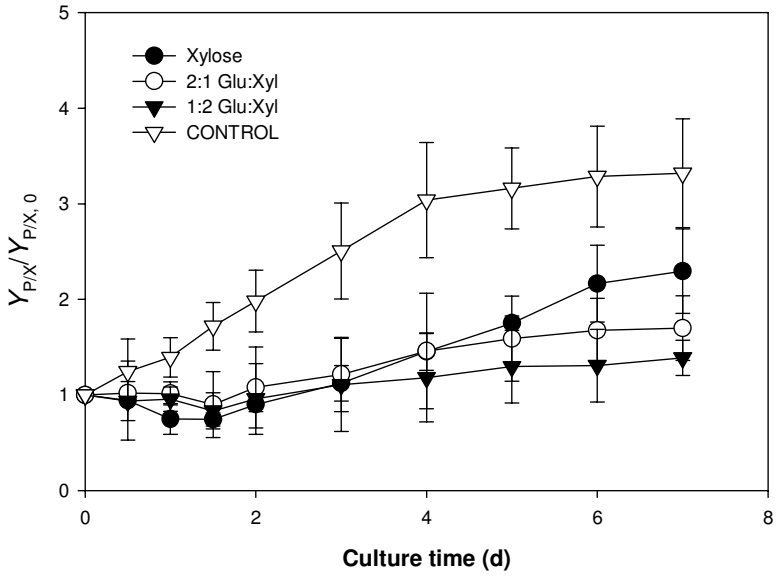

Figure 8.7: Effect of glucose and xylose co-fermentation on time profile of normalized lipid content (% CDW) of activated sludge biomass.

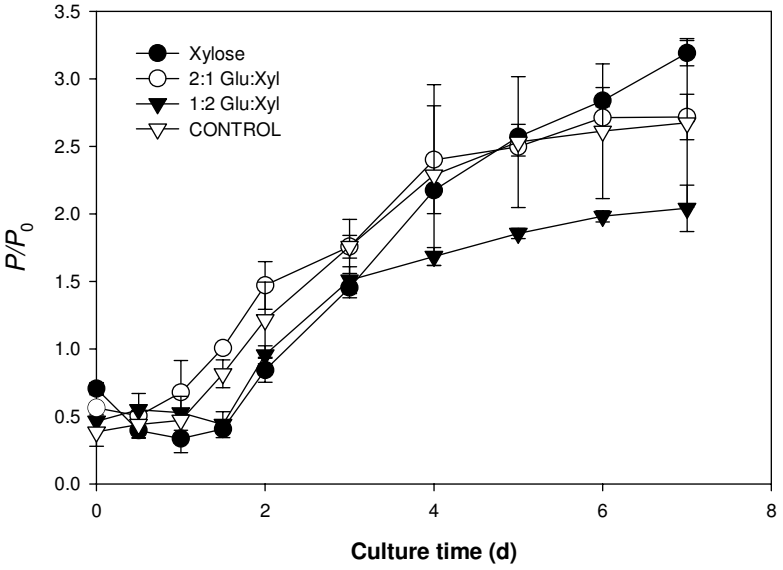

Figure 8.8: Effect of glucose and xylose co-fermentation on time profile of normalized volumetric lipid yield (g/L) of activated sludge biomass.

yield coefficients obtained in this study from activated sludge microorganisms were lower than typical oleaginous microorganisms utilizing xylose as sole carbon source or mixed with other types of sugars. However, the results from these studies similarly indicated that the use of xylose resulted in better biomass lipid contents and yield coefficients compared with other sugars such as in the case of the oleaginous yeast *Candida curvata*, wherein biomass containing 48.6 % lipids by weight was achieved using xylose with a conversion of 17.4 g lipids per 100 g xylose [Evans and Ratledge, 1983]. In some cases though, biomass and lipid production by activated sludge microorganisms using xylose were comparable to some oleaginous yeasts species belonging to the genera *Rhodosporidium, Trichosporon,* and *Rhodotorula* wherein the resulting total biomass and lipid production from xylose were found in the range of 4.2 to 7.2 g/L and 4 to 20 % CDW, respectively, while the maximum $Y_{P/S}$ obtained was 11 % [Li, et al., 2005]. Based on these findings, it appears that xylose is a better substrate for microbial biomass and lipid production due to its slow uptake rate thus is more efficiently utilized by microorganisms leading to higher yield coefficients. Therefore, experimental conditions need to be optimized or fermentation times may need to be extended to further enhance the utilization of xylose in the fermentation process for the production of lipids. While this is the case, lignocellulose hydrolyzates usually contain mixtures of sugars with varying proportions of mostly glucose and xylose. Based on the results obtained from this study and in others, glucose is always assimilated first before xylose regardless of their proportions. In these cases, glucose dominant sugar mixtures (e.g., 2:1 ratio) gave good results in terms of lipid contents, such as in the case of *Lipomyces starkeyi,* which resulted in a maximum lipid content of 61 % wt. [Zhao, et al., 2008]. The activated

sludge also performed better in terms of both biomass growth and lipid accumulation at 2:1 compared with 1:2 glucose-to-xylose substrate loading. However, in terms of lignocellulose hydrolysis, milder reaction conditions usually give higher proportions of xylose than glucose while minimizing inhibitor production and increasing the glucose yield usually requires more severe hydrolysis conditions. If lowering the cost of sugar production and minimizing the production of degradation by-products is to be taken into account, further investigations on improving xylose conversion to lipids by microorganisms using xylose dominant sugar mixtures must be pursued.

Lipid Analysis

The resulting lipid composition profiles in terms of the saponifiable fraction and fatty acid distribution are shown in Figs. 8.9 and 8.10, respectively. Fig. 8.9 shows that although the maximum lipid activated sludge biomass lipid content was obtained using pure xylose (21.5 % CDW), the highest saponifiable lipid fraction, hence the saponifiable lipid yield, was still obtained from the treatment using glucose as sole carbon source (10.2 % CDW). In the pure xylose treatment run, the saponifiable fraction constituted only around 40 % of the total lipid extract yield, corresponding to an 8.3 % biodiesel yield by dry sludge mass. This biodiesel yield is comparable with that obtained from the fermentation run using a 2:1 glucose/xylose mixture at 8.1 % (CDW) while the lowest biodiesel yield was obtained from activated sludge biomass generated using a 1:2 glucose/xylose mixture (6.4 %). Among the treatments investigated, the lipid extracts produced using glucose as sole carbon source or mixed with xylose contained 50 – 60 % of saponifiable lipids while that obtained using pure xylose was reduced to 40 %,

possibly indicating the biosynthesis of some lipid types that are slightly different from that produced using glucose. As it has been observed in the previous phases of the study, the lipid and biodiesel yields from sugar-grown activated sludge microorganisms were likewise higher that those obtained from raw activated sludge (Fig. 8.9), indicating an enhanced sludge biomass for increased lipid extraction and biodiesel production.

In terms of the fatty acid composition of the lipid extracts, Fig. 8.10 shows that the type of sugar used as substrate has little effect on the distribution of fatty acids. The major fatty acids composing the lipid extracts were in the C_{16} to C_{18} range similar to some plant-based oils, rendering it suitable for biodiesel production. Whereas in raw activated sludge palmitic (C16:0), palmitoleic (C16:1), and oleic (C18:1) acids were the dominant components at 17, 13, and 23 % of the total FAMEs, respectively, the final lipid extracts obtained using either glucose, xylose, or glucose/xylose mixtures were dominated mainly by unsaturated fatty acids which is mainly oleic acid at 40 – 45 % followed by palmitic acid (17 – 21 %) and stearic acid (C18:0) at 9 – 13 %. In addition, the fraction of unclassified fatty acyl residues were also lower in lipids extracted from sugar-grown activated sludge (> 10 %) whereas in raw activated sludge, the percentage of unclassified residues was close to 30 %. As mentioned in earlier chapters, the enhanced unsaturated fatty acid concentration due to oleic acid relative to the saturated fatty acids (mostly palmitic acid) in glucose- and/or xylose-grown activated sludge was comparable with a target soybean oil composition to produce biodiesel with improved cold flow, ignition quality (cetane number), oxidative stability, and presumably reduced nitrogen oxide emissions due to very low levels of linolenic acid (C18:3) [Bringe, 2005]. The concentration levels were within the error range for all the treatments investigated, hence

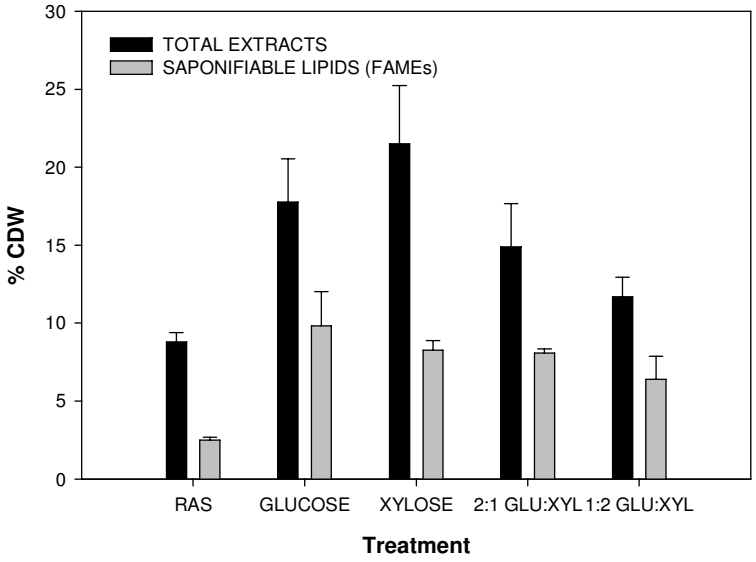

Figure 8.9: Effect of glucose and xylose co-fermentation on total and saponifiable lipid fractions of activated sludge biomass. (RAS: raw activated sludge).

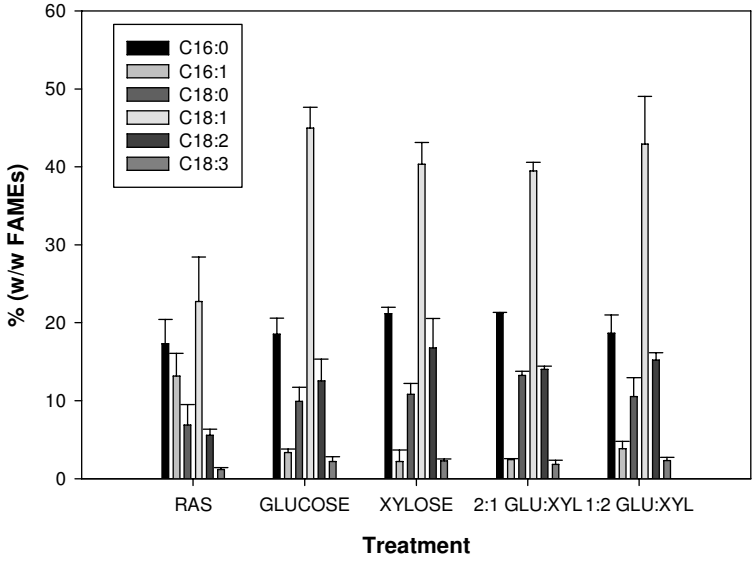

Figure 8.10: Effect of glucose and xylose co-fermentation on the fatty acid profile fractions of activated sludge biomass. (RAS: raw activated sludge).

they could be considered similar to each other. The only significant difference observed was the slightly higher levels of linoleic acid (C18:2) found in lipid extracts derived form activated sludge grown in pure xylose. The results obtained hereunto were similar to those obtained in previous studies involving pure oleaginous strains such as *Candida curvata* [Evans and Ratledge, 1983] and *Lipomyces starkeyi* [Zhao, et al., 2008] in terms of oleic acid concentrations, each showing oleate percentages of 43 and 49 %, respectively compared with 40 – 45 % in cultured activated sludge regardless of whether glucose or xylose was used as the fermentation substrate. Stearic acid levels in cultured activated sludge (10 – 12 %) were also similar with 12 – 14 % in *C. curvata* and about twice as high than that in *L. starkeyi* (6.2 %). The only major difference observed was the relatively higher proportion of saturated fatty acids which is mainly palmitic acid (30 – 40 %) in the two oleaginous yeast strains mentioned.

Conclusion

The results obtained in this phase of the research shows than in addition to glucose; pentose sugars such as xylose could be utilized by activated sludge microorganisms for biomass growth and enhancement of lipid content for improved biodiesel yields. As sole carbon sources, fermentation of glucose and xylose produced comparable biomass yields but the maximum total biomass lipid content (21.5 % CDW) was obtained using pure xylose. However, the saponifiable lipid fraction and hence, the biodiesel yield was still highest when using glucose as sole carbon source. When glucose/xylose mixtures were used as substrate, the glucose-dominant mixture (2:1 glucose:xylose) produced both higher total and saponifiable lipid yields compared with

the xylose dominant mixture (1:2 glucose:xylose) but lower than when pure glucose and xylose were used. The resulting fatty acid distribution using all sugar combinations were found to be similar and suitable for biodiesel application due to the dominance of C_{16} and C_{18} fatty acids and the enhanced proportion of unsaturated fatty acids (mainly oleic acid) relative to the saturated fatty acids (mainly palmitic acid) contributes to improved biodiesel properties being similar with a target oil composition for use as biodiesel feedstock mentioned in literature. Furthermore, the biomass and lipid yield coefficients with xylose as sole carbon source or mixed with glucose were higher than pure glucose, indicating that xylose is likely more efficiently utilized by the activated sludge microorganisms for biomass and lipid production. Further investigations are necessary in order to improve process conditions and microbial adaptation for enhanced xylose consumption in order to fully utilize the abundant amounts of fermentable sugars from waste lignocellulose biomass and potentially improve the economics of the process.

CHAPTER IX

EVALUATION OF FED-BATCH AND CONTINUOUS FERMENTATION OF LIGNOCELLULOSE HYDROLYZATE FOR ENHANCED LIPID ACCUMULATION IN ACTIVATED SLUDGE

Introduction

In Chapter VII, results on batch glucose fermentation experiments with furfural and acetic acid additions have shown that high initial levels of these inhibitors, particularly furfural severely inhibited cell biomass growth and lipid formation by activated sludge microorganisms. In the case of high acetic acid levels, cell growth appeared to be enhanced but lipid accumulation was inhibited as well. It was speculated that this apparent reduction in the microbial growth and metabolism was due to the *in situ* detoxification of inhibitor compounds by microorganisms; specifically, the conversion of furfural to the supposedly less toxic furfuryl alcohol and furoic acid and the intracellular neutralization of acetic acid via an active proton pump. Numerous strategies have been proposed before to mitigate the toxic effects of these lignocellulose degradation compounds on microorganisms, the most common of which are physical and chemical pretreatment of lignocellulose hydrolyzates prior to fermentation [Palmqvist and Hahn-Hagerdal, 2000a]. However, these methods could add to feedstock and production costs for microbial lipid production. A possible alternative is to apply fermentation techniques

designed to minimize residual inhibitor concentrations in microbial cultures and assist in the *in situ* degradation of inhibitors by discontinuous or gradual feeding of hydrolyzates or allow for the adaptation of microorganisms to acquire tolerance towards these compounds. In this phase of the study, different fermentation modes for lignocellulose hydrolyzates have been tested for the enhanced lipid accumulation by activated sludge microorganisms. Specifically, batch, discontinuous fed batch, semicontinuous fed batch, and continuous cultures for enhanced lipid accumulation by activated sludge microorganisms have been evaluated. Kinetic analysis of the fermentation data was conducted to assess the performance of activated sludge microorganisms in terms of biomass and lipid yields and production rates, and substrate consumption rates at the different fermentation modes investigated.

Methodology

Fermentation experiments were conducted using an artificially prepared model lignocellulose hydrolyzate shown in Table 9.1. The composition was chosen based on the average values for corn stover hydrolyzate; however, the components have been reduced to those listed in Table 9.1 with representative hexose (glucose) and pentose (xylose) sugars and inhibitors that are present in relatively higher concentrations so as to simplify sample analysis and fermentation kinetics interpretation. No detoxification or any other treatment of the hydrolyzate was carried out prior to fermentation. Batch fermentation was conducted using the same protocols mentioned in Chapter IV using 60 g/L of the model hydrolyzate as carbon source and 1.62 g/L of ammonium sulfate as the nitrogen

Table 9.1: Composition of synthetic model lignocellulose hydrolyzate.

Component	% (w/w)
Glucose	26.7
Xylose	59.2
Acetic acid	12.8
Furfural	1.3

source, such that the initial mass C:N ratio of the medium was 70:1. The total substrate loading was 180 g based on a culture volume of 3 L. Fermentation conditions (i.e., temperature, aeration rate, etc.) were the same for all the fermentation modes investigated, with the exception of the feeding patterns. The fermentation time was also extended beyond the usual seven days to allow for complete utilization of all components of the hydrolyzate mixture.

For the discontinuous fed batch culture, the bioreactor initially contained 2.4 L of the synthetic wastewater medium inoculated with 600 mL of activated sludge to a total culture volume of 3 L. The concentration of ammonium sulfate and other nutrients in the medium remained the same but the initial glucose concentration was 20 g/L (60 g total for 3 L culture). Hence, the initial C:N ratio was set at approximately 23:1 to favor cell biomass production. The initial batch culture (Stage I) was conducted until the residual glucose concentration drops below 5 g/L, at which time 60 g of the model hydrolyzate was dissolved in a required volume of liquid to re-establish the culture volume to 3 L after sample aliquots were obtained from the culture for analysis and to re-set the substrate concentration in the culture back to 20 g/L. No further additions of the nitrogen source (ammonium sulfate) and other nutrients were done and two subsequent batch cultures were conducted after each addition at a high C:N ratio (Stages II and III).

The total substrate loading of the overall process is 180 g similar with the batch culture. Fermentation time was also extended until all hydrolyzate components have been at least 90 % consumed.

In the semicontinuous experiment, an initial 3-L batch culture was conducted using 20 g/L glucose as the sole carbon source. Nutrient composition in the initial synthetic wastewater medium was the same as in the batch culture, with an initial ammonium sulfate concentration of 1.62 g/L corresponding to an initial C:N ratio of 23:1 to enhance biomass growth. After 48 h of the initial batch culture (Stage I), semicontinuous fermentation (Stage II) was commenced by pumping into the culture a 1-L synthetic hydrolyzate mixture containing 120 g of the total mass of the components at the rate of 8.3 mL/h using one of two 12-RPM constant speed pumps in the fermenter cabinet to reach a final volume between 3.7 – 3.9 L after 5 d. The flow rate on a 12-RPM constant speed pump using a 1.6-mm ID silicone tubing at 100 % revolution cycle is 79.2 mL/h according to the fermentor manual and has been verified experimentally. Hence, the pump flow rate was adjusted and calibrated to the desired value by varying the pump set point to a certain percentage of the pump period required to deliver a specific volume of fluid within a specified time span. In this case, the pump period was set at 10 s and the set point required to deliver 8.3 mL/h of the hydrolyzate mixture was calculated to be approximately 10 %. The feed rate was chosen so that the total substrate loading after a total of 7 d of the initiation (I) and processing (II) stages was 180 g for comparison with batch and discontinuous fed batch modes and the final working volume is 4 L, which is within 80 % of the fermenter vessel volume.

For the continuous culture, an initial 3-L batch culture using 20 g/L of glucose as sole carbon source was conducted similar to the semicontinuous fermentation experiment. Nutrient composition in the initial synthetic wastewater medium was the same as in the batch culture, with an initial ammonium sulfate concentration of 1.62 g/L corresponding to an initial C:N ratio of 23:1 to enhance biomass growth. After 48 h of the initial batch culture (Stage I), the continuous fermentation stage (Stage II) was commenced by pumping into the culture a 40 g/L solution of the model synthetic hydrolyzate at the rate of 25 mL/h using a 12-RPM constant speed pump set at 31 % over a pump period of 10 s. This flow rate has been selected so as to have a complete turnover of the initial 3 L media within 5 d for a total culture time of 7 d. The volume of the culture was maintained at approximately 2.8 L by means of level probe, which triggers the other 12-RPM constant speed pump running at a higher setpoint of 60 % corresponding to a higher flow rate of approximately 48 mL/h. The total substrate loading after 5 d of continuous culture (7 d total) was 180 g similar to the batch, fed batch, and semicontinuous experiments.

Biomass, lipid extracts, and supernatant samples from the cultures were analyzed using the analytical methods described in detail in Chapter IV. Kinetic parameter estimates for each of the fermentation modes investigated were obtained using the model equations and solution methods enumerated in Chapter IV.

Results and Discussion

Different fermentation modes for enhanced lipid accumulation by activated sludge were tested using as the substrate a model lignocellulose hydrolyzate mixture (Table 9.1) with a composition having a higher proportion of pentose (xylose) than hexose (glucose) sugars and low to medium levels of inhibitor compounds, which typically results from milder hydrolysis conditions. Furthermore, an artificially-prepared hydrolyzate was used in this study instead of one derived from actual hydrolysis of lignocellulose biomass in order to avoid the expected variation of hydrolyzate compositions from batch to batch. The investigation of hydrolysis conditions and different biomass types to attain a specific target hydrolyzate composition is beyond the scope of this study.

Batch Fermentation

The resulting batch fermentation profiles using the model hydrolyzate are shown in Figure 9.1. The activated sludge biomass growth profiles showed an initial lag phase within the first 2 d of cultivation while the lipid content of the cells remained relatively constant at ≈ 6 % CDW before increasing slightly to approximately 9.5 % CDW, which was actually the highest lipid content achieved in the batch culture. The onset of the exponential growth phase from 2 to 3 d of fermentation resulted in rapid increase in the biomass concentration. Although the stationary phase could not be readily observed, the biomass concentration in the culture further increased continuously at a lower rate until it reached the highest value of 23 g/L after 11 d. However, along with the biomass increase, a rapid decrease in the intracellular lipid content was observed during the exponential

phase from 9.5 down to 4 % CDW, which was even lower than the initial lipid content in raw activated sludge. The lipid content then remained fairly constant at this level until the end of the experiment. Although this is the case, the volumetric lipid concentration exhibited a similarly increasing trend along with the total biomass concentration, reaching a maximum of 1.0 g/L. The enhanced biomass production with reduction in intracellular lipid content has also been observed previously in Chapter VII with binary mixtures of acetic acid and furfural and can be attributed to the complex interaction between the stimulatory effect of acetate on biomass production with the inhibitory effect of furfural on both biomass and lipid production as described previously in Chapter VII.

The substrate concentration profiles shown in Fig. 9.1(b) also exhibited a diauxic or sequential utilization trend similar to the results obtained in Chapters VII and VIII. Similar with results obtained from Chapter VII, the furfural utilization rate (0.03 g/L·h) was slightly higher than the glucose uptake rate (0.007 g/L·h) during the lag phase, in which the activated sludge microorganisms exhibited a higher affinity towards the consumption of furfural and conversion to less toxic compounds such as furfuryl alcohol and furoic acid as it has been mentioned in the earlier chapters and elsewhere[Taherzadeh, et al., 1999a] . As the culture progressed towards the exponential phase (1 to 2 d) and furfural concentrations become smaller, the glucose uptake rate increased while the furfural consumption rate decreased. At the same time no xylose consumption has yet been detected while acetic acid in the culture increased in

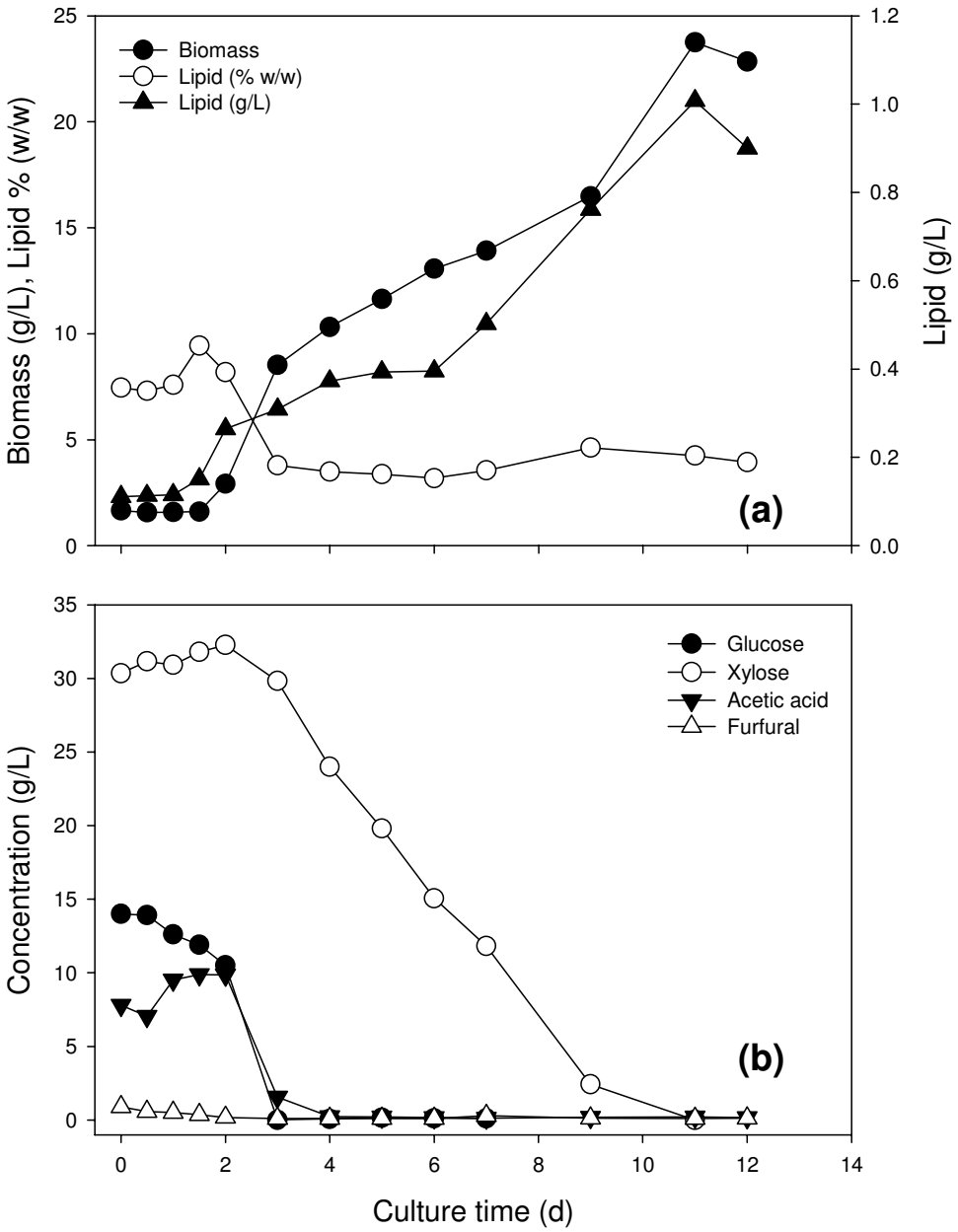

Figure 9.1: Fermentation profiles of a batch culture of activated sludge cultivated under nitrogen-limited conditions using artificial hydrolyzate as carbon source.

concentration possibly due to its production and release by acid-producing members of the activated sludge microbiota. During the exponential phase between days 2 and 3 of cultivation, glucose was rapidly depleted (0.43 g/ L·h) and at the same time acetic acid and xylose consumption started at rates of 0.35 and 0.001 g/L·h, respectively. After majority of the acetic acid has been depleted between 4 and 5 d of cultivation, xylose utilization rate increased dramatically to a maximum of 0.24 g/L·h and was depleted after 11 d of cultivation. Based on these calculated rates and the concentration profiles in Fig. 9.1, the components of the model hydrolyzate are consumed in the following sequence (first to last): furfural, glucose, acetic acid, and xylose.

In order to aid in the investigation of the other fermentation modes, the batch fermentation kinetics were described using growth, lipid formation, and substrate consumption rate equations based on the Monod rate law and the kinetic parameters were estimated via linear regression of the double reciprocal (Lineweaver-Burke) plot of the growth (non lipid biomass production) and lipid production rates with substrate concentration data as described previously in Chapter V and the parameter estimates are summarized in Table 9.2.

Discontinuous Fed Batch Fermentation

Figure 9.2 shows the resulting fermentation profiles in the discontinuous fed-batch experiment involving an initial batch culture at low C:N ratio (Stage I) followed by two successive batch feedings of the model hydrolyzate mixture at high C:N ratio (Stages II and III). In this manner, the overall substrate loading of 180 g was divided into three portions of 60 g each, which led to lower initial concentrations of the hydrolyzate

components, particularly the inhibitor compounds acetic acid and furfural. The initial amount of nitrogen supplied into the medium prior to the initial batch culture was identical to that in the batch fermentation experiment described previously. In Stage I, a short lag period in biomass growth occurred in the first 12 h of cultivation followed by the exponential phase in which the biomass concentration more than doubled to reach its maximum value at 3.11 g/L. Similar to the batch experiment, the increase in biomass concentration was accompanied by a sharp reduction in the intracellular lipid content from approximately 8 down to 6 % CDW, although this was expected since Stage I was conducted under a low C:N ratio. The volumetric lipid yield profile however followed the biomass concentration profile. The substrate utilization profiles also followed a sequential pattern, in which glucose was consumed fastest followed by acetic acid and furfural. Xylose consumption did not begin until after 24 of cultivation and was rapidly consumed to less than 10 % of its initial supply after 36 h. At this point, the total substrate residual was 1.57 g/L; hence the first batch addition (Stage II) of hydrolyzate was made and the culture was run a new batch culture.

In Stage II of the experiment, no further addition of nitrogen and other nutrients were made and IC analysis of the culture found that nitrogen levels were in the range of 20 – 25 mg/L compared with approximately 300 – 400 mg/L initially. The consequence is evident in the resulting biomass production profiles, wherein the biomass increased slightly from 3.11 to 4.11 g/L from 36 to 96 h and remained fairly constant. Intracellular lipid contents also remained constant over the time span of Stage II and again, volumetric lipid concentration followed the biomass production trend. Unlike the initial batch stage however, glucose and xylose were consumed simultaneously with glucose having a

slightly higher consumption rate. Glucose was depleted after 60 of Stage II (4 d total) while xylose was reduced from 13 to 2.4 g/L over a period of 108 h in Stage II (6 d total). The concentration profiles of acetic acid and furfural showed an initial build-up in the levels of these compounds in the culture. Furfural was then gradually consumed while acetic acid levels increased again starting from 5 to 6 d of the overall culture, possibly due to the production of acetic acid by some members of the activated sludge microbial community *in situ* during the fermentation process.

After 108 h of Stage II (4.5 d, 6 d total culture), the second batch addition (Stage III) of hydrolyzate was performed and again no further additions of nutrients were made. In this stage, the total biomass concentration fluctuated slightly with no substantial increase towards the end of the experiment. On the other hand, the activated sludge biomass lipid content increased slightly from 5.8 to 6 % CDW within the first 2 d of Stage III (6 to 8 d total culture) and increased significantly to approximately 10 % CDW and the volumetric lipid concentration followed a similar pattern. Glucose and xylose were consumed by the activated sludge microorganisms at roughly the same rates and the former was depleted after 2 d of Stage III (8 d total) while a residual xylose concentration of 8 g/L was observed after 3 d (9 d total) due to the lower initial level of glucose compared to xylose. Similar to Stage II, acetic acid levels increased slightly initially possibly due to *in situ* generation during the fermentation process while furfural levels remained fairly low. Unfortunately, the experiment was terminated after 9 d due to an unexpected power failure; hence any further increase in the lipid content after this time span cannot be confirmed.

As shown in Table 9.2, the maximum specific growth rate (μ_{max}) found in Stage I of the discontinuous fed batch experiment was higher than that in the single stage batch fermentation due to the lower initial C:N ratio in the former; however, the non lipid biomass ($Y_{X/S}$) and lipid ($Y_{P/S}$) yield coefficients were both higher in the single stage batch experiment, due perhaps to the higher initial substrate concentration although the lipid productivity was comparable in both setups. Kinetic analysis of Stage II fermentation data found a significantly lower μ_{max} than in Stage I due to the higher starting C:N ratio in the former. Although the $Y_{X/S}$ obtained in Stage II was lower that that in Stage I as expected, the kinetic data indicated negligible lipid production at this stage due to the lack of nutrients in the culture to support microbial cell multiplication. The same was also observed during Stage III wherein no growth parameters could be estimated due to negligible biomass concentration increases; however, a non growth-associated lipid production constant, productivity, and yield were obtained. Lipid accumulation in the single stage batch culture and in Stage I of the fed batch culture was found to be more influenced by cell multiplication rather than intracellular lipid content increase since $m > n$ in both cases, a fact that was evident in Figure 9.2 for the constant lipid content profile while the total biomass concentration increased. Calculation of the overall $Y_{X/S}$ and $Y_{P/S}$ for the discontinuous fed-batch experiment found a lower biomass yield and a comparable lipid yield with a single stage batch culture of hydrolyzate; hence the use of this method shows no obvious advantage over the single stage batch in terms

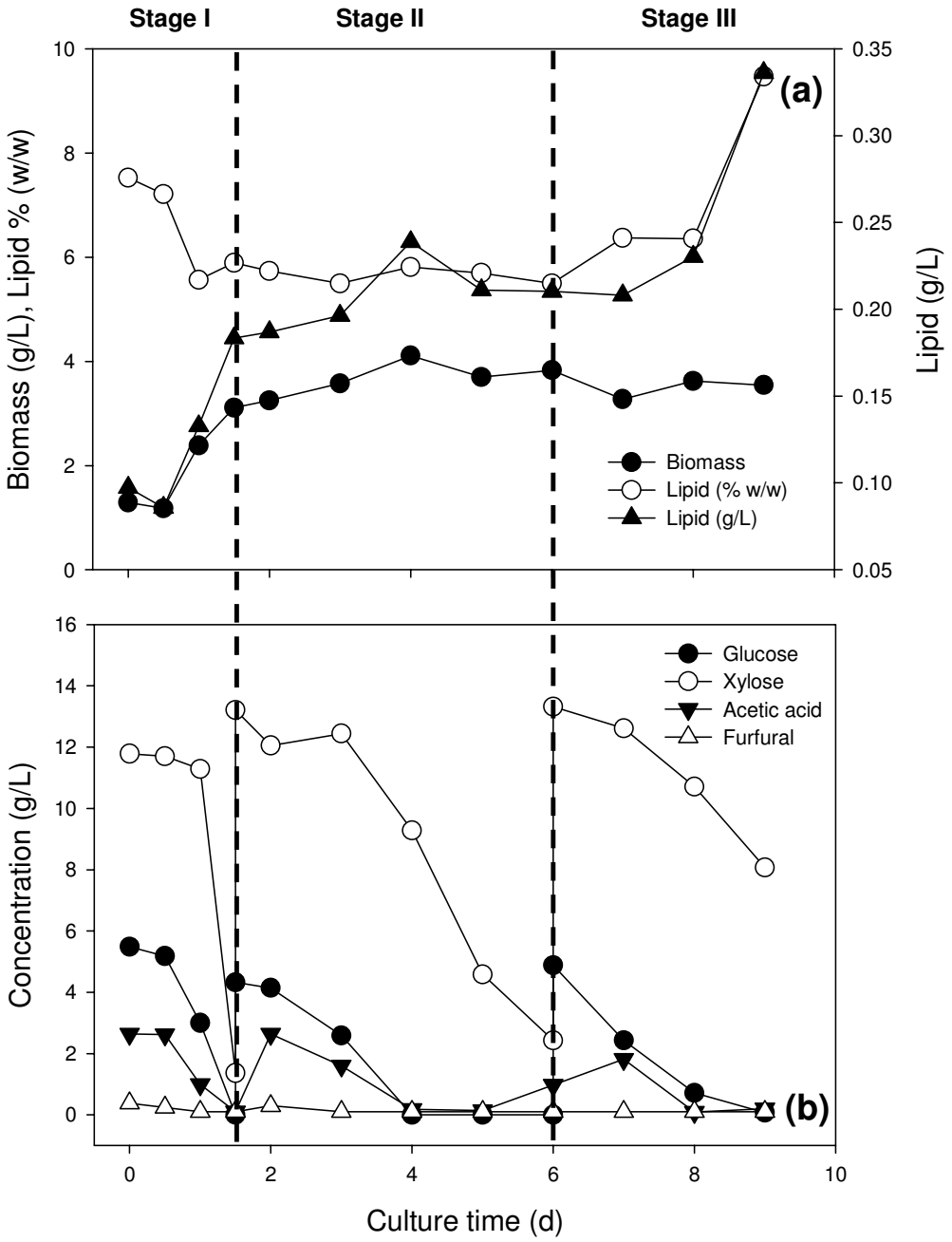

Figure 9.2: Fermentation profiles of a discontinuous fed batch culture of activated sludge cultivated under nitrogen-limited conditions using artificial hydrolyzate as carbon source.

of productivity. The only improvement brought about by sequential additions of smaller substrate amounts as opposed to a single addition of higher substrate amount was the enhanced uptake rates for all four components of the model hydrolyzate as seen in Table 9.2 during Stage I especially with the inhibitor compounds acetic acid and furfural, in which their consumption rates were around thrice than those in the single stage batch culture. However, consumption rates were no better in Stages II and III. The reduced growth and lipid production performance of the activated sludge microorganisms in these later stages was most likely due to the negligible levels of nutrients relative to the carbon source. Hence, future attempts in conducting a discontinuous fed batch culture should also include nutrient supplementation in addition to the carbon source.

Semicontinuous Fermentation

Another strategy that was considered in order to improve the biomass and lipid productivity of activated sludge microorganisms involved an initial batch culture (Stage I) using glucose (20 g/L) followed by the semicontinuous culture wherein a 120 g/L model hydrolyzate mixture was fed continuously into the culture without harvesting for 5 d (Stage II). Glucose has been used in the initial batch culture to improve biomass productivity in preparation for the lipid accumulation phase. Indeed, the indicated biomass and lipid profiles in Figure 9.3 and kinetic parameter estimates in Table 9.2 for Stage I show improved biomass and lipid production using glucose than with hydrolyzate due to the higher μ_{max}, lipid productivity, $Y_{X/S}$ and $Y_{P/S}$ and lower K_S values. After 2 d of the initial batch culture, the semicontinuous culture stage was commenced (Stage II)

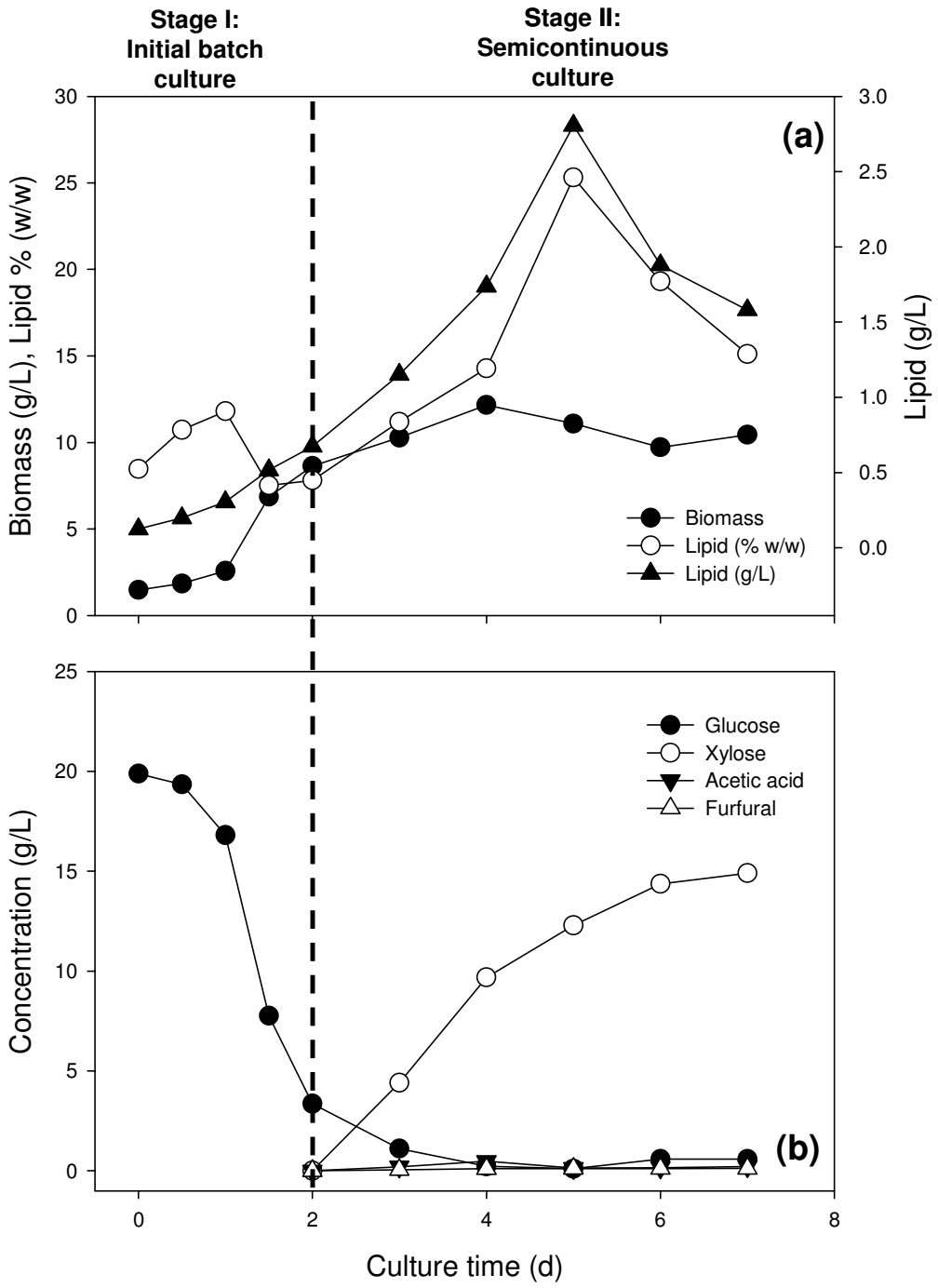

Figure 9.3: Fermentation profiles of a semicontinuous culture of activated sludge. Stage I: Initial batch culture using glucose. Stage II. Semicontinuous feeding of artificial hydrolyzate.

wherein the biomass concentration increased gradually to a maximum of ≈ 12.2 g/L after 2 d (4 d total) and decreased gradually to a range of 10.5 – 10 g/L after 5 d (7 d total). Biomass lipid contents (% CDW) and lipid concentration in the culture also increased significantly to reach maximum levels of 25.3 % CDW and 2.81 g/L, respectively, both after 3 d of semicontinuous culture, after which they decreased towards the end of the 7-d experiment. It should also be noted that the culture volume was also continuously changed by 1-L and multiplying the instantaneous volume with the concentrations gives the total biomass and lipid levels, which was also found to follow the same trend as the concentration profiles. Similar to the discontinuous fed batch experiments and unlike the single stage batch culture, the hydrolyzate components appeared to be consumed simultaneously with different rates. In Figure 9.3b, it can be seen that after starting the continuous feed of substrate, glucose, acetic acid, and furfural concentrations remained relatively low with minor fluctuations whereas xylose levels in the culture continuously build-up. As shown in Table 9.2, the overall glucose consumption rate was the highest followed by xylose, acetic acid, and furfural. When the consumption rates were compared with the calculated overall supply rates of each component (in g/L·h: glucose 0.27, xylose 0.59, acetic acid 0.13, furfural 0.13), one can see that the consumption rates were only slightly less than the supply rates except for xylose, in which the overall consumption rate was only around 22 % of the supply rate; hence the trend observed in Figure 9.3.

Overall, the calculated lipid productivities and $Y_{X/S}$ and $Y_{P/S}$ values for the 5-d semicontinuous culture (Stage II) shown in Table 9.2 indicated a reduced non lipid biomass production at the expense of a significantly improved lipid yield (0.015 and 0.065 g/g, respectively) compared with those obtained in the single stage batch culture

(0.386 and 0.015 g/g). On the other hand, non lipid biomass production in the semicontinuous culture stage was slightly higher and the lipid yield was almost 50 times than those in the overall discontinuous fed batch culture, which implies a superior performance of the semicontinuous process over the discontinuous fed batch and single stage batch. Although in all cases, lipid production was mostly growth –associated ($m > n$), the use of the semicontinuous fermentation mode improved the contribution of intracellular lipid content increase compared with the single stage batch and discontinuous fed batch due to the relatively higher magnitude of the parameter n in the former as shown in Table 9.2. The gradual addition of the substrate as opposed to initial charging was beneficial in improving lipid productivity by keeping sugar and inhibitor concentrations low so as to avoid possible inhibitory effects. Inhibitor consumption/degradation rates were also improved significantly with continuous substrate feeding at a low flow rate. However, the rather short time span of lipid accumulation was perhaps due to the lack of nutrient supplementation relative to the substrate supply leading to low microbial cell numbers involved in the accumulation of lipids since majority of the lipid accumulation by the activated sludge consortia was growth dependent as it has been found in previous experiments. Hence, in future semicontinuous experiments, lipid accumulation feed solutions with high C:N ratios must be formulated with nutrient supplementation as well as opposed to the carbon source alone.

Continuous Fermentation

The use of a continuous culture is considered to be a more viable strategy for the utilization of lignocellulose biomass hydrolyzate for microbial lipid accumulation in an industrial scale due to the advantage of having a continuous output of product with supposedly consistent characteristics [Gill, et al., 1977]. Similar to the semicontinuous experiment, a startup batch culture using glucose was conducted for 2 d after which simultaneous feeding of the substrate (40 g/L hydrolyzate) and culture withdrawal at supposedly the same flow rate (25 mL/h) and dilution rate (D) of 0.008 h^{-1} with no further nutrient supplementation. Hence the culture residence time (τ), which is the reciprocal of the operating dilution rate, was 125 h. As mentioned earlier, these operating parameters were so chosen as to acquire the same overall substrate loading as the other fermentation schemes investigated. However, the continuous culture stage (Stage II) proved to be unsuccessful as the biomass concentration declined immediately as shown in Fig. 9.4. Biomass lipid content and the lipid concentration in the culture increased initially within the first 24 h of Stage 2 but declined gradually afterwards and as a consequence no kinetic parameters were obtained for this stage. Furthermore, the consumption rates of the hydrolyzate components were lower than those obtained from the discontinuous fed-batch and semicontinuous experiments. These observations all indicate a possible washout event under the operating conditions mentioned above. In order to verify this, a plot similar to that shown in Fig. 5.3 in Chapter V was constructed using Equations 5.33 and 5.36 from Chapter V of this manuscript at different D values to graphically determine the optimum D for maximum biomass productivity and the critical D above which

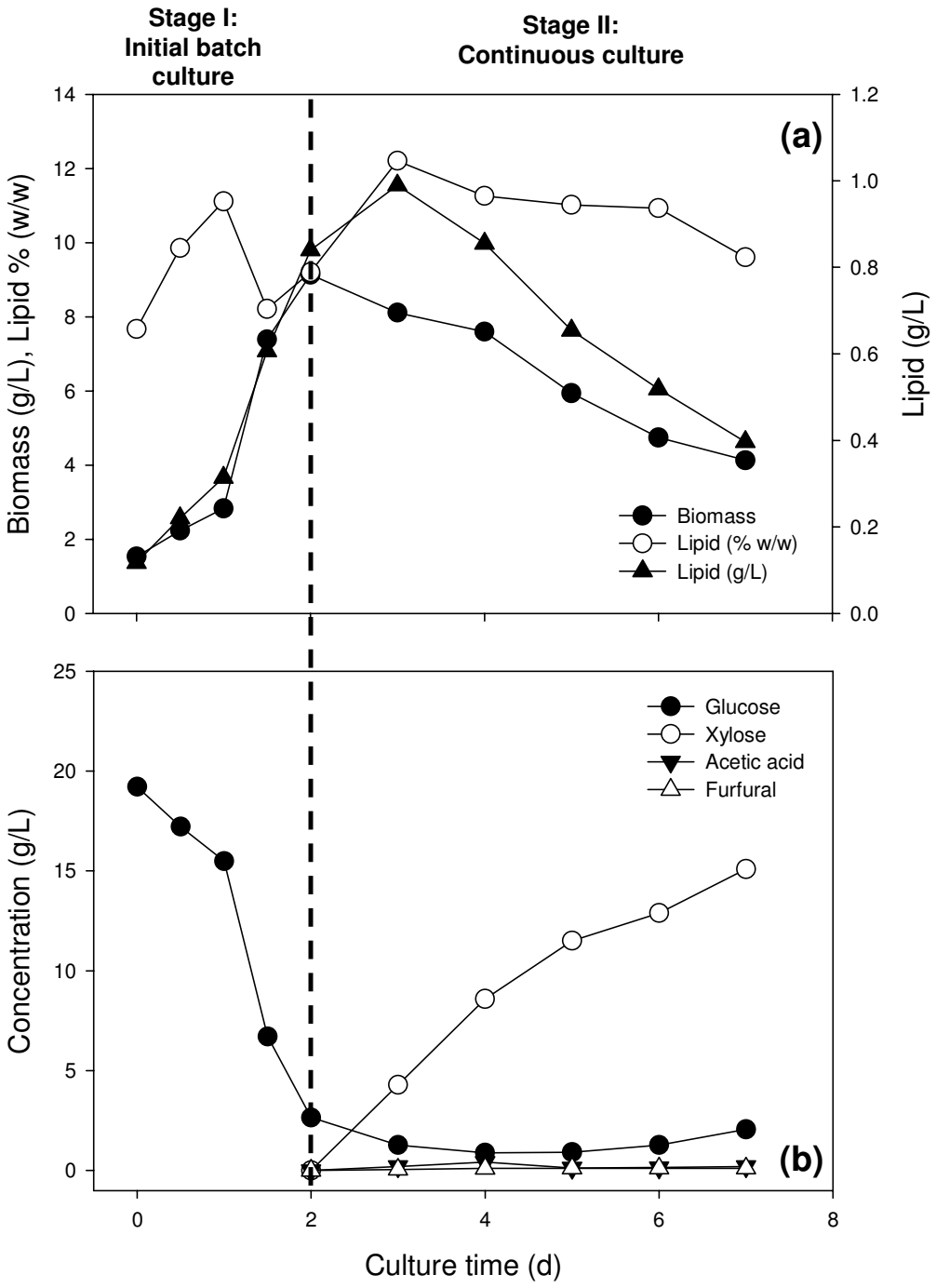

Figure 9.4: Fermentation profiles of a continuous culture (D = 0.008 h^{-1}) of activated sludge. Stage I: Initial batch culture using glucose. Stage II. Continuous mode using artificial hydrolyzate.

washout occurs. These D values were also calculated using Equations 5.34 and 5.36. The values of μ_{max}, $Y_{X/S}$, and K_S used were those from Stage II of the semicontinuous culture as this closely approximates the conditions of substrate feeding and nutrient levels in the continuous culture. The resulting plots are shown in Fig. 9.5 where it can be seen that under the initial conditions prior to the performance of the continuous culture (Stage II), the optimum D for maximum biomass productivity is approximately 0.0029 h^{-1} (τ = 345 h) while the critical D for washout was around 0.0037 h^{-1} (τ = 270 h). Clearly, the operating D in this experiment was higher than the critical D, hence washout was presumed to have occurred in the experiment rendering it unsuccessful. However, the calculated D_{opt} here is very small and at a culture volume of 3 L, the required feed/effluent flow rate is also very small (8.7 mL/h), such that errors could be associated with setting and controlling fermenter pumps to achieve this flow rate. The washout that occurred could also be attributed again to the negligible nutrient (ammonium-nitrogen) levels during the continuous culture stage; therefore feed solutions for lipid accumulation (i.e., high C:N ratio) should be formulated with nutrient supplements in addition to the substrate to ensure sufficient biomass levels in the culture.

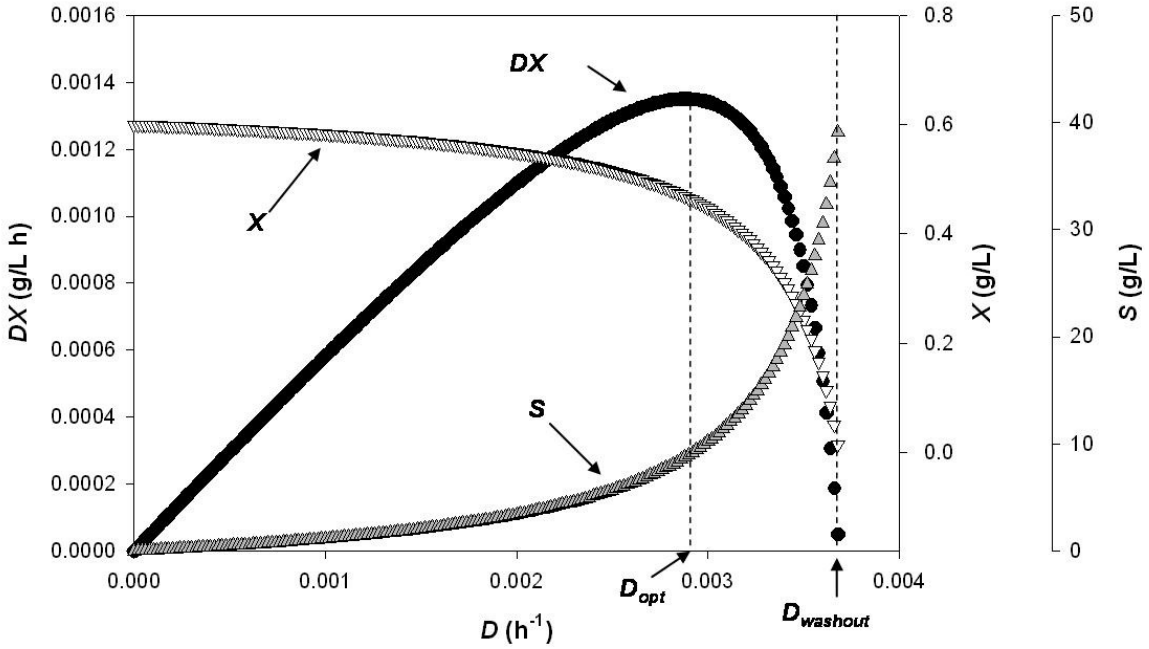

Figure 9.5: Plot of substrate *(S)* and non lipid biomass (*X)* and biomass production rate (*DX)* as a function of dilution rate (*D)* for the determination of the optimum and washout *D* in the continuous activated sludge culture experiment.

Table 9.2: Summary of kinetic parameter estimates for the fermentation of lignocellulose hydrolyzate by activated sludge for lipid production.

Parameters	Units	Batch	Fed Batch			Semicontinuous		Continuous	
			I	II	III	I	II	I	II
μ_{max}	h^{-1}	0.018	0.051	0.011	-	0.054	0.004	0.047	-
K_S	g/L	14.0	9.88	26.0	-	1.84	3.4	1.51	-
Lipid Productivity	g/L·h	0.0027	0.0024	0.0002	0.0017	0.011	0.008	0.015	-
m	g/g·h	0.223	0.491	-	-	0.0378	0.539	0.057	-
n	g/g	3.5×10^{-4}	0.005	2.4×10^{-5}	4.7×10^{-5}	0.0058	0.05	0.0067	-
$Y_{X/S}$	g/g	0.386	0.093	0.049	-	0.40	0.015	0.415	-
Overall				0.011		0.159		0.039	
$Y_{P/S}$	g/g	0.015	0.0046	0.0019	0.012	0.033	0.065	0.044	0.023*
Overall				0.0013		0.03		0.005	
Consumption Rates									
Glucose	g/L·h	0.065	0.152	0.04	0.067	0.344	0.249	0.345	0.072
Xylose	g/L·h	0.115	0.289	0.1	0.073	-	0.131	-	0.072
Acetic Acid	g/L·h	0.027	0.071	-	0.011	-	0.121	-	0.041
Furfural	g/L·h	0.0027	0.0075	3.5×10^{-5}	1.4×10^{-4}	-	0.009	-	0.003

*Lipid yield based on the lipid content increase in the initial 24 h of the continuous culture.

Lipid Analysis

One of the major requirements for the successful performance of any fermentation process in the large scale in addition to a constant production rate over prolonged cultivation times is the consistency of the products over time and from batch to batch [Shuler and Kargi, 2002]. In the case of proposed lipid production process by activated sludge microorganisms using lignocellulose hydrolyzate, consistency of the fatty acid profile and saponifiable lipid fraction of the lipids with time, especially it these are intended for biofuels production is a must. Therefore, lipid extracts from cultivated sludge generated using four different fermentation modes were analyzed by gas chromatography and at different fermentation times. Figure 9.6 shows the variation of the saponifiable lipid fraction in the sludge biomass with culture time under batch, fed-batch, semicontinuous, and continuous processes in relation to the total lipid contents. As it has been observed before with glucose as the sole carbon source (Chapter VI), saponifiable lipid fractions in raw sludge constitute on average less than 2 % of the total biomass and 25 % of the total lipid extracts. In glucose-fed cultures, these levels remained throughout the lag phase, after which the saponifiable fraction based on the total lipids increased to around 50 - 60 % and then its concentration based on the dry biomass weight increased with time at the same rate as the total lipids while maintaining the same ratio of 50 -60 % (w/w). In the single stage batch fermentation of the model hydrolyzate however, the total lipid content initially increased and then decreased while the saponifiable lipid fraction increased and after 3 d of cultivation, the proportion of the saponifiable lipids within the total extracts was close to 60 % (w/w) and remained fairly constant along with the total

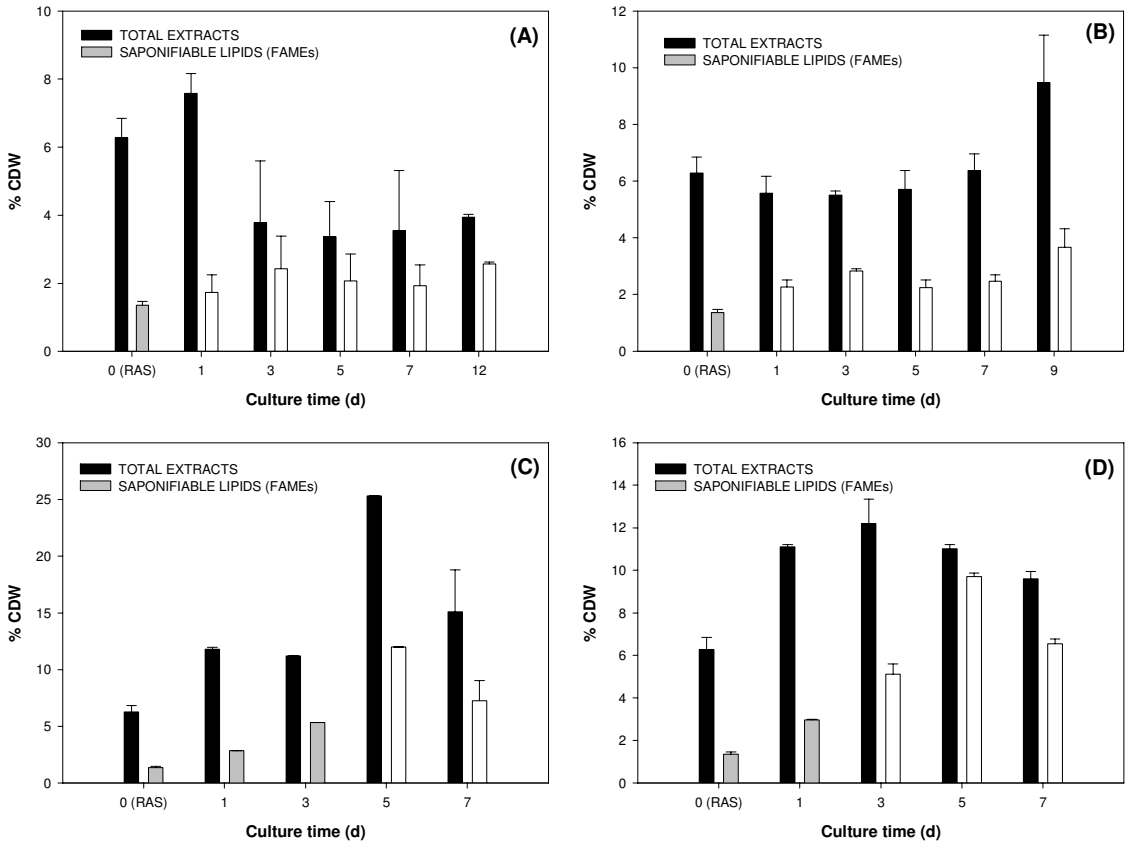

Figure 9.6: Total and saponifiable lipid fractions of activated sludge biomass grown on model hydrolyzate under (A) batch, (B) discontinuous fed-batch, (C) semicontinuous, and (D) continuous cultures.

lipids. This implies that initially, majority of the lipid components were unsaponifiable and after further fermentation, the unsaponifiables were degraded while the saponifiable lipids increased slightly. Furthermore, the final total saponifiable fraction in the biomass, which represents the biodiesel yield, was much lower (≈ 2.5 % CDW) compared with the maximum achieved previously using only glucose (≈ 10 % CDW). In Fig. 9.6(B), it can be seen that the variation in saponifiable lipid fractions in the discontinuous fed batch culture was very similar with that in the single stage batch, with a slightly higher final

saponifiable lipid yield (3.6 % CDW), however, the proportion of the saponifiable lipids with respect to the total extracts was slightly lower (40 % w/w) while the sudden increase in the total lipids from 8 to 9 d was due to the increase in the fraction of unsaponifiables. In the semicontinuous culture (Fig. 9.6 C), the saponifiable fraction relative to the total lipid extracts increased to approximately 50 % (w/w) after 1 d of semicontinuous cultivation (3 d total); hence a maximum saponifiable lipid (biodiesel) yield of 12 % CDW was achieved after 3 d of semicontinuous fermentation, during which time the maximum total lipid yield of 25.3 % was achieved. Both saponifiable and total lipids then decreased towards the end of the run (5 d semicontinuous, 7 d total). Interestingly, while the total lipid fraction of biomass decreased between 3 and 5 d of continuous fermentation (Fig. 9.6D), the saponifiable lipid fraction increased dramatically to around 88 % of the total lipid mass corresponding to 9.7 % CDW biodiesel yield.

Fig. 9.7 shows the distribution of the major fatty acids in the lipid extracts from the model lignocellulose hydrolyzate-grown activated sludge biomass. All percentages reported in this section are relative to the total mass of saponifiable lipids. Similar to activated sludge grown on glucose, C_{16} and C_{18} fatty acids dominated the lipids obtained via fermentation of the model lignocellulose hydrolyzate, making them suitable for biodiesel production as well. For the single stage batch process (Fig. 9.6A), no significant changes in the concentration of palmitic (C16:0), palmitoleic (C16:1), stearic (C18:0), linoleic (C18:2), and linolenic (C18:3) acids were seen relative to the initial composition in raw activated sludge oil, while oleic acid (C18:1) levels increased significantly with

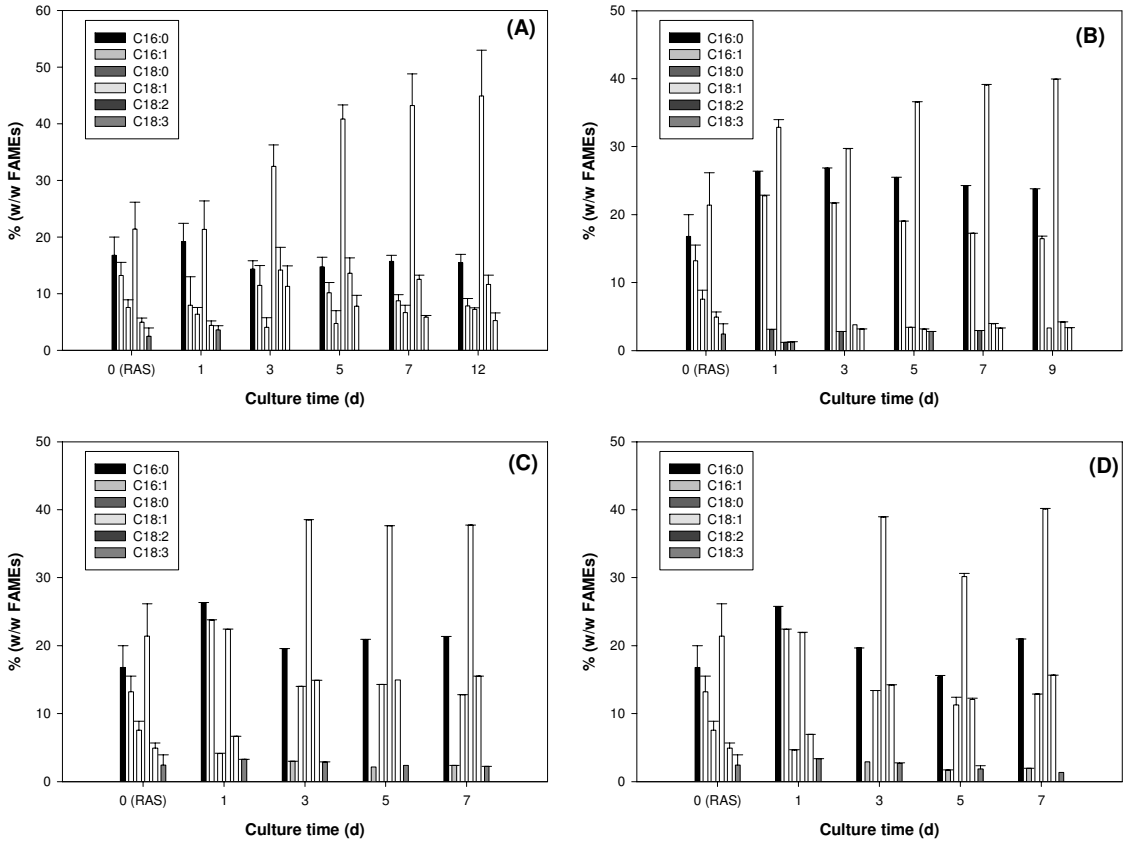

Figure 9.7: Fatty acid profile of lipid extracts from activated sludge biomass grown on model hydrolyzate under (A) batch, (B) discontinuous fed-batch, (C) semicontinuous, and (D) continuous cultures.

cultivation time from around 21 to 45 % after 12 d. On the other hand for the discontinuous fed batch culture (Fig. 9.6B), palmitic acid levels increased from 17 to 27 % palmitoleic acid levels increased from 13 to 27 %, and oleic acid concentration increased from 20 to 30 % (w/w FAMEs) within 24 h of the initial startup stage using hydrolyzate as the substrate. The remaining fatty acyl resides decreased to less than 5 % each. During the cultivation time span encompassing the next two batch feedings (3 – 9 d), the concentration of oleic acid increased further from 30 to 40 % (w/w FAMEs).

Palmitic and palmitoleic acids decreased slightly within the range of 27 - 23 % and 23 - 16.5 % (w/w FAMEs), which were both higher that those in the single stage batch culture.

Similar fatty acid profiles were observed in the semicontinuous and continuous culture as seen in Fig. 9.6C and D. The startup phases in both experiments (0 and 1 d) were characterized by increases in palmitic and palmitoleic acid level similar to Stage I of the discontinuous fed batch cultures but unlike the latter, oleic acid concentrations remained fairly constant at approximately 22 %. This difference could be due to the fact that glucose instead of the hydrolyzate was used as the substrate in the startup batch cultures in the semicontinuous and continuous cultures. After the initial batch culture during which semicontinuous and continuous feeding the hydrolyzate was conducted, the fatty acid profile obtained consisted of approximately 20 % palmitic acid and 40 % oleic acid. Stearic and linoleic acids were also present in significant amounts both in the range of 14 – 16 %, unlike in the single stage batch and discontinuous fed-batch cultures where palmitoleic acid was a dominant fatty acid along with oleic and palmitic acid.

Furthermore, the fatty acid profile of the lipids produced from the semicontinuous culture remained fairly constant from 3 to 7 d of fermentation whereas that from the continuous experiment showed a decrease in the oleic acid level at 5 d and increased again to its level at 3 d while the other fatty acid concentration remained the same As such, it can be inferred that the goal of producing lipids with a rather consistent profile suitable for biodiesel or green diesel application can be achieved through gradual substrate in the semicontinuous and continuous processes. For the continuous culture

however, the observed fluctuations might be due to quantification errors associated with the washout condition that occurred during the continuous fermentation experiments.

Conclusion

Different fermentation strategies were evaluated for the fermentation of a model lignocellulose hydrolyzate for the enhanced lipid accumulation by activated sludge microorganisms with the objective of improving lipid yield and productivity and the *in situ* degradation of the inhibitor compounds acetic acid and furfural. Biomass yields were highest but lipid production was severely limited in single stage batch culture using hydrolyzate as the carbon substrate due to the additive inhibitory effect of acetic acid and furfural. Results showed that the semicontinuous fermentation with an initial batch glucose startup culture resulted in the highest attained lipid content (25.3 % CDW), lipid concentration (2.81 g/L), lipid coefficient (0.03 g/g), and saponifiable lipid yield (12 % CDW), due to the constant feeding of the hydrolyzate resulting in low inhibitor and substrate concentrations, after which these levels eventually decreased. Although the fatty acid profiles in the semicontinuous and continuous fermentation experiments did not vary significantly during the later stage of the culture, the experiments failed to achieve a consistent output of lipids due to the cessation of biomass production caused by very low nutrient (N and P) levels. In the case of the continuous culture, the operating dilution rate was found to be above the critical values, thus washout of the culture occurred and no steady state biomass, substrate, and product levels were obtained. Therefore, in the performance of semicontinuous and continuous cultures, feed solutions for lipid accumulation must be formulated with nutrients in addition to the carbon source must be

used to sustain a viable microbial cell concentration that could continuously accumulate lipids.

CHAPTER X

MICROBIAL COMMUNITY ANALYSIS OF ACTIVATED SLUDGE IN AEROBIC BIOREACTORS FOR LIPID ACCUMULATION

Introduction

In addition to studying the bulk behavior (i.e., fermentation kinetics) of activated sludge in aerobic fermentation systems for the production of microbial lipids as discussed in earlier chapters, analysis of the dynamics of the activated sludge microbial population at the molecular level is necessary in order to have a full understanding of the proposed fermentation process. Changes in the composition of the microbial consortium in activated sludge in terms of organism types and species could be correlated with lipid accumulation patterns in activated sludge cultivated under various process conditions. This analysis can be done using a variety of techniques such as light microscopy, biochemical tests, cultivation-dependent methods, and non cultivation-dependent procedures such as the use of oligonucleotide staining probes, signature molecules such as PLFA's (phospholipid fatty acids), and 16S rRNA (rDNA) sequencing [Yan, et al., 2007]. For this study, the effect of the carbon-to-nitrogen ratio in the fermentation medium, identified as the variable that has the most significant effect on the lipid accumulation of activated sludge microorganisms (Chapter VI), on the composition of the bacterial population in activated sludge was investigated using a full cycle rRNA (rDNA)

approach based on bacterial 16S rRNA subunit as employed in previous studies for activated sludge systems [Snaidr, et al., 1997; Wagner and Loy, 2002]. In this manner, dominant microbial groups and specific microbial strains that may be responsible for enhanced lipid concentration in activated sludge can be identified and may be isolated for pure culture fermentations in the production of high amounts of lipids for biodiesel application. Knowledge of the ecology of microbial communities in activated sludge related to lipid production could also lead to the development of strategies to enhance wastewater treatment conditions favorable for the dominance of lipid producing microbial strains and enhance lipid yields from municipal sewage sludge.

Methodology

Activated sludge biomass culture broth samples from batch fermentation experiments operating at C:N ratios of 10:1, 40:1, and 70:1 as mentioned in Chapter VI at the following time points: 0 (raw sludge), 3 d, and 7 d were obtained, processed, and analyzed according to the specific protocols discussed in Chapter IV. Gene clone libraries based on the 16S rRNA were developed from DNA extracted from the activated sludge biomass samples obtained from the said time points and conditions. The clone libraries were then sequenced, analyzed, and compared with sequence libraries to determine the composition of the activated sludge microbial composition in terms of bacterial groups and genera. The abundance of a specific microbial group was expressed in terms of percent of the total number of sequences in a library.

Results and Discussion

The variation in the composition of the activated sludge microbial population with fermentation time and C:N ratio is illustrated in Figs. 10.1 – 10.3. Although the composition of activated sludge microbiota has been studied previously [Snaidr, et al., 1997], to our knowledge this is the first time sludge microbial communities have been studied under conditions conducive to enhanced lipid accumulation. 16S rRNA gene clone libraries were developed from the samples obtained at different C:N ratios since C:N ratio was found to exert a significant effect on lipid accumulation in activated sludge. As shown in Fig. 10.1, members of the *Proteobacteria* (gram-negative bacteria) phylum dominated the raw sludge samples (Day 0) prior to the treatments (58.4 %) followed by *Bacteriodetes* (26.6 %). Similar results have been found in previous studies conducted by other researchers on different activated sludge systems [Wagner and Loy, 2002; Eschenhagen, et al., 2003]. Among the *Proteobacteria,* gamma- and beta-like sequences dominated, accounting for 40.5 and 29.3 % of the *Proteobacteria* sequences, respectively. Alpha and delta-like Proteobacteria sequences were approximately 14.6 and 13.1 % of the total *Proteobacteria* sequences, respectively. On the other hand, most of the *Bacteriodetes* sequences identified (85 %) were found to be closely related to *Sphingobacteria*. *Verrucomicrobia*-like sequences were close to 7 % of the Day 0 library, while other groups represented less than 1 % each (i.e., gram-positive bacteria or *Firmicutes*, TM7, *Gemmatimonadetes*, OP10, SR1, *Chloroflexi*).

Significant changes in microbial composition were observed for each of the treatments after 3 d, which corresponded to the onset of the stationary phase and lipid

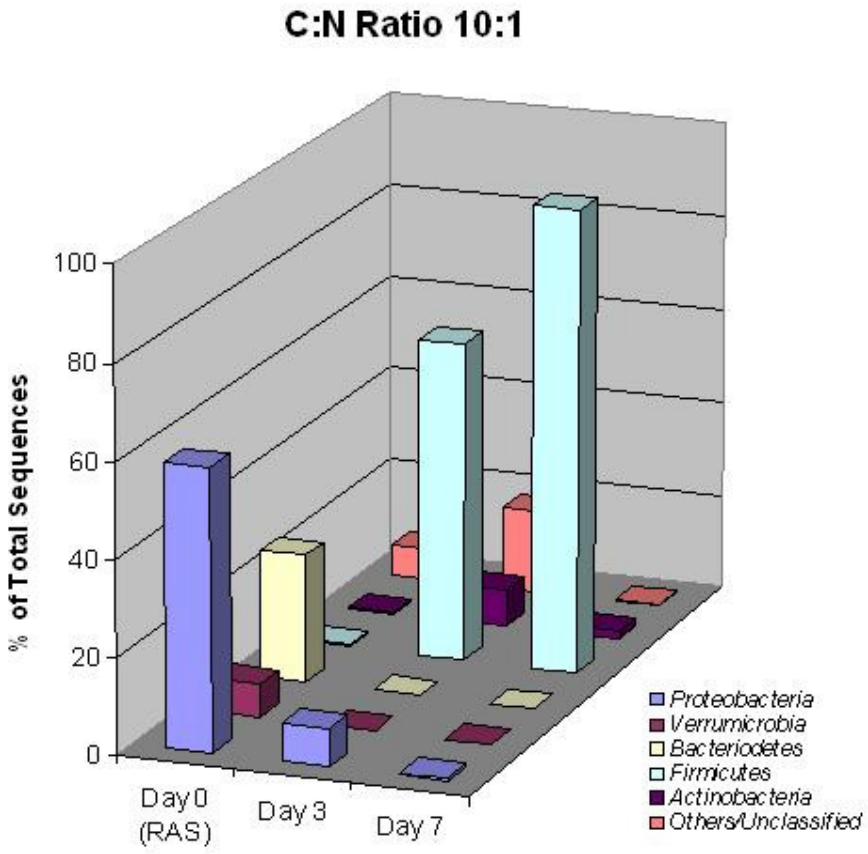

Figure 10.1: Variation in activated sludge microbial composition with cultivation time at C:N ratio 10:1. Total number of sequences: Day 0 (274), Day 3 (166), and Day 7 (180).

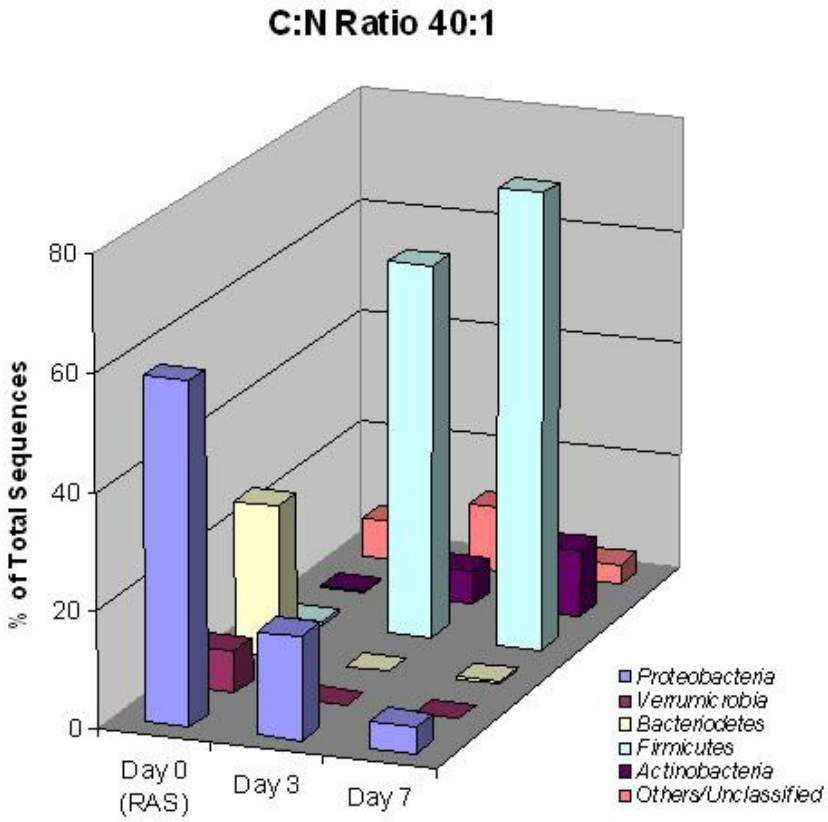

Figure 10.2: Variation in activated sludge microbial composition with cultivation time at C:N ratio 40:1. Total number of sequences: Day 0 (274), Day 3 (185), and Day 7 (183).

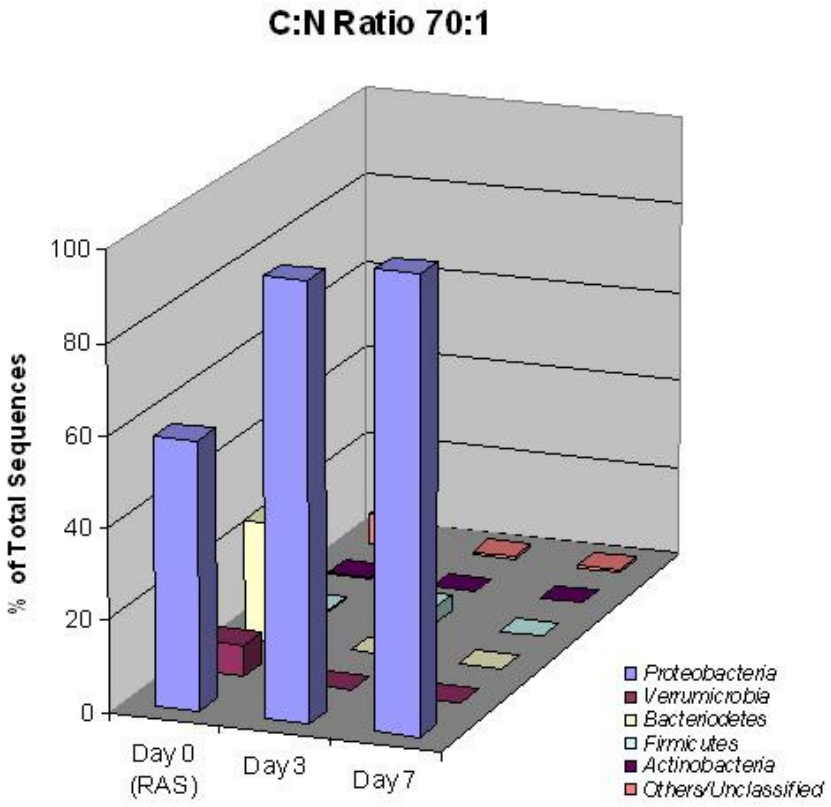

Figure 10.3: Variation in activated sludge microbial composition with cultivation time at C:N ratio 70:1. Total number of sequences: Day 0 (274), Day 3 (175), and Day 7 (189).

accumulation in the case of C:N ratio 70:1 (Fig. 10.3). At C:N ratio 10:1 (Fig. 10.1) and C:N ratio 40:1 (Fig. 10.2), *Firmicutes* increased from 0.6 to 67 and 65 % of all sequences, respectively. Most *Firmicutes* sequences (78-86 %) were closely related to members of the *Clostridia* class and the rest belong to the *Erysipelotrichi* class. *Proteobacteria* decreased considerably in numbers, representing less than 18% (i.e., 7.8 % for C: N 10:1 and 17.8 % for C:N 40:1) of the sequences, most of which were gamma-like sequences. In contrast, *Actinobacteria* increased to 7.8 and 5.9 % in the C:N ratio 10:1 and C:N ratio 40:1 Day 3 libraries, respectively and no *Bacteroidetes* sequences were found in any of the treatments. After 7 d, *Firmicutes* proportion increased further to 97.2 and 79.2 % of the total sequences at C:N ratio 10:1 and C:N ratio 40:1, respectively. In this group, *Clostridia* was the dominant class, accounting for around 85 % of the *Firmicutes* sequences. Within the *Clostridia* class, *Sporacetigenium*- and *Turicibacter*-like sequences were the majority. Similar to other *Clostridia*-, *Sporacetigenium*- and *Turicibacter*-type species are considered obligate anaerobic bacteria. The fact that these microorganisms dominated in aerated bioreactors suggest that some of their close relatives might be tolerant to aerobic conditions or that there are microniches within these systems that can promote anaerobic growth. It is also possible that although the bioreactor dissolved oxygen probe readings showed sufficient oxygen levels in the culture broth, flocs could have formed causing limited oxygen mass transfer into the microorganisms. The changes in composition favoring *Clostridia* as abundant bacteria in the C:N ratio 10:1 and C:N ratio 40:1 samples can be explained by the utilization of

potentially available carbohydrates such as glycerol, a process that could result in the production of value added products such as butanol [Taconi, et al., 2009].

As shown in Fig. 10.3, the C:N ratio 70:1 microbial community was vastly dominated by Proteobacteria (96 %) after 3 d, most of which were gamma *Proteobacteria* (90.4 % of *Proteobacteria* sequences). Some of the most abundant gamma *Proteobacteria* at this stage of the fermentation were members of orders *Enterobacteriales, Pseudomonadales,* and *Aeromonadales*, which were below detection limits in the initial sludge community. In a previous study, some members of these orders (genera *Pseudomonas* and *Aeromonas*) have been isolated from municipal sewage sludge as producers of polyhydroxyalkanoates (PHA) under similar conditions with the present study [Reddy, et al., 2008]. Further, extracellular polysaccharide (EPS) formation has been detected in bacteria of the orders *Rhodospirillales, Sphingomonadales, Xanthomonadales, Enterobacteriales* and *Pseudomonadales* [Vu, et al., 2009]. These microbial storage products could possible take into account the unsaponifiable fraction of the lipids not converted to biodiesel, which constitutes a significant fraction (40 to 50 %) of the total lipid extracts.

Nearly all of the C:N ratio 70:1 sequences (99%) were alpha *Proteobacteria* after 7 d, indicating a significant shift in microbial composition, specifically from gamma to alpha *Proteobacteria*, at which time span maximal lipid contents in the activated sludge biomass were obtained. Most of the alpha-like sequences (99.5 % of total *Proteobacteria* sequences) were closely related to *Acidomonas methanolica*, a member of the *Rhodospirillales* order under the *Acetobacteraceae* family, which are known acetic acid

producers [Wilkinson, 1988], which interestingly was not detected in the initial sludge community. No mention has yet to be found in literature regarding lipid accumulation by any member/s of this bacterial groups; however, the dominance of oleic acid (C18:1) followed by palmitic acid (C16:0) in the fatty acid profile of lipid extracts obtained from activated sludge grown in the same conditions could be accounted for by the dominance of this particular group in the late stages of the C:N ratio 70:1 culture. Bacteria belonging to the *Acetobacteraceae* family have characteristic fatty acid profiles having 70 – 80 % oleic acid and 10 – 20 % palmitic acid [Wilkinson, 1988] while the final activated sludge biomass contained lipids with 50 – 60 % oleic acid and around 20 % palmitic acid. It should be noted however that the lower oleate levels in activated sludge compared with the specific *Acetobacteraceae* family is probably due to the fact that activated sludge is a mixed culture. Despite the apparent dominance of one family in the total bacteria, it should also be considered that other microbial groups such as yeasts and fungi have not been investigated for their population dynamics in activated sludge; hence it is possible that these eukaryotes are present in the sludge community as well contributing to the enhanced lipid production.

Conclusion

The composition of the microbial community in municipal sewage sludge was analyzed at different initial C:N ratios of the fermentation media for enhanced lipid accumulation. Results showed that the microbial composition of activated sludge changed considerably from being in its raw form in the municipal wastewater treatment plant and after aerobic cultivation in synthetic wastewater supplemented with sugars

(glucose) at different initial C:N ratios. After 3 and 7 d of fermentation, the microbial composition of cultured activated sludge was very similar at low (10:1) and medium (40:1) C:N ratios and both were different from that at obtained at high C:N ratio (70:1). The results also suggested that prolonged exposure to any of these conditions led to a significant reduction in the diversity of the activated sludge microbiota, in terms of the bacterial population. Since it was found in the earlier phases of the study that the lipid productivity of activated sludge microorganisms was highest at C:N ratio 70:1, the dominance of members of the alpha *Proteobacteria* group in the resulting activated sludge culture at this condition could point to the specific microorganisms potentially responsible for high lipid accumulation among the numerous members of the activated sludge microbiota for potential isolation and use in pure culture fermentations. Although C:N ratio was the only variable considered in this analysis, the observed changes in the culture pH and dissolved oxygen could have also affected the variation of the microbial composition of activated sludge; hence, their effects needed to be considered in future studies as well.

Still, the bacterial groups responsible for lipid production, specifically the saponifiable fraction for conversion to biodiesel, in these consortia have yet to be conclusively determined; although some of the potential bacterial groups were identified. The molecular data obtained from this study could allow for further investigation of these identified groups using quantitative group-specific assays. Furthermore, it is possible that not all members of the community are contributing in a similar manner to lipid production, or complex microbial interactions occurring in diverse microbial

communities such as activated sludge could influence the overall lipid productivity of activated sludge. In this regard, understanding the microbial composition of amended activated sludge samples is relevant in order to develop functionally stable engineered systems in wastewater treatment facilities configured for enhanced sludge oil production and recovery.

CHAPTER XI

ENGINEERING SIGNIFICANCE

Introduction

In this chapter, several engineering aspects of the proposed fermentation process for the enhancement of lipid and biodiesel yields from municipal sewage activated sludge are discussed in order to determine its feasibility in industrial applications. Continuous process simulations were performed using computer software to obtain projected biomass and lipid productivities, biodiesel yields, and substrate consumption rates. Preliminary design calculations were them made to estimate the required bioreactor size required for specific calculation bases; specifically the assumed substrate conversion or yield coefficients for lipids and biodiesel production. An economic analysis was conducted to determine capital investment, production costs, and optimal product selling price. Finally, energy balance calculations were made to determine the applicability of employing the lipid and biodiesel outputs of the proposed process for energy-intensive industrial processes.

Continuous Process Simulation

Based on the results of the laboratory-scale cultivation experiments conducted in this study, the proposed fermentation process for the conversion of lignocellulose sugars into storage lipids could be applied to aerobic activated sludge bioreactors for the enhancement of its lipid content and subsequently its saponifiable lipid fraction or biodiesel yield. Since initial trials of a small-scale continuous fermentation process using the model hydrolyzate mixture were unsuccessful (Chapter IX), the single stage batch kinetic parameters obtained at an initial C:N ratio 70:1 and substrate (hydrolyzate) concentration of 60 g/L shown previously in Table 9.1 were used to design a large scale continuous lipid accumulation process and estimate the fermentation profiles under the same initial conditions. These kinetic parameters and their corresponding values are again shown in this Chapter in Table 11.1. It was also concluded that in order to sustain microbial growth and hence lipid accumulation, the culture must also be supplemented with nutrients (N and P sources) during the continuous feeding and harvesting and these could be accomplished by using raw wastewater as the feed media.

First, the optimum dilution rate (D_{opt}) for maximum biomass productivity was calculated using Equation 5.36 given previously:

$$D_{opt} = \mu_{max}\left(1 - \sqrt{\frac{K_S}{K_S + S_0}}\right) \tag{5.36}$$

Table 11.1: Single-stage batch fermentation kinetic parameters at 60 g hydrolyzate per L initial loading and C:N ratio 70:1 used for estimation of continuous culture profiles.

Parameter	Symbol	Units	Value
Maximum specific growth rate	μ_{max}	h^{-1}	0.018
Saturation constant	K_S	g/L	14.0
Empirical constant for growth-associated lipid production	m	g/g	0.223
Empirical constant for non growth-associated lipid production	n	g/g·h	3.5×10^{-4}
Non lipid biomass yield coefficient	$Y_{X/S}$	g.g	0.39
Optimum dilution rate	D_{opt}	h^{-1}	0.01

Table 11.2: Performance parameters of model simulated continuous fermentation of lignocellulose hydrolyzate for enhanced lipid accumulation of activated sludge.

Dilution rate, D	h^{-1}	0.01
Feed Substrate Concentration S_0	g/L	60
Initial Non Lipid Biomass Concentration, X_0	g/L	1.0
Initial Lipid Content,	% CDW	9.1
Initial Lipid Concentration P_0	g/L	0.1
Steady State		
Time to Reach Steady State	h (d)	3243 (135)
Non Lipid Biomass Concentration X	g/L	32.4
Lipid Content	% CDW	20.5
Lipid Concentration P	g/L	8.4
Substrate Concentration S	g/L	18.2
Non Lipid Biomass Productivity	g/L·h	0.32
Lipid Productivity	g/L·h	0.08
Substrate Loading Rate	g/L·h	0.61
Substrate Effluent Rate	g/L·h	0.18
Substrate Consumption Rate	g/L·h	0.43
Non Lipid Biomass Yield Based in Substrate Consumed $Y_{X/S}$	g/g	0.39
Lipid Yield Based on Substrate Consumed $Y_{P/S}$	g/g	0.20

to give D_{opt} = 0.01 h^{-1}. Assuming initial non lipid (X_0) and lipid (P_0) concentrations of 1.0 and 0.1 g/L respectively corresponding to an initial lipid content of 9 % w/w of total biomass based on the initial characteristics of raw sludge, and a lipid yield coefficient $Y_{P/S}$ of 0.20 g/g, the simulated time profiles of non lipid biomass (X), substrate (S), and lipid (P) were obtained by integration of their respective rate equations given by Equations 5.27, 5.28, and 5.39 as shown previously in Chapter V:

$$\frac{dX}{dt} = \left(\mu_g - D\right)X \tag{5.27}$$

$$\frac{dS}{dt} = DS_0 - DS - \frac{\mu_{net}X}{Y_{X/S}} - \frac{q_P X}{Y_{P/S}} \tag{5.28}$$

$$\frac{dP}{dt} = q_P X - DP = nX + m\mu_g X - DP \tag{5.39}$$

Integration of these differential equations was carried out using the Runge-Kutta-Fehlberg (RK45) algorithm of the ordinary differential equations program of Polymath® Professional 6.1 (CACHE Corpn., USA). The resulting fermentation profiles are shown in Figure 11.1 and the fermentation performance parameters and predicted steady state conditions are shown in Table 11.2. These numerical values can then be applied to the design of a large scale lipid accumulation process in a wastewater treatment plant employing the activated sludge process.

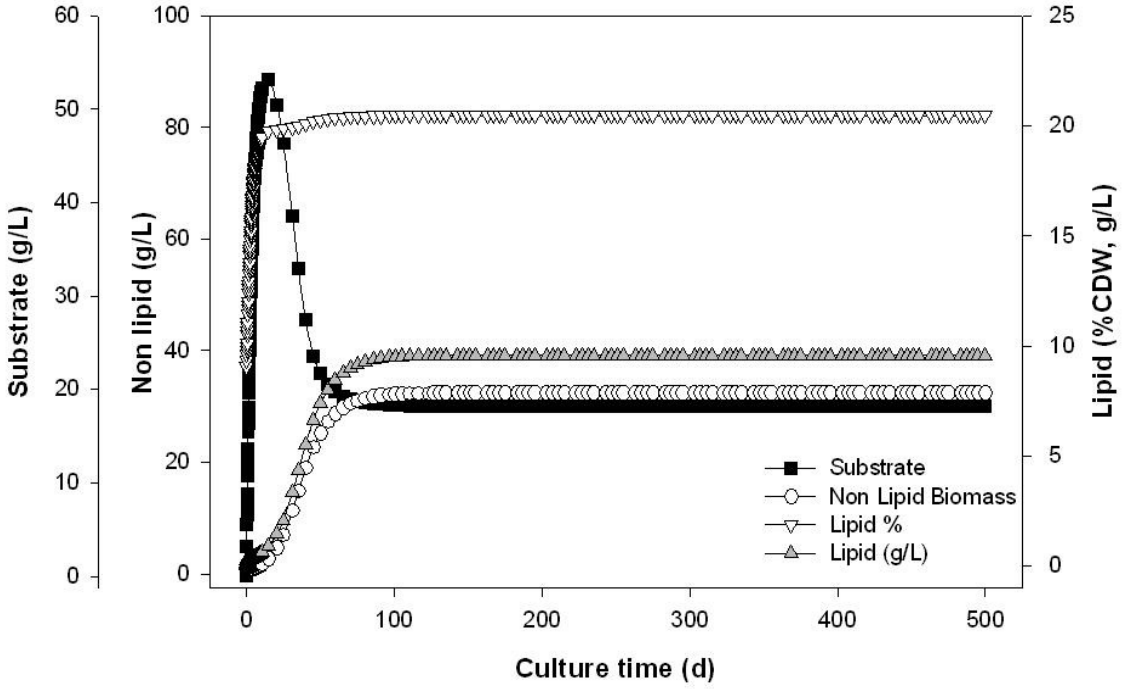

Figure 11.1: Model simulation for the continuous fermentation of model lignocellulose hydrolyzate at 60 g/L hydrolyzate feed concentration, C:N ratio 70:1, D = 0.01 h^{-1}.

Process Scale-Up and Economic Analysis

For the process scale-up calculations, the municipal wastewater treatment plant from which the activated sludges used in this study were obtained was considered. The said wastewater treatment plant is located in Tuscaloosa, AL, USA and is rated with an average daily capacity of 30 MGD (million gallons per day). For the proposed lipid enhancement process for activated sludge based on Figure 1.7, it was assumed that 2 % of the total average daily capacity will be used as the influent media stream; hence the basis of the design was:

$$\begin{aligned}\text{Design influent flow rate} &= 0.02(30) = 0.6\,\text{MGD} \\ &= 80{,}200\ \text{ft}^3/\text{d} \\ &= 2.3\times10^6\ \text{L/d}\end{aligned} \tag{11.1}$$

The total substrate loading rate shown in Table 11.2 (0.61 g/L·h) was obtained by multiplying the influent substrate concentration (S_0 = 60 g/L) with the design dilution rate (0.01 h^{-1}). Thus, the substrate loading for the proposed large scale process was calculated as

$$\begin{aligned}\text{Total substrate loading} &= FS_0 \\ &= \left(2.3\times10^6\ \text{L/d}\right)\left(60\times10^{-3}\ \text{kg/L}\right) \\ &= 1.4\times10^5\ \text{kg/d} \\ &= 5.0\times10^7\ \text{kg/yr}\end{aligned} \tag{11.2}$$

To express these parameters in terms of BOD_5, the conversion factor of 224 mg/L BOD_5 for a standard 300 mg/L of glucose solution for the standard BOD_5 analysis method was used [APHA, et al., 1998] and the calculated BOD_5 equivalent of the initial substrate concentration of 60 g/L was 44800 mg BOD_5/L . Hence, the BOD_5 loading was calculated as 681 lb BOD_5/1000 ft^3·d. The required total working volume of the bioreactor or aeration basin for the proposed process was then calculated from the dilution rate and design flow rate as

$$\begin{aligned}V_R = \frac{F}{D} = \frac{9.5\times10^4\ \text{L/h}}{0.01\ \text{h}^{-1}} &= 9.3\times10^6\ \text{L} \\ &= 9.3\times10^3\ \text{m}^3 \\ &= 3.3\times10^5\ \text{ft}^3 \\ &= 2.5\times10^6\ \text{gal}\end{aligned} \tag{11.2}$$

or based on the equivalent BOD_5 loading

$$
\begin{aligned}
V_R &= 2.2\times10^5 \ \frac{\text{lb BOD}_5}{\text{d}}\left(\frac{1000 \text{ ft}^3 \text{ d}}{681 \text{ lb BOD}_5}\right) \\
&= 2.5\times10^6 \text{ gal} \\
&= 3.3\times10^5 \text{ ft}^3
\end{aligned} \tag{11.3}
$$

The bioreactor/aeration basin dimensions were then sized based on the design guideline for completely-mixed systems, wherein the typical length-to-width ratios are between 1.5:1 and 2:1 at depths less than 5 m (16.4 ft) [Celenza, 2000]. Although most activated sludge aeration basins are designed in plug flow configurations having length-to-width ratios of at least 5:1 or in many cases even greater than 10:1, the use of the plug flow for this particular application was considered inappropriate due to the existence of concentration gradients along the length of the basin [Celenza, 2000]. Assuming a liquid depth of 5.5 m (18 ft) and length-to-diameter ratio of 2:1, the bioreactor length and width are calculated to be 58.2 m (191 ft) and 29.1 m (95.5 ft), respectively.

The effluent substrate flow rate was calculated in a similar method as with the influent substrate loading in Equation 11.1 to give

$$
\begin{aligned}
\text{Effluent substrate flow rate} &= FS \\
&= \left(2.3\times10^6 \text{ L/d}\right)\left(18.2\times10^{-3} \text{ kg/L}\right) \\
&= 4.1\times10^4 \text{ kg/d} \\
&= 1.5\times10^7 \text{ kg/yr}
\end{aligned} \tag{11.4}
$$

Hence, the overall substrate consumption can be estimated by taking the difference of the total substrate loading and the effluent substrate loading to obtain 9.9×10^4 kg/d or 3.5×10^7 kg/yr. Similarly, the BOD_5 concentration and loading of the effluent was calculated as 13580 mg BOD_5/L and 206.5 lb BOD_5/1000 ft^3·d. These levels are still too

high for discharge in stabilization ponds; hence the effluent should be routed back to the head of the wastewater treatment plant for BOD_5 degradation. Furthermore, due to its significant residual substrate content, the effluent could likewise be recycled into the fermentation process for further utilization by the activated sludge microorganisms for lipid production by lowering the sugar requirement and costs.

The non lipid biomass and lipid production rates were also calculated from steady state data using the same approach as shown in Equations 11.2 and 11.4 as

$$\begin{aligned}\text{Non lipid biomass production} &= FX \\ &= \left(2.3\times10^{6}\ \text{L/d}\right)\left(32.4\times10^{-3}\ \text{kg/L}\right) \\ &= 7.5\times10^{4}\ \text{kg/d} \\ &= 2.7\times10^{7}\ \text{kg/yr}\end{aligned} \tag{11.5}$$

and

$$\begin{aligned}\text{Lipid production} &= FP \\ &= \left(2.3\times10^{6}\ \text{L/d}\right)\left(8.4\times10^{-3}\ \text{kg/L}\right) \\ &= 1.9\times10^{4}\ \text{kg/d} \\ &= 6.9\times10^{6}\ \text{kg/yr}\end{aligned} \tag{11.6}$$

where lipid production can also be calculated by multiplying the lipid yield coefficient $Y_{P/S}$ with the sugar consumption rate using the assumed value of 0.20 g lipids/g substrate consumed. Based on the experimental results obtained in the earlier sections of this study, a total FAMEs (biodiesel) yield of 60 % by mass of the lipid extracts from the enhanced activated sludge was assumed, which is higher compared with around 25 % in raw activated sludge. Hence the total estimated biodiesel production from activated sludge following the enhancement process is 1.1×10^{4} kg/d or 4.2×10^{6} kg/yr. Converting these

mass production rates to volume using the density of 0.88 g/mL yields 4.7×10^6 L/yr or 1.3×10^6 kg/yr of biodiesel production capacity.

In order to determine the economic feasibility of the proposed process, a cost analysis approach employed previously for biodiesel production from raw sewage sludge via *in situ* transesterification [Mondala, et al., 2009] was used in the current study to estimate the production cost and break even price of biodiesel obtained from the enhanced sludge and the results are shown in Table 11.3. The basis for the cost analysis is one year of continuous operation of the sequential lipid accumulation cultures of activated sludge and the *in situ* biodiesel production from the enhanced sludge biomass. It also assumed that the sugar cost is the only contribution of the former process to the total direct operating cost (DOC). No additional construction of bioreactors was necessary since the fermentation process could be conducted in available activated sludge aeration basins in the wastewater treatment plant; hence no equipment and capital costs are incurred in this manner. The sugar cost was estimated at $0.20/lb as the average of the monthly sugar price from Jan. – Sep. 2010 as found in the International Monetary Fund webpage listing of fuel and non-fuel commodity prices [IMF, 2010] and was calculated accordingly per gallon of biodiesel produced based on the yield assumptions mentioned in the preceding paragraph (Table 11.3 Item B.1.a). Additionally, the process effluent stream still contains significant quantities of the substrate (18.2 g/L); hence it was assumed that the effluent streams were recycled following separation of the oil-rich sludge biomass to fully utilize the sugar supply into the process. All the sludges being

Table 11.3: Annual cost estimates for *in-situ* transesterification of enhanced activated sludge. Bases: 1.25×10^6 gallons/yr (4.73×10^6 L/yr) capacity.

Item	Unit Cost	Total Cost
A. Total capital investment cost, TCC (FCC + WCC)[a]		$788,376.10
1. Equipment cost, EC (In $1000/8000 ton annual cap.)		$186,126.08
a. Transesterification reactor	$284.75	$14,502.89
b. Neutralization reactor	$21.25	$68,612.18
c. Washing column	$97.75	$109,977.71
d. FAME distillation column	$153.85	$2,459.44
e. Heat exchangers	$3.40	$32,839.70
f. Pumps	$45.05	$32,381.90
g. Others	$44.20	$186,126.08
2. Contingencies and fees, CFC (18 % of EC)		$80,441.98
3. Total basic module cost, TBMC (EC + CFC)		$527,341.87
4. Auxiliary facility cost, AFC (30% of TBMC)		$158,202.56
5. Fixed capital cost, FCC (TBMC + AFC)		$685,544.43
6. Working capital, WCC (15 % of FCC)		$102,831.66
B. Total annual production cost, TAPC (DOC+IOC+DEPC+GE)[b]		$6,034,992.06
1. Direct operating costs, DOC		$5,709,099.79
a. Sugars for fermentation[c]	$2.52/gal	$3,150,860.10
b. Feedstock (sludge) preparation, centrifugation, and drying[d]	$1.72/gal	$2,147,746.12
c. Methanol	$0.08/gal	$102,578.33
d. Acid catalyst and solvent	$0.15/gal	$58,880.00
e. Labor[d]	$0.10/gal	$124,868.96
f. Heating oil[e]	$0.008/L	$37,810.32
g. Electricity[e]	$0.002/L	$9,452.58
h. Cooling water[e]	$0.0013/L	$6,144.18
i. Steam[e]	$0.0009/L	$4,253.66
j. Wash water[e]	$0.0001/L	$472.63
k. Maintenance and repairs (6 % of FCC)		$2,147,746.12
l. Operating supplies (15 % of maintenance and repairs)		$102,578.33
m. Lab charges (15 % of labor)		$58,880.00
2. Indirect operating costs, IOC		$88,632.26
a. Overhead, packing, storage (60% of labor)		$74,921.38
b. Local taxes (1.5 % of FCC)		$10,283.17
c. Insurance (0.5 % of FCC)		$3,427.72
3. Depreciation, DEPC (10 % of FCC)		$68,554.44
4. General expenses, GE		$168,705.56
a. Administrative expenses (25 % of overhead)		$18,730.34
b. Distribution and selling (≈10 % of TPC)		$99,983.48
c. Research and development (≈5 % of TPC)		$49,991.74
C. Total revenues from biosolids fertilizer sale	$35.80/ton[f]	$961,475.09
D. Net annual production costs (B-C)		$5,073,516.98
Price of biodiesel per gallon to break even		**$4.06**

[a]Costs were estimated based on the values reported in $1000 per 8000 tons of biodiesel per yr using the conversion equation of capacity: $Cost_B = Cost_A(Capacity_B/Capacity_A)^{0.65}$ [You, et al., 2008].
[b]Itemized production costs were based on the costs reported by You *et al.* (2008) unless specified otherwise.
[c]Sugar cost of $0.22/lb converted to per gallon of biodiesel produced [IMF, 2010]
[d][Dufreche, et al., 2007].
[e][Nelson and Schrock, 2006].
[f][Sullivan, et al., 2007].

produced were harvested and processed for *in situ* transesterification and there was no sludge recycle stream.

For estimation of the operating costs related to the *in situ* transesterification of the activated sludge biomass with enhanced lipid contents, the same assumptions applied in the previous paper was similarly used in the current study. The required amounts of methanol and sulfuric acid for the transesterification process were calculated based on the optimum experimental conditions of 12:1 mass ratio of methanol to sludge biomass and 5 % (v/v) sulfuric acid in methanol. It was also assumed that the used methanol were recovered via distillation and reused for approximately 40 batch cycles before disposal. As it was assumed earlier that there were no capital costs related to the fermentation process, the fixed capital investment cost (FCC) (Table 11.3 Item A.5.) only accounted for the fabrication of biodiesel production equipment based on the calculated production capacity and their respective contingencies and fees and auxiliary facilities (Table 11.3 Items A.1.-A.6.) according to the methods employed in another paper [You, et al., 2008]. The FCC was then used to estimate the total capital investment cost (TCC) and total annual production cost (TAPC) as seen in Table 11.3 Items A and B, respectively similarly using the approach used by You and colleagues [2008]. As mentioned previously, the auxiliary facilities cost, which includes the purchase of land, installation of electrical and water systems, and construction of internal roads (AFC, Table 11.3 Item A.4.) may be significantly lowered it the biodiesel facility was built in the same site or within close proximity of the wastewater treatment plant, as well as the feedstock transportation costs [Mondala, et al., 2009]. In order to recover some of the TAPC and

reduce the fraction of feedstock cost attributed to the sugars, the use and sale of the spent biomass (biosolids) after *in situ* transesterification or lipid extraction as fertilizer replacement has been considered. These solids theoretically still contain nitrogen and phosphorus from the microbial cell materials that may be utilized nutrient sources for agricultural applications at an estimated cost of $35.80 per dry ton [Sullivan, et al., 2007]. Based on the overall non lipid biomass output of the fermentation and transesterification assuming complete separation of lipidic materials (2.7×10^4 tons/yr), the estimated yearly revenues from the sale of the spent biosolids was projected to be $961,475.09, and subtracting this value from the TAPC gives the net annual production cost (Table 11.3 Item D). Therefore, the break even price of the biodiesel exclusive of profits, income taxes, and product transportation cost was calculated as $4.06/gallon of processed biodiesel, This price estimate was around 26 % higher than the estimated cost for biodiesel from raw sewage sludge ($3.23/gallon) and the fraction of the TAPC attributed to the feedstock including the sugar used for fermentation in the current study was found to be around 88 % compared to 53 % using raw sewage sludge as shown in the previous paper [Mondala, et al., 2009]. Based on these price estimates, it appears that the assumed 20 % total lipid yield based on substrate consumption was not sufficient to achieve a similar price with the unamended sludge biodiesel although the experimental results showed a significant improvement in the lipid feedstock quality (fatty acid profile) for use in biodiesel application following cultivation in lignocellulose sugars. However, using the maximum theoretical yield of lipids from sugars (glucose) of 33 g/100 g of sugar [Ratledge, 1982] as the assumed value for the total lipid yield gives a biodiesel

break even price of $3.25/gal which is now roughly the same as with that using raw activated sludge.

In addition to these, the cost of the sugar substrate for fermentation was also found to be a limiting factor in terms of the biofuel costs. The five-year plan (2007-2011) of the US Department of Energy includes as one of its primary goals the reduction of the cost of lignocellulose sugars for fermentation to bioethanol and other biofuel applications from $0.15 - $0.20 to around $0.50 - $0.64 per lb in order to reduce the price of ethanol from $2.72/gallon down to $1.07/gallon [U.S. DOE, 2006]. Therefore, a sensitivity analysis was conducted by determining the impact of different sugar costs on the projected biodiesel break even price. Based on the results shown in Table 11.4, a lignocellulose sugar cost between $0.12 and $0.14 per lb is needed to match a similar break even price for biodiesel obtained from raw sewage sludge. Decreasing the sugar cost further to $0.10 per lb drops the biodiesel price below the $3.00/gal mark ($2.80), which is lower than the current average diesel price of $3.07 in the U.S. from January to September 2010 [EIA, 2010].

Energetic Analysis and Potential Applications

Figure 11.2 shows the resulting energy inputs and outputs of the proposed lipid accumulation process and subsequent biodiesel production from activated sludge biomass with enhanced lipid contents, as well as its potential applications in powering energy-intensive water and wastewater treatment processes and unit operations. One day of operation for the combined processes was set as the calculation basis. For the proposed

Table 11.4: Projected biodiesel feedstock cost fraction and break even price at different assumed sugar costs.

Sugar Cost ($/lb)	Feedstock Cost Fraction (%)	Break Even Price ($/gallon)
0.20	87.8	4.06
0.18	87.1	3.81
0.16	86.4	3.56
0.14	85.5	3.31
0.12	84.6	3.05
0.10	83.5	2.80
0.08	82.2	2.55
0.06	80.8	2.30
0.04	79.1	2.04

continuous fermentation process, the energy inputs consist of the energy content of the substrate, assumed to be that of monosaccharide sugars in general equivalent to 0.017 MJ/g [FAO, 2003] multiplied with the daily total mass inflow of substrate as calculated in earlier in this chapter. The required aeration rate (in SCFM or standard cubic feet per minute) for respiration and mixing, blower pressure, and the estimated energy input based on the daily BOD_5 loading, water depth, and typical blower efficiency (0.12) were calculated as follows [Tchobanoglous, et al., 2003; Hoffland Environmental Inc., 2010]:

$$\begin{aligned}\text{Aeration rate} &= \left(681\times10^3 \text{ lb BOD}_5/\text{d}\right)\left[1.25 \text{ SCFM}/\left(\text{lb BOD}_5 \text{ d}\right)\right] \\ &= 8.5\times10^5 \text{ SCFM}\end{aligned} \tag{11.7}$$

$$\begin{aligned}\text{Blower Pressure} &= \text{water depth } (\text{ft}) \times 0.43 \text{ psi/ft} + 2 \text{ psi line loss} \\ &= (15 \text{ ft})(0.43 \text{ psi/ft}) + 2 \text{ psi} \\ &= 8.45 \text{ psig}\end{aligned} \tag{11.8}$$

$$\begin{aligned}
&\text{Motor Power Rating (hp)} \\
&= \frac{\text{Aeration rate (SCFM)} \times \text{Blower Pressure (psig)} \times 0.00076}{\text{Blower Efficiency}} \\
&= \frac{\left(8.5\times10^{5}\ \text{SCFM}\right)\left(8.5\ \text{psig}\right)\left(0.00076\right)}{0.12} \\
&= 4.6\times10^{4}\ \text{hp} \\
&= 2.9\times10^{6}\ \text{MJ/d}
\end{aligned} \tag{11.9}$$

Based on the experimental results, it was found that oleic acid was primarily the most dominant fatty acid in the total lipid extracts and biodiesel from activated sludge. Therefore, the energy content of the product lipids and biodiesel were estimated based on the literature values of the heat of combustion for triolein (8389 kcal/mol or 39.6 MJ/g) and oleic acid methyl ester (2828 kcal/mol or 39.9 MJ/g), respectively [Knothe, 2005]. While automotive or transportation applications may not be readily accepted due to the sewage undertones, biodiesel produced via *in situ* transesterification of the enhanced activated sludge biomass containing the said lipids with the calculated energy contents can then be utilized by diesel-powered generators for electricity generation to drive energy-intensive water and wastewater treatment processes. The activated sludge process in itself requires large amounts of energy, estimated on average to be between 1000 and 2400 MJ of electricity to process each 1000 m^3 of wastewater, majority of which (≈ 56 %) is applied for activated sludge aeration [Tchobanoglous, et al., 2003]. Tertiary treatment processes such as UV disinfection (190 MJ/1000 m^3), reverse osmosis (1900 MJ/1000 m^3), and ozonation (302 MJ/1000 m^3) [Tchobanoglous, et al., 2003] were also considered as possible users of the electric power generated from the combustion of activated sludge biodiesel due to their high calculated energy requirements based on the

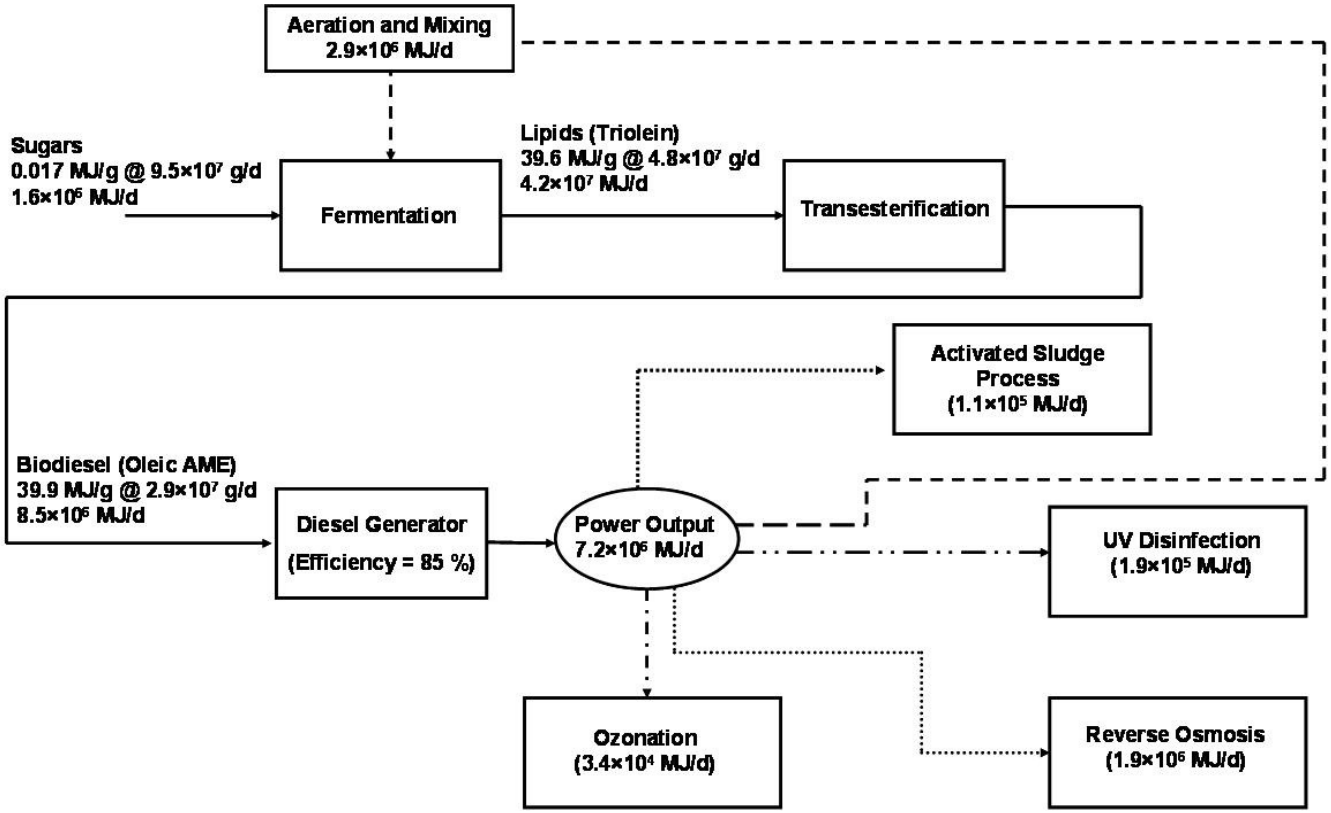

Figure 11.2: Energetic analysis of enhanced lipid accumulation by activated sludge and potential applications for energy-intensive water and wastewater treatment processes.

assumed total daily treatment capacity of 30 MGD (million gallons per day) as shown in Fig. 11.2. Assuming a generator efficiency of 85 %, the electric power output using the activated sludge biodiesel as fuel was calculated as 7.2×10^6 MJ/d, which may be able to provide electrical energy to drive any of the wastewater treatment processes considered, as well as the aeration requirements for the fermentative activated sludge lipid accumulation process. These findings show that a self-sustaining wastewater treatment facility able to generate its own fuel and electricity for the performance of various water and wastewater treatment processes could be realized by applying the fermentation process investigated in this study.

Conclusion

The engineering calculations and analyses of the proposed enhanced lipid accumulation process by activated sludge via fermentation of lignocellulose sugars presented in this chapter show that it has a high potential for producing biofuel feedstock lipids for biodiesel production. Biodiesel production costs and its break even price can be further minimized by increasing the total lipid yield coefficient or the conversion of substrate (sugars) to lipids, which can be accomplished through further experiments and optimization studies of the continuous fermentation process or by reducing the price of sugar substrate used for the fermentation process. Energetic analysis of the combined lipid accumulation and *in situ* transesterification process showed that the activated sludge-derived biodiesel can be used for electric power generation to drive energy-intensive water and wastewater treatment processes such as aeration, UV disinfection, reverse osmosis, or ozonation; hence it could lead to a self-sustaining and energy-

independent wastewater treatment facility. This could lead to reduced treatment costs in publicly-owned treatment works often shouldered by the general public and to a better effluent water quality for environmental discharge and subsequent domestic usage.

CHAPTER XII

OVERALL CONCLUSIONS AND RECOMMENDATIONS

Conclusions

Based on the results obtained in this research, the proposed aerobic cultivation process of municipal sewage activated sludge using lignocellulose sugars as carbon source improved the applicability, quality, and economic competitiveness of activated sludge as a source of feedstock lipids for the production of biofuels such as biodiesel and renewable diesel. This process could then be conducted in an industrial scale using existing wastewater treatment plant infrastructure, specifically conventional activated sludge aeration basins, which serve as bioreactors for the growth of municipal wastewater microorganisms resulting from the degradation of the organic content of the wastewater influent stream. The observed lipid contents, fatty acid profiles, and saponifiable lipid fraction corresponding to the total FAME or biodiesel yield of the "enhanced" activated sludge biomass showed significant improvements compared to those of raw activated sludge. The specific conclusions are summarized as follows:

- Preliminary testing using different initial glucose levels (20 – 60 g/L) and C:N ratios (10:1 – 70:1) in batch fermentation experiments indicated that the activated sludge microbial communities exhibited oleaginicity; hence the ability to increase its overall intracellular lipid content when cultivated in a

high initial glucose loading (60 g/L) and carbon-to-nitrogen ration (C:N) of 70:1. An increase in the initial C:N ratio from 10:1 to 70:1 led to a decreased total biomass yield and increased lipid and biodiesel yields. At a constant C:N ratio 70:1, initial glucose loadings greater than 20 g/L showed improved lipid and biodiesel yields as well as greater total biomass production. The maximum gravimetric lipid yield of 17 % (CDW) with a corresponding biodiesel yield of 10 % (CDW) was obtained at these conditions compared with the other treatments. These values are significantly higher than those obtained in raw activated sludge (10 % CDW total lipids, 2.8 % CDW biodiesel yield). Analysis of the fermentation kinetics showed that the maximum specific growth rates based on non lipid biomass production were lower at the optimum conditions for lipid accumulation (high C:N ratio, high glucose loading) as opposed to the conditions favored for biomass production (low C:N ratio, high glucose loading). The resulting fatty acid profiles indicated that lipids derived from activated sludge grown aerobically in glucose-containing synthetic wastewater medium consisting mainly of C_{16} and C_{18} fatty acids is suitable for the production of biodiesel with improved properties.

- The presence of furfural at relatively low levels (0.5 – 1.5 g/L), a lignocellulose degradation by-product and a known inhibitor compound in microbial fermentation processes, in batch cultures caused significant inhibition of cell growth, lipid accumulation, and glucose uptake by activated

sludge microorganisms. Biomass and lipid production were likewise reduced under a low acetic acid loading (2 g/L) while a higher biomass and lower lipid productivities were obtained under a high initial acetic acid/acetate loading (10 g/L) compared with a control run using containing glucose and no inhibitors. Binary mixtures of acetic acid and furfural exhibited an additive effect on the fermentation profiles of activated sludge in glucose resembling a stepwise detoxification of furfural and then followed by acetic acid/acetate. Biomass production and glucose uptake were inhibited initially as long as furfural was still present in the culture, after which biomass growth increased significantly when acetic acid/acetate remained in the culture. However, lipid accumulation was likewise due to the effect of the residual acetic acid in the culture. Similar with fermentation runs with no inhibitors and glucose as sole carbon source, biodiesel (FAME) yields from the total extracts obtained from batch cultures containing furfural and/or acetic acid were consistent at 50 - 60 % (w/w total extracts) while oleic acid was found to be the most dominant fatty acid residue in the lipids extracts.

- Pentose sugars such as xylose could be utilized by activated sludge microorganisms for biomass growth and enhancement of lipid content for improved biodiesel yields. As sole carbon sources, fermentation of glucose and xylose produced comparable biomass yields but the maximum total biomass lipid content (21.5 % CDW) was obtained using pure xylose. When glucose/xylose mixtures were used as substrate, the glucose-dominant mixture

(2:1 glucose:xylose) produced both higher total and saponifiable lipid yields compared with the xylose dominant mixture (1:2 glucose:xylose) but lower than when pure glucose and xylose were used. Overall, the use of glucose in activated sludge fermentations still resulted in the highest saponifiable lipid fraction and subsequently, the biodiesel yield. The resulting fatty acid distribution using all sugar combinations were found to be similar and suitable for biodiesel application due to the dominance of C_{16} and C_{18} fatty acids. The enhanced proportion of unsaturated fatty acids (mainly oleic acid) relative to the saturated fatty acids (mainly palmitic acid) contributes to improved biodiesel properties similar to the target oil composition used as biodiesel feedstock mentioned in literature. Furthermore, the biomass and lipid yield coefficients with xylose as sole carbon source or mixed with glucose were higher than pure glucose, indicating that xylose is likely more efficiently utilized by the activated sludge microorganisms for biomass and lipid production.

- In testing different fermentation strategies to reduce the inhibitory effect of acetic acid and furfural in a model lignocellulose hydrolyzate, the results showed that biomass yields were highest but lipid production was severely limited in single stage batch culture. Semicontinuous fermentation with an initial batch glucose startup culture resulted in the highest attained lipid content (25.3 % CDW), lipid concentration (2.81 g/L), lipid coefficient (0.03 g/g), and saponifiable lipid yield (12 % CDW), due to the constant feeding of

the hydrolyzate at low rates resulting in low inhibitor and substrate concentrations, after which these levels eventually decreased. In the case of the continuous culture, the operating dilution rate was found to be above the critical values, thus washout of the culture occurred and steady state of the biomass, substrate, and product levels was not obtained. Therefore, in the performance of semicontinuous and continuous cultures, feed solutions for lipid accumulation must be formulated with nutrients (in addition to the carbon source) to sustain a viable microbial cell concentration that could continuously accumulate lipids.

- Analysis of the composition of activated sludge microbial communities via 16S rRNA sequence analysis indicated that cultivation of activated sludge in glucose-fed aerobic batch cultures resulted in a significant reduction in the microbial diversity of the activated sludge microflora. On average, the raw activated sludge microbiota consisted mainly of 58.4 % *Proteobacteria* and 26.6 % *Bacteriodetes* groups. Following cultivation for seven days under low (10:1) and medium (40:1) C:N ratios, the *Firmicutes* group became the dominant group (65 %), whereas at a high C:N ratio (70:1), the activated sludge microbiota almost consisted entirely of the *Proteobacteria* group (96-99 %). This could indicate that specific microbial strains belonging to the *Proteobacteria* proliferated at high C:N ratios and could include potential lipid producers within the group as evident in the observed increase in the

cellular lipid contents of activated sludge biomass grown in bioreactors operating at C:N ratio 70:1.

- According to the engineering and economic analyses, the production of activated sludge biomass with enhanced lipid contents via fermentation of sugars could lead to increased biodiesel production from sludge with a slightly higher break even price ($4.06/gal) than that obtain in a previous study from raw sewage sludge ($3.23/gal) at a sugar substrate cost of $0.20/lb. The biodiesel price could be lowered by reducing the production cost associated with the sugar substrate, which could be accomplished by improvements in lignocellulose processing conditions.

Recommendations

Further studies on this research topic are recommended in order to optimize process conditions and economics, specifically on the following aspects:

- Evaluation of the use of lignocellulose hydrolyzate of actual biomass materials as substrates for the fermentation experiments;
- Testing of domestic wastewater or other industrial wastewaters obtained from as cultivation media. Other wastewater streams such as those from food processing plants, pulp and paper industries, and animal farms contain large amounts of carbonaceous organic matter and nutrients such that these could be used as a stand-alone media requiring neither sugar or nutrient supplementation;

- Extended continuous fermentation trials with nutrient supplementation (in addition to the carbon source) in addition to the carbon source designed to simulate an actual wastewater plant aeration process;
- Microbial community analysis expanded to eukaryotes (yeasts, molds, algae) in addition to the bacterial population conducted in this study to determine the variation of their relative abundances in the activated sludge cultivated under different C:N ratios or substrate loading; and
- Comprehensive chemical analysis of the enhanced sludge biomass and lipids to determine its full composition in terms of high value chemicals such as triacylglycerols, polyhydroxyalakanoates, extracellular polysaccharides, and similar materials. This could potentially increase the value of enhanced activated sludge biomass by fully utilizing the unsaponifiable fractions (those that were not converted to biodiesel) as well as the spent biosolids after lipid extraction or *in situ* transesterification.

BIBLIOGRAPHY

Agbogbo, F.K., Wagner, K.S. 2007. "Production of ethanol from corn stover hemicellulose hydrolyzate using *Pichia stipitis*." *Journal of Industrial Microbiology and Biotechnology,* 34, 723-727.

Alvarez, H.M., Mayer, F., Fabritius, D., Steinbuchel, A. 1996. "Formation of intracytoplasmic lipid inclusions by *Rhodococcus opacus* strain PD630." *Archives of Microbiology,* 165, 377-386.

Alvarez, H.M., Kalscheuer, R., Steinbuchel, A. 2000. "Accumulation and mobilization of storage lipids by *Rhodococcus opacus* PD630 and *Rhodococcus ruber* NCIMB 40126." *Applied Microbiology and Biotechnology,* 54, 218-223.

Alvarez, H.M., Steinbuchel, A. 2002. "Triacylglycerols in prokaryotic microorganisms." *Applied Microbiology and Biotechnology,* 60, 367-376.

Amartey, S., Jeffries, T. 1996. "An improvement in *Pichia stipitis* fermentation of acid-hydrolyzed hemicellulose achieved by overliming (calcium hydroxide treatment) and strain adaptation." *World Journal of Microbiology and Biotechnology,* 12, 281-283.

American Soybean Association 2009. "Soy stats." Online posting. Last Accessed 19 October 2010: http://www.soystats.com/2009/Default-frames.htm.

Anderson, A.J., Dawes, E.A. 1990. "Occurrrence, metabolism, metabolic role, and industrial uses of bacterial polyhydroxylakanoates." *Microbiological Reviews,* 54, 450-472.

Angerbauer, C., Siebehofer, M., Mittelbach, M., Guebitz, G.M. 2008. "Conversion of sewage sludge into lipids by *Lipomyces starkeyi* for biodiesel production." *Bioresource Technology,* 99, 3051-3056.

American Oil Chemists Society 2010. "The Lipid Library." Online posting. Last Accessed 18 August 2010: http://lipidlibrary.aocs.org/index.html.

APHA, AWWA, WEF 1998. *Standard Methods for the Examination of Water and Wastewater 20th Ed.,* American Public Health Association, Washington, D.C.

Arnold, C.N., McElhanon, J., Lee, A., Leonhart, R., Siegele, D.A. 2001. "Global analysis of *Escherichia coli* gene expression during acetate-induced acid tolerance response." *Journal of Bacteriology,* 183, 2178-2186.

American Type Culture Collection 2002. "Trace mineral supplement formulation." Online posting. Last Accessed 7 September 2010: http://www.atcc.org/Portals/1/Pdf/MD_TMS.pdf.

Banerjee, N., Bhatnagar, R., Viswanathan, L. 1981. "Inhibition of glycolysis by furfural in *Saccharomyces cerevisiae.*" *European Journal of Applied Microbiology and Biotechnology,* 11, 224-228.

Bengtsson, S., Werker, A., Christensson, M., Welander, T. 2008. "Production of polyhydroxyalkanoates by activated sludge treating a paper mill wastewater." *Bioresource Technology,* 99, 509-516.

Biomass Research and Development Board 2008. "National Biofuels Action Plan" Online posting. Last Accessed 15 August 2010: http://www1.eere.energy.gov/biomass/pdfs/nbap.pdf.

Bligh, E.G., Dyer, W.J. 1959. "A rapid method for total lipid extraction and purification." *Canadian Journal of Biochemistry and Physiology,* 37, 911-917.

Boocock, D.G.B., Konar, S.K., Leung, A., Ly, L.D. 1992. "Fuels and chemicals from sewage sludge 1. The solvent extraction and composition of a lipid from a raw sewage sludge." *Fuel,* 71, 1283-1289.

Boocock, D.G.B., Konar, S.K., Mackay, A., Cheung, P.T.C., Liu, J. 1992. "Fuels and chemicals from sewage sludge 2. The production of alkanes and alkenes by the pyrolysis of triglycerides over activated alumina." *Fuel,* 71, 1291-1297.

Boyer, L., Vega, J., Klasson, K., Clausen, E., Gaddy, J. 1992. "The effects of furfural on ethanol production by *Saccharomyces cerevisiae* in batch culture." *Biomass and Bioenergy,* 3, 41-48.

Boyer, L.J., Vega, K., Klasson, K.T., Clausen, E.C., Gaddy, J.L. 1992. "The effects of furfural on ethanol production by *Saccharomyces cerevisiae.*" *Biomass Bioengineering,* 3, 41-48.

Brandberg, T., Karimi, K., Taherzadeh, M.J., Franzen, C.J., Gustafsson, L. 2007. "Continuous fermentation of wheat-supplemented lignocellulose hydrolyzate with different types of cell retention." *Biotechnology and Bioengineering,* 98, 80-90.

Brennan, P.J. 1988. "Mycobacterium and other actinomycetes." *Microbial Lipids, vol. 1,* Academic Press, London, 203-298.

Bringe, N.A. 2005. "Soybean oil composition for biodiesel." *The Biodiesel Handbook,* AOCS Press, Champaign, IL, 161-164.

Carvalho, W., Batista, M.A., Canilha, L., Santos, J.C., Converti, A., Silva, S.S. 2004. "Sugarcane bagasse hydrolysis with phosphoric and sulfuric acids and hydrolysate detoxification for xylitol production." *Journal of Chemical Technology and Biotechnology,* 79, 1308-1312.

Carvalho, W., Batista, M.A., Canilha, L., Santos, J.C., Coverti, A., Silva, S.S. 2004. "Sugarcane bagasse hydrolysis with phosphoric and sulfuric acids and hydrolysate detoxification for xylitol production." *Journal of Chemical Technology and Biotechnology,* 79, 1308-1312.

Celenza, G.J. 2000. *Industrial Waste Treatment Process Engineering: Biological Processes, Vol.II.,* Technomic Publishing Co., Inc., Lancaster, PA.

Center for American Progress 2006. "America is addicted to oil." Online posting. Last Accessed 13 July 2010: http://www.americanprogress.org/issues/2006/02/b1408771.html.

Chen, X., Li, Z., Zhang, X., Hu, F., Ryu, D.D.Y., Bao, J. 2009. "Screening of oleaginous yeast strains tolerant to lignocellulose degradation compounds." *Applied Biochemistry and Biotechnology,* 159, 591-604.

Chipasa, K.B., Medrzycka, K. 2000. "Adaptive response of microbial communities to soluble microbial products." *Journal of Industrial Microbiology and Biotechnology,* 31, 384-390.

Choi, S.Y., Ryu, D.D.W., Rhee, J.S. 1982. "Production of microbial lipid: effects of growth rate and oxygen on lipid synthesis and fatty acid composition of *Rhodotorula gracilis.*" *Biotechnology and Bioengineering,* 24, 1165-1172.

Christie, W.W. 2003. *Lipid analysis: Isolation, separation, identification, and structural analysis of lipids,* The Oily Press, Bridgewater, England.

Chum, H.L., Johnson, D.K., Black, S.K., Overend, R.P. 1990. "Pretreatment-catalyst effects and the combined severity parameter." *Applied Biochemistry and Biotechnology,* 24/25, 1-14.

Chung, I., Lee, Y. 1985. "Ethanol fermentation of crude acid hydrolyzate of cellulose using high-level yeast inocula." *Biotechnology and Bioengineering,* 27, 308-315.

Chung, I.S., Lee, Y.Y. 1985. "Ethanol fermentation of crude acid hydrolyzate of cellulose using high-level yeast inocula." *Biotechnology and Bioengineering,* 27, 308-315.

Claassen, P.A.M., van Lier, J.B., Lopez Contreras, A.M., van Niel, E.W.J., Sijtsma, L., Stams, A.J.M., de Vries, S.S., Weusthuis, R.A. 1999. "Utilisation of biomass for the supply of energy carriers" *Applied Microbiology and Biotechnology,* 52, 741-755.

Clark, T., Mackie, K.L. 1984. "Fermentation inhibitors in wood hydrolyzates derived from the softwood *Pinus radiata.*" *Journal of Chemical Technology and Biotechnology,* 34, 101-110.

Cole, J.R., Wang, Q., Cardenas, E., Fish, E., Chai, B., Farris, R.J., Kulam-Syed-Mohideen, A.S., McGarrell, D.M., Marsh, T., Garrity, G.M., Tiedje, J.M. 2008. "The Ribomosomal Database Project: improved alignments and new tools for rRNA analysis" *Nucleic Acids Research,* 37, D141-D145.

Converti, A., Perego, P., Torre, P., da Silva, S.S. 2000. "Mixed inhibitions by methanol, furfural, and acetic acid on xylitol production by *Candida guilliermondii.*" *Biotechnology Letters,* 22, 1861-1865.

Dai, C., Tao, J., Xie, F., Dai, Y., Zhao, M. 2007. "Biodiesel generation from oleaginous yeast *Rhodotorula glutinis* with xylose assimilating capacity." *African Journal of Biotechnology,* 6, 2130-2134.

Davies, R.J. 1988. "Yeast oil from cheese whey-process development." *Single Cell Oil,* Longmans, London, 99-145.

Davies, R.J., Holdsworth, J.E., Reader, S.L. 1990. "The effect of low oxygen uptake on the fatty acid profile of the oleaginous yeast *Apiotrichum curvatum.*" *Applied Microbiology and Biotechnology,* 33, 569-573.

Davies, R.J., Holdsworth, J.E. 1992. "Synthesis of lipids in yeasts biochemistry, physiology, production." *Advances in Applied Lipid Research,* JAI Press Ltd., Greenwich, CT, 119-159.

De Andres, C., Espuny, M.J., Robert, M., Mercade, M.E., Manresa, A., Guinea, J. 1991. "Cellular lipid accumulation by *Pseudomonas aeruginosa* 44T1." *Applied Microbiology and Biotechnology,* 35, 813-816.

Diaz de Villegas, M.E., Villa, P., Guerra, M., Rodriguez, E., Redondo, D., Martinez, A. 1992. "Conversion of furfural to furfuryl alcohol by *Saccharomyces cerevisiae* 354." *Acta Biotechnologica,* 12, 351-354.

Diaz, M.J., Ruiz, E., Romero, I., Cara, C., Moya, M., Castro, E. 2009. "Inhibition of *Pichia stipitis* fermentation of hydrolysates from olive tree cuttings." *World Journal of Microbiology and Biotechnology,* 25, 891-899.

Dionex Corp. 2008. "Application Note 141: Determination of inorganic cations and ammonium in environmental waters by ion chromatography using the CS16 IonPac column" Online posting. Last Accessed August 1, 2008: http://www.dionex.com/en-us/webdocs/4211_AN141_V15.pdf.

Dionex Corp. 2010. "Dionex Corporation - Company profilem business description, history, background information on Dionex Corporation." Online posting. Last Accessed 8 September 2010: http://www.referenceforbusiness.com/history2/41/Dionex-Corporation.html.

Don, M.M., Shoparwe, N.F. 2010. "Kinetics of hyaluronic acid production by *Streptococcus zooepidemicus* considering the effect of glucose." *Biochemical Engineering Journal,* 49, 95-103.

Dostalek, M. 1986. "Production of lipid from starch by a nitrogen-controlled mixed culture of *Saccharomyces fibuligera* and *Rhodosporidium toruloides.*" *Applied Microbiology and Biotechnology,* 24, 19-23.

Du, J., Wang, H.X., Jin, H.L., Yang, K.L., Zhang, X.Y. 2007. "Fatty acids production by fungi growing in sweet potao starch processing waste water." *Chinese Journal of Bioprocess Engineering,* 51, 33-36.

Dufreche, S., Hernandez, R., French, T., Sparks, D., Zappi, M., Alley, E. 2007. "Extraction of lipids from municipal wastewater plant microorganisms for production of biodiesel." *Journal of the American Oil Chemists Society,* 84, 181-187.

Easterling, E.R., French, W.T., Hernandez, R., Licha, M. 2009. "The effect of glycerol as a sole and secondary substrate on the growth and fatty acid composition of *Rhodotorula glutinis.*" *Bioresource Technology,* 100, 356-361.

U.S. Energy Infromation Administration 2010. "Gasoline and Diesel Fuel Update" Online posting. Last Accessed 19 October 2010: http://www.eia.doe.gov/oog/info/gdu/gasdiesel.asp.

Enebo, L., Iwamoto, H. 1966. "Effects of cultivation temperature on fatty acid composition in *Rhodotorulla gracilis.*" *Acta Chemica Scandinavia,* 20, 439-443.

Eschenhagen, M., Schuppler, M., Roske, I. 2003. "Molecular characterization of the microbial community structure in two activated sludge systems for the advanced treatment of domestic effluents." *Water Research,* 37, 3224-3232.

Evans, C.T., Ratledge, C. 1983. "A comparison of the oleaginous yeast, *Candida curvata*, grown on different carbon sources in continuous and batch culture." *Lipids,* 18, 623-629.

Evans, C.T., Ratledge, C. 1984. "Effect of nitrogen source on lipid accumulation in oleaginous yeasts." *Journal of General Microbiology,* 130, 1693-1704.

Fakas, S., Papanikolaou, S., Batsos, A., Galiotou-Panayatou, M., Mallouchos, A., Aggelis, G. 2009. "Evaluating renewable carbon sources as substrates for single cell oil production by *Cunninghamella echinulata* and *Mortierella isabellina.*" *Biomass and Bioenergy,* 33, 573-580.

Food and Agricultural Organization 2003. "Food energy - methods of analysis and conversion factors." Online posting. Last Accessed 18 October 2010: http://www.fao.org/docrep/006/y5022e/y5022e04.htm.

Felipe, M., Alves, L., Silva, S., Roberto, I., Mancilha, I., Almeida e Silva, J. 1996. "Fermentation of eucalyptus hemicellulosic hydrolysate to xylitol by *Candida guiliermondii.*" *Bioresource Technology,* 56, 281-283.

Fengel, D., Wegener, G. 1984. *Wood: Chemistry, Ultrastructure, Reactions.,* Walter de Gruyter & Co., Berlin.

Ferrante, G., Kates, M. 1986. "Characteristics of the oleoyl- and linoleoyl-CoA desaturase and hydroxylase systems in cell fractions from soybean cell suspension cultures." *Biochimica et Biophysica Acta,* 876, 429-437.

Ferrari, R.A., Oliveira, V., Scabio, A. 2005. "Oxidative stability of biodiesel from soybean oil fatty acid ethyl esters." *Scientia Agricola,* 62, 291-295.

Fogler, H.S. 2006. *Elements of Chemical Reaction Engineering, 4th ed.,* Pearson Education, Inc., Upper Saddle River, NJ.

Foidl, N., Foidl, G., Sanchez, M., Mittlebach, M., Hackel, S. 1996. "*Jatropha curcas* L. as a source for the production of biofuel in Nicaragua." *Bioresource Technology,* 58, 77-82.

Freedman, B., Butterfield, R.O., Pryde, E.H. 1986. "Transesterification kinetics of soybean oil." *Journal of the American Oil Chemists Society,* 63, 1375-1380.

Galbe, M., Zacchi, G. 2002. "A review of the production of ethanol from softwood." *Applied Microbiology and Biotechnology,* 59, 618-628.

Ghose, T.K., Tyagi, R.D. 1979. "Rapid ethanol fermentation of cellulose hydrolyzate I. Batch versus continuous systems." *Biotechnology and Bioengineering,* 21, 1387-1400.

Ghosh, S., LaPara, T.M. 2004. "Removal of carbonaceous and nitrogenous pollutants from a synthetic wastewater using a membrane-coupled bioreactor." *Journal of Industrial Microbiology and Biotechnology,* 31, 353-361.

Gill, C.O., Hall, M.J., Ratledge, C. 1977. "Lipid accumulation in an oleaginous yeast (*Candida* 107) growing on glucose in single-stage continuous culture." *Applied and Environmental Microbiology,* 33, 231-239.

Goodson, M., Rowbury, R.J. 1989. "Habituation to normally lethal acidity by prior growth of *Escherichia coli* at a sub-lethal acid pH value." *Letters in Applied Microbiology,* 8, 77-79.

Gorsich, S.W., Dien, B.S., NIchols, N.N., Slininger, P.J., Liu, Z.L., Skory, C.D. 2006. "Tolerance to furfural-induced stress is associated with pentose phosphate pathway genes ZWF1, GND1, RPE1, and TKL1 in *Saccharomyces cerevisiae.*" *Applied Microbiology and Biotechnology,* 71, 339-349.

Gottschalk, G. 1987. "Control of product formation in anaerobes." *Dechema-Monographs,* 105, 43-53.

Gouveia, L., Oliveira, A.C. 2009. "Microalgae as a raw material for biofuels production." *Journal of Industrial Microbiology and Biotechnology,* 36, 269-274.

Guerzoni, M.E., Lambertini, P., Lercker, G., Marchetti, R. 1985. "Technological potential of some starch degrading yeasts." *Starch,* 37, 52-57.

Haas, M.J., Foglia, T.A. 2005. "Alternate feedstocks and technologies for biodiesel production" *The Biodiesel Handbook,* AOCS Press, Champaign, IL, 42-61.

Haddad, P.R., Jackson, P.E. 1990. *Ion Chromatography: Principles and Applications,* Elsevier, Burlington, MA.

Hadi, S.M., Shahabuddin, R.A. 1989. "Specificity of the interaction of furfural with DNA." *Mutation Research,* 225, 101-106.

Hahn-Hagerdal, B., Karhumaa, K., Fonseca, C., Spencer-Martins, I., Gorwa-Grauslund, M.F. 2007. "Towards industrial pentose-fermenting yeast strains." *Applied Microbiology and Biotechnology,* 74, 937-953.

Hall, M.J., Ratledge, C. 1977. "Lipid accumulation in an oleaginous yeast (*Candida* 107) growing on glucose under various conditions in a one- and two-stage continuous culture." *Applied and Environmental Microbiology,* 33, 577-584.

Hoffland Environmental Inc. 2010. "Design Worksheet for Activated Sludge Bio-Treatment Systems." Online posting. Last Accessed 19 October 2010: http://www.hoffland.net/img/bio_systems.doc.

Holdsworth, J.E., Ratledge, C. 1988. "Lipid turnover in oleaginous yeasts." *Journal of General Microbiology,* 134, 339-346.

Horvath, I.S., Franzen, C.J., Taherzadeh, M.J., Niklasson, C., Liden, G. 2003. "Effects of furfural on the respiratory metabolism of *Saccharomyces cerevisiae* in glucose-limited chemostats." *Applied and Environmental Microbiology,* 69, 4076-4086.

Hu, C., Zhao, X., Zhao, J., Wu, S., Zhao, Z.K. 2009. "Effects of biomass hydolysis by-products on oleaginous yeast *Rhodosporidium toruloides.*" *Bioresource Technology,* 100, 4843-4847.

Hu, Q., Sommerfeld, M., Jarvis, E., Ghirardi, M., Posewitz, M., Seibert, M., Darzins, A. 2008. "Microalgal triacylglycerols as feedstocks for biofuel production: perspectives and advances." *The Plant Journal,* 54, 621-639.

Huang, C., Zong, M.-h., Wu, H., Liu, Q.-p. 2009. "Microbial oil production from rice straw hydrolysate by *Trichosporon fermentans.*" *Bioresource Technology,* 100, 4535-4538.

Illman, A.M., Scragg, A.H., Shales, S.W. 2000. "Increase in *Chlorella* strains calorific values when grown in low nitrogen medium." *Enzyme and Microbial Technology,* 27, 631-635.

International Monetary Fund 2010. "IMF Primary Commodity Prices." Online posting. Last Accessed 17 October 2010: http://www.imf.org/external/np/res/commod/index.asp.

International Monetary Fund 2010. "IMF Primary Commodity Prices" Online posting. Last Accessed 17 October 2010: http://www.imf.org/external/np/res/commod/index.asp.

Ingram, M. 1959. "Comparison of different media for counting sugar tolerant yeasts in concentrated orange juice." *Journal of Applied Microbiology,* 22, 234-247.

Jarde, E., Mansuy, L., Faure, P. 2005. "Organic markers in the lipidic fraction of sewage sludges." *Water Research,* 39, 1215-1232.

Jensen, J., Morinelly, J., Aglan, A., Mix, A., Shonnard, D.R. 2008. "Kinetic characteristic of biomass dilute sulfuric acid hydrolysis: mixtures of hardwoods, softwood, and switchgrass." *AIChE Journal,* 54, 1637-1645.

Jonsson, L.J., Palmqvist, E., Nilvebrant, N.O., Hahn-Hagerdal, B. 1998. "Detoxification of wood hydrolyzates with laccase and peroxidase from the white-rot fungus *Trametes versicolor.*" *Applied and Environmental Microbiology,* 46, 691-697.

Juang, D.F., Chiou, L.J. 2007. "Microbial population structures in activated sludge before and after the application of synthetic polymer." *International Journal of Environmental Science and Technology,* 4, 119-125.

Kadam, K.L., McMillan, J.D. 2003. "Availability of corn stover as a sustainable feedstock for bioethanol production." *Bioresource Technology,* 88,

Kalscheuer, R., Stolting, T., Steinbuchel, A. 2006. "Microdiesel: *Escherichia coli* engineered for fuel production." *Microbiology,* 25, 187-191.

Karanth, N.G., Sattur, A.P. 1991. "Mathematical modeling of production of microbial lipids Part II: Kinetics of lipid accumulation." *Bioprocess Engineering,* 6, 241-248.

Kargbo, D.M. 2010. "Biodiesel production from municipal sewage sludges." *Energy & Fuels,* 24, 2791-2794.

Karp, G. 2008. *Cell and Molecular Biology Concepts and Experiments 5th ed.,* John Wiley & Sons, Inc., New York.

Keating, J.D., Panganiban, C., Mansfield, S.D. 2006. "Tolerance and adaptation of ethanologenic yeasts to lignocellulose inhibitory compounds." *Biotechnology and Bioengineering,* 93, 1196-1206.

Kessell, R.H.J. 1968. "Fatty acids of *Rhodotorulla gracilis:* Fat production in submerged culture and the particular effect of pH value." *Journal of Applied Bacteriology,* 31, 220-231.

Khan, Q.A., Hadi, S.M. 1994. "Inactivation and repair of bacteriophage lamba by furfural." *Biochemistry and Molecular Biology Internationl,* 32, 379-385.

Klimek, J., Ollis, D.F. 1980. "Extracellular microbial polysaccharides: Kinetics of *Pseudomonas* sp., *Azotobacter vinelandii,* and *Aureobasidium pullulans* batch fermentations" *Biotechnology and Bioengineering,* 22, 2321-2342.

Knothe, G. 2005. "Introduction: What is Biodiesel?" *The Biodiesel Handbook,* AOCS Press, Champaign, IL, 1-3.

Knothe, G. 2005. "Fuel Properties: Cetane numbers-heat of combustion-why vegetable oils and their derivatives are suitable as a diesel fuel." *The Biodiesel Handbook,* AOCS Press, Champaign, IL, 76-80.

Konar, S.K., Boocock, D.G.B., Mao, V., Liu, J. 1994. "Fuels and chemicals from sewage sludge: 3. Hydrocarbon liquids from the catalytic pyrolysis of sewage sludge lipids over activated alumina." *Fuel,* 73, 642-645.

Kong, X.L., Liu, B., Zhao, Z.B., Feng, B. 2007. "Microbial production of lipids by cofermentation of glucose and xylose with *Lipomyces starkeyi* 2#." *Chinese Journal of Bioprocess Engineering,* 5, 36-41.

Kulkarni, M.G., Dalai, A.K. 2006. "Waste cooking oil - an economic source for biodiesel: a review." *Industrial and Engineering Chemistry Research,* 45, 2901-2913.

Lal, R. 2004. "World crop residues production and implications of its use as biofuels." *Environment International,* 31, 575-584.

Larsson, S., Palmqvist, E., Hahn-Hagerdal, B., Tengborg, C., Stenberg, K., Zacchi, G., Nilvebrant, N.O. 1998. "The generation of fermentation inhibitors during dilute acid hydrolysis of softwood." *Enzyme and Microbial Technology,* 24, 151-159.

Lee, K.T., Foglia, T.A., Chang, K.S. 2002. "Production of alkyl esters as biodiesel fuel from fractionated lard and restaurant grease." *Journal of the American Oil Chemists Society,* 79, 191-195.

Leonard, R.H., Hajny, G.J. 1945. "Fermentation of wood sugars to ethanol." *Industrial and Engineering Chemistry Research,* 37, 390-395.

Li, Q., Wang, M.Y. 1997. "Use food industry waste to produce microbial oil." *Science and Technology of Food Industry,* 6, 65-69.

Li, Q., Du, W., Liu, D. 2008. "Perspectives of microbial oils for biodiesel production." *Applied Microbiology and Biotechnology,* 80, 749-756.

Li, Y., Liu, B., Sun, Y., Zhao, Z.H., Bai, F.W. 2005. "Screening of oleaginous yeasts for broad-spectrum carbohydrates assimilating capacity." *China Biotechnology,* 25, 39-44.

Li, Y.H., Zhao, Z.B., Bai, F.W. 2007. "High-density cultivation of oleaginous yeast *Rhodosporidium toruloides* Y4 in fed-batch culture." *Enzyme and Microbial Technology,* 41, 312-317.

Liden, G., Jacobsson, V., Niklasson, C. 1993. "The effect of carbon dioxide on xylose fermentation by *Pichia stipitis.*" *Applied Biochemistry and Biotechnology,* 38, 27-40.

Lin, J., Lee, I.S., Frey, J., Slonczewski, J.L., Foster, J.W. 1995. "Comparative analysis of extreme acid survival in *Salmonella typhimurium, Shigella flexneri,* and *Escherichia coli.*" *Journal of Bacteriology,* 177, 4097-4104.

Liu, B., Zhao, Z. 2007. "Biodiesel production by direct methanolysis of oleaginous microbial biomass." *Journal of Chemical Technology and Biotechnology,* 82, 775-780.

Liu, S.J., Yang, W.B., Shi, A.H. 2000. "Screening of the high lipid production strains and studies on its flask culture conditions." *Microbiology,* 27, 93-97.

Liu, Z.L., Slininger, P.J., Dien, B.S., Berhow, M.A., Kurtzman, C.P., Gorsich, S.W. 2004. "Adaptive response of yeasts to furfural and 5-hydroxymethylfurfural and new chemical evidence of HMF conversion to 2,5-bis-hydroxymethylfuran." *Journal of Industrial Microbiology and Biotechnology,* 31, 345-352.

Losel, D.M. 1988. "Fungal lipids." *Microbial Lipids, Vol. 1,* Academic Press, London, 699-806.

Lu, X.B., Zhang, Y.M., Yang, J., Liang, Y. 2007. "Enzymatic hydrolysis of corn stover after pretreatment with dilute sulfuric acid." *Chemical Engineering Technology,* 30, 938-944.

Ma, Z., Gong, S., Richard, H., Tucker, D.L., Conway, T., Foster, J.W. 2003. "GadE (YHiE) activates glutamate decarboxylase-dependent acid resistance in *Escherichia coli* K-12." *Molecular Microbiology,* 49, 1309-1320.

Mainul, H., Philippe, J.B., Louis, M.G., Alain, P. 1996. "Influence of nitrogen and iron limitations on lipid production by *Cryptococcus curvatus* grown in batch and fed-batch culture." *Process Biochemistry,* 31, 355-361.

Makula, R.A., Lockwood, P.J., Finnerty, W.R. 1975. "Comparative analysis of lipids of *Acinetobacter* species grown on hexadecane." *Journal of Bacteriology,* 121, 250-258.

Martin, C., Marcet, M., Almazan, O., Jonsson, L.J. 2007. "Adaptation of a recombinant xylose-utilizing *Saccharomyces cerevisiae* strain to a sugarcane bagasses hydrolyzate with high content of fermentation inhibitors." *Bioresource Technology,* 98, 1767-1773.

McNair, H.M., Miller, J., M. 1998. *Basic Gas Chromatography,* John Wiley & Sons, Inc., New York.

Meesters, P., Huijberts, G., Eggink, G. 1996. "High cell density cultivation of the lipid accumulating yeast *Cryptococcus curvatus* using glycerol as a carbon source." *Applied Microbiology and Biotechnology,* 45, 575-579.

Mehandjiyska, L. 1995. "Microbiological analysis of activated sludge in municipal wastewater treatment plant at 'kremikovtzi' holding." *Journal of Culture Collections,* 1, 18-22.

Meng, X., Yang, J., Xu, X., Zhang, L., Nie, Q., Xian, M. 2009. "Biodiesel production from oleaginous microorganisms." *Renewable Energy,* 34, 1-5.

Michalski, R. 2006. "Ion chromatography as a reference method for determination of inorganic ions in water and wastewater." *Critical Reviews in Analytical Chemistry,* 36, 107-127.

Miller, E.N., Jarboe, L.R., Yomano, L.P., York, S.W., Shanmugam, K.T., Ingram, L.O. 2009. "Silencing of NAPDH-dependent oxidoreductases (yqhD and dkgA)) in furfural-resistant ethanologenic *Escherichia coli.*" *Applied and Environmental Microbiology,* 75, 4315-4323.

Mills, T.Y., Sandoval, N.R., Gill, R.T. 2009. "Cellulosic hydrolysate toxicity and tolerance mechanisms in *Escherichia coli.*" *Biotechnology for Biofuels,* 2, 26-36.

Modig, T., Liden, G., Taherzadeh, M.J. 2002. "Inhibition effects of furfural on alcohol dehydrogenase, aldehyde dehydrogenase, and pyruvate dehydrogenase." *Biochemical Journal,* 363, 769-776.

Mondala, A., Liang, K., Toghiani, H., Hernandez, R., French, T. 2009. "Biodiesel production by *in situ* transesterification of municipal primary and secondary sludges." *Bioresource Technology,* 100, 1203-1210.

Moreton, R.S. 1988. "Physiology of lipid accumulating yeast." *Single Cell Oil,* Longman Scientific and Technical, London, 1-32.

Morimoto, S., Hirashima, T., Matutani, N. 1969. "Studies on fermentation product from furfural by yeast, III. Identification of furoin and furil." *Journal of Fermentation Technology,* 47, 486-490.

Myers, H.M., Montgomery, D.C. 1991. *Response surface methodology: process and product optimization using designed experiments.,* Wiley-Interscience, New York.

National Biodiesel Board 2009. "Benefits of biodiesel." Online posting. Last Accessed 15 August 2010: http://www.biodiesel.org/pdf_files/fuelfactsheets/Benefits%20of%20Biodiesel.Pdf.

National Biodiesel Board 2010a. "Energy content." Online posting. Last Accessed 15 August 2010: http://www.biodiesel.org/pdf_files/fuelfactsheets/BTU_Content_Final_Oct2005.pdf.

National Biodiesel Board 2010b. "Environmental and safety information." Online posting. Last Accessed 15 August 2010: http://www.biodiesel.org/pdf_files/fuelfactsheets/Environment_Safety.pdf.

National Biodiesel Board 2010c. "Performance." Online posting. Last Accessed 15 August 2010: http://www.biodiesel.org/pdf_files/fuelfactsheets/Performance.PDF.

National Biodiesel Board 2010d. "Esimated US biodiesel production by fiscal year (Oct 1-Sept 30)." Online posting. Last Accessed 15 August 2010: http://www.biodiesel.org/pdf_files/fuelfactsheets/Production_Graph_Slide.pdf.

National Biodiesel Board 2010e. "U.S. biodiesel production capacity." Online posting. Last Accessed 15 August 2010: http://www.biodiesel.org/pdf_files/fuelfactsheets/Production_Capacity.pdf.

National Biodiesel Board 2010f. "Estimated US biodiesel production by calendar year." Online posting. Last Accessed 15 August 2010: http://www.biodiesel.org/pdf_files/fuelfactsheets/Estimated_Production_Calendar_Years_05-09.ppt.

National Renewable Energy Laboratory 2004. "Biomass oil analysis: Research needs and recommendations." Online posting. Last Accessed 15 August 2010: http://www.eere.energy.gov/biomass/pdfs/34796.pdf.

Nelson, R.D., Schrock, M.D. 2006. "Energetic and economic feasibility associated with the production processing, and conversion of beef tallow to a substitute diesel fuel." *Biomass and Bioenergy,* 30, 584-591.

New Brunswick Scientific Co., I. 2007. *Guide to Operations: BioFlo 310 Benchtop Fermenter/Bioreactor.,* NBSC, Edison, NJ.

Nielsen, J.L., Nielsen, P.H. 2002. "Quantification of functional groups in activated sludge by microautoradiography." *Water Science and Technology,* 46, 389-395.

Nielsen, P.H., Thomsen, T.R., Nielsen, J.L. 2004. "Bacterial composition of activated sludge - importance for floc and sludge properties." *Water Science and Technology,* 49, 51-58.

Nilsson, A., Taherzadeh, M.J., Liden, G. 2001. "Use of dynamic step response for control of fed-batch conversion of lignocellulose hydrolyzates to ethanol." *Journal of Biotechnology,* 89, 41-53.

Nogueira, R., Melo, L.F., Purkhold, U., Wuertz, S., Wagner, M. 2002. "Nitrifying and heterotrophic population dynamics in biofilm reactors: Effects of hydraulic retention time and presence of organic carbon." *Water Research,* 36, 469-481.

O'Leary, W.M., Wilkinson, S.G. 1988. "Gram-positive bacteria." *Microbial Lipids, vol. 1,* Academic Press, London, 117-202.

Oehmen, A., Vives, M.T., Lu, H., Yuan, Z., Keller, J. 2005. "The effect of pH on the competition between polyphosphate-accumulating organisms and glycogen-accumulating organisms." *Water Research,* 39, 3727-3737.

Okabe, S., Oozawa, Y., Hirata, K., Watanabe, Y. 1996. "Relationship between population dynamics of nitrifiers in biofilms and reactor performance at various C:N ratios." *Water Research,* 30, 1563-1572.

Olsson, L., Hahn-Hagerdal, B. 1993. "Fermentative performance of bacteria and yeasts in lignocellulose hydrolysates." *Process Biochemistry,* 28, 249-257.

Olsson, L., Hahn-Hagerdal, B., Zacchi, G. 1995. "Kinetics of ethanol production by recombinant *Escherichia coli* KO11." *Biotechnology and Bioengineering,* 45, 356-365.

Olsson, L., Hahn-Hagerdal, B. 1996. "Fermentation of lignocellulose hydrolyzates for ethanol production." *Enzyme and Microbial Technology,* 18, 312-331.

Olukoshi, E.R., Packter, N.M. 1994. "Importance of stored triacylglycerols in *Streptomyces*: possible carbon source for antibiotics." *Microbiology,* 140, 931-943.

Oura, E. 1977. "Reaction products of yeast fermentations." *Process Biochemistry,* 12, 19-21.

Palmqvist, E., Hahn-Hagerdal, B., Galbe, M., Stenberg, K., Szengyel, Z., Tengborg, C., Zacchi, G. 1996. "Design and development of a bench-scale process development unit for the production of ethanol from lignocellulosics." *Bioresource Technology,* 58, 171-179.

Palmqvist, E., Hahn-Hagerdal, B., Galbe, M., Zacchi, G. 1996. "The effect of water-soluble inhibitors fom steam-pretreated willow on enzymatic hydrolysis and ethanol fermentation." *Enzyme and Microbial Technology,* 19, 470-476.

Palmqvist, E., Hahn-Hagerdal, B., Szengyel, Z., Zacchi, G., Reczey, K. 1997. "Simultaneous detoxification and enzyme production of hemicellulose hydrolyzates obtained after steam pretreatment." *Enzyme and Microbial Technology,* 19, 470-476.

Palmqvist, E., Galbe, M., Hahn-Hagerdal, B. 1998. "Evaluation of cell recycling in continuous fermentation of enzymatic hydrolysis of spruce with *Saccharomyces cerevisiae* and on-line monitoring of glucose and ethanol." *Applied Biochemistry and Biotechnology,* 50, 545-551.

Palmqvist, E., Almeida, J., Hahn-Hagerdal, B. 1999. "Influence of anaerobic glycolytic kinetics of *Saccharomyces cerevisiae* in batch culture." *Biotechnology and Bioengineering,* 62, 447-454.

Palmqvist, E., Grage, H., Meinander, N.Q., Hahn-Hagerdal, B. 1999. "Main and interaction effects of acetic acid, furfural, and *p*-hydroxybenzoic acid on growth and ethanol productivity of yeasts." *Biotechnology and Bioengineering,* 63, 46-55.

Palmqvist, E., Hahn-Hagerdal, B. 2000. "Fermentation of lignocellulose hydrolysates. II: Inhibitors and mechanisms of inhibition." *Bioresource Technology,* 74, 25-33.

Palmqvist, E., Hahn-Hagerdal, B. 2000a. "Fermentaion of lignocellulose hydrolysates. I: inhibition and detoxification." *Bioresource Technology,* 74, 17-24.

Palmqvist, E., Hahn-Hagerdal, B. 2000b. "Fermentation of lignocellulose hydrolysates. II: Inhibitors and mechanisms of inhibition." *Bioresource Technology,* 74, 25-33.

Pampuhla, M.E., Loureiro-Dias, M.C. 1990. "Activity of glycolytic enzymes of *Saccharomyces cerevisiae* in the presence of acetic acid." *Applied Microbiology and Biotechnology,* 34, 375-380.

Pan, J.G., Kwak, M.Y., Rhee, J.S. 1986. "High denisty cell culture of *Rhodotorula glutinins* using oxygen enriched-air." *Biotechnology Letters,* 8, 715-718.

Patterson, G. 1970. "Effect of temperature on fatty acid composition of *Chlorella sorokiniana.*" *Lipids,* 5, 597-600.

Pederson, T.A. 1962. "Lipid formation in *Cryptococcus terricolus* II." *Acta Chemica Scandinavia,* 16, 1015-1026.

Petersson, A., Liden, G. 2007. "Fed-batch cultivation of *Saccharomyces cerevisiae* on lignocellulosic hydrolyzate." *Biotechnology Letters,* 29, 219-225.

Ratledge, C. 1968. "Production of fatty acids and lipid by a *Candida* sp. growing on a fraction of *n*-alkanes predominating in tridecane." *Biotechnology and Bioengineering,* 10, 511-533.

Ratledge, C., Hall, M.J. 1977. "Oxygen demand by lipid-accumulating yeasts in continuous culture." *Applied and Environmental Microbiology,* 34, 230-231.

Ratledge, C. 1982. "Microbial oils and fats: an assessment of their commercial potential." *Progress in Industrial Microbiology,* 16, 119-206.

Ratledge, C. 1988. "Biochemistry, stoichiometry, substrates, and economics." *Single Cell Oil,* Longmans, Harlow, 33-70.

Ratledge, C. 2002. "Regulation of lipid accumulation in oleaginous microorganisms." *Biochemical Society Transactions,* 30, 1047-10050.

Ratledge, C., Wynn, J.P. 2002. "The biochemistry and molecular biology of lipid accumulation in oleaginous microorganisms." *Advances in Applied Microbiology,* 51, 1-51.

Ratledge, C. 2005. "Single cell oils for the 21st century." *Single cell oils,* AOCS Press, Champaign, IL, 1-20.

Rattray, J.B.M. 1988. "Yeasts." *Microbial Lipids, vol. 1,* Academic Press, London, 555-698.

Reddy, S.V., Thirumala, M., Reddy, T.V.K., Mahmood, S.K. 2008. "Isolation of bacteria producing polyhydroxyalkanoates (PHA) from municipal sewage sludge." *World Journal of Microbiology and Biotechnology,* 24, 2949-2955.

Reveille, V., Mansuy, L., Jarde, E., Garnier-Sillam, E. 2003. "Characterisation of sewage sludge-derived organic matter: lipids and humic acids." *Organic Geochemistry,* 34, 615-627.

Revellame, E., Hernandez, R., French, W., Holmes, W., Alley, E. 2010. "Biodiesel from activated sludge through *in situ* transesterification." *Journal of Chemical Technology and Biotechnology,* 85, 614-620.

Rittman, B.E., McCarty, P.L. 2001. *Environmental Biotechnology: Principles and Applications,* McGraw-Hill, New York.

Rose, A.H. 1989. "Influence of the environment on microbial lipid composition." *Microbial Lipids, Vol. 2,* Academic Press, London, 255-278.

Rottenberg, H. 1979. "The measurement of membrane potential and the pH in cells, organelles, and vesicles." *Methods in Enzymology,* 55, 547-569.

Russell, J.B. 1992. "Another explanation for the toxicity of fermentation acids at low pH: anion accumulation versus uncoupling." *Journal of Applied Bacteriology,* 73, 363-370.

Saha, B.C. 2004. "Lignocellulose biodegradation and applications in biotechnology." *Lignocellullose Biodegradation,* American Chemical Society, Washington, D.C., 2-35.

Salvado, H., Mas, M., Menendez, S., Garcia, M.P. 2001. "Effects of shock loads of salt on protozoan communities of activated sludge algae." *Acta Biotechnologica,* 40, 177-185.

Sattur, A.P., Karanth, N.G. 1989a. "Production of microbial lipids: I. Development of a mathematical model." *Biotechnology and Bioengineering,* 34, 863-867.

Sattur, A.P., Karanth, N.G. 1989b. "Production of microbial lipids: II. Influence of C/N ratio - model prediction." *Biotechnology and Bioengineering,* 34, 868-871.

Sattur, A.P., Karanth, N.G. 1989c. "Production of microbial lipids III: Influence of C/N ratio - experimental observations." *Biotechnology and Bioengineering,* 34, 872-874.

Sattur, A.P., Karanth, N.G. 1991. "Mathematical modeling of production of microbial lipids. Part I: Kinetics of biomass growth." *Bioprocess Engineering,* 6, 227-234.

Schell, D.J., Farmer, J., Newman, M., McMIllan, J.D. 2003. "Dilute-sulfuric acid pretreatment of corn stover in pilot-scale reactor." *Applied Biochemistry and Biotechnology,* 105, 69-85.

Schuchardt, U., Sercheli, R., Vargas, R.M. 1998. "Transesterification of vegetable oils: a review." *Journal of the Brazilian Chemical Society,* 9, 199-210.

Schweizer, E. 1989. "Biosynthesis of fatty acids and related compounds." *Microbial Lipids, Vol. 2,* Academic Press, London, 3-50.

Shuler, M.L., Kargi, F. 2002. *Bioprocess Engineering Basic Concepts, 2nd Edition,* Prentice Hall, Inc., Upper Saddle River, NJ.

Singh, J., Walker, T.K. 1956. "Influence of pH of the medium on the characterisitics and composition of *Aspergillus nidulans* fat." *Journal of Scientific and Industrial Research,* 15C, 222-224.

Snaidr, J., Amann, R., Huber, I., Ludwig, W., Schleifer, K.H. 1997. "Phylogenetic analysis and *in situ* identification of bacteria in activated sludge." *Applied and Environmental Microbiology,* 63, 2884-2896.

Sorger, D., Daum, G. 2003. "Triacylglycerol biosynthesis in yeast." *Applied Microbiology and Biotechnology,* 61, 289-299.

Sullivan, D.M., Cogger, C.G., Bary, A.I. 2007. "Fertilizing with Biosolids." Online posting. Last Accessed 19 October 2010: http://extension.oregonstate.edu/catalog/pdf/pnw/pnw508-e.pdf.

Taconi, K.A., Venkataramanan, K.P., Johnson, D.T. 2009. "Growth and solvent production by *Clostridium pasteurianum* ATCC 6013 utilizing biodiesel-derived crude glycerol as the sole carbon source." *Environmental Progress and Sustainable Energy,* 28, 100-110.

Taherzadeh, M.J., Eklund, R., Gustafsson, L., Niklasson, C., Liden, G. 1997. "Characterization and fermentation of diltue-acid hydrolyzates from wood." *Industrial and Engineering Chemistry Research,* 36, 4659-4665.

Taherzadeh, M.J., Niklasson, C., Liden, G. 1997. "Acetic acid - friend or foe in anaerobic batch conversion of glucose to ethanol by *Saccharomyces cerevisiae.*" *Chemical Engineering Science,* 52, 2653-2659.

Taherzadeh, M.J., Eklund, R., Gustafsson, L., Niklasson, C., Liden, G. 1997a. "Characterization and fermentation of diltue-acid hydrolyzates from wood." *Industrial and Engineering Chemistry Research,* 36, 4659-4665.

Taherzadeh, M.J., Niklasson, C., Liden, G. 1999a. "Conversion of dilute-acid hydrolyzates of spruce and birch to ethanol by fed-batch fermentation." *Bioresource Technology,* 69, 59-66.

Taherzadeh, M.J., Gustafsson, L., Niklasson, C., Liden, G. 1999b. "Conversion of furfural in aerobic and anaerobic batch fermentation of glucose by *Saccharomyces cerevisiae.*" *Journal of Bioscience and Bioengineering,* 87, 169-174.

Taherzadeh, M.J., Gustasson, L., Niklasson, C., Liden, G. 2000. "Inhibition effects of furfural on aerobic batch cultivation of *Saccharomyces cerevisiae* growing on ethanol and/or acetic acid." *Journal of Bioscience and Bioengineering,* 90, 374-380.

Taherzadeh, M.J., Niklasson, C., Liden, G. 2000b. "On-line control of fed-batch fermentation of dilute-acid hydrolyzates." *Biotechnology and Bioengineering,* 69, 330-338.

Taherzadeh, M.J., Gustafsson, L., Niklasson, C., Liden, G. 2000c. "Physiological effects of 5-hydroxymethyl furfural on *Saccharomyces cerevisiae.*" *Applied Microbiology and Biotechnology,* 53, 701-708.

Taherzadeh, M.J., Karimi, K. 2007. "Acid-based hydrolysis processes for ethanol from lignocellulosic materials: A review." *BioResources,* 2, 472-499.

Taherzadeh, M.J., Karimi, K. 2007. "Acid-based hydrolysis process for ethanol from lignocellulosic materials: a review." *Bioresources,* 2, 472-499.

Talebnia, F., Taherzadeh, M.J. 2006. "In situ detoxification and continuous cultivation of dilute-acid hydrolyzates." *Biotechnology and Bioengineering,* 69, 330-338.

Tchobanoglous, G., Burton, F.L., Stensel, H.D. 2003. *Wastewater Engineering Treatment and Reuse,* McGraw-Hill, New York.

Thomann, W.R., Hill, G.B. 1986. "Modified extraction procedure for gas-liquid chromatography applied to the identification of anaerobic bacteria." *Journal of Clinical Microbiology,* 23, 392-394.

Thomas, K.C., Hynes, S.H., Ingledew, W.M. 2002. "Influence of medium buffering capacity on inhibition of *Saccharomyces cerevisiae* growth my acetic and lactic acids." *Applied and Environmental Microbiology,* 68, 1616-1623.

U.S. Department of Energy, Energy Information Administration 2010. "United States energy profile." Online posting. Last Accessed 15 August 2010: http://tonto.eia.doe.gov/country/country_energy_data.cfm?fips=US.

U.S. Department of Energy 2006. "Five Year Plan FY 2007-FY2011 Vol. I." Online posting. Last Accessed http://www.smartgrids.eu/documents/DOE_Office_of_Science_5%20years_plan.pdf.

U.S. Energy Information Administration 2004. "Biodiesel performance, costs, and use." Online posting. Last Accessed 15 August 2010: http://www.eia.doe.gov/oiaf/analysispaper/biodiesel/.

U.S. Environmental Protection Agency 1999. "Biosolid Generation, Use, and Disposal in the United States" Online posting. Last Accessed 16 August 2010: http://www.biosolids.org/docs/18941.PDF.

U.S. Environmental Protection Agency 2008. "Clean watersheds needs survey." Online posting. Last Accessed 16 August 2010: http://epa.gov/cwns/cwns2008rtc/cwns2008rtc.pdf.

Van Gerpen, J., Knothe, G. 2005. "Basics of the transesterification reaction." *The Biodiesel Handbook,* AOCS Press, Champain, IL, 26-41.

Van Zyl, C., Prior, B.A., Du Preez, J.C. 1988. "Production of ethanol from sugar cane bagasse hemicellulose hydrolyzate by *Pichia stipitis* CBS 5776." *Enzyme and Microbial Technology,* 8, 439-44.

Verduyn, C., Postma, E., Scheffers, W.A., Van Dijken, J.P. 1990a. "Energetics of *Saccharomyces cerevisiae* in anaerobic glucose-limited chemostat cultures." *Journal of General Microbiology,* 136, 405-412.

Verduyn, C., Postma, E., Scheffers, W.A., Van Dijken, J.P. 1990b. "Physiology of *Saccharomyces cerevisiae* in anerobic glucose-limited chemostats." *Journal of General Microbiology,* 136, 395-403.

Vicente, G., Bautista, L.F., Rodriguez, R., Gutierrez, F.J., Sadaba, I., Ruiz-Vazquez, R.M., Torres-Martinez, S., Garre, V. 2009. "Biodiesel production from biomass of an oleaginous fungus." *Biochemical Engineering Journal,* 48, 22-27.

Vu, B., Chen, M., Crawford, R.J., Ivanova, E.P. 2009. "Bacterial extracellular polysaccharides involved in biofilm formation." *Molecules,* 14, 2535-2554.

Wagner, M., Loy, A. 2002. "Bacterial community composition and function in sewage treatment systems." *Current Opinion in Biotechnology,* 13, 218-227.

Weigert, B., Klein, K., Rizzi, M., Lauterbach, C., Dellweg, H. 1988. "Influence of furfural on the aerobic growth of the yeast *Pichia stipitis.*" *Biotechnology Letters,* 10, 895-900.

Weiss, R.M., Ollis, D.F. 1980. "Extracellular microbial polysaccharides. I. Substrate, biomass, and product kinetic equations for batch xanthan gum fermentation." *Biotechnology and Bioengineering,* 22, 859-873.

Wikandari, R., Millati, R., Syamsiyah, S., Muriana, R., Ayuningish, Y. 2010. "Effect of furfural, hydroxymethylfurfural, and acetic acid on indigenous microbial isolate for bioethanol production." *Agricultural Journal,* 5, 105-109.

Wilkinson, S.G. 1988. "Gram-negative bacteria." *Microbial Lipids, vol. 1,* Academic Press, London, 299-488.

Wilson, J.J., Deshcatelets, L., Nishikawa, N.K. 1989. "Comparative fermentability of enzymatic and acid hydrolysis of steam pretreated aspenwood hemicellulose by *Pichia stipitis* CBS 5776." *Applied Microbiology and Biotechnology,* 31, 592-596.

Wood, B.J.B. 1988. "Lipids of algae and protozoa." *Microbial Lipids, vol. 1,* Academic Press, London, 807-868.

Woodbine, M. 1959. "Microbial fat: microorganisms as potential fat producers." *Progress in Industrial Microbiology,* 1, 179-245.

Wynn, J.P., Hamid, A.A., Li, Y., Ratledge, C. 2001. "Biochemical events leading to the diversion of carbon into storage lipids in the oleaginous fungi *Mucor circinelloides* and *Mortierella alpina.*" *Microbiology,* 147, 2857-2864.

Yamaguchi, H., Mori, H., Kobayashi, T., Shimizu, S. 1983. "Mass production of lipids by *Lipomyces starkeyi* in microcompouter-aided-fed-batch culture." *Journal of Fermentation Technology,* 61, 275-280.

Yan, S., Subramanian, B., Surampali, R.Y., Narasiah, S., Tyagi, R.D. 2007. "Isolation, characterization, and identification of bacteria from activated sludge and soluble microbial products in in wastewater treatment systems." *Canadian Practice Periodical of Hazardous, Toxic, and Radioactive Waste Management,* 11, 240-258.

Ykema, A., Verbree, E.C., Kater, M.M., Smit, H. 1988. "Optimization of lipid production in the oleaginous yeast *Apiotrichum curvatum* in whey permeate." *Applied Microbiology and Biotechnology,* 29, 211-218.

Ykema, A., Bakels, R.H.A., Verwoert, I.I.G.S., Smit, H., Van Verseveld, H.W. 1989. "Growth yield, maintenance requirements, and lipid formation in the oleaginous yeast *Apiotrichum curvatum.*" *Biotechnology and Bioengineering,* 34, 1268-1276.

You, Y.-D., Shie, J.-L., Chang, C.-Y., Huang, S.-H., Pai, C.-Y., Yu, Y.-H., Chang, C.-H. 2008. "Economic cost analysis of biodiesel production: case in soybean oil." *Energy & Fuels,* 22, 182-189.

YSI Inc. Life Sciences 2000. "YSI 2700 Select Biochemistry Analyzer User's Manual" Online posting. Last Accessed 9 September 2010: www.ysi.com.

YSI Inc. Life Sciences 2008. "Application Note No. 328: Rapid measurement of xylose and glucose monitoring corn stover fermentation in bioethanol production." Online posting. Last Accessed 8 September 2010: www.ysilifesciences.com.

Zaldivar, J., Ingram, L.O. 1999. "Effect of organic acids on the growth and fermentation of ethanologenic *Escherichia coli* LY01." *Biotechnology and Bioengineering,* 66, 203-210.

Zaldivar, J., Nielsen, J., Olsson, L. 2001. "Fuel ethanol production from lignocellulose: a challenge for metabolic engineering and process integration." *Applied Microbiology and Biotechnology,* 56, 17-34.

Zhao, X., Kong, X., Hua, Y., Feng, B., Zhao, Z. 2008. "Medium optimization for lipid production through co-fermentation of glucose and xylose by the oleaginous yeast *Lipomyces starkeyi.*" *European Journal of Lipid Science and Technology,* 110, 405-412.

Zhila, N.O., Kalacheva, G.S., Volova, T.G. 2005. "Effect of nitrogen limitation on the growth and lipid consumption of the green alga *Botryococcus braunii* Kutz IPPAS H-252." *Russian Journal of Plant Physiology,* 52, 311-319.

Zhu, L.Y., Zong, M.H., Wu, H. 2008. "Efficient lipid production with *Trichosporon fermentans* and its use for biodiesel preparation." *Bioresource Technology,* 99, 7881-7885.

APPENDIX A

GC-FID CHROMOTOGRAMS FOR FAME ANALYSIS OF LIPIDS FROM ACTIVATED SLUDGE

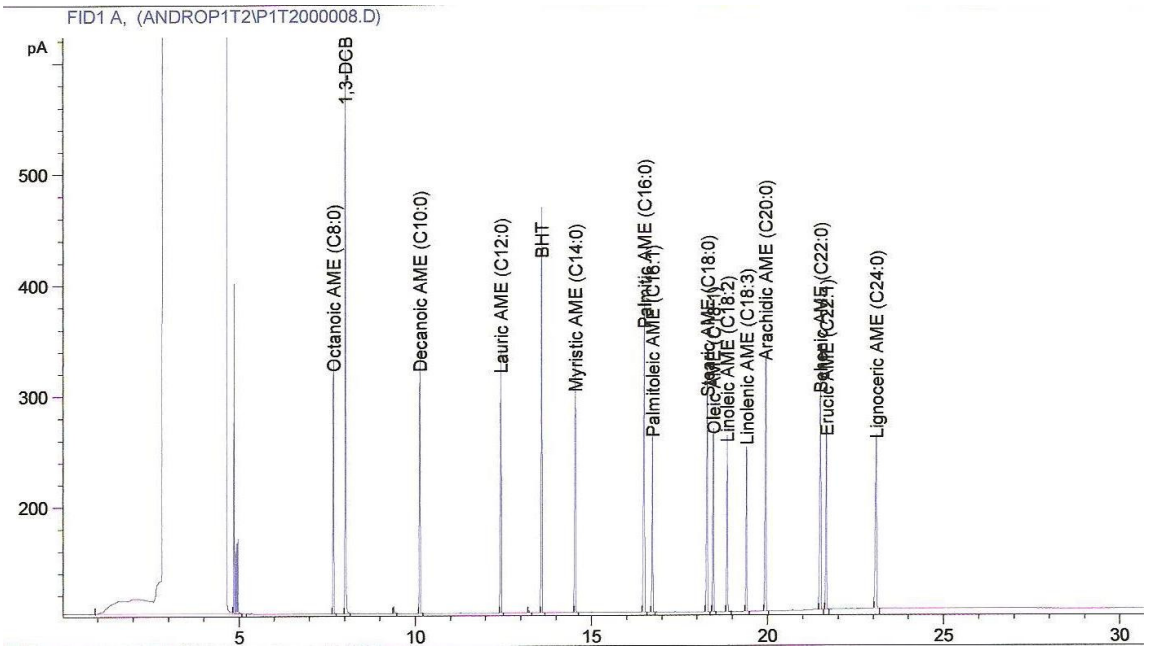

Figure A.1: GC-FID chromatogram of a standard FAME mix solution used for calibration.

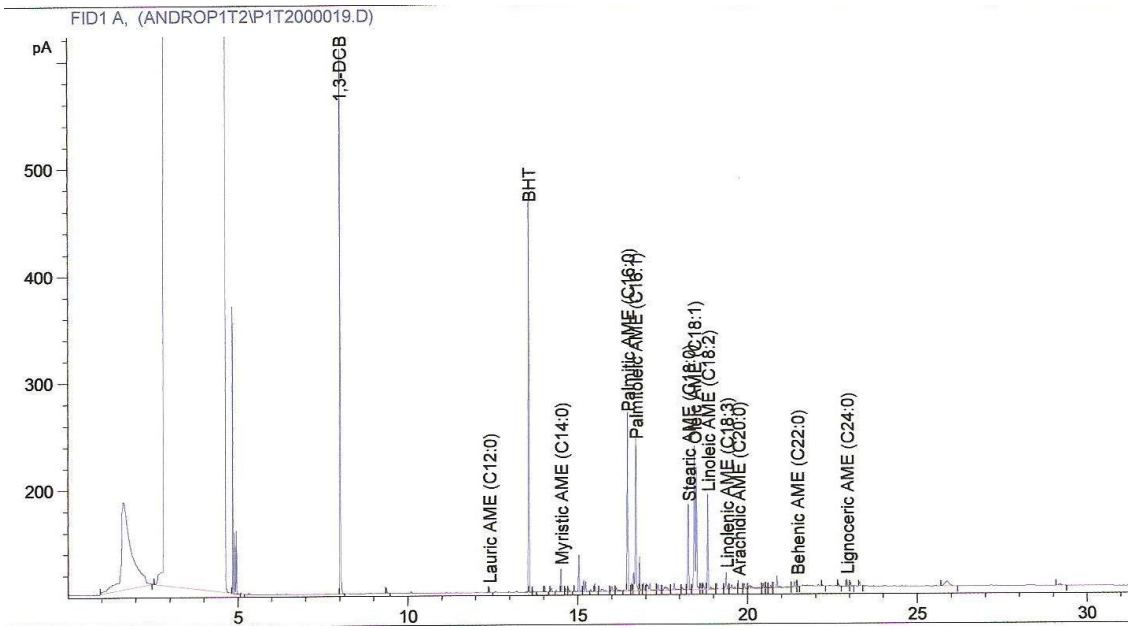

Figure A.2: Representative GC-FID chromatogram of a lipid extract from raw activated sludge.

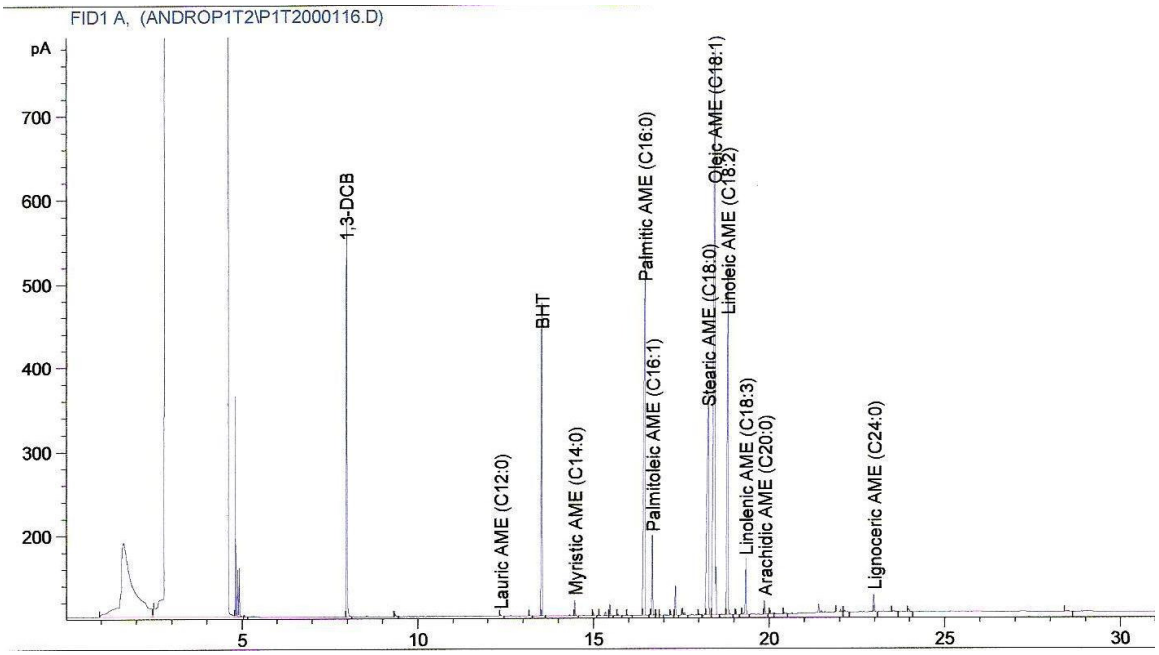

Figure A.3: Representative GC-FID chromatogram of a lipid extract from enhanced activated sludge.

APPENDIX B

KINETIC MODELING CALCULATIONS WITH POLYMATH® PROFESSIONAL 6.1

Table B.1: Sample nonlinear regression report for estimation of non lipid biomass growth kinetic parameters.

POLYMATH Report
Nonlinear Regression (L-M)

Model: X = Xo*2.718^(umax*t)/(1-Xo*(1-2.718^(umax*t))/Xmax)

Variable	Initial guess	Value	95% confidence
Xo	1.31101	1.149606	0.6155485
umax	0.02372	0.0454734	0.019152
Xmax	7.2575	6.663179	0.637424

Nonlinear regression settings
Max # iterations = 64

Precision

R^2	0.9674724
R^2adj	0.9581789
Rmsd	0.1180183
Variance	0.1989759

General

Sample size	10
Model vars	3
Indep vars	1
Iterations	10

Source data points and calculated data points

	t	X	X calc	Delta X
1	0	1.35	1.149606	0.2003943
2	12	1.68	1.763111	-0.083111
3	24	1.9	2.552453	-0.6524533
4	36	4.03	3.446617	0.5833831
5	48	4.42	4.324491	0.0955086
6	72	5.58	5.63912	-0.0591201
7	96	6.07	6.28021	-0.2102096
8	120	6.17	6.529475	-0.3594751
9	144	6.48	6.617675	-0.1376753
10	168	7.26	6.64783	0.6121705

Table B.2: Sample nonlinear regression report for estimation of lipid accumulation kinetic parameters.

POLYMATH Report
Nonlinear Regression (L-M)

Model: P = 0.24+m*(X-1.40829)+n*(16.5076/0.05163)*(0.05163*t+ln(1.40829/X))

Variable	Initial guess	Value	95% confidence
m	0.0576	0.0474106	0.0782845
n	0.0007	0.0003971	0.0002483

Nonlinear regression settings
Max # iterations = 64

Precision

R^2	0.956278
R^2adj	0.9508127
Rmsd	0.0300681
Variance	0.0113011

General

Sample size	10
Model vars	2
Indep vars	2
Iterations	5

Source data points and calculated data points

	X	t	P	P calc	Delta P
1	1.35	0	0.13	0.2426032	-0.1126032
2	1.68	12	0.18	0.3091431	-0.1291431
3	1.9	24	0.21	0.3826088	-0.1726088
4	2.55	36	0.31	0.4547282	-0.1447282
5	4.42	48	0.51	0.5522114	-0.0422114
6	5.58	72	0.73	0.734938	-0.004938
7	6.07	96	0.89	0.9048011	-0.0148011
8	6.17	120	1.12	1.064786	0.0552143
9	6.48	144	1.3	1.230577	0.0694226
10	7.26	168	1.39	1.410446	-0.0204456

Table B.3: Sample nonlinear regression report for estimation of sugar consumption kinetic parameters.

POLYMATH Report
Nonlinear Regression (L-M)

Model: S = 58.54-B*(6.66318/0.04547)*(0.04547*t+ln(1.14961/X))-a*(X-1.14961)

Variable	Initial guess	Value	95% confidence
B	0.04004	0.0048324	0.0110979
a	4.94854	5.028514	1.216805

Nonlinear regression settings
Max # iterations = 64

Precision

R^2	0.9762195
R^2adj	0.9732469
Rmsd	0.5762086
Variance	4.150204

General

Sample size	10
Model vars	2
Indep vars	2
Iterations	5

Source data points and calculated data points

	t	X	S	S calc	Delta S
1	0	1.35	58.54	57.64612	0.8938786
2	12	1.68	57.57	55.75518	1.814815
3	24	1.9	52.63	54.34967	-1.719666
4	36	2.55	46.43	50.90311	-4.473105
5	48	4.42	39.72	41.5029	-1.782905
6	72	5.58	36.03	35.06208	0.9679191
7	96	6.07	33.19	31.88493	1.305066
8	120	6.17	31.17	30.62087	0.5491258
9	144	6.48	28.22	28.32397	-0.1039697
10	168	7.26	23.6	23.70944	-0.1094364

Table B.4: Program code and sample report for Runge-Kutta-Fehlberg (RK45) integration of non lipid (Logistic Model), lipid, and substrate (Leudeking-Piret Model) rate equations for batch cultures.

POLYMATH Report
Ordinary Differential Equations

Calculated values of DEQ variables

	Variable	Initial value	Minimal value	Maximal value	Final value
1	a	5.02851	5.02851	5.02851	5.02851
2	B	0.00483	0.00483	0.00483	0.00483
3	m	0.07969	0.07969	0.07969	0.07969
4	n	0.000977	0.000977	0.000977	0.000977
5	P	0.13	0.13	1.410577	1.410577
6	S	58.54	26.72743	58.54	26.72743
7	t	0	0	168.	168.
8	Um	0.04547	0.04547	0.04547	0.04547
9	X	1.14961	1.14961	6.647834	6.647834
10	Xm	6.66318	6.66318	6.66318	6.66318

Differential equations

1 d(S)/d(t) = -B*X-a*Um*X*(1-X/Xm)
2 d(P)/d(t) = n*X+m*Um*X*(1-X/Xm)
3 d(X)/d(t) = Um*X*(1-X/Xm)

Explicit equations

1 B = 0.00483
2 a = 5.02851
3 m = 0.07969
4 n = 0.000977
5 Xm = 6.66318
6 Um = 0.04547

General

Total number of equations	9
Number of differential equations	3
Number of explicit equations	6
Elapsed time	0.000 sec
Solution method	RKF_45
Step size guess. h	0.000001
Truncation error tolerance. eps	0.000001

Table B.5: Program code and sample report for Runge-Kutta-Fehlberg (RK45) integration of non lipid (Monod Rate Law), lipid, and substrate (Leudeking-Piret Model) rate equations for continuous cultures.

POLYMATH Report
Ordinary Differential Equations

Calculated values of DEQ variables

	Variable	Initial value	Minimal value	Maximal value	Final value
1	D	0.010161	0.010161	0.010161	0.010161
2	Ks	14.00773	14.00773	14.00773	14.00773
3	m	0.223	0.223	0.223	0.223
4	n	0.00035	0.00035	0.00035	0.00035
5	P	0.1	0.1	0.6250327	0.6250327
6	qp	-0.0019159	-0.0019159	0.0011534	0.00035
7	S	0	0	45.67287	18.19179
8	t	0	0	1.25E+04	1.25E+04
9	u	0	0	0.0137637	0.010161
10	um	0.017985	0.017985	0.017985	0.017985
11	X	1.	1.	18.14558	18.14558
12	Yps	0.01495	0.01495	0.01495	0.01495
13	Yxs	0.38642	0.38642	0.38642	0.38642

Differential equations

1 d(S)/d(t) = -((u-D)*X/Yxs)-qp*X/Yps+D*(60-S)

Rate of substrate consumption

2 d(P)/d(t) = qp*X-D*P

Rate of lipid production

3 d(X)/d(t) = (u-D)*X

Rate of nonlipid biomass production

Explicit equations

1 um = 0.017985

Maximum specific growth rate

2 n = 0.00035

3 Ks = 14.00773

Saturation constant

4 u = um*S/(Ks+S)

Monod Rate Law

5 D = 0.010161

6 Yps = 0.01495

7 Yxs = 0.38642

8 m = 0.223

9 qp = m*(u-D)+n

APPENDIX C

16S rRNA SEQUENCES OF ACTIVATED SLUDGE BIOMASS

AGAGTTTGATCCTGGCTCAGGATGAACGCTAGCGGCAGGCTTAATACATG

CAAGTCAAGGGGTCAGCAATGGCACCGGCGGACGGGTGAGTAACGCGTAC

ACAACGTACCTTTAACTGGGGGATAGCATTTGGAAACGAGTGGTAATACC

GCATGTGGTTGCAGGGAGGCATCTTTTTGCAACTAAAACTCAGGTGGTTA

AAGATCGGTGTGCGTCCGATTAGCTTGTTGGTGAGGTAATGGCTCACCAA

GGCGACGATCGGTAGGGGGCGTGAGAGCGTGAACCCCCACACGGGTACTG

AGACACGGACCCGACTCCTACGGGAGGCAGCAGTAAGGAATATTGGTCAA

TGGAGGCAACTCTGAACCAGCCATGCCGCGTGGAGGAAGAAGGCGCTATG

CGTTGTAAACTTCTTTTGGGTGGGAAGAAAATGGTCAATTTATTGACAAC

TGACGGTACCATCAGAATAAGCACCGGCTAACTCCGTGCCAGCAGCCGCG

GTAATACGGAGGGTGCAAGCGTTATCCGGAATCACTGGGTTTAAAGGGTG

CGTAGGTGGTCTGATAAGTCAGTTGTGAAATTCCTCGGCTTAACCGAGTG

GACTGCGATTGATACTGTCAGACTTGAATCAGGTTGAGGTAGGCGGAATG

TGACATGTAGCGGTGAAATGCTTAGATATGTCATAGAACACCGATTGCGA

AGGCAGCTTGCTGGGCTTAGATTGACGCTGAGGCACGAAAGCGTGGGGAG

CAAACAGGATTAGATACCCTGGTAGTCC

Figure C.1: 16S rRNA sequence of raw activated sludge microbial community.

GAGTTTGATCCTGGCTCAGGACGAACGCTGGCGGCGTGCCTAACACATGC

AAGTCGAGCGAATGAAGTTCCTTCGGGAACGGATTTAGCGGCGGACGGGT

GAGTAACACGTGGGCAACCTGCCTCATAGAGGGGAATAGCCTTCCGAAAG

GGAGATTAATACCGCATAAGATTGTAGTACCGCATGGTACAGCAATTAAA

GGAGCAATCCGCTATGAGATGGGCCCGCGGCGCATTAGCTAGTTGGTGAG

GTAACGGCTCACCAAGGCGACGATGCGTAGCCGACCTGAGAGGGTGATCG

GCCACATTGGGACTGAGACACGGCCCAGACTCCTACGGGAGGCAGCAGTG

GGGAATATTGCACAATGGGGGAAACCCTGATGCAGCAACGCCGCGTGAGT

GATGACGGCCTTCGGGTTGTAAAGCTCTGTCTTCAGGGACGATAATGACG

GTACCTGAGGAGGAAGCCACGGCTAACTACGTGCCAGCAGCCGCGGTAAT

ACGTAGGTGGCGAGCGTTGTCCGGATTTACTGGGCGTAAAGGGAGCGTAG

GCGGATTTTTAAGTGAGATGTGAAATACTCGGGCTTAACCTGAGTGCTGC

ATTTCAAACTGGAAGTCTAGAGTGCAGGAGAGGAGAAGGGAATTCCTAGT

GTAGCGGTGAAATGCGTAGAGATTAGGAAGAACACCAGTGGCGAAGGCGC

TTCTCTGGACTGTAACTGACGCTGAGGCTCGAAAGCGTGGGGAGCAAACA

GGATTAGATACCCTGGTAGTCC

Figure C.2: 16S rRNA sequence of activated sludge microbial community at C:N ratio 10:1 after 3 d.

GGACTACCAGGGTATCTAATCCTGTTTGCTCCCCACGCTTTCGAGCCTCA

GCGTCAGTTACAGTCCAGAGAATCGCCTTCGCCACTGGTGTTCTTCCTAA

TCTCTACGCATTTCACCGCTACACTAGGAATTCCATTCTCCTCTCCTGCA

CTCTAGACTTCCAGTTTGAAATGCAGCACCCAAGTTGAGCCTGGGTATTT

CACATCTCACTTAAAAGTCCGCCTACGCTCCCTTTACGCCCAGTAAATCC

GGACAACGCTCGCCACCTACGTATTACCGCGGCTGCTGGCACGTAGTTAG

CCGTGGCTTCCCCCTCAGGTACCGTCATTATCGTCCCTGAAGACAGAGCT

TTACAACCCGAAGGCCGTCATCACTCACGCGGCGTTGCTGCATCAGGGTT

TCCCCCATTGTGCAATATTCCCCACTGCTGCCTCCCGTAGGAGTCTGGGC

CGTGTCTCAGTCCCAATGTGGCCGATCACCCTCTCAGGTCGGCTACGCAT

CGTCGCCTTGGTAAGCCGTTACCTTACCAACTAGCTAATCAGACGCGGGT

CCATCCTGTACCGCAAAAGCTTTGATACTTCTACCATGCGATAAAAGTAT

ATTATCTCGTATTAGCATACCTTTCGGTATGTTATCCGTGTGTACAGGGC

AGGTTACCCACGCGTTACTCACCCGTCCGCCGCTCTTTACAGAAGTAAAT

CGCTCGACTTGCATGTGTTAGGCACGCCGCCAGCGTTCATCCTGAGCCAG

GATCAAACTCT

Figure C.3: 16S rRNA sequence of activated sludge microbial community at C:N ratio 10:1 after 7 d.

AGAGTTTGATCCTGGCTCAGGATGAACGCTGGCGGCGTGCCTAACACATG

CAAGTCGAGCGATTTACTTCGGTAAAGAGCGGCGGACGGGTGAGTAACGC

GTGGGTAACCTGCCCTATACACACGGATAACGTACCGAAAGATACGCTAA

TACGAGATAACATATTTTTATCGCATGGTAAGAATATCAAAGCTCCGGCG

GTATAGGATGGACCCGCGTCTGATTAGCTGGTTGGTAAGGTAACGGCTTA

CCAAGGCGACGATCAGTAGCCGACCTGAGAGGGTGATCGGCCACATTGGA

ACTGAGACACGGTCCAAACTCCTACGGGAGGCAGCAGTGGGGAATATTGC

ACAATGGGCGAAAGCCTGATGCAGCAACGCCGCGTGAGCGATGAAGGCCT

TAGGGTCGTAAAGCTCTGTCCTCAAGGAAGATAATGACGGTACTTGAGGA

GGAAGCCCCGGCTAACTACGTGCCAGCAGCCGCGGTAATACGTAGGGGGC

TAGCGTTATCCGGAATTACTGGGCGTAAAGGGTGCGTAGGTGGTTTCTTA

AGTCAGAGGTGAAAGGCTACGGCTCAACCGTAGTAAGCCTTTGAAACTGA

GAAACTTGAGTGCGGGAGAGGAGAGTAGAATTCCTAGTGTAGCGGTGAAA

TGCGTAGATATTAGGAGGAATACCAGTTGCGAAGGCGGCTCTCTGGACTG

TAACTGACACTGAGGCACGAAAGCGTGGGGAGCAAACAGGATTAGATACC

CTGGTAGTCC

Figure C.4: 16S rRNA sequence of activated sludge microbial community at C:N ratio 40:1 after 3 d.

GGACTACCAGGGTATCTAATCCTGTTTGCTCCCCACGCTTTCGTGCCTCA

GTGTCAGTTACAGTCCAGAGAGCCGCCTTCGCAACTGGTGTTCCTCCTAA

TATCTACGCATTTCACCGCTACACTAGGAATTCCACTCTCCTCTCCTGCA

CTCAAGTTTCCCAGTTTCAAAGGCTTACTACGGTTGAGCCGTAGCCTTTC

ACCTCTGACTTAAGAAACCACCTACGCACCCTTTACGCCCAGTAATTCCG

GATAACGCTAGCCCCCTACGTATTACCGCGGCTGCTGGCACGTAGTTAGC

CGGGGCTTCCTCCTCAAGTACCGTCATTATCTTCCTTGAGGACAGAGCTT

TACGACCCGAAGGCCTTCATCGCTCACGCGGCGTTGCTGCATCAGGCTTT

CGCCCATTGTGCAATATTCCCCACTGCTGCCTCCCGTAGGAGTTTGGACC

GTGTCTCAGTTCCAATGTGGCCGATCACCCTCTCAGGTCGGCTACTGATC

GTCGCCTTGGTAAGCCGTTACCTTACCAACTAGCTAATCAGACGCGGGTC

CATCCTGTACCGCAAAAGCTTTGATACTTCTACCATGCGATAAAAGTATA

TTATCTCGTATTAGCATACCTTTCGGTATGTTATCCGTGTGTACAGGGCA

GGTTACCCACGCGTTACTCACCCGTCCGCCGCTCTTTACCGAAGTAAATC

GCTCGACTTGCATGTGTTAGGCACGCCGCCAGCGTTCATCCTGAGCCAGG

ATCAAACTCT

Figure C.5: 16S rRNA sequence of activated sludge microbial community at C:N ratio 40:1 after 7 d.

GGACTACCAGGGTATCTAATCCTGTTTGCTCCCCACGCTTTCGCACCTGA

GCGTCAGTCTTTGTCCAGGGGGCCGCCTTCGCCACCGGTATTCCTCCAGA

TCTCTACGCATTTCACCGCTACACCTGGAATTCTACCCCCCTCTACAAGA

CTCTAGCTGGACAGTTTTAAATGCAATTCCCAGGTTGAGCCCGGGGCTTT

CACATCTAACTTATCCAACCGCCTGCGTGCGCTTTACGCCCAGTAATTCC

GATTAACGCTTGCACCCTCCGTATTACCGCGGCTGCTGGCACGGAGTTAG

CCGGTGCTTCTTCTGCGAGTAACGTCACAGCCAGCAGGTATTAGCTACTG

ACCTTTCCTCCTCGCTGAAAGTGCTTTACAACCCGAAGGCCTTCTTCACA

CACGCGGCATGGCTGCATCAGGGTTTCCCCCATTGTGCAATATTCCCCAC

TGCTGCCTCCCGTAGGAGTCTGGACCGTGTCTCAGTTCCAGTGTGGCTGG

TCATCCTCTCAGACCAGCTAGGGATCGTCGCCTGGGTGAGCCATTACCCC

ACCTACTAGCTAATCCCATCTGGGCACATCTGATGGCATGAGGCCCGAAG

GTCCCCCACTTTGGTCTTGCGACGTTATGCGGTATTAGCTACCGTTTCCA

GTAGTTATCCCCCTCCATCAGGCGGTTTCCCAGACATTACTCACCCGTCC

GCCGCTCGTCACCCGAGAGCAAGCTCTCTGTGCTACCGCTCGACTTGCAT

GTGTTAGGCCTGCCGCCAGCGTTCAATCTGAGCCAGGATCAAACTCT

Figure C.6: 16S rRNA sequence of activated sludge microbial community at C:N ratio 70:1 after 3 d.

AGAGTTTGATCCTGGCTCAGAGCGAACGCTGGCGGCATGCTTAACACATG

CAAGTCGCACGAGGGTTTCGGCCCTAGTGGCGGACGGGTGAGTAGCGCGT

AGGGATCTATCCATGGGTGGGGGATAACACTGGGAAACTGGTGCTAATAC

CGCATGATGCCTGAGGGCCAAAGGCGCAAGTCGCCTGTGGAGGAGCCTGC

GTTCGATTAGCTTGTTGGTGGGGTAAAGGCCTACCAAGGCGATGATCGAT

AGCTGGTCTGAGAGGATGATCAGCCACACTGGGACTGAGACACGGCCCAG

ACCCCTACGGGAGGCAGCAGTGGGGAATATTGGACAATGGGGGCAACCCT

GATCCAGCAATGCCGCGTGTGTGAAGAAGGTCTTCGGATTGTAAAGCACT

TTCGACGGGGACGATGATGACGGTACCCGTAGAAGAAGCCCCGGCTAACT

TCGTGCCAGCAGCCGCGGTAATACGAAGGGGGCTAGCGTTGCTCGGAATG

ACTGGGCGTAAAGGGCGCGTAGGCGGTTGACACAGTCAGATGTGAAATTC

CAGGGCTTAACCTTGGGGCTGCATTTGAGACGTGTTGACTGGAGTTCGAG

AGAGGGTTGTGGAATTCCCAGTGTAGAGGTGAAATTCGTAGATATTGGGA

AGAACACCGGTGGCGAAGGCGGCAACCTGGCTCGATACTGACGCTGAGGC

GCGAAAGCGTGGGGAGCAAACAGGATTAGATACCCTGGTAGTCC

Figure C.7: 16S rRNA sequence of activated sludge microbial community at C:N ratio 70:1 after 7 d.